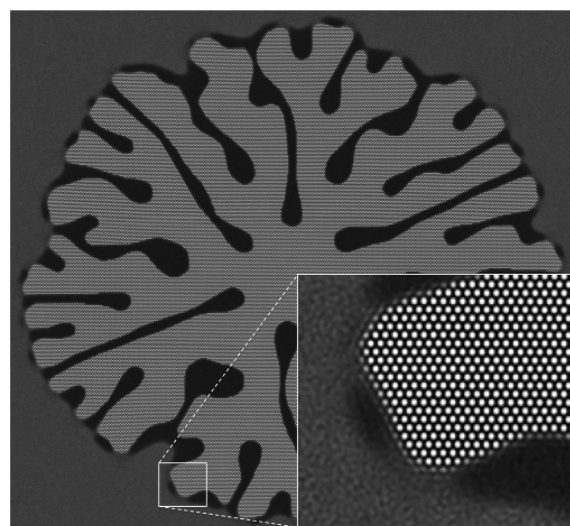
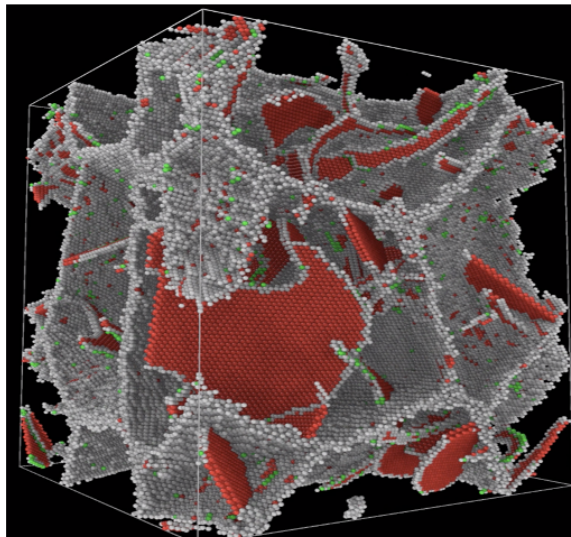


Thermodynamics & Kinetics of Phase Transformations

Nikolas Provatas



Department of
Physics, McGill
University

© NP, October 2023, Ed.1.3

Contents

Preface	ii
1 Thermodynamics and Phase Coexistence	1
1.1 Energy, Work, Heat and The First Law of Thermodynamics	1
1.2 Entropy, Heat and The Second Law of Thermodynamics	2
1.3 Thermodynamic Potentials	2
1.3.1 Internal energy	3
1.3.2 Helmholtz free energy	3
1.3.3 Gibbs free energy	4
1.3.4 Enthalpy	4
1.3.5 Grand potential	4
1.4 Extrema of Thermodynamic Potentials	5
1.5 Extensive Variables and Homogeneous Functions	5
1.5.1 Helmholtz free energy	6
1.5.1.1 Description in terms of solute concentration variables	7
1.5.2 Grand potential	8
1.5.2.1 Description in terms of solute concentration variables	9
1.5.3 Gibbs free energy	10
1.5.3.1 Description in terms of solute concentration variables	10
1.5.3.2 Alternate derivation of the inter-diffusion potential of a mixture	11
1.6 Intensive Variables	12
1.7 Equilibrium Phase Coexistence	13
1.7.1 Pure materials	13
1.7.1.1 Pressure at co-existence in a pure material	14
1.7.2 Binay Alloys	15
1.7.2.1 Gibbs phase rule	15
1.7.2.2 Equilibrium conditions	15
1.7.2.3 Recasting equilibrium conditions in term of concentration and density	16
1.7.2.4 Final form of coexistence conditions in terms of concentration and density	17
1.7.2.5 Recasting equilibrium conditions in terms of molar free energies	18
1.7.2.6 Dimensionless representation	19
1.7.2.7 Special case of equal densities	20
2 Nucleation	21
2.1 Fokker Plank Equation: Evolution of Nuclei in Size Space	21
2.1.1 Determination of mesoscale coefficients A and B in the size flux	26
2.2 Classical Nucleation Theory From a Microscopic Perspective	27

2.2.1	Preliminaries	27
2.2.2	Non-equilibrium attachment kinetics governing the growth of nuclei	28
2.2.3	Equilibrium steady state conditions	29
2.2.4	Non-equilibrium steady-state conditions	29
2.3	Nucleation Rate in a Binary Mixture	31
2.3.1	Work of formation in a binary mixture	32
3	Phase Transformation Kinetics	36
3.1	Supersaturation-Driven Grain Growth	36
3.2	Grain Growth Dynamics Subject to Mass Conservation	39
3.2.1	Conditions controlling the kinetics of a phase boundary in an alloy	39
3.2.2	Early-time grain growth kinetics	40
3.2.3	Late-time grain growth kinetics	41
3.2.4	Scaling of particle size distribution in the late time coarsening regime	43
4	Interface Instabilities and the Emergence of Solidification Microstructures	47
4.1	Sharp-Interface Model of Solidification of a Pure Substance	48
4.2	Solidification of an Undercooled Spherical Liquid Drop	50
4.3	Stability of an Undercooled Spherical Liquid Drop	53
4.4	Beyond Linear Stability: Dendritic Growth Forms	58
4.5	Limitations of Sharp Interface Models	59
5	Topics in Mean Field Theory	61
5.1	Landau Theory of Solids	61
5.1.1	Vacancy order parameter	61
5.1.2	Vacancy-strain coupling in the free energy	63
5.1.3	Vacancies in the stress tensor	63
5.2	Fluctuations in Ginzburg-Landau Theory	65
5.2.1	Expansion of partition function around the mean field solution	65
5.2.2	Gaussian integration of Q_V	67
5.2.3	Renormalization of free energy coefficients	70
6	Hydrodynamics of Solids	71
6.1	Microscopic Operators and Conservation Laws	71
6.1.1	Averages of microscopic operators	73
6.2	Adding Momentum into Thermodynamics	74
6.2.1	Mechanics of the moving volume ΔV	75
6.2.2	Statistical mechanics of the moving volume ΔV	76
6.2.3	Thermodynamics of the moving volume ΔV	78
6.3	Entropy Production and Hydrodynamic Fluxes	80
6.3.1	Specialization to liquids	83
6.3.2	Specialization to solids	83
6.4	Hydrodynamics of Solids: Displacement Modes	84
7	Classical Density Functional Theory	86
7.1	Statistical Mechanics Preliminaries	86
7.2	Adding Spatial Variations in the Grand Partition Function	88
7.3	The Intrinsic Free Energy Functional	89

7.4	Equilibrium Density and Thermodynamic Driving Forces	90
7.5	Correlation Functions	91
7.5.1	Generating the n -point density from the grand partition function	91
7.5.2	Generating density correlation functions from the grand potential	93
7.5.3	Generating direct correlation functions from the excess free energy	95
7.5.3.1	Non-Interacting ideal gas	95
7.5.3.2	Interacting systems	96
7.5.3.3	Definition of Direct correlation functions	97
7.5.3.4	Orstein-Zernike relation for $C^{(2)}(\mathbf{q}_1, \mathbf{q}_2)$	97
7.6	Density Functional Theory of Freezing	100
7.6.1	Relation of $C_0^{(2)}(\mathbf{x}, \mathbf{x}')$ to the structure factor	101
7.6.2	Moving on to phase field crystal models	102
8	Phase Field Crystal (PFC) Theory	103
8.1	Simplifying cDFT Theory	103
8.2	Recovering the Traditional PFC Model	104
8.3	Structural PFC Model (XPFC)	105
8.4	Equilibrium Properties of the XPFC model	106
8.4.1	Crystallography of the single mode expansion	106
8.4.2	Mean field free energy density of BCC solid-liquid system	107
8.4.2.1	Interaction free energy	107
8.4.2.2	Local free energy terms	108
8.4.2.3	Total BCC-liquid mean field free energy	109
8.4.3	Phase Coexistence and Construction of Diagrams	109
9	Dynamics in Classical Field Theories	112
9.1	Dynamic Density Functional Theory (DDFT)	112
9.1.1	Non-equilibrium statistical mechanics	112
9.1.2	Density evolution as a Markov process	113
9.2	Model B Limit of DDFT: PFC Dynamics	115
9.3	“Quasi-Phononic” PFC Dynamics	117
9.3.1	Two-time dynamics in the PFC model	117
9.3.2	A constitutive equation for $\rho(\mathbf{x}, t)$	119
9.4	Dissipation tensor	120
9.4.1	Modified PFC (<i>MPFC</i>) model and its simplifications	121

Preface

These notes comprise select tutorials on phase field modelling, classical density functional theory and non-equilibrium phase transformations. They provide supplementary reading for the introductory text *Phase Field Methods in Materials Science and Engineering* in [24] by N. Provatas and K. Elder, and that text will be referenced frequently. Reference [24] takes a somewhat practical approach for deriving phase field theories. The present notes (most of which will end up in the next edition the aforementioned text) introduce select topics in phase field theory at a more advanced level. The level is aimed at graduate students familiar with or following a classical condensed matter physics curriculum.

The first chapter of these notes is a review of thermodynamic potentials and their applications to phase coexistence in multi-component materials. This topic is crucial for analyzing the mean field properties of phase field models and determining their phase diagrams¹. Chapters 2-4 examine classical particle growth kinetics, from nucleation to particle growth and coarsening, and interface instabilities that are quintessential to pattern formation in microstructure evolution. The fifth chapter studies two topics in mean field theory that are not usually covered in traditional treatments of the topic. The first topic derives a mean field model for a solid that incorporates a vacancy order parameter alongside the density and strain order parameters typically used to describe solids. The second topic derives the classic Ginzburg-Landau “Model A” free energy directly from the partition function. Chapter 6 derives mesoscale conservations laws for mass, momentum and energy from microscopic principles. Combining these with the appropriate fluxes derived from entropy dissipation yields dynamical equations that are the basis for the evolution of density, displacement and temperature in solids. These compliment the dynamical equations derived in Ref. [24] for order parameters describing phase changes. Combining an order parameter with hydrodynamics modes can then yield a complete set of equations for the evolution of mass, heat, and strain during microstructure formation, which is the basis of many papers on phase transformations in solid state materials. Chapter 7 moves on to review the statistical mechanics of inhomogeneous fluids, from which is derived a classical density functional theory (CDFT) of solidification. In this formalism, the emergence of an ordered phase (e.g. crystal) is seen as the localization of order in the fluid phase. Chapter 8 studies a simplification of CDFT that give rise to a class of phase field models that have been coined “phase field crystal” (PFC) models. The equilibrium thermodynamics and non-equilibrium kinetics of a PFC model is analyzed. Chapter 8 deals with dynamics in cDFT and PFC type theories.

Many topics presented herein that require some familiarity advanced topics in statistical mechanics and condensed matter physics. Such topics are reviewed briefly here, as required, in order to not break the flow from the main topic of phase field modelling; they are, however, covered in depth in other primary references, to which the reader is referred for further reading.

I wish to thank my graduate students and my many collaborators for the many discussions which helped shape the flow and content of this book. As with anything in print, this book likely contains

¹I apologize in advance to the purists for swapping the variable $G \leftrightarrow F$ for the Helmholtz and Gibbs free energies; I enjoy using G over F for the former.

typos and oversights. I would be delighted to hear from readers about any such errors or omissions. Please do not hesitate to contact me at Nikolaos.Provatas@McGill.ca

Chapter 1

Thermodynamics and Phase Coexistence

This Chapter begins with a basic tutorial on thermodynamic potentials. We get some concepts and definitions out of the way, as well as some relationships between thermodynamic variables and the concept of thermodynamic potentials and their extrema. Material developed in the first tutorial will be used to derive conditions of equilibrium phase coexistence in a pure material and a binary alloy by considering their description in terms of both mass density and alloy concentration, respectively.

1.1 Energy, Work, Heat and The First Law of Thermodynamics

The *first law of thermodynamics* dictates that we can break the *internal energy* of a closed system into two contributions,

$$dE = dW + dQ \quad (1.1)$$

where dW is the work done on/by the system and dQ is the heat energy added or removed from the system through non-mechanical means (friction, heating up the system, etc). It is instructive to explore the meaning of the terms dW and dQ and their roles in changing dE .

The term dW is usually expressed in terms of mechanical work. For example, in an isotropic material such as a fluid (gas or liquid), an applied pressure does work $dW = -pdV$ on the system, where p is the pressure of the system and dV is its volume change¹. In the case of an ideal gas, the work imparted onto a system by small change in volume dV imparts an increase in kinetic energy of the surface atoms colliding with the surface, which is rapidly distributed into an increased average kinetic energy of the gas' constituent particles. In a solid, atoms or molecules are fixed to specific lattice sites (on average). Here, work can also impart kinetic energy through the surface of the atomic vibrations. However, the larger contribution to a materials internal energy comes in the form of increased potential energy as the "bond-springs" holding atoms in place are stretched or compressed.

Heat flow dQ into a system can occur when a system is in contact with another system at a different temperatures. In this case, the flow of heat into a system represents an change in the average kinetic energy of its constituent particles. Another case, to be discussed in more detail in the next section, is one where heat flowing into/out of the system causes the system to change between different

¹Pressure has units of force/area, and can be applied in various ways. In what follows, we imagine it is applied uniformly around the container walls. To visualize this, take a soft plastic bottle and remove much of the air from within by placing into it a lit match and sealing the bottle cap. As the flame depletes most of the oxygen, the bottle will start to "uniformly" squeeze inwards from many surfaces simultaneously. Adding up $-p\Delta V$ over all surface elements will give the total work done on the system of box.

equilibrium states that all consistent with a given temperature, i.e., isothermally. These states can be encoded by the system *entropy* (denoted by S), and the change in heat flow between these state of entropy is represented by $dQ = TdS$, where T is the system temperature. Entropy (S) is abstraction that captures the number of configurations (e.g., momenta and coordinates) of the system that are consistent with a given internal energy.

1.2 Entropy, Heat and The Second Law of Thermodynamics

The fundamental thermodynamic connection between entropy and heat transfer in and out of a system during some change must be more formally defined to be more generally applicable. It is couched in the form of of a law, namely *The Second Law of Thermodynamics*. Consider measuring the heat flow into and out of a system during some cyclic process that is broken into infinitesimal steps. Doing so for *any* process, it is always observed that the integral of the ratio dQ/T over the cyclic process satisfies

$$\oint \frac{dQ}{T} \leq 0 \quad (1.2)$$

The equality holds for any *reversible, quasi-static* processes. For a reversible process, Eq. (1.2) becomes path independent and can be equivalently expressed in terms of a state function, which is a function of the state variables of the system. We denote this state function as the *entropy* S , and make the association

$$dS = \frac{dQ}{T} \quad (1.3)$$

For an irreversible process, the inequality holds in Eq. (1.2). To understand what this means, decompose the path integral of Eq. (1.2) into an irreversible process path from states $a \rightarrow b$ and then a reversible processes along a path form $b \rightarrow a$. Denote the entropy change along the reversible path $b \rightarrow a$ as ΔS , and note that it is the *minus* of the reversible process from $a \rightarrow b$. The complete path integral of Eq. (1.2) for the process $a \rightarrow b$ and $b \rightarrow a$ thus becomes,

$$\oint \frac{dQ}{T} = \int_{a \rightarrow b} \frac{dQ}{T} - \Delta S_{a \rightarrow b}^{\text{rev}} < 0 \quad (1.4)$$

This implies that, in general, for *any* given irreversible process path (let us drop the notation $a \rightarrow b$), the change of the entropy function of a system satisfies,

$$\Delta S > \int \frac{dQ}{T} \quad (1.5)$$

The inequality in Eq. (1.5) implies that we can have, for an irreversible process, $\Delta S > 0$ even when $\Delta Q = 0$. An intuitive example is the rapid expansion of a gas into a thermally shielded (adiabatic) container. In the case of a reversible process on the other hand, Eq. (1.3) and Eq. (1.1) allows for a quantity of heat absorbed from a reservoir to do useful work (e.g. expand a piston) in one part of a cycle, and then for work to be done to transfer a quantity of heat back into the reservoir in another part of the process; in both part of such an exchange, the heat transferred is expressible by the changes in the entropy state of the system.

1.3 Thermodynamic Potentials

We saw that the internal energy E is relatable to heat and work through the first law of thermodynamics, but since work is related to changes in volume, internal energy a function of the state of system's

entropy S and volume V . Internal energy is an example of a thermodynamic potential. There are other such potentials as well. For example, entropy S is also a thermodynamic potential dependent on the temperature T and volume V . In this section we use the first and second laws to derive other thermodynamic potentials, and their state variable dependencies.

1.3.1 Internal energy

Revisiting the first law, we use Eq. (1.3) to replace $dQ \rightarrow TdS$ in the 1st law of Eq. (1.1) and, assuming an isotropic material, write the change in internal energy of a closed system as

$$dE = TdS - pdV \quad (1.6)$$

Before we continue, there is one contribution to the change of internal energy that is missing and very important to discuss. In the case of a permeable system, we can also change the energy of system by adding or removing particles into the system. This change in the energy of the system is quantified by increment $\mu\Delta N$, where dN is the change in the total number of particles in the system, and μ is referred to as the *chemical potential*. The chemical potential describes changes to the internal energy due to the change in chemical bonding that arise due to the change of particles in a system. It is different from the kinetic energy contribution to the internal energy, which change the motional energy of atoms, or the work done on a system which also accounts for changes potential energy that arise from "stretching" bonds between a given number of atoms/molecules.

Taking the changes of chemical potential into account allows us to write the change in *internal energy* E of a system as

$$dE = TdS - pdV + \mu dN \quad (1.7)$$

Equation 1.7 has three terms. The first relates to heat flow, expressed through the entropy –which itself is related to the number of states accessible to a system. The second relates to the external work done on the system. The last relates to number of particles contained in the system. We can think of Eq. (1.7) as the total differential of multi-variable function of the variables (S, V, N) . In other words we can write the internal energy as $E = E(S, V, N)$.

1.3.2 Helmholtz free energy

While the volume V and particle number N can be measured in many situations, entropy is not something we can readily measure. We can get around this problem by performing a *Legendre transformation* to E in order create another potential with different natural variables. Here is an example. Define a new thermodynamic function G by

$$G = E - TS \quad (1.8)$$

Why is this useful? To see this take the differential of Eq. (1.8),

$$\begin{aligned} dG &= dE - TdS - SdT = TdS - pdV - TdS - SdT + \mu dN \\ &= -SdT - pdV + \mu dN \end{aligned} \quad (1.9)$$

If we again interpret Eq. (1.9) in the context of a function of multiple variables, we conclude that $G = G(T, V, N)$. The function G is called the *Helmholtz free energy* and is also thermodynamic potential. Thus, by the Legendre transformation we made a state functions that changed the description of the system from the variables (S, V, N) to (T, V, N) .

1.3.3 Gibbs free energy

We can also describe the state of the system knowing only temperature, pressure and number of particles. We can define another function, through a Legendre transformation of the Helmholtz free energy according to

$$F = G + PV \quad (1.10)$$

As before, taking differentials of Eq. (1.10), we obtain

$$\begin{aligned} dF &= dG + pdV + Vdp = -SdT - pdV + \mu dN + pdV + Vdp \\ &= -SdT + Vdp + \mu dN \end{aligned} \quad (1.11)$$

This defines the *Gibbs free energy* as a potential of T, p, N , i.e., $F = F(T, p, N)$.

1.3.4 Enthalpy

One last potential is the *enthalpy*, defined by a Legendre transformation of the internal energy according to

$$H = E + PV \quad (1.12)$$

Taking differentials and using Eq. (1.7) yields

$$\begin{aligned} dH &= dE + pdV + Vdp = TdS - pdV + \mu dN + pdV + Vdp \\ &= TdS + Vdp + \mu dN, \end{aligned} \quad (1.13)$$

which makes the enthalpy a state function of S, p, N , i.e., $H = H(S, p, N)$.

Figure (1.1) provides an easy mnemonic for remembering the derivatives of Eqs. (1.7), (1.9), (1.11) and (1.13) with respect to their natural state variables, e.g., $(\partial G/\partial T)_V = -S$ or $(\partial H/\partial S)_p = -T$, etc. Note that the chemical potential is not shown in Fig. (1.1) as it is always the derivative of a

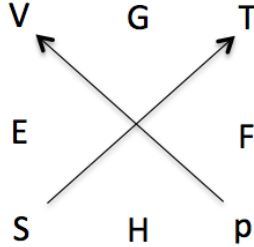


Figure 1.1: The functions E, G, F, H are flanked by their respective natural variables (on either side or top and bottom). For example, $G = G(V, T)$. Derivatives with respect to one argument, with the other held fixed, gives a variable along one of the diagonals, either with or against the direction of the arrow. Going against the arrows yields a negative sign, e.g., $(\partial G/\partial T)_V = -S$.

potential function with respect to the number of particles while holding all other natural variables fixed.

1.3.5 Grand potential

An important thermodynamic function that is useful is the *grand potential*, defined by a Legendre transformation of G according to

$$\Omega = G - \mu N \quad (1.14)$$

As before, taking differentials yields

$$\begin{aligned}
d\Omega &= dG - \mu dN - N d\mu \\
&= -SdT - pdV + \mu dN - \mu dN - N d\mu \\
&= -SdT - pdV - N d\mu
\end{aligned} \tag{1.15}$$

The grand potential is a function of T, V, μ , i.e., $\Omega = \Omega(T, V, \mu)$.

1.4 Extrema of Thermodynamic Potentials

The functions S, E, H, G, F and Ω are usually called *thermodynamic potentials*. The analogy with a potential is made because equilibrium can be defined as an extremum of these "potentials" with respect to the variables with which they are defined. For example, inspection of Eqs. (1.7), (1.9), (1.11), (1.13) and (1.15) gives

$$\begin{aligned}
(dS)_{E,V,N} &= 0 \\
(dE)_{S,V,N} &= 0 \\
(dH)_{S,p,N} &= 0 \\
(dG)_{T,V,N} &= 0 \\
(dF)_{T,p,N} &= 0 \\
(d\Omega)_{T,V,\mu} &= 0
\end{aligned} \tag{1.16}$$

where the subscripts in Eqs. (1.16) denote what thermodynamic variables are held fixed in each case when defining equilibrium via any of the potentials. Expanded discussions of this topic are also found in Chapter 3 of Ref. [5] and Ref. [27].

The extremum properties in Eqs. (1.16) are powerful tools. They require that a thermodynamic potential written with respect to any variable *other* than the ones being held fixed is in a minimum with respect to that variable. As written, Eqs. (1.16) appear to apply to a single homogeneous system. However, they also apply to a system comprised of multiple, coexisting homogeneous phases or sub-regions. In this case, the system can depend on additional *internal variables* [27]. These can describe, for example, the volume of a contained phase β , V_β , relative to the fixed system volume V , or the number of elemental particles N_α^β in a phase β relative to the fixed number of particles N . Thermodynamic potentials can be then minimized with respect to internal variables such as V_α or N_α^β , subject to any constraints these variables obey relative to V or N . We will see some examples of this below.

1.5 Extensive Variables and Homogeneous Functions

The potentials S, E, H, G, F and Ω are called *extensive*, which means they become larger in proportion to the size of their natural extensive variable (e.g., V or N) as the system they describe is scaled up, while maintaining a homogeneous density in any given sub-volume of that system ². We next illustrate the extensiveness and homogeneity property on some of the thermodynamic potentials and some interesting results that arise from these properties.

²It is noted that said "system" can be a homogenous material within a volume, or a phase within a volume containing multiple phases.

1.5.1 Helmholtz free energy

Consider a multi-component system. The Helmholtz free energy is generalized to $G(T, V, \{N_i\})$, where V is the volume of a system and $\{N_i\} \equiv \{N_1, N_2, \dots, N_n\}$ is the set of numbers of particles of each component indexed by the label i . Assume for the moment, we are just taking about a "black box" with homogenous properties within. Since G is an extensive quantity it should get larger as its volume and number of particles go to infinity. But since we said the system is homogeneous, the ratio of N_i/V should be fixed, otherwise the system would not remain homogeneous in particle density as it becomes larger. In that way, the "extensive" and "homogeneous" attributes can be simultaneously satisfied. This also implies that the Helmholtz free energy should be written as [5]

$$G(T, V, \{N_i\}) = Vg(T, \{n_i\}), \text{ where } \{n_i\} \equiv \left\{ \frac{N_1}{V}, \frac{N_2}{V}, \dots, \frac{N_m}{V} \right\} \quad (1.17)$$

where g is the Helmholtz free energy *density* of the system and $n_i = N_i/V$ is the density of the component i , where $i = 1, \dots, m$. Let's specialize this discussion to just two components for the moment to keep things simple. From the two-component version of Eq. (1.9) we have

$$p = - \left. \frac{\partial G}{\partial V} \right|_{T, N_A, N_B} = - \left. \frac{\partial}{\partial V} (Vg(T, n_A, n_B)) \right|_{T, n_A, n_B} = V \frac{N_A}{V^2} \frac{\partial g}{\partial n_A} + V \frac{N_B}{V^2} \frac{\partial g}{\partial n_B} - g \quad (1.18)$$

Eq. (1.18) leads to the well known relation between pressure, p , and the free energy density,

$$p = - \left(g - n_A \frac{\partial g}{\partial n_A} - n_B \frac{\partial g}{\partial n_B} \right) = - (g - n_A \mu_A - n_B \mu_B) \quad (1.19)$$

where

$$\mu_i \equiv \left. \frac{\partial G}{\partial N_i} \right|_{T, V, N_k \neq N_i} = \left. \frac{\partial g}{\partial n_i} \right|_{T, n_k \neq n_i} \quad (1.20)$$

is the definition of the chemical potential of species $i = \{A, B\}$, given here in terms of the Helmholtz free energy or in terms of the Helmholtz free energy density. Equation (1.20) also applicable to a system with m components.

It is often convenient to work with component number fractions, $c_i = N_i/N$, also called the *concentration* of component i . To do so, we express the overall system density by $\bar{\rho} = N_A/\nu_o$, with N_A being Avogadro's number and ν_o the *molar volume* (m^3/mole). In terms of these variables, the concentration can be written in several ways,

$$c_i = \frac{N_i}{N} = \frac{n_i}{\bar{\rho}} = \frac{\nu_o}{N_A} n_i \quad (1.21)$$

Through the variable transformation in Eq. (1.21), the free energy density g can be transformed to a function of the c_i , which we denote $\tilde{g}(T, \{c_i\})$, where $\{c_i\}$ is the set of component concentrations. By the chain rule, the right hand side of Eq. (1.20) then leads to

$$\tilde{\mu}_i = \left. \frac{\partial \tilde{g}}{\partial c_i} \right|_{T, c_k \neq c_i} \quad (1.22)$$

where $\tilde{\mu}_i = (N_A/\nu_o) \mu_i$ is defined as the chemical potential in units of joules/m³ (units of μ_i are joules/particle). It is noted that Eq. (1.22) tacitly assumes that the molar volume (or density) of the whole system remains fixed; this is a fairly good approximation, particularly for so-called *substitutional alloys* where the molar volume is set by the crystal lattice of the solvent.

1.5.1.1 Description in terms of solute concentration variables

It is often the case in the description of mixtures such as metal alloys that the thermodynamic potentials are written in terms of the concentrations of the so-called minority species or the *solutes*, while not explicitly referencing the concentration of the majority species, also called the *solvent*. To transform to this description, we begin by relating the individual particle number to the total number of particles in the system to N by

$$\sum_{i=1}^m N_i = N, \quad (1.23)$$

where m denotes the number of particle species (or components). In terms of component densities, Eq. (1.23) becomes

$$\sum_{i=1}^m n_i = \frac{N}{V} = \bar{\rho} = \frac{N_A}{\nu_o}, \quad (1.24)$$

Equation (1.23) can be used to eliminate one of the components in the description of the free energy. Here, we pick to eliminate the component N_m , where “ m ” denotes the index of the solvent, although the steps that follow will be true regardless of which concentration is eliminated. This implies we can describe the system through the free energy as

$$G_m(T, V, \{N_\alpha\}_{m-1}, N) = V g_m(T, \{n_\alpha\}_{m-1}, \bar{\rho}), \quad (1.25)$$

where the subscript m signifies that the component N_m has been eliminated from the free energy G in terms of N via Eq. (1.23) or n_m has been eliminated from g in terms of $\bar{\rho}$ via Eq. (1.24).

To proceed, we adapt the differential law in Eq. (1.9) to m components as

$$dG = -SdT - pdV + \sum_{i=1}^m \mu_i dN_i \quad (1.26)$$

We eliminate the dN_m term in the sum of Eq. (1.26) using

$$dN_m = dN - \sum_{i=1}^{m-1} dN_i \quad (1.27)$$

Using Eq. (1.27) to eliminate the last term of Eq. (1.26) yields the differential of G_m , i.e.,

$$dG_m = -SdT - pdV + \sum_{i=1}^{m-1} (\mu_i - \mu_m) dN_i + \mu_m dN, \quad (1.28)$$

from which is obtained

$$\left. \frac{\partial G_m}{\partial N_i} \right|_{T, V, N, N_k \neq N_i} = \mu_i - \mu_m \equiv \Delta\mu_i, \quad (1.29)$$

where it is implied that i spans the *solute* components $i = 1, \dots, m-1$ and k represents any component other than i . The difference $\Delta\mu_i$ is often referred to as the *inter-diffusion potential*.

To obtain $\Delta\mu_i$ in terms of g_m , we keep V (the volume of the whole system) fixed, and divide Eq. (1.28) by V , recalling that $G_m = V g_m$. This gives

$$dg_m = -s dT + \sum_{i=1}^{m-1} \Delta\mu_i dn_i + \mu_m d\bar{\rho} \quad (1.30)$$

where $s = S/V$ and $\bar{\rho} = 1/\nu_o$ is the total system density. From Eq. (1.30) is obtained

$$\frac{\partial g_m}{\partial n_i} \Big|_{T, \bar{\rho}, n_k \neq n_i} = \Delta \mu_i \quad (1.31)$$

We can further define $\tilde{g}_m(T, \{c_i\}_{m-1})$ as the free energy density g_m written in terms of species concentrations c_i . Using the relations $n_i = \bar{\rho}c_i$ and $\tilde{\mu} = (N_A/\nu_o)\mu_i$ then gives

$$\frac{\partial \tilde{g}_m}{\partial c_i} \Big|_{T, \nu_o, n_k \neq n_i} = \Delta \tilde{\mu}_i \quad (1.32)$$

The free energy $\tilde{g}_m(T, \{c_i\}_{m-1})$ and Eq. (1.32) are quite frequently used as descriptors of the thermodynamics of metallic alloys in the physical metallurgy literature. It is noted that Eq. (1.32) holds the total molar volume of the system fixed. This is a good approximation to assume holds in dilute mixtures and will be tacitly assumed hereafter.

1.5.2 Grand potential

We begin by extending the definition of the grand potential defined in Section (1.3.5) to m components,

$$\Omega = G - \sum_{i=1}^m \mu_i N_i \quad (1.33)$$

Using Eq. (1.26), the m -component analogue of Eq. (1.15) thus becomes

$$d\Omega = -SdT - pdV + \sum_{i=1}^m N_i d\mu_i, \quad (1.34)$$

from which we directly obtain

$$N_i = -\left. \frac{\partial \Omega}{\partial \mu_i} \right|_{T, V, \mu_k \neq \mu_i} \quad (1.35)$$

The extensiveness property applied to Ω becomes

$$\Omega(T, V, \{\mu_i\}) = V\omega(T, \{\mu_i\}), \quad (1.36)$$

where ω is the grand potential density and the notation $\{\mu_i\}$ represents the set of all component chemical potentials ³, each indexed by i . Equation (1.34) together with Eq. (1.36) give

$$\left. \frac{\partial \Omega}{\partial V} \right|_{T, \{\mu_i\}} = -p = \omega(T, \{\mu_i\}) = g - \sum_{i=1}^m n_i \mu_i, \quad (1.37)$$

where the right-most equality in Eq. (1.37) is obtained by dividing Eq. (1.33) by V . The analogue of Eq. (1.35) in terms of component densities is obtained by substituting Eq. (1.36) in Eq. (1.35), which leads to

$$n_i = -\left. \frac{\partial \omega}{\partial \mu_i} \right|_{T, \mu_k \neq \mu_i} \quad (1.38)$$

³Note that there the set of densities $\{n_i\}$ do not explicitly appear in descriptor $\omega(T, \{\mu_\alpha\})$ since in the grand potential ensemble, the densities are functions of the chemical potentials.

Equation (1.38) is equivalently derived by taking the derivative of ω in Eq. (1.37) with respect to μ_i and using the right-most equality in Eq. (1.20).

Equation (1.37) shows that the pressure is equal to the grand potential density. Since in thermal equilibrium the pressures of any two parts of a system are the same, this implies that the grand potential densities of any two parts of a system are also the same. This will be a valuable tool later for determining the conditions for the coexistence between two phases.

1.5.2.1 Description in terms of solute concentration variables

As in Section 1.5.1.1, we can write the grand potential in terms of the concentrations of the solute components of a material. We will again relate the individual particle numbers to the total number of particles N and use Eq. (1.23) to eliminate component N_m of the *solvent*. We begin by using Eq. (1.23) to eliminate N_m in the terms of Eq. (1.33), which gives

$$\Omega_m = G_m(T, \{n_\alpha\}_{m-1}, \bar{\rho}) - \sum_{i=1}^{m-1} N_i(\mu_i - \mu_m) - \mu_m N, \quad (1.39)$$

where, as above, the notation Ω_m indicates that we are expressing Ω using the free energy in which the N_m component has been replaced in terms of the other components, $i = 1, 2, \dots, m-1$. We next divide Ω_m by V , after re-expressing $G_m = Vg_m$ in Eq. (1.39). This gives

$$\omega_m = g_m(T, \{n_\alpha\}_{m-1}, \bar{\rho}) - \sum_{i=1}^{m-1} n_i(\mu_i - \mu_m) - \mu_m \bar{\rho}, \quad (1.40)$$

Taking the variation of ω_m in Eq. (1.40) gives

$$d\omega_m = dg_m(T, \{n_\alpha\}_{m-1}, \bar{\rho}) - \sum_{i=1}^{m-1} \Delta\mu_i dn_i - \mu_m d\bar{\rho} - \sum_{i=1}^{m-1} n_i \Delta\mu_i - \bar{\rho} d\mu_m, \quad (1.41)$$

where we have again used the shorthand notation $\Delta\mu_i \equiv \mu_i - \mu_m$. Substituting Eq. (1.30) for dg_m in Eq. (1.41) gives

$$d\omega_m = -sdT - \sum_{i=1}^{m-1} n_i d(\Delta\mu_i) - \bar{\rho} d\mu_m, \quad (1.42)$$

Keeping the chemical potential of the solvent atoms, μ_m , fixed, Eq. (1.42) gives

$$-n_i = \left. \frac{\partial \omega_m}{\partial (\Delta\mu_i)} \right|_{T, \mu_m, \Delta\mu_k \neq \Delta\tilde{\mu}_i} \quad (1.43)$$

Moreover, by rescaling the chemical potentials as $\Delta\tilde{\mu} = (N_A/\nu_o) \Delta\mu_i$, and recalling that $c_i = (\nu_o/N_a) n_i$, Eq. (1.43) can also be re-cast as

$$-c_i = \left. \frac{\partial \tilde{\omega}_m}{\partial (\Delta\tilde{\mu}_i)} \right|_{T, \mu_m, \Delta\tilde{\mu}_k \neq \Delta\tilde{\mu}_i} \quad (1.44)$$

where $\tilde{\omega}_m$ denotes the grand potential density ω_m expressed in terms of the $\Delta\tilde{\mu}_i$. It is noted that Eq. (1.44) holds the chemical potential $\tilde{\mu}_m$ of the solvent fixed. This is a good approximation to assume holds true for dilute mixtures and will be tacitly assumed hereafter. Equation (1.44) is important when developing a phase field models (or most theories of mixtures, actually) of alloys from a grand potential functional, where the free energy measured is in terms of solutes and the ‘chemical potential’ usually written as ‘ μ ’ in the literature tacitly assumes $\Delta\tilde{\mu}$.

1.5.3 Gibbs free energy

This section ends by applying the “extensiveness” property to the Gibbs free energy. The m -component analogue of Eq. (1.11) is given by

$$dF = -SdT + Vdp + \sum_{i=1}^m \mu_i dN_i, \quad (1.45)$$

where N_i denotes the total number of particles of component i . From Eq. (1.45) we directly obtain

$$\left. \frac{\partial F}{\partial N_i} \right|_{T,p,N_k \neq N_i} = \mu_i \quad (1.46)$$

The extensive form of the Gibbs free energy is written as

$$F(T, p, \{N_i\}) = N\tilde{f}(T, p, \{c_i\}) \text{ where } \{c_i\} \equiv \left\{ \frac{N_1}{N}, \frac{N_2}{N}, \dots, \frac{N_m}{N} \right\}, \quad (1.47)$$

where N is the total number of particles and c_i denote the concentration of particle species i , defined previously. If we fix the total number of particles in the system, N , and dividing Eq. (1.45) by N , we obtain

$$\left. \frac{\partial \tilde{f}}{\partial c_i} \right|_{T,p,c_k \neq c_i} = \mu_i \quad (1.48)$$

Equivalently, we can arrive at Eq. (1.48) by substituting $F = N\tilde{f}$ directly into the left-hand side of Eq. (1.46) and using the chain $dc_i/dN_i = 1/N$.

1.5.3.1 Description in terms of solute concentration variables

As with the Helmholtz and grand potentials, we can also represent the Gibbs free energy in terms of the solute concentrations of a system, removing explicit dependence of the solvent. Re-writing Eq. (1.23) in terms of concentrations (i.e., $c_i = N_i/N$) gives

$$\sum_{i=1}^m c_i = 1, \quad (1.49)$$

which implies that we can eliminate one of the component or concentration variables from F or \tilde{f} , respectively. This is often the solvent element in a mixture or alloy. As we have done previously, let us denote the solvent species by $i = m$. We thus can express F as

$$F_s(T, p, \{N_i\}_{m-1}, N) = Nf_s(T, p, \{c_i\}_{m-1}), \quad (1.50)$$

where here we use the notation F_s to denote that the solvent component N_m has been eliminated from the free energy F and f_s to denote that the solvent concentration c_m has been eliminated from \tilde{f} . Also, the notation $\{c_i\}_{m-1}$ denotes the subset of $\{c_i\}$ with c_m removed (analogously for the notation $\{N_i\}_{m-1}$). In physical metallurgy f_s is typically the free energy density of an alloy measured as a function of the solute concentrations in thermodynamic databases. Using the relation

$$dN_m = dN - \sum_{i=1}^{m-1} dN_i \quad (1.51)$$

to eliminate the m^{th} term in the sum of Eq. (1.45) yields

$$dF_s = SdT + Vdp + \sum_{i=1}^{m-1} (\mu_i - \mu_m) dN_i + \mu_m dN, \quad (1.52)$$

from which we directly obtain

$$\left. \frac{\partial F_s}{\partial N_i} \right|_{T,p,N,N_k \neq N_i} = \mu_i - \mu_m \equiv \Delta\mu_i \quad (1.53)$$

Keeping the total number of particles in the system (N) fixed, dividing Eq. (1.52) by N and using Eq. (1.50) gives

$$\left. \frac{\partial f_s}{\partial c_i} \right|_{T,p,c_k \neq c_i} = \mu_i - \mu_m = \Delta\mu_i \quad (1.54)$$

Equation (1.54) is a relation for $\Delta\mu_i \equiv \mu_i - \mu_m$, which is also sometimes called the *inter-diffusion potential* and measures the chemical potential of solute component i with respect to the solvent of the mixture or alloy. In some literature, $\Delta\mu_i$ is just referred to as the “chemical potential” of the mixture or phase, etc.

1.5.3.2 Alternate derivation of the inter-diffusion potential of a mixture

It is instructive to follow an alternate path for deriving $\Delta\mu_i$ in term of $f_s(T, p, \{c_i\}_{m-1})$, which is the free energy typically measured experimentally. For generality in this subsection, we will index the solute component by c_s rather than c_m as we did above. Doing so and applying the chain rule to F_s , which gives

$$\mu_i = \left. \frac{\partial F_s}{\partial N_i} \right|_{T,p,N_k \neq N_i} = N \sum_{\substack{\alpha=1 \\ \alpha \neq s}}^m \frac{\partial f_s}{\partial c_\alpha} \frac{\partial c_\alpha}{\partial N_i} + f_s \frac{\partial N}{\partial N_i}, \quad (1.55)$$

where μ_i is the chemical potential of the i^{th} component, which is assumed to be different from s . From the definition of $c_i = N_i/N$ and Eq. (1.23), we arrive at

$$\mu_i = f_s + (1 - c_i) \frac{\partial f_s}{\partial c_i} - \sum_{\substack{\alpha=1 \\ \alpha \neq s,i}}^m c_\alpha \frac{\partial f_s}{\partial c_\alpha}, \quad (1.56)$$

where the sum now excludes both eliminated component ($\alpha = s$) and the component $\alpha = i$. For the important special case of a two-component (binary) mixture, Eq. (1.56) gives

$$\mu_i = f_s + (1 - c_i) \frac{\partial f_s}{\partial c_i} \quad (1.57)$$

Note the difference in chemical potentials calculated via the Gibb's free energy versus that obtained via the Helmholtz free energy (Eq. (1.20)).

It is instructive to consider the important special case of a binary alloy, whose components are denoted $i = A, B$, where A is typically labelled the solvent and B the solute. Eq. (1.57) gives

$$\begin{aligned} \mu_B &= f_A(c_B) + (1 - c_B) \frac{\partial f_A(c_B)}{\partial c_B} \\ \mu_A &= f_B(c_A) + (1 - c_A) \frac{\partial f_B(c_A)}{\partial c_A} \end{aligned} \quad (1.58)$$

It is noted that $f_A(c_A) = f_B(c_B) = \tilde{f}(c_A, c_B)$. Moreover, since $c_A = 1 - c_B$, we have $\partial f_B / \partial c_A = -\partial f_A / \partial c_B$. As a result, the difference $\mu_B - \mu_A$ becomes

$$\mu_B - \mu_A = \frac{\partial f_A(c_B)}{\partial c_B} \quad (1.59)$$

which could also have been obtained directly from Eq. (1.54).

1.6 Intensive Variables

Intensive variables are thermodynamic descriptors of the state of the system that do not depend on the extent of the system, which we saw includes the total energy (E), entropy (S), free energy (F) etc, or the values of any extensive variables with which the system size scales (e.g., N and V). Another important property of intensive variables is that they are constant through a system in thermodynamic equilibrium. Here we illustrate three important intensive variables seen previously and which are the most commonly used thermodynamics state descriptors in materials science: the temperature T , pressure p and chemical potential μ .

We can illustrate intensive variables using a simple example of entropy extremization. Consider a thermally isolated system (i.e. one in which heat cannot enter or leave) partitioned into two subsystems occupying two physical regions in space. Variables associated with the two regions are denoted by subscripts "1" and "2", respectively. Imagine that the two regions are separated by an imaginary, movable, massless and frictionless divider, and which can interact thermally. Due to extensivity of the total entropy, internal energy, volume and number of particles, we have

$$\begin{aligned} N_{\text{tot}} &= N_1 + N_2 \\ V_{\text{tot}} &= V_1 + V_2 \\ E_{\text{tot}} &= E_1 + E_2 \\ S_{\text{tot}} &= S_1 + S_2 \end{aligned} \quad (1.60)$$

Since the system is isolated the totals on the left hand side of Eqs. (1.60) don't change, i.e. $\Delta E_{\text{tot}} = \Delta S_{\text{tot}} = \Delta N_{\text{tot}} = \Delta V_{\text{tot}} = 0$, and so

$$\begin{aligned} \Delta N_1 &= -\Delta N_2 = -\Delta \bar{N} \\ \Delta V_1 &= -\Delta V_2 = -\Delta \bar{V} \\ \Delta E_1 &= -\Delta E_2 = -\Delta \bar{E} \end{aligned} \quad (1.61)$$

Consider next a small change in total system entropy, written as via the corresponding changes of its sub-systems, i.e., $\Delta S_{\text{tot}} = \Delta S_1 + \Delta S_2$. Using Eq.(1.7) for each region (sub-system), let us write ΔS_{tot} in terms of the changes of internal energy, volume, and particle number of the sub-systems, each constrained by Eq. (1.61). This gives,

$$\Delta S_{\text{tot}} = \left(\frac{1}{T_1} - \frac{1}{T_2} \right) \Delta \bar{E} + \left(\frac{p_1}{T_1} - \frac{p_2}{T_2} \right) \Delta \bar{V} - \left(\frac{\mu_1}{T_1} - \frac{\mu_2}{T_2} \right) \Delta \bar{N} \quad (1.62)$$

For a system in equilibrium, $(\Delta S_{\text{tot}})_{E,V,N} = 0$ requires that ΔS_{tot} be a minimum with respect to each of $\bar{E}, \bar{V}, \bar{N}$, each of which act as an internal degree of freedom. This gives,

$$T_1 = T_2 \quad (1.63)$$

$$p_1 = p_2 \quad (1.64)$$

$$\mu_1 = \mu_2 \quad (1.65)$$

This, of course, is a well known result about the equality of pressure, temperature and chemical potentials between sub-systems in equilibrium with each other. Similar results can be obtained using other thermodynamic potentials. As mentioned above, temperature, pressure and chemical potential are known as *intensive variables* are independent of the extent of the system and are only a function of its thermodynamic state. On the other hand, extensive variables such as N_1, N_2, V_1, V_2 are internal to the system and depend on the extent of its sub-systems.

1.7 Equilibrium Phase Coexistence

One of the most powerful applications of thermodynamics is in the description of phase transformations. A phase transformation occurs when one phase of matter transforms into two or more phases. This occurs in certain regions of material's phase space. There are generally two types of phase transformations: first order and second order transformations. The latter are associated with a so-called critical point. A description of a system close to a critical point possesses certain universal properties that do not require an accurate description of the free energy to describe. Phase transformations across the critical point exhibit smooth derivatives of the thermodynamic potentials. Phase separation is spontaneously activated below the critical point and microstructure displays self-affine scaling in the characteristic length scale characterizing coexisting phases. Most phase transformations in metal alloys are first order. First order phase transformations exhibit discontinuous derivatives of thermodynamic potentials across the transition point, which signals a discontinuous change of order, latent heat release, etc. First order phase transitions also require nucleation to activate the growth of stable phases. Moreover, they do not exhibit length scaling near the phase transition transition point, but rather maintain atomically sharp interfaces that require complex *sharp-interface models* to describe the kinetics of inter-phase boundaries. This book has more to say about models and continuum theories that emulate such kinetic sharp interface models in the limit of first order transformations. Before we go there however, let us first use the thermodynamics concepts derived in this chapter to derive the equilibrium properties of coexisting phase that emerge in a phase transformation.

1.7.1 Pure materials

Consider first a pure material system that is in a state of coexistence of two phases, solid(s) and liquid(L). We wish to describe this coexistence in terms of thermodynamic variables. Specifically, these will be the density, temperature and pressure. To proceed, we require a thermodynamic potential of this system on which to apply the minimization procedure of the thermodynamic potentials discussed in Section (1.4). Assume the system as a whole occupies a volume V , has a total of N particles and is at a temperature T . Exploiting the assumed homogeneity of a phase and the corresponding extensivity of its free energy, Eq. (1.17) is used to write the total Helmholtz free energy of the system as

$$G(T, V, N) = V_s g_s(T, n_s) + V_L g_L(T, n_L), \quad (1.66)$$

where V_s is the volume of the solid, V_L the volume of the liquid, while $n_s \equiv N_s/V_s$ and $n_L \equiv N_L/V_L$ are the relative number densities of solid or liquid phases, respectively. The functions g_s/g_L are the Helmholtz free energy densities of a single homogeneous phase of solid/liquid, respectively. Note that V_L, V_s , are actually implicit functions of the internal variables n_L, n_s through the conservation laws $V_L + V_s = V, N_s + N_L = N$, which together imply

$$\begin{aligned} n_s \chi_s + n_L \chi_L &= n_o \\ \chi_L + \chi_s &= 1 \end{aligned} \quad (1.67)$$

where

$$\chi_s \equiv \frac{V_s}{V}, \quad \chi_L \equiv \frac{V_L}{V}, \quad n_o \equiv \frac{N}{V} \quad (1.68)$$

Solving Eqs. (1.67) yields

$$\begin{aligned} V_s &= \left(\frac{n_L - n_o}{n_L - n_s} \right) V \\ V_L &= \left(\frac{n_o - n_s}{n_L - n_s} \right) V, \end{aligned} \quad (1.69)$$

which constitutes a so-called *lever rule*. Substituting Equations (1.69) into Eq. (1.66) gives a unified free energy of the entire system of the form $G = Vg(T, n_o)$, where $n_o = N/V$.

Applying the extremum condition $(dG)_{T,V,N} = 0$ implies minimizing with respect to the *internal* densities n_s and n_L , while keeping V, N (or $N/V = n_o$) fixed. This yields

$$\begin{aligned} \frac{\partial}{\partial n_s} \{V_s g_s(T, n_s) + V_L g_L(T, n_L)\} &= V_s \frac{\partial g_s}{\partial n_s} + g_s \frac{\partial V_s}{\partial n_s} + g_L \frac{\partial V_L}{\partial n_s} = 0 \\ \frac{\partial}{\partial n_L} \{V_s g_s(T, n_s) + V_L g_L(T, n_L)\} &= V_L \frac{\partial g_L}{\partial n_L} + g_s \frac{\partial V_s}{\partial n_L} + g_L \frac{\partial V_L}{\partial n_L} = 0 \end{aligned} \quad (1.70)$$

Through the use of Eqs. (1.69) it is straightforward to arrive at

$$\begin{aligned} \frac{g_L - g_s}{n_L - n_s} &= \mu_s \\ \frac{g_L - g_s}{n_L - n_s} &= \mu_L, \end{aligned} \quad (1.71)$$

which implies that $\mu_s = \mu_L$, while from Eq. (1.20) we have,

$$\begin{aligned} \mu_s &\equiv \left. \frac{\partial g_s}{\partial n_s} \right|_T = \mu^{\text{eq}} \\ \mu_L &\equiv \left. \frac{\partial g_L}{\partial n_L} \right|_T = \mu^{\text{eq}}, \end{aligned} \quad (1.72)$$

where μ^{eq} is the equilibrium value of the chemical potential that coexisting phase must both equal, as we saw from Section (1.6). For each temperature Eqs. (1.71)-(1.72) can be solved to yield unique n_l , n_s and μ^{eq} or, equivalently, for a unique μ_{eq} and some n_o consistent with n_L and n_s .

1.7.1.1 Pressure at co-existence in a pure material

Another approach to obtain the previous results is to minimize the Helmholtz free energy analogously to how we minimized the entropy in Section (1.6). This will yield the well-known result that the chemical potential, temperature and pressure of coexisting phases must be equal in equilibrium. Then, using Eq. (1.19) for the pressure, we would arrive at

$$g_s - n_s \mu_s = g_L - n_L \mu_L = -p, \quad (1.73)$$

while the chemical potentials of the two phases must satisfy $\mu_s = \mu_L = \mu^{\text{eq}}$. This and Eq. (1.73) are identical to Eqs. (1.71)-(1.72).

Notice that Eqs. (1.71) and (1.72) actually comprise three distinct equations in three unknowns $\{n_s, n_L, \mu^{\text{eq}}\}$, all of which are functions of temperature T . For each T , $n_s(T)$ and $n_L(T)$ comprise the so-called *solidus* and *liquids* coexistence lines in the (n, T) space of the phase diagram of a pure material. Once we solve these equations for a given T , either of the equalities of Eq. (1.73) gives the coexistence pressure, from which we can obtain the phase coexistence line in the (T, P) space of the material.

1.7.2 Binay Alloys

An alloy is a mixture of different metal atoms or metal-based compounds. The simplest is a binary mixture, which comprises two types of atoms, species “A” and species “B”. We characterize a binary alloy by the ratio of $c = N_B/(N_A + N_B)$ where N_A is the number of A atoms and N_B the number of B atoms. Usually, species A is referred to as the solvent and B as the solute. Alloys can exist in different homogenous phases or can exist as two or more coexisting homogenous phases. Coexistence in the case of a binary alloy is trickier than in a pure material because one more degree of freedom, c , is introduced. A complete description of phase coexistence requires a four-dimensional phase diagram, with cuts in (T, p) , (n, T) , and (c, T) space. **Before launching into the math of this topic**, it is instructive to review an interesting theorem about coexistence in general.

1.7.2.1 Gibbs phase rule

Understanding phase coexistence in complex materials is made easier by considering the question of how many phases can coexist for a given set of thermodynamic variables, or alternatively, what minimum number of thermodynamic variables need to be specified in order to describe coexistence between a given number of phases. To determine this, we are guided by a concept called the *Gibbs Phase rule* [15]. This states that for a system in equilibrium, the number of degrees of freedom (i.e. free thermodynamic variables) f , the number of components (i.e. atomic species) n and the number of phases r are related by

$$f = n - r + 2 \quad (1.74)$$

So, for example, in a pure material ($n = 1$), Eq. (1.74) gives $f = 2$ for a single phase and $f = 1$ for two-phase coexistence. As an example, recall that for a pure material examined in Section (1.7.1), we only needed to specify one intensive variable, temperature T , and two-phase equilibrium can be achieved for some pressure p (or equivalently chemical potential μ) and a corresponding range of average densities n_o , thus yielding 2D phase coexistence at a point in (T, p) space or a region in (T, n_o) space. In an alloy there are 2 components ($n = 2$) and so two-phase coexistence can be completely described by specifying any $f = 2 - 2 + 2 = 2$ of the available thermodynamic variables of the system. Thus, if we specify the temperature T and pressure p in a binary mixture, 2-phase coexistence is defined by a point in (T, p, μ) space and/or a corresponding range of average concentrations c_o in (T, p, c_o) space, or alternatively in (T, p, n_o) space. It is noted that if c_o range has a finite extent, each endpoint of this range specifies the concentration of each of coexisting phases. Similarly for coexistence in (T, p, n_o) space. For details see Landau and Lifshitz volume on Statistical Physics [15].

1.7.2.2 Equilibrium conditions

To elucidate the conditions of the Gibbs phase rule with a concrete example, we consider here phase co-existence in a binary alloy, we begin with the results of Section (1.6) and equate expressions for chemical potential of each species and expressions for pressure between phases and make them constants of the system, i.e. *intensive variables*. This is expressed as

$$\begin{aligned} \mu_A^s(\rho_A^s, \rho_B^s) &= \mu_A^L(\rho_A^L, \rho_B^L) = \mu_A^{\text{eq}} \\ \mu_B^s(\rho_A^s, \rho_B^s) &= \mu_B^L(\rho_A^L, \rho_B^L) = \mu_B^{\text{eq}} \\ \omega_s(\rho_A^s, \rho_B^s) &= \omega_L(\rho_A^L, \rho_B^L) = p, \end{aligned} \quad (1.75)$$

where here ρ_I^J denotes the density (assumed here in [moles/m³]) of component $I (= A, B)$ in phase $J (= s, L)$ and

$$\mu_I^J(\rho_A^J, \rho_B^J) \equiv (\partial g_J(\rho_A^J, \rho_B^J)/\partial \rho_I^J)_{T, N} \quad (1.76)$$

denotes the chemical potential (assumed here in [J/mole]) of component I in phase J , with g_J being the Helmholtz free energy density [J/m^3]. Moreover,

$$\omega_J(\rho_A^J, \rho_B^J) = \sum_I \rho_I^J \mu_I^J(\rho_A^J, \rho_B^J) - g_J(\rho_A^J, \rho_B^J) \quad (1.77)$$

denotes the grand potential density, or pressure, of phase J . The right hand sides of Eqs. (1.75) are, respectively, the equilibrium chemical potentials of component A (μ_A^{eq}) and B (μ_B^{eq}) and the equilibrium pressure p of the system. **The notation used for derivatives in Eq. (1.76) (and elsewhere) is shorthand for**

$$\partial g_J(\rho_A^J, \rho_B^J) / \partial \rho_I^J \equiv \partial g_J(\rho_A, \rho_B) / \partial \rho_I|_{\rho_A=\rho_A^J, \rho_B=\rho_B^J}, \quad (1.78)$$

where the index $I = A, B$.

Equations (1.75) comprise six non-linear equations in eight unknowns,

$$(\rho_A^s, \rho_B^s, \rho_A^L, \rho_B^L, \mu_A^{\text{eq}}, \mu_B^{\text{eq}}, T, p) \quad (1.79)$$

The Gibbs phase rule requires that we fix two the degrees of freedom to completely specify phase co-existence between two alloy phases. This implies that we can fix, for example, T , p , and uniquely specify an equilibrium states of $\{\rho_A^s, \rho_B^s, \rho_A^L, \rho_B^L, \mu_A^{\text{eq}}, \mu_B^{\text{eq}}\}$.

For what follows, it will be useful to continue from Eqs. (1.75) written in a more explicit form,

$$\begin{aligned} \frac{\partial g_s(\rho_A^s, \rho_B^s)}{\partial \rho_A^s} &= \frac{\partial g_L(\rho_A^L, \rho_B^L)}{\partial \rho_A^L} = \mu_A^{\text{eq}} \\ \frac{\partial g_s(\rho_A^s, \rho_B^s)}{\partial \rho_B^s} &= \frac{\partial g_L(\rho_A^L, \rho_B^L)}{\partial \rho_B^L} = \mu_B^{\text{eq}} \\ \rho_A^s \frac{\partial g_s(\rho_A^s, \rho_B^s)}{\partial \rho_A^s} + \rho_B^s \frac{\partial g_s(\rho_A^s, \rho_B^s)}{\partial \rho_B^s} - g_s(\rho_A^s, \rho_B^s) &= \rho_A^L \frac{\partial g_L(\rho_A^L, \rho_B^L)}{\partial \rho_A^L} + \rho_B^L \frac{\partial g_L(\rho_A^L, \rho_B^L)}{\partial \rho_B^L} - g_L(\rho_A^L, \rho_B^L) = p \end{aligned} \quad (1.80)$$

1.7.2.3 Recasting equilibrium conditions in term of concentration and density

It is instructive to convert to variables that can typically used to describe metal alloys. This is done by transforming to *phase densities* and *phase concentration*,

$$\begin{aligned} \rho_J &= \rho_A^J + \rho_B^J, \quad J = s, L \\ c_J &= \frac{\rho_B^J}{\rho_A^J + \rho_B^J}, \quad J = s, L \end{aligned} \quad (1.81)$$

The mapping between new and old variables is given by

$$\begin{aligned} \rho_B^J &= \rho_J c_J, \quad J = s, L \\ \rho_A^J &= (1 - c_J) \rho_J, \quad J = s, L \end{aligned} \quad (1.82)$$

It will also be convenient in what follows to introduce a new variable,

$$\mu^{\text{eq}} \equiv \mu_B^{\text{eq}} - \mu_A^{\text{eq}}, \quad (1.83)$$

which was defined in Section (1.5.3) as the *inter-diffusion* potential.

To switch between variable representations via Eqs. (1.82), we introduce two new **free energy density** functions, $G_s(c_s, \rho_s)$ and $G_L(c_L, \rho_L)$, defined through

$$\begin{aligned} g_s(\rho_A^s, \rho_B^s) &\equiv G_s(c_s(\rho_A^s, \rho_B^s), \rho_s(\rho_A^s, \rho_B^s)) \\ g_L(\rho_A^L, \rho_B^L) &\equiv G_L(c_L(\rho_A^L, \rho_B^L), \rho_L(\rho_A^L, \rho_B^L)) \end{aligned} \quad (1.84)$$

In terms of G_s and G_L , and the chain rule, we derive

$$\begin{aligned} \frac{\partial g_s(\rho_A^s, \rho_B^s)}{\partial \rho_A^s} &= \underbrace{\frac{\partial G_s(c_s, \rho_s)}{\partial c_s}}_{-c_s/\rho_s} \underbrace{\frac{\partial c_s}{\partial \rho_A^s}}_{1} + \underbrace{\frac{\partial G_s(c_s, \rho_s)}{\partial \rho_s}}_{1} \underbrace{\frac{\partial \rho_s}{\partial \rho_A^s}}_{1} \\ \frac{\partial g_L(\rho_A^s, \rho_B^s)}{\partial \rho_A^L} &= \underbrace{\frac{\partial G_L(c_L, \rho_L)}{\partial c_L}}_{-c_L/\rho_L} \underbrace{\frac{\partial c_L}{\partial \rho_A^L}}_{1} + \underbrace{\frac{\partial G_L(c_L, \rho_L)}{\partial \rho_L}}_{1} \underbrace{\frac{\partial \rho_L}{\partial \rho_A^L}}_{1} \\ \frac{\partial g_s(\rho_A^s, \rho_B^s)}{\partial \rho_B^s} &= \underbrace{\frac{\partial G_s(c_s, \rho_s)}{\partial c_s}}_{(1-c_s)/\rho_s} \underbrace{\frac{\partial c_s}{\partial \rho_B^s}}_{1} + \underbrace{\frac{\partial G_s(c_s, \rho_s)}{\partial \rho_s}}_{1} \underbrace{\frac{\partial \rho_s}{\partial \rho_B^s}}_{1} \\ \frac{\partial g_L(\rho_A^s, \rho_B^s)}{\partial \rho_B^L} &= \underbrace{\frac{\partial G_L(c_L, \rho_L)}{\partial c_L}}_{(1-c_L)/\rho_L} \underbrace{\frac{\partial c_L}{\partial \rho_B^L}}_{1} + \underbrace{\frac{\partial G_L(c_L, \rho_L)}{\partial \rho_L}}_{1} \underbrace{\frac{\partial \rho_L}{\partial \rho_B^L}}_{1} \end{aligned} \quad (1.85)$$

Using Eqs. (1.85) and the above variable transformations, Eqs. (1.80) become

$$\frac{-c_s}{\rho_s} \frac{\partial G_s(c_s, \rho_s)}{\partial c_s} + \frac{\partial G_s(c_s, \rho_s)}{\partial \rho_s} = -\frac{-c_L}{\rho_L} \frac{\partial G_L(c_L, \rho_L)}{\partial c_L} + \frac{\partial G_L(c_L, \rho_L)}{\partial \rho_L} = \mu_A^{\text{eq}} \quad (1.86)$$

$$\frac{1-c_s}{\rho_s} \frac{\partial G_s(c_s, \rho_s)}{\partial c_s} + \frac{\partial G_s(c_s, \rho_s)}{\partial \rho_s} = \frac{1-c_L}{\rho_L} \frac{\partial G_L(c_L, \rho_L)}{\partial c_L} + \frac{\partial G_L(c_L, \rho_L)}{\partial \rho_L} = \mu_B^{\text{eq}} \quad (1.87)$$

$$\rho_s \frac{\partial G_s(c_s, \rho_s)}{\partial \rho_s} - G_s(\rho_s, c_s) = \rho_L \frac{\partial G_L(c_L, \rho_L)}{\partial \rho_L} - G_L(\rho_L, c_L) = p \quad (1.88)$$

The six equations that are generated from Eqs. (1.86)-(1.88) can now be, in principle, be solved for $\{\rho_s, \rho_L, c_s, c_L, \mu_A^{\text{eq}}, \mu_B^{\text{eq}}\}$, assuming T and p are specified. For future reference, it is noted that the last of Eq. (1.80) generates another equation,

$$(c_s \rho_s - c_L \rho_L) \mu^{\text{eq}} + (\rho_s - \rho_L) \mu_A^{\text{eq}} = -[G_L(c_L, \rho_L) - G_s(c_s, \rho_s)], \quad (1.89)$$

which is not independent of the set in Eqs. (1.86)-(1.88), but which will be useful for relating the inter-potential μ_E to the other variable of this system.

1.7.2.4 Final form of coexistence conditions in terms of concentration and density

In this subsection, Eqs. (1.86)-(1.89) will be further simplified by: (1) replacing μ_B^{eq} in favour of μ_E ; (2) explicitly solving out for μ_A^{eq} , thus reducing the set of coexistence conditions to five equations in the five unknowns $\{\rho_s, \rho_L, c_s, c_L, \mu^{\text{eq}}\}$, assuming, as always, that T and p are specified.

We begin by subtracting Eq. (1.87) from Eq. (1.86), which gives the following two new equations,

$$\begin{aligned} \frac{1}{\rho_s} \frac{\partial G_s(c_s, \rho_s)}{\partial c_s} &= \mu^{\text{eq}} \\ \frac{1}{\rho_L} \frac{\partial G_L(c_L, \rho_L)}{\partial c_L} &= \mu^{\text{eq}} \end{aligned} \quad (1.90)$$

Another new equation is obtained by re-arranging the first (i.e. the left side) equation in either of Eq. (1.86) or Eq. (1.87) (doesn't matter which), and substituting for the corresponding derivatives with respect to concentration by μ^{eq} using Eqs. (1.90). This yields

$$\frac{\partial G_L(c_L, \rho_L)}{\partial \rho_L} - \frac{\partial G_s(c_s, \rho_s)}{\partial \rho_s} = (c_L - c_s) \mu^{\text{eq}} \quad (1.91)$$

Finally, use the liquid and solid expressions for p in Eq. (1.88) to eliminate the derivatives with respect to solid and liquid density in Eq. (1.91), respectively, yielding

$$(c_L - c_s) \mu^{\text{eq}} - \left(\frac{1}{\rho_L} - \frac{1}{\rho_s} \right) p = \frac{G_L(\rho_L, c_L)}{\rho_L} - \frac{G_s(\rho_s, c_s)}{\rho_s} \quad (1.92)$$

(Alternatively, Eq. (1.92) could have been derived as follows. Replace μ_A^{eq} in Eq. (1.89) by the leftmost expression of μ_A^{eq} in Eq. (1.86), and use the first of Eqs. (1.90) to eliminate the derivative with respect to solid concentration (c_s) by μ^{eq} . This yields

$$\rho_L (c_L - c_s) \mu^{\text{eq}} + (\rho_L - \rho_s) \frac{\partial G_s}{\partial \rho_s} = G_L(\rho_L, c_L) - G_s(\rho_s, c_s) \quad (1.93)$$

Eq. (1.92) is then obtained by substituting the solid expression for p from Eq. (1.88) into Eq. (1.93)).

The final system of coexistence equations used hereafter is found by collecting the two equations in Eq. (1.90), Eq. (1.92), and the two pressure equations in Eq. (1.88). These are collected here again for convenience and future reference,

$$\begin{aligned} \frac{1}{\rho_s} \frac{\partial G_s(c_s, \rho_s)}{\partial c_s} &= \mu^{\text{eq}} \\ \frac{1}{\rho_L} \frac{\partial G_L(c_L, \rho_L)}{\partial c_L} &= \mu^{\text{eq}} \\ \rho_s \frac{\partial G_s(c_s, \rho_s)}{\partial \rho_s} - G_s(c_s, \rho_s) &= p \\ \rho_L \frac{\partial G_L(c_L, \rho_L)}{\partial \rho_L} - G_L(c_L, \rho_L) &= p \\ \frac{G_L(c_L, \rho_L)}{\rho_L} - \frac{G_s(c_s, \rho_s)}{\rho_s} &= (c_L - c_s) \mu^{\text{eq}} - \left(\frac{1}{\rho_L} - \frac{1}{\rho_s} \right) p, \end{aligned} \quad (1.94)$$

Equations (1.94) are supplemented with the additional equation that gives μ_A^{eq} one the other equilibrium states are known, i.e.,

$$\mu_A^{\text{eq}} = \{p + G_s(c_s, \rho_s)\} / \rho_s - c_s \mu^{\text{eq}}, \quad (1.95)$$

which is just the explicit solution of μ_A^{eq} . With p specified, Eqs. (1.94) comprise five equations for the five variables ($c_s, c_L, \rho_s, \rho_L, \mu^{\text{eq}}$). It might appear that T is not in the problem but it is buried implicitly in the setting of G_s , G_L , the forms of which vary with T .

1.7.2.5 Recasting equilibrium conditions in terms of molar free energies

In the metallurgical literature (where most experiments on metallic alloys are reported), free energy is often quoted in units of J/mole not J/m^3 . Moreover, it is typical to speak of *molar volumes* of a phase rather than density. Molar volume has units of m^3/mole , the inverse of a density. Equations (1.94) are

significantly simplified -and made more intuitive- by switching to molar volumes and molar energies. Specifically we define

$$\nu_J \equiv \frac{1}{\rho_J}, \quad J = s, L \quad (1.96)$$

$$\mathcal{G}_J(\nu_J, c_J) \equiv \frac{G_J}{\rho_J} = \nu_J G_J(1/\nu_J, c_J), \quad J = s, L \quad (1.97)$$

where $[\mathcal{G}_{s,L}] = J/mole$ and $[\nu_{s,L}] = m^3/mole$. In terms of \mathcal{G} and ν , Eqs. (1.94) simplify to

$$\begin{aligned} \frac{\partial \mathcal{G}_s(c_s, \nu_s)}{\partial c_s} &= \mu^{\text{eq}} \\ \frac{\partial \mathcal{G}_L(c_L, \nu_L)}{\partial c_L} &= \mu^{\text{eq}} \\ \frac{\partial \mathcal{G}_s(c_s, \nu_s)}{\partial \nu_s} &= -p \\ \frac{\partial \mathcal{G}_L(c_L, \nu_L)}{\partial \nu_L} &= -p \\ \mathcal{G}_L(c_L, \nu_L) - \mathcal{G}_s(c_s, \nu_s) &= (c_L - c_s) \mu^{\text{eq}} - (\nu_L - \nu_s) p, \end{aligned} \quad (1.98)$$

The third and fourth of Eqs. (1.98) are obtained from the third and fourth of Eqs. (1.94) by noting that $\rho_J \partial G_J / \partial \rho_J - G_J = \rho_J^2 \partial \mathcal{G}_J / \partial \rho_J$ and that $\partial \nu_J / \partial \rho_J = -1/\rho_J^2$.

The system of Eqs. (1.98) are easy to intuit. They define a plane as a function of molar volume and concentration (ν, c) that is simultaneously tangent to the free energy functions \mathcal{G}_s and \mathcal{G}_L at the co-ordinates (ν_s, c_s) and (ν_L, c_L) . The projection of line between (ν_s, c_s) and (ν_L, c_L) onto the $\nu = 0$ plane has slope μ_E , while on the $c = 0$ plane is equal to p . **Equations (1.98) comprise a common tangent plane construction**, the 3D analogue of the more commonly known *common plane* construction when we consider concentration as the only relevant variable -as is typically done in most materials science books.

1.7.2.6 Dimensionless representation

The system of equations in Eqs. (1.94) can be re-written as a function of the following dimensionless variables:

$$\bar{G}_{s,L} \equiv \frac{G_{s,L}}{RT\rho_o}, \quad \bar{\mu}^{\text{eq}} \equiv \frac{\mu^{\text{eq}}}{RT}, \quad \bar{p} \equiv \frac{p}{RT\rho_o}, \quad \bar{\rho}_{s,L} \equiv \frac{\rho_{s,L}}{\rho_o}, \quad (1.99)$$

where ρ_o is a reference density and R is the natural gas constant. These units are convenient to make contact with those used in some phase field crystal models (studied later in the course), where density is scaled by a reference density ρ_o of the liquid phase at coexistence at some (T, p) , and the free energy density is made dimensionless by scaling by the energy density $RT\rho_o$. In these units, Eqs. (1.94)

become

$$\begin{aligned}
\frac{1}{\bar{\rho}_s} \frac{\partial \bar{G}_s(c_s, \bar{\rho}_s)}{\partial c_s} &= \bar{\mu}^{\text{eq}} \\
\frac{1}{\bar{\rho}_L} \frac{\partial \bar{G}_L(c_L, \bar{\rho}_L)}{\partial c_L} &= \bar{\mu}^{\text{eq}} \\
\bar{\rho}_s \frac{\partial \bar{G}_s(c_s, \bar{\rho}_s)}{\partial \bar{\rho}_s} - \bar{G}_s(c_s, \bar{\rho}_s) &= \bar{p} \\
\bar{\rho}_L \frac{\partial \bar{G}_L(c_L, \bar{\rho}_L)}{\partial \bar{\rho}_L} - \bar{G}_L(c_L, \bar{\rho}_L) &= \bar{p} \\
\frac{\bar{G}_L(c_L, \bar{\rho}_L)}{\bar{\rho}_L} - \frac{\bar{G}_s(c_s, \bar{\rho}_s)}{\bar{\rho}_s} &= (c_L - c_s) \bar{\mu}^{\text{eq}} + \left(\frac{1}{\bar{\rho}_s} - \frac{1}{\bar{\rho}_L} \right) \bar{p},
\end{aligned} \tag{1.100}$$

Another convenient scaling of Eqs. (1.98) is in terms of molar quantities, which has units of $m^3/mole$. Let ν_o denote a reference molar volume of the liquid, and define

$$\bar{\mathcal{G}}_{s,L} \equiv \frac{\nu_o \mathcal{G}_{s,L}}{RT}, \quad \bar{\mu}^{\text{eq}} \equiv \frac{\mu^{\text{eq}}}{RT}, \quad \bar{p} \equiv \frac{\nu_o p}{RT}, \quad \bar{\nu}_{s,L} \equiv \frac{\nu_{s,L}}{\nu_o} \tag{1.101}$$

With these re-scalings, Eqs. (1.98) become

$$\begin{aligned}
\frac{\partial \bar{\mathcal{G}}_s(c_s, \bar{\nu}_s)}{\partial c_s} &= \bar{\mu}^{\text{eq}} \\
\frac{\partial \bar{\mathcal{G}}_L(c_L, \bar{\nu}_L)}{\partial c_L} &= \bar{\mu}^{\text{eq}} \\
\frac{\partial \bar{\mathcal{G}}_s(c_s, \bar{\nu}_s)}{\partial \bar{\nu}_s} &= -\bar{p} \\
\frac{\partial \bar{\mathcal{G}}_L(c_L, \bar{\nu}_L)}{\partial \bar{\nu}_L} &= -\bar{p} \\
\bar{\mathcal{G}}_L(c_L, \bar{\nu}_L) - \bar{\mathcal{G}}_s(c_s, \bar{\nu}_s) &= (c_L - c_s) \bar{\mu}^{\text{eq}} - (\bar{\nu}_L - \bar{\nu}_s) \bar{p},
\end{aligned} \tag{1.102}$$

1.7.2.7 Special case of equal densities

For the special case where the solid and liquid densities are equal and set to the reference alloy density, i.e. $\nu_L = \nu_s$, the number of unknowns reduces to $(c_s, c_L, \mu^{\text{eq}})$. These three parameters are found by solving the first two and last of Eqs. (1.98),

$$\begin{aligned}
\frac{\partial \mathcal{G}_s(c_s)}{\partial c_s} &= \mu^{\text{eq}} \\
\frac{\partial \mathcal{G}_L(c_L)}{\partial c_L} &= \mu^{\text{eq}} \\
\mathcal{G}_L(c_L) - \mathcal{G}_s(c_s) &= (c_L - c_s) \mu^{\text{eq}}
\end{aligned} \tag{1.103}$$

Equations (1.103) comprise the usual common tangent construction. The pressure is specified via either of the third or fourth of Eq. (1.98), if the free energy is known as a function of the molar volume (or density).

Chapter 2

Nucleation

This chapter discusses the kinetics of nucleation. We do so in the context of solidification, although the discussion is general enough to easily be extended to nucleation in other first order phase transitions. The first section of this chapter follows closely the approach of Landau and Lifshitz [18]. The second section follows the paper of James E. McDonald [21]. As the primary focus of this chapter be the physics of nucleation rate theory, we will consider pure substances to keep the algebra to a minimum. The last part of the chapter adapts the nucleation rate theory derived for a pure material to binary mixtures.

2.1 Fokker Plank Equation: Evolution of Nuclei in Size Space

During a first order phase transition, a meta-stable liquid transforms, given enough time, to a more stable solid state. This is initiated by a process of *nucleation*, whereby an embryo of solid of a critical size large enough to overcome the energy barrier imposed by surface energy begone to grow. Throughout the nucleation process (from the quench to meta-stability to the growth of the first stable solid), there is a distribution function that governs the probability of a nucleus of any size. This distribution is peaked at small nucleus sizes at early time, but broadens to include all sizes after a period known as an "incubation time" wherein meta-stable fluctuations allow nuclei to grow progressively larger, until their size surpasses the aforementioned critical nucleus size. We denote this function by $f(a, t)$ and note that $f(a, t) da$ gives the probability per volume of finding a nucleus between the size ranges a and $a + da$. Since nucleation growth and dissolution in the melt is governed by stochastic processes of atoms sticking to or detaching from a nucleus, the evolution of $f(a, t)$ is governed by a Fokker-Plank equation given by,

$$\frac{\partial f(a, t)}{\partial t} = -\frac{\partial}{\partial a} \left(A f(a, t) - B \frac{\partial f(a, t)}{\partial a} \right), \quad (2.1)$$

where both A and B are in general functions of size "a". The Fokker-Plank equation can be written as

$$\frac{\partial f(a, t)}{\partial t} = -\frac{\partial J(a, t)}{\partial a} \quad (2.2)$$

where

$$J = A f(a, t) - B \frac{\partial f(a, t)}{\partial a} \quad (2.3)$$

Is the flux of nuclei in size space. The units of J are $\#/m^3/s$ (number of nuclei per volume per second that pass through size "a"), while the units of f are $\#/m^4$.

The functional relationship between the A and B parameters can be found by considering what happens in equilibrium. In that situation the $J = 0$ since nuclei simply fluctuate into and out of existence over some fluctuation time scale since both solid and liquid can coexist at equilibrium. In this situation, statistical mechanics informs us that for small values of a the distribution of nuclei is given by

$$f_o(a) \propto e^{-\frac{R_{\min}(a)}{k_B T}}, \quad (2.4)$$

where

$$R_{\min}(a) = -\frac{8\pi\gamma}{3a_{cr}}a^3 + 4\pi\gamma a^2 \quad (2.5)$$

is the familiar work of forming a nucleus of size “ a ” ¹. Here, γ is the surface energy of a solid-liquid interface and a_{cr} is the critical size of nucleus referred to above ². Substituting Equation (2.4) into Eq. (2.3), with $J = 0$, gives

$$A = -\frac{B}{k_B T} R'_{\min}(a) \quad (2.6)$$

where $R'_{\min}(a)$ in Eq. (2.6) denotes differentiation with respect to a .

It is instructive to consider $R_{\min}(a)$ a little deeper to facilitate the calculations that follow. It contains two terms, the first being the change of bulk (i.e. volumetric) free energy in transforming a spherical liquid of radius a to solid nucleus of the same radius, while the second term is the surface energy of maintaining an interface between said nucleus and the liquid. The quadratic (surface) term dominates at low sizes, while the cubic (volumetric) term dominates at large sizes. Figure (2.1) shows a plot of $R_{\min}(a/a_{cr})$ as a function of size a/a_{cr} , showing a maximum where the aforementioned effects cross over. This defines the maximum radius $a = a_{cr}$. To make some of the algebra that follows tractable, we will be using the second order expansion of $R_{\min}(a)$ around $a = a_{cr}$, given by

$$R_{\min}(a) \approx \frac{4}{3}\pi\gamma a_{cr}^3 - 4\pi(a - a_{cr})^2 \quad (2.7)$$

This approximation of $R_{\min}(a)$ is shown superimposed on top $R_{\min}(a)$ in Fig. (2.1).

Very rapidly following a quench to a meta-stable [liquid] state, a steady state is attained, whereby the flux J approaches a constant; this means that the flux of nuclei from smaller to larger sizes is constant across all sizes (up to an upper value we’ll discuss later). Denoting this steady state flux by $J = s$, gives

$$s = A f(a, t) - B \frac{\partial f(a, t)}{\partial a} = \text{constant} \quad (2.8)$$

We will see later that A will be seen later to play a role of a nuclear “velocity” coefficient, and B a nuclear “diffusion” coefficient. At sizes below the critical (stable) size, nuclei appear at larger sizes through diffusive fluctuations in size space controlled by the second term in Eq. (2.8), while for sizes above the critical size threshold, nuclei appear predominantly through the constant forward growth rate of those post-critical nuclei that have managed to grow past $a = a_{cr}$ (again, up to some maximum size that where a grain can still be called a nucleus). More on this later. Right now, let us explore the properties of Eq. (2.8) with the aim of working out a tractable expression for s .

¹The work of formation is defined as the change of free energy required to change required to a spherical volume of radius a from liquid to solid. This is given by $R_{\min}(a) = (4\pi a^3/3)\Delta G + (4\pi a^2)\gamma$, where ΔG is the exothermic enthalpy of formation of a solid and γ is the solid-liquid surface energy. The critical nucleus is found by the extremum of $R_{\min}(a)$, which is straightforward to do and gives $a_{cr} = -2\gamma/\Delta G$. Substituting $\Delta G = -2\gamma/a_{cr}$ into $R_{\min}(a)$ gives Eq. (2.5).

²The normalization of Eq. (2.4) is given by $a_{cr}^2 \rho_s \rho_L$ [18], where ρ_s and ρ_L are the densities of the solid and liquid, respectivley. This expression will be deduced later when we consider nucleation from a more microscopic perspective.

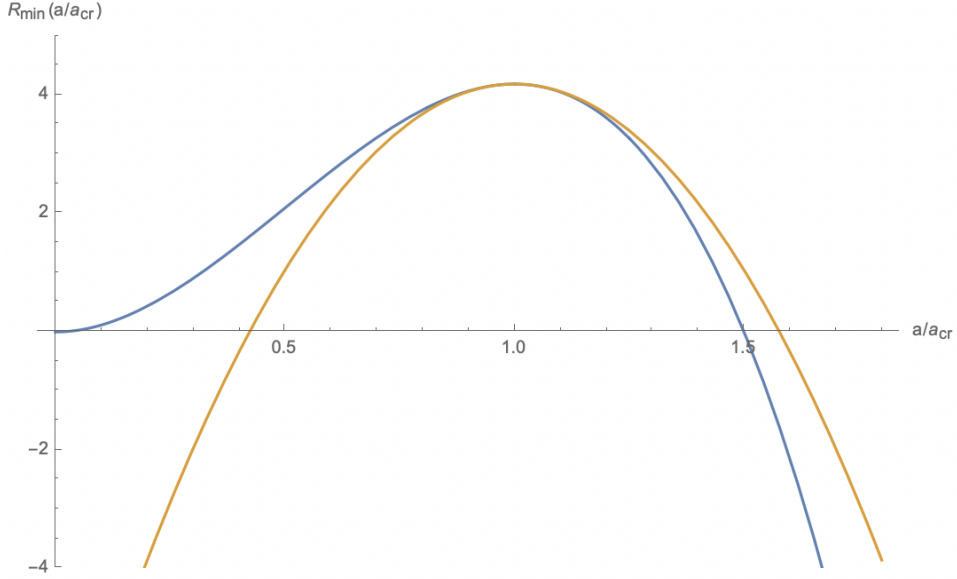


Figure 2.1: Blue curve: work of formation of a nucleus $R_{\min}(a/a_{\text{cr}})$ versus of size a/a_{cr} . Orange curve: expansion of $R_{\min}(a)$ around the critical nucleus size.

To proceed further, Eq. (2.4) can be used to give $df_o/da = - \left(R'_{\min}(a)/k_B T \right) f_o$, which allows us to re-write Eq. (2.8) for s as

$$-B f_o \frac{\partial}{\partial a} \left(\frac{f(a)}{f_o(a)} \right) = s \quad (2.9)$$

Integrating Eq. (2.9) gives

$$\frac{f(a)}{f_o(a)} = -s \int^a \frac{da'}{B f_o(a')} + D \quad (2.10)$$

The constant D can be found by imposing sensible boundary conditions on the nuclear distribution $f(a)$. In particular, we expect that even for $T < T_m$ (T_m is the melting temperature), the size distribution $f(a, t)$ should give similar statistics to the equilibrium distribution $f_o(a)$ at small a , since nuclei appearing and disappearing in this regime resemble equilibrium-like fluctuations of a metastable liquid. Mathematically, this is expressed as

$$f/f_o \rightarrow 1, \text{ as } a \rightarrow 0 \quad (2.11)$$

On the other end of the size spectrum, we clearly do not expect that the number density of nuclei at sizes larger than the critical size $a = a_{\text{cr}}$ can be given by $f_o(a)$. This can be seen quite clearly in Fig. (2.2) which plots the equilibrium size distribution in Eq. (2.4), using Eq. (2.5). While $f_o(a)$ makes perfect sense at small values of a/a_{cr} , it is nonsense in the range $a > a_{\text{cr}}$, as we certainly do not expect an ever-increasing probability of large nuclei to somehow emerge as $a \gg a_{\text{cr}}$. Indeed, this is precisely because the steady state nucleus size distribution we seek, $f(a)$, describes a *non-equilibrium* situation, where the number density of nuclei emergent in the liquid beyond $a = a_{\text{cr}}$ does not follow equilibrium fluctuation theory. Indeed, in this range the *predominant* mechanism for nuclei to appear at sizes larger than $a = a_{\text{cr}}$ is through the steady forward growth of the *small* number of “lucky”, or so-called *post-critical*, nuclei that have managed to grow, through random fluctuations, through

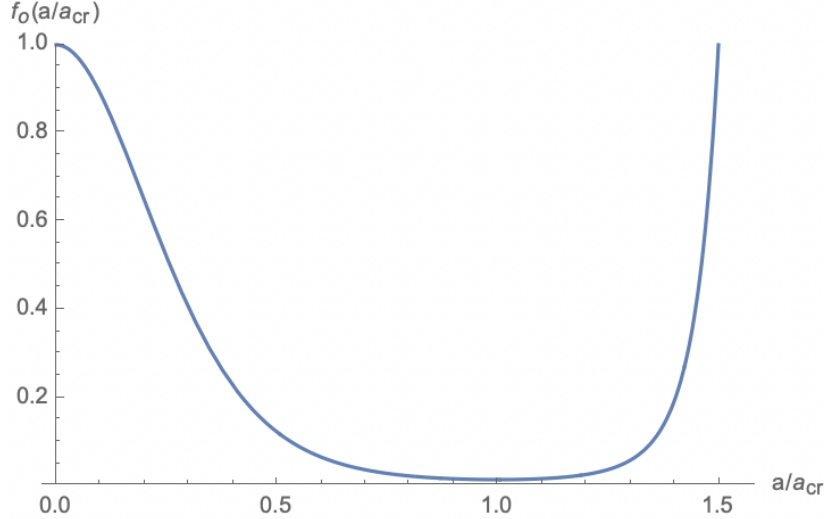


Figure 2.2: Plot of the equilibrium nucleus size distribution $f_o(a)$ as a function of size a . The normalization constant has been set to one.

the size $a = a_{\text{cr}}$. These considerations imply that $f/f_o \ll 1$, for $a > a_{\text{cr}}$. This condition is most practically satisfied by setting the large-size boundary condition of $f(a)$ to

$$f(a)/f_o(a) \rightarrow 0, \text{ as } a/a_{\text{cr}} \rightarrow \infty \quad (2.12)$$

Applying the boundary conditions Eq. (2.11) and Eq. (2.12) to Eq. (2.10) gives a closed form for the nuclear size distribution under state conditions, i.e.,

$$\frac{f(a)}{f_o(a)} = s \int_a^\infty \frac{da'}{B f_o(a')} \quad (2.13)$$

with s (the steady state flux of nuclei in the direction of increasing size) given by

$$s = \left\{ \int_0^\infty \frac{da'}{B f_o(a')} \right\}^{-1} \quad (2.14)$$

As a reminder, it is recalled that the steady state flux has units of nuclei per unit volume per unit time, i.e., $[s] = \#/(m^3 s)$.

An explicit form for s can be approximated by replacing $R_{\min}(a)$ in f_o by its expanded form in Eq. (2.7). The difference is small as shown in Fig. (2.3). This approximation simplifies Eq. (2.14) to the more tractable –and illuminating– form of a Gaussian integral, i.e.,

$$s = f_o(a_{\text{cr}}) \left\{ \int_0^\infty \frac{e^{-\frac{4\pi\gamma(a'-a_{\text{cr}})^2}{k_B T}}}{B} da' \right\}^{-1} \quad (2.15)$$

Since the $1/f_o(a)$ decays exponentially, it is reasonable to approximate the [as yet unknown] function $B(a)$ in the integrand of Eq. (2.15) as a constant, $B(a) \approx B(a_{\text{cr}})$, which can then be removed out of

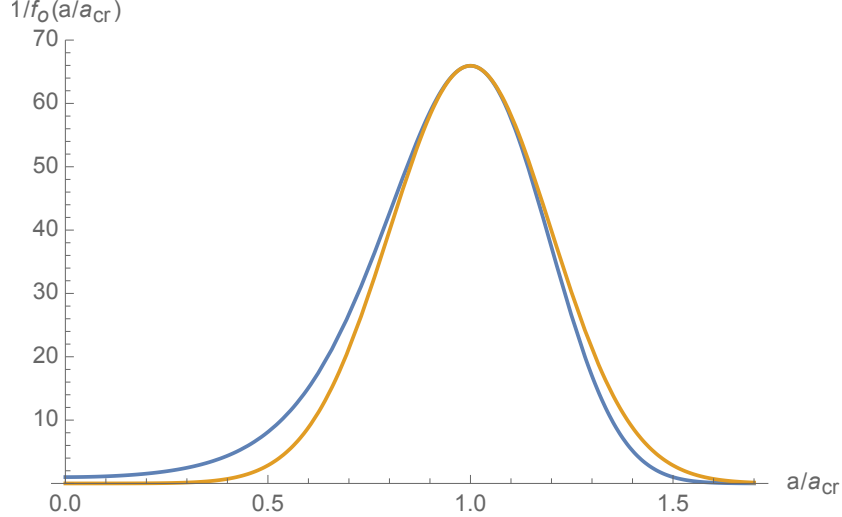


Figure 2.3: Comparison of the inverse of equilibrium nucleus size distribution, $1/f_o(a)$ using $R_{\min}(a)$ in Eq. (2.5)(Blue) and its expansion in Eq. (2.7) (orange). For simplicity, γ and $k_B T$ have been set to one.

the integral in Eq. (2.15). This then gives

$$s = f_o(a_{\text{cr}}) B(a_{\text{cr}}) \left\{ \int_0^\infty e^{-\frac{4\pi\gamma(a'-a_{\text{cr}})^2}{k_B T}} da' \right\}^{-1} \quad (2.16)$$

Making a change of variables in Eq. (2.16) from a' to $\eta = a' - a_{\text{cr}}$ gives

$$\int_0^\infty e^{-\frac{4\pi\gamma(a'-a_{\text{cr}})^2}{k_B T}} da' = \int_{-a_{\text{cr}}}^\infty e^{-\frac{4\pi\gamma\eta^2}{k_B T}} d\eta \approx \int_{-\infty}^\infty e^{-\frac{4\pi\gamma\eta^2}{k_B T}} d\eta = \sqrt{\frac{k_B T}{4\gamma}}, \quad (2.17)$$

We can thus finally approximate the steady state flux of nuclear sizes, s , by

$$s = 2\sqrt{\frac{\gamma}{k_B T}} f_o(a_{\text{cr}}) B(a_{\text{cr}}) \quad (2.18)$$

Figure (2.4) shows a plot of $f(a/a_{\text{cr}})/f_o(a_{\text{cr}})$ using Eq. (2.13) with s given by Eq. (2.18), where the approximation $B \approx B(a_{\text{cr}})$ has been made in the integrand of Eq. (2.13), and where we have set $\gamma/k_B T = 1$ for convenience.

It is noteworthy that Eq. (2.8) shows that a steady state flux s that is constant at all sizes (up to some size beyond $a = a_{\text{cr}}$) and can also be represented at any size a as a sum of two contributions, $f(a)$ and its derivative, weighted by the constants A and B , respectively. Figure (2.4) shows that for $a < a_{\text{cr}}$, both terms can generally contribute to the flux. However, for $a > a_{\text{cr}}$, the derivative of $f(a)$ becomes negligible compared to the $f(a)$ itself and the flux is represented at any general value of a as

$$s \approx A(a)f(a), \quad (2.19)$$

This can also be seen by the following argument: The derivative term in the flux J in Eq. (2.3) is akin to a diffusive term in size space, i.e. it represents random, diffusive-type, jumps in size space

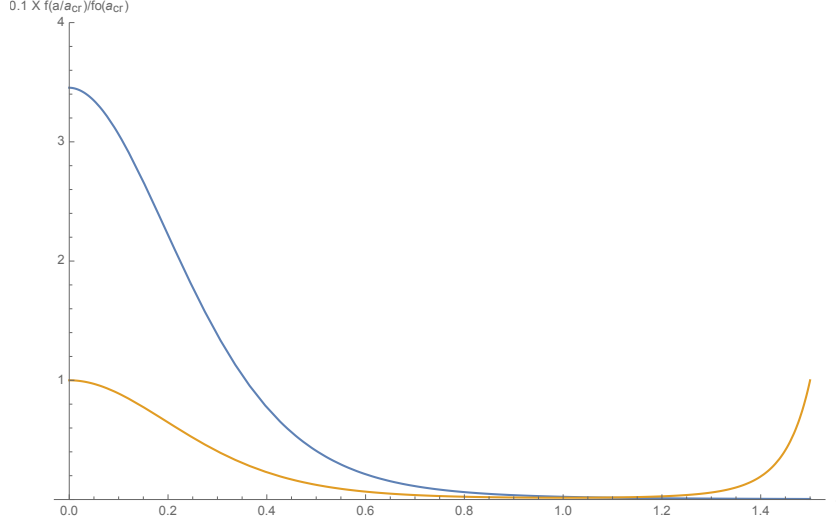


Figure 2.4: Comparison of the nuclear size distribution $f(a/a_{\text{cr}})/f_o(a/a_{\text{cr}})$ in Eq. (2.13) with $B = 1$ (blue) and the equilibrium nucleus size distribution, $f_o(a/a_{\text{cr}})$ (orange). The distribution f/f_o has been scaled by a factor of 1/10 to make the two plots visible on the same axes, and the normalization in f_o has been set to one.

that ‘‘ride down’’ the gradient of $f(a)$. However, for $a > a_{\text{cr}}$, very few nuclei jump from $a \longleftrightarrow a + \delta a$ through such random diffusive jumps in size. Indeed, nuclei appear in this regime due to the constant forward growth rate of a few post-critical nuclei (i.e. crystals), a very different mechanism. We can thus neglect the derivative term in J , leading to form of s given by Eq. (2.19). Comparing the units of f ($1/m^4$) and the units of flux ($1/m^2 s$), we can deduce that A has units of velocity, which suggests that $A(a)$ corresponds to the growth rate of stable crystals, which is typically found to scale in proportion to the their size according $A(a) \propto (a - a_{\text{cr}})$. It is noted that while A increases with a , its multiplication by a decreasing number density $f(a)$ can still maintain s constant, at least up to some size $a^* > a_{\text{cr}}$ where it even makes sense to speak of ‘‘nuclei’’³.

2.1.1 Determination of mesoscale coefficients A and B in the size flux

Equation (2.18) gives an explicit form for computing the steady state diffusion rate. But to do so, we first need a form for $B(a_{\text{cr}})$. It turns out that the is a quantity that can be calculated from mesoscale models of the growth of post-critical particles, which we can tackle with mean field arguments or computer simulation, without needing to explicitly resort to microscopic considerations. This is discussed further in this sub-section.

Calculating $R'_{\min}(a)$ and substituting it back into Eq. (2.6) gives

$$B(a) = \frac{k_B T}{8\pi\gamma} \frac{A(a)}{(a - a_{\text{cr}})} \quad (2.20)$$

³This argument tacitly assumes that $f(a)$ represents *only* the decreasing density of nuclei that grow through diffusive fluctuations in size space up to some maximum size $a^* > a_{\text{cr}}$, which most theories of nucleation leave unspecified, and after which they generally set $f(a > a^*) = 0$. Practically, the distribution $f(a)$ can be approximated as a small, but finite, constant for the size range $a_{\text{cr}} < a < a^*$, to reflect the fact that there is a constant number of nuclei in any given volume (in a system of infinite size) since there is a constant number per volume/time passing $a = a_{\text{cr}}$ and vanishing beyond $a = a^*$, under steady state nucleation conditions.

We next assume that the “nuclear velocity” coefficient $A(a)$ can be deduced analytically or computationally from models that can track the growth rate of crystal size, ie. $da(t)/dt$, through the form

$$A(a) = \frac{da(t)}{dt} \approx g(a_{\text{cr}})(a - a_{\text{cr}}), \text{ as } a \rightarrow a_{\text{cr}} \quad (2.21)$$

where the proportionality constant $g(a_{\text{cr}})$ is added to create a concrete place holder for a quantity to be computed from some kinetic growth model of a process of interest. Substituting this form of $A(a)$ into Eq. (2.20) gives

$$B(a_{\text{cr}}) = \frac{k_B T}{8\pi\gamma} g(a_{\text{cr}}) \quad (2.22)$$

In the case of vapour nucleation, $B(a_{\text{cr}})$ can be calculated by considering the hydrodynamics of vapour growth. In the case of nucleation from solid-phase (i.e solid-state precipitate) or solidification, nucleation, we can consider mass transport of solute diffusing across a moving [spherical] interface to and from the surrounding matrix.

2.2 Classical Nucleation Theory From a Microscopic Perspective

The previous section examined nucleation as a stochastic process in size space and defined the nucleation rate in terms of coefficients (A and B) that could be in principle deduced from mesoscale models of particle growth. This is a powerful technique that is in keeping with the spirit of mean-field type theories, which deduce microscopic properties from emergent or “slow” quantities that define their mesoscale behaviour. It is instructive however, to re-consider nucleation from a microscopic perspective that considers the growth rate of nuclei specifically through atomic attachment kinetics. This is done next.

2.2.1 Preliminaries

We begin by getting some definitions out of the way. The first is the volume v of a unit grain, which is considered to be one atom big, i.e. the *atomic volume*. The second is the surface area S of said unit grain, which is the atomic surface area. Clearly, we are considering a purely classical picture of atoms here, which suffices the study of physical kinetics. Of these two quantities only v is “fundamental” as S can be expressed in terms of the molar volume through the atomic radius as

$$S = (36\pi)^{1/3} v^{2/3} \quad (2.23)$$

It is also noted for future reference that the atomic volume v is related to the *solid density* by $\rho_s = 1/v$; the *liquid density* will be denoted by ρ_L .

Let’s re-visit the work of formation of a nucleus of radius am given by Eq. (2.5). This quantity can be expressed in terms of the number of atoms, n , in a cluster of radius a . Specifically, the volume of a cluster of size a , denoted by V_a , is given by

$$V_a = 4\pi a^3 / 3 = vn, \quad (2.24)$$

which makes the surface area of the cluster, denoted by A_a ,

$$A_a = 4\pi a^2 = Sn^{2/3}, \quad (2.25)$$

In terms of v and S , Eq. (2.5) can thus be recast as

$$R_{\min}(n) = vn\Delta G + Sn^{2/3}\gamma \quad (2.26)$$

The number of atoms in a critical nucleus, n_{cr} , is found by the extremum of Eq. (2.26), which gives

$$n_{\text{cr}} = \left\{ \frac{2S\gamma}{3v(-\Delta G)} \right\}, \quad (2.27)$$

where the minus is associated with ΔG , which is inherently negative in an exothermic reaction like solidification, condensation, etc. Using the definitions of the quantities above, it is also straightforward to write n_{cr} as

$$n_{\text{cr}} = \frac{4\pi}{3} a_{\text{cr}}^3 \rho_s \quad (2.28)$$

The two expressions for n_{cr} will be useful in that follows.

Another important quantity that we will emerge in our calculations that follow is the so-called *Zeldovich number*, Z , which often discussed in the nucleation literature. It is related the curvature of the work function $R_{\min}(a_{\text{cr}})$ and is proportional to the rate at which a post-critical can fluctuate back below the critical size a_{cr} . The Zeldovich number is defined by

$$Z = \left(-\frac{1}{k_B T} \left. \frac{d^2 R_{\min}}{dn^2} \right|_{n_{\text{cr}}} \right)^{1/2} \quad (2.29)$$

Taking the second derivative of Eq. (2.26), substituting n^* from Eq. (2.28) and using Eq. (2.23) gives,

$$Z = \left(\frac{4\pi}{81} \right)^{1/6} \left(\frac{2\gamma}{k_B T} \right) \rho_s^{-1/3} (n_{\text{cr}})^{-2/3} \quad (2.30)$$

This can be re-cast in an alternative form by eliminating γ through the relation $a_{\text{cr}} = 2\gamma/(-\Delta G)$. Substituting this into Eq. (2.30) gives after some trivial algebra,

$$Z = \frac{\sqrt{3}}{4\pi} \left(\frac{(-\Delta \bar{G})}{k_B T} \right)^{1/2} \frac{1}{\rho_s a_{\text{cr}}^3}, \quad (2.31)$$

where here $\Delta \bar{G}$ is the total work of formation of a nucleus of radius $a = a_{\text{cr}}$ (i.e., $[\bar{G}] = J$).

2.2.2 Non-equilibrium attachment kinetics governing the growth of nuclei

With the above definitions and quantities out worked out, we now turn our attention to the kinetics of nuclei growing through the random attachment/detachment (called “condensation” and “evaporation”) of atoms onto their surface. We denote by N_g the density (number/volume) of crystal nuclei containing g atoms, under general conditions of non-equilibrium. We denote by C_g the rate at which *one* atom jumps from the liquid to the a nucleus of size g , turning it into, by virtue of this jump, a nucleus of size $g + 1$. Similarly, we denote by E_g the rate at which *one* atom jumps off a nucleus of size g (i.e., into the liquid), turning it into, by virtue of this jump, a nucleus of size $g - 1$. The net rate of nuclei jumping from size $g \rightarrow g + 1$ is given by

$$I_g = C_g N_g - E_{g+1} N_{g+1}, \quad (2.32)$$

which is the difference of how many nuclei *increase* past size g (by one atom) minus how many nuclei fall back from size $g + 1$ to g . Similarly I_{g-1} gives the ate of change of nuclei from size $g - 1 \rightarrow g$. Form Eq. (2.32), we note that a positive value for I_g or I_{g-1} implies that there is a net increase in the number of nuclei (per volume) growing from the smaller size to the larger size. The time rate of change of the nucleus density *at the size g* is thus given by the difference of the number (per

volume) of nuclei jumping from a smaller size ($g - 1$) to g minus the number (per volume) leaving the size g and jumping to size $g + 1$, i.e.,

$$\frac{dN_g}{dt} = I_{g-1} - I_g, \quad (2.33)$$

Equation (2.33) can be seen as a microscopic transport equation that gives us the rate of change of N_g due as a difference in rate entering compared to leaving the size g . Its differential form implies we can use it to describe the change of N_g due to individual atomic jump events (i.e. dt is on the order of individual atomic vibration times), which is why the rates I_g can be bases on the jump rate of individual atoms onto/off a nucleus.

2.2.3 Equilibrium steady state conditions

In equilibrium, N_g satisfies $dN_g/dt = 0$, and represents a statistically unchanging distribution, which we denote by n_g . Under these conditions, Eq. (2.33) satisfies

$$C_g n_g = E_{g+1} n_{g+1} \quad (2.34)$$

Equation (2.34) is satisfied by a form n_g proportional to Eq. (2.4), except with a slightly different normalization used in n_g to describe the number of nuclei per unit volume, i.e.,

$$n_g = \rho_L e^{-R_{\min}(g)/k_B T}, \quad (2.35)$$

where it is recalled that ρ_L is the density of liquid. Equation (2.35) gives the total number of atomic sites of the liquid that are likely to become site to host a nucleus of size g , under equilibrium conditions. As discussed above, this form can only be assumed to hold over some range $0 < g < g^*$, where $g^* > g_{\text{cr}}$ and g_{cr} is the number of atoms in a nucleus of critical size $a = a_{\text{cr}}$.

2.2.4 Non-equilibrium steady-state conditions

Under non-equilibrium, but steady-state, conditions that exist following some transient time after a thermodynamic driving force is applied to bias nuclei to grow from smaller to larger sizes (i.e. to initiating a first order phase transition), there is a uniform non-zero flow rate, I , of nuclei at all sizes g (up to the aforementioned post-critical size, which for consistency of notation we denote in this sub-section as g^*), after which the distribution of nuclei can be assumed to go to zero. This implies that

$$I_g = I = C_g f_g - E_{g+1} f_{g+1} = \text{constant, for all } 0 < g < g^* \quad (2.36)$$

where we have denoted by f_g the non-equilibrium steady state distribution, to avoid confusion with n_g and N_g defined previously.

To proceed, we algebraically re-manipulate Eq. (2.36) to the form

$$I = C_g n_g \left\{ \frac{f_g}{n_g} - \frac{E_{g+1} f_{g+1}}{C_g n_g} \right\} \quad (2.37)$$

Using Eq. (2.34) reduces Eq. (2.37) to

$$I = C_g n_g \left\{ \frac{f_g}{n_g} - \frac{f_{g+1}}{n_{g+1}} \right\} \quad (2.38)$$

Denoting $\Lambda(g) \equiv f_g/n_g$ and $\Lambda(g+1) \equiv f_{g+1}/n_{g+1}$, and noting that $g \rightarrow g + 1$ can be represented as $g \rightarrow g + \Delta g$, where $\Delta g/g \ll 1$, allows us to re-write

$$\frac{f_g}{n_g} - \frac{f_{g+1}}{n_{g+1}} \rightarrow -\frac{d\Lambda(g)}{dg} \quad (2.39)$$

Thus, the microscopic rate equation in Eq. (2.37) can be cast as the following differential equation,

$$\frac{I}{C_g n_g} = -\frac{d}{dg} \left(\frac{f_g}{n_g} \right) \quad (2.40)$$

or, alternatively, in the slightly more illuminating form

$$I = C_g n_g \left\{ -\frac{d}{dg} \left(\frac{f_g}{n_g} \right) \right\} \quad (2.41)$$

In what follows, we will expand on the term in the brackets and show that that is where the Zeldovich number comes from as a multiplicative correction to the more traditional pre-factor, which we'll see is just gives standard (i.e., uncorrected) rate of post-critical nuclei.

Equation (2.40) is next integrated from $g = 1$ (i.e. a 1-atom “cluster”) to some $g = G > g_{\text{cr}}$, which yields

$$\frac{f_G}{n_G} - \frac{f_1}{n_1} = - \int_1^G \left(\frac{I}{C_g n_g} \right) dg \quad (2.42)$$

Equation (2.42) is simplified by noting that: (a) I is constant; (b) $f_G/n_G \ll 1$, or practically $f_G \approx 0$ as alluded to above; (c) the distribution of nuclei at the smallest sizes approximates the equilibrium distribution, $f_1/n_1 \approx 1$. Thus, Equation (2.42)

$$I = - \left\{ \int_1^G \left(\frac{1}{C_g n_g} \right) dg \right\}^{-1} \quad (2.43)$$

It is recalled that n_g in Eq. (2.43) is given by Eq. (2.35), while C_g is the rate at which atoms in the liquid attach to a nucleus of size g . This depends on the rate of atomic vibrations in the liquid, denoted ν_o , the probability that an atom can actually overcome the energy barrier ΔG_A required to integrate itself into the solid at the solid-liquid interface and the number of surface sites available around the nucleus of size g , which is given as the area of the cluster divided by the atomic surface S area defined previously (it is assumed can all act as attachment sites in a pure substance). Explicitly, the form of C_g is

$$C_g = \nu_o \times e^{-\Delta G_A/k_B T} \times g^{2/3} \quad (2.44)$$

This expression $g^{2/3}$ can be recast with the aid of Eq. (2.25) and Eq. (2.23) as

$$g^{2/3} = \left(\frac{16\pi^2}{9} \right) a^2 \rho_s^{2/3}, \quad (2.45)$$

where a is the radius of a g -atom nucleus and where it is recalled that $v = 1/\rho_s$. Substituting Eq. (2.45) into Eq. (2.44) gives C_g as

$$C_g = \left(\frac{16\pi^2}{9} \right) a^2 \nu_o \rho_s^{2/3} e^{-\Delta G_A/k_B T} \quad (2.46)$$

To proceed further, we note from Eq. (2.35) and inspection of Fig. 2.3 that $1/n_g$ is sharply peaked around the critical nucleus size, i.e., $g = g_{\text{cr}}$ and decays exponentially away from the peak. We can thus expand $R_{\min}(g)$ to second order around g_{cr} , yielding

$$\begin{aligned} R_{\min}(g) &= R_{\min}(g_{\text{cr}}) + \frac{1}{2} \left. \frac{d^2 R_{\min}(g)}{dg^2} \right|_{g_{\text{cr}}} (g - g_{\text{cr}})^2 \dots \\ &\approx R_{\min}(g_{\text{cr}}) - \frac{Q}{2} (g - g_{\text{cr}})^2 \dots \end{aligned} \quad (2.47)$$

where we have defined $Q = R''_{\min}(g_{\text{cr}})$ for convenience. Substituting the second line of Eq. (2.47) into $1/n_g$ in the integral on the RHS of Eq. (2.43) gives

$$\int_1^G \left(\frac{1}{n_G C_g} \right) dg = \int_1^G \left(\frac{e^{\frac{R_{\min}(g)}{k_B T}}}{\rho_L C_g} \right) dg \approx \left(\frac{e^{\frac{R_{\min}(g_{\text{cr}})}{k_B T}}}{\rho_L C_{g_{\text{cr}}}} \right) \int_1^G e^{\frac{-Q}{2k_B T}(g-g_{\text{cr}})^2} dg \quad (2.48)$$

The last integral in Eq. (2.48) is approximated by a standard Gaussian integral from $-\infty$ to ∞ by making a change of variables $\xi = g - g_{\text{cr}}$, which changes the limits to $g = 1 \rightarrow \xi = 1 - g_{\text{cr}} \ll 0$ and $g = G \rightarrow \xi = G - g_{\text{cr}} \gg 0$. This gives,

$$\int_1^G \left(\frac{1}{n_G C_g} \right) dg \approx \left(\frac{e^{\frac{R_{\min}(g_{\text{cr}})}{k_B T}}}{\rho_L C_{g_{\text{cr}}}} \right) \sqrt{\frac{2\pi k_B T}{Q}}, \quad (2.49)$$

as a result of which Eq. (2.43) finally becomes,

$$I = \rho_L C_{g_{\text{cr}}} e^{\frac{R_{\min}(g_{\text{cr}})}{k_B T}} \sqrt{\frac{-R''_{\min}(g_{\text{cr}})}{2\pi k_B T}}, \quad (2.50)$$

The square root is equal to the so-called Zeldovich number and was derived in Eq. (2.30) (where $n_{\text{cr}} \rightarrow g_{\text{cr}}$). Substituting the relation $g_{\text{cr}} = (4\pi/3)a_{\text{cr}}^3\rho_s$ and Eq. (2.46) for $C_{g_{\text{cr}}}$ gives after some trivial algebra,

$$I = 2 \left(\frac{\gamma}{k_B T} \right)^{1/2} \left\{ \left(\frac{\sqrt{\pi}}{36} \right)^{1/3} \frac{\nu_o}{a_{\text{cr}}^2 \rho_s^{4/3}} e^{-\Delta G_A/k_B T} \right\} \left\{ a_{\text{cr}}^2 \rho_s \rho_L e^{-R_{\min}(g_{\text{cr}})/k_B T} \right\}, \quad (2.51)$$

The expression in Eq. (2.51) has been manipulated intentionally in a form that is comparable to Eq. (2.18) for the nucleation rate derived previously using mesoscale considerations. It is evident that the second bracketed factor in Eq. (2.51) corresponds to $B(a_{\text{cr}})$ while the factor in the last bracket of Eq. (2.51) corresponds to $f_o(a_{\text{cr}})$.

2.3 Nucleation Rate in a Binary Mixture

The nucleation rate theory applied in the previous sections of this chapter assumed a pure substance when evaluating the work of formation and any other thermodynamic quantity. The physical kinetics we considered throughout, however, are to lowest order independent of whether nucleation occurs in a liquid of a pure substance or a solution that is a mixture. This last section of this chapter adapts the expression for the steady state nucleation rate to the metastable liquid in a binary alloy, which amounts to formulating the work of formation of a critical nucleus for a binary mixture, denoted in this section by ΔF^* . The steady state nucleation rate in a metastable liquid of a binary mixture is given by a form analogous to Eq. (2.50), adapted here to match the form frequently shown in the literature, i.e.,

$$J = \rho_L \beta^* Z \exp(-\Delta F^*/kT), \quad (2.52)$$

where ρ_L is the usual nucleation site density, $\beta^* \sim C_{g^*}$ is a frequency factor proportional to the inverse of characteristic nucleation time, Z is the Zeldovich factor and k is the Boltzmann constant.

2.3.1 Work of formation in a binary mixture

Consider a large closed thermodynamic system of volume V containing a homogeneous undercooled liquid phase in contact with a thermal reservoir at temperature T . Let $f_L(c, T)$ be the composition and temperature-dependent free energy density of this liquid. Similarly, let $f_s(c, T)$ be the composition and temperature-dependent free energy density of the solid phase whose nucleation we are considering. These free energy curves are illustrated for typical metallic alloys in Fig. (2.5). Figure 2.5 shows a typical composition dependence of f_L for a binary alloy at a fixed temperature. Notice that in order for the liquid to be in a metastable state, its composition c_0 must be smaller than the coexistence liquid composition, c_L^{eq} , obtained via the common tangent construction with the solid phase curve. Thus, the initial free energy of the system is

$$F_0 = f_L(c_0, T)V. \quad (2.53)$$

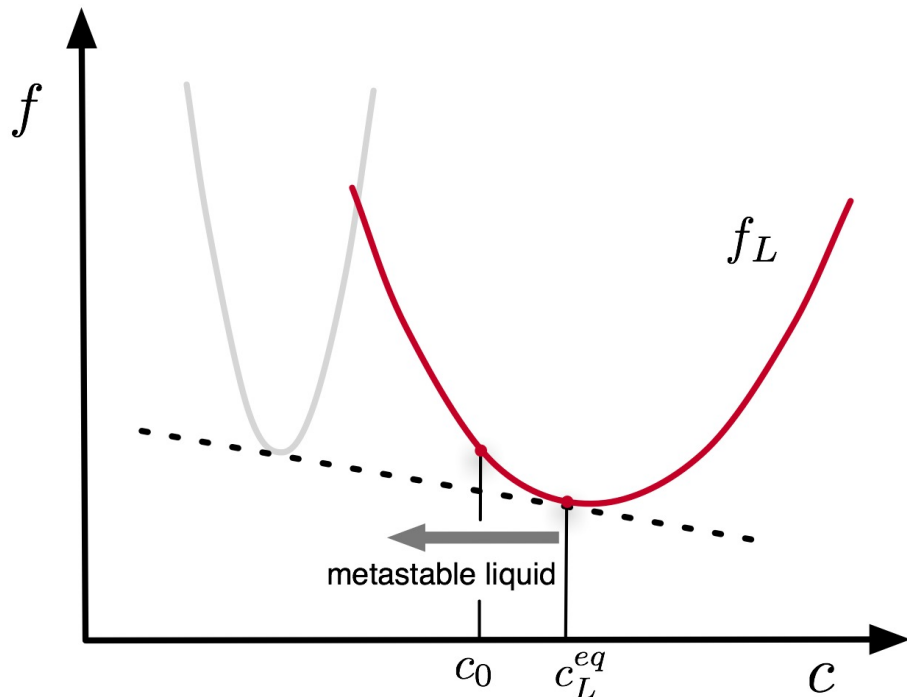


Figure 2.5: Typical forms for the free energy of a liquid or solid binary alloy mixture.

Now consider that in the bulk liquid, a fluctuation gives rise to small spherical solid nucleus of size V_N and composition c_N (see Fig. 2.6). The free energy of the system is now written as

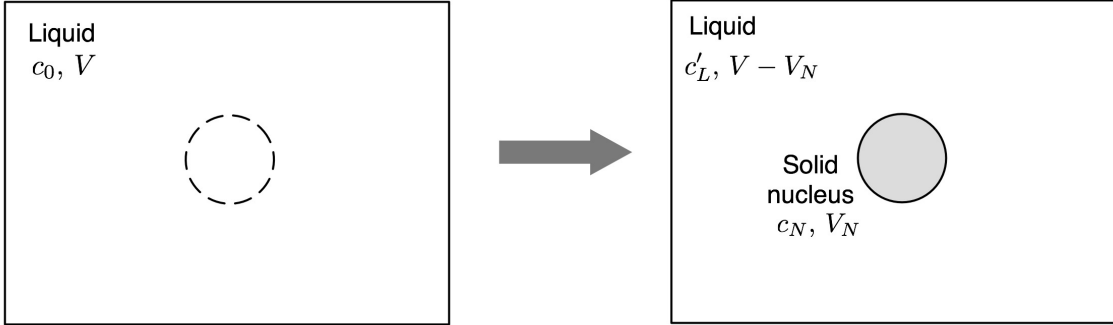


Figure 2.6: Nucleation event

$$F = f_S(c_N, T)V_N + f_L(c'_L, T)(V - V_N) + \gamma A_N, \quad (2.54)$$

where f_S is the extensive free energy of the solid, γ is the solid-liquid interfacial energy (here we consider it to be orientation independent), A_N is the surface area of the nucleus and c'_L is the composition of the liquid after the nucleus has been formed; it is different from c_0 because $c_N < c_0$ and the average composition for the whole system must remain constant. Since we are assuming that the transformation is isothermal, it is convenient to drop the explicit dependence of temperature in the equations. Moreover, since we are considering an isothermal system at fixed total volume, the associated work of formation of the nucleus is equal to the change in free energy, i.e.,

$$\begin{aligned} \Delta F &= F - F_0 \\ &= f_S(c_N)V_N + f_L(c'_L)(V - V_N) + \gamma A_N - f_L(c_0)V \\ &= [f_S(c_N) - f_L(c_0)]V_N + [f_L(c'_L) - f_L(c_0)V](V - V_N) + \gamma A_N. \end{aligned} \quad (2.55)$$

In the equation above it is also implied that the density of the solid nucleus is the same as the liquid. We also have the solute conservation equation, which is a consequence of considering a closed system:

$$c_0V = c_NV_N + c'_L(V - V_N) \quad (2.56)$$

Since the system is large, $V_N \ll V$ and c'_L is close to c_0 . Therefore, we can write $f_L(c'_L)$ as an expansion (to first order) of f_L around c_0 :

$$\begin{aligned} f_L(c'_L) &= f_L(c_0) + \frac{\partial f_L}{\partial c} \Big|_{c_0} (c'_L - c_0) \\ &= f_L(c_0) + \mu_L(c_0)(c'_L - c_0), \end{aligned} \quad (2.57)$$

where $\mu_L(c_0)$ (which from now on we denote as μ_0) is the excess chemical potential of the liquid at c_0 . Substituting $f_L(c'_L)$ from (2.57) and $V - V_N$ from (2.56) into (2.55) we get

$$\Delta F = \underbrace{[f_S(c_N) - f_L(c_0) - \mu_0(c_N - c_0)]V_N}_{\Delta F_B} + \underbrace{\gamma A_N}_{\Delta F_I}. \quad (2.58)$$

Note that we can identify two contributions to the change in free energy: the bulk contribution ΔF_B and the interface contribution ΔF_I . Since the former is associated with the change from a metastable

phase (liquid) into a stable phase (solid), ΔF_B is always negative. In contrast, ΔF_I is always positive because it is associated with the creation of an interface. Now, because of the relation between V_N and A_N (remember we are considering a spherical geometry) the surface term will always dominate for small sizes and the bulk term will start to dominate beyond a certain size. Thus, ΔF as a function of size will have a maximum which corresponds to the nucleation barrier ΔF^* . The critical nucleus size V_N^* must satisfy

$$\left. \frac{\partial \Delta F}{\partial V_N} \right|_{V_N^*} = 0 \quad (2.59)$$

But before finding V_N^* and ΔF^* we still need to specify the concentration selected by the nucleus, c_N . Since nucleation is a fluctuation driven event and thermodynamics tells us that the fluctuation most likely to occur is the one associated with the smallest cost in energy, we can determine c_N by finding the minimum of ΔF with respect to the concentration in the solid. Since the dependence of ΔF on c_N is only on the bulk part, minimizing ΔF is equivalent to minimizing $\Delta f_B = \Delta F_B/V_N$ or, alternatively, maximizing $D_F \equiv -\Delta f_B$ which we can express as

$$\frac{\partial D_F}{\partial c_N} = 0, \quad (2.60)$$

where D_F is the called the thermodynamic driving force for nucleation and it is proportional to the undercooling of the original liquid phase. Obtaining D_F from (2.58) and solving (2.60) give us

$$\frac{\partial f_S}{\partial c_N} = \mu_S(c_N) = \mu_0, \quad (2.61)$$

where $\mu_S(c_N)$, which from now on we denote as μ_N is the solid excess chemical potential at concentration c_N . Eq. 2.61 states that the selected nucleus concentration c_N is such that the chemical potential of the solid and liquid phases is the same. We can write now the driving force for nucleation as

$$\begin{aligned} D_F &= [f_L(c_0) - \mu_0 c_0] - [f_S(c_N) - \mu_0 c_N] \\ &= -(\omega_S(c_N(\mu_0)) - \omega_L(c_0(\mu_0))) \\ &= -\Delta\omega_B(\mu_0), \end{aligned} \quad (2.62)$$

where $\omega_J(\mu_0)$ ($J = S, L$) is the grand potential density of each phase evaluated at μ_0 , the chemical potential of the unstable liquid.⁴ Graphically, the driving force for nucleation is represented in figure 2.7. Note that the condition that $\mu_N = \mu_0$ means that the slopes of the lines tangent to $f_S(c_N)$ and $f_L(c_0)$ are the same. However, these lines have different intercepts.

⁴At this point it is important to clarify the distinction between the physical meaning of Δf_B and $\Delta\omega_B$ to avoid confusion. Δf_B refers to the total change in bulk free energy of the entire system associated with the creation of the nucleus divided by the nucleation volume, whereas $\Delta\omega_B$ refers to the difference of the grand potential density (grand potential per unit volume) between the solid and that of the original liquid phase.

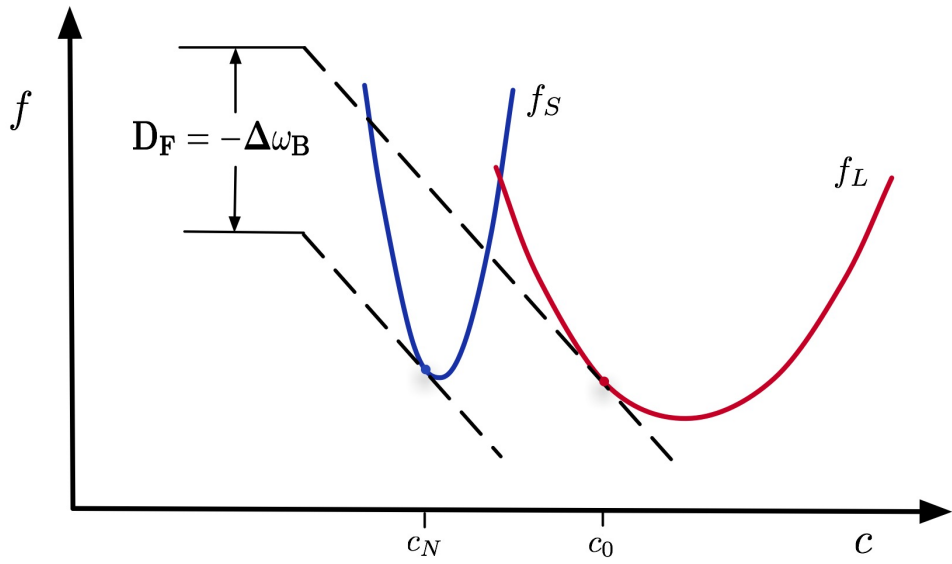


Figure 2.7: Graphical representation of driving force for nucleation.

We now write equation (2.58) as

$$\Delta F = \Delta\omega_B V_N + \gamma A_N. \quad (2.63)$$

Finally, finding the maximum of ΔF with respect to V_N (according to (2.59)) gives us the critical nucleus size, which, in terms of its radius R^* , is given by

$$R^* = -\frac{2\gamma}{\Delta\omega_B}, \quad (2.64)$$

and the free energy barrier ΔF^* ,

$$\Delta F^* = \frac{16\pi\gamma^3}{3\Delta\omega_B^2}. \quad (2.65)$$

Chapter 3

Phase Transformation Kinetics

Nucleation leads to post-critical [stable] particles that grow into the liquid (or a solid matrix in solid state transformations). Their growth kinetics and interaction is ultimately what determines the final microstructure of a system. The word “microstructure” has become a catch-all word that encompasses the amount of, types and patterning of stable phases that emerge in a phase transformation. This first two sections of the chapter examine the kinetics of first order phase transformations under two conditions. The first is one wherein particle growth is determined predominately by supersaturation, or thermodynamic driving force, and curvature effects can be ignored. Moreover, in this regime, growth is not affected very much by any conservation law (e.g. conservation of mass) that may apply to the system. This can, for example, describe magnetic domain growth in the Ising model, or solidification in a highly supercooled liquid of a pure substance. The second situation examined is one where particle growth is driven by supersaturation at early time but transitions to curvature-driven growth at late times. In the latter regime, any conservation law that are applicable must be taken into consideration in calculating the particle growth dynamics. This situation is a good description of particle coarsening out of a homogeneous two-component mixture.

3.1 Supersaturation-Driven Grain Growth

We begin by considering the fraction of a stable phase (denoted here by α) that grows into and consumes a metastable phase (denoted here by β) as a function of time in a first order phase transition. To maintain consistency with previous chapter we will continue to use the language of solidification here, although the arguments presented here hold for any first order phase transformation. The previous chapter derived the rate at which post-critical nuclei of a metastable first phase appear. It is thus expected that the fraction of α created, denoted f_s , should be a function of the particle nucleation rate *and* the growth rate of post-critical nuclei, which we will denote by v . The solid fraction at time t can be written as

$$f_s(t) = \int_0^t dt' I(t') \left(\frac{4\pi}{3} R^3(t, t') \right), \quad (3.1)$$

where $I(t)$ is the nucleation rate, which we saw is constant for homogeneous nucleation, and $R(t, t')$ is the average radius of a grain at time t , which has been growing since the time t' when it was nucleated from the metastable phase¹. To progress further, we next need to derive the form of $R(t, t')$.

¹It should be noted here that Eq. (3.1) is really only true when grains grow under a constant driving force and don’t interact. As a result, the theory presented in this sub-section is only reasonable for domain coarsening in systems like the Ising model described by a so-called order parameter that need not be conserved, thus allowing for grains can completely consume the metastable phase. It can also be a reasonable description for solidification of a rapidly solidified material

A cardinal rule of non-equilibrium phase transformations is that the local speed of a two-phase interface (e.g. a solid-liquid interface in solidification (or a solid-solid interface in solid state precipitation) is proportional to the difference of an appropriate thermodynamic potential (e.g. free energy or grand canonical potential, etc) between the stable and metastable phases, i.e.,

$$v \propto \Delta G_{\text{drive}}, \quad (3.2)$$

where for the case of solidification that we have been considering ΔG_{drive} is proportional to undercooling for the case of solidification/precipitation of a pure material (i.e. $\sim T - T_m$, the difference between the quench temperature and the melting temperature). For solidification/precipitation of binary mixtures, the driving force is proportional to the *supersaturation* at a particular temperature of interest. Supersaturation can be determined from the equilibrium phase diagram such as that in Fig. 3.1, which is typical of dilute metal alloys that we'll be considering in what follows ². Since the

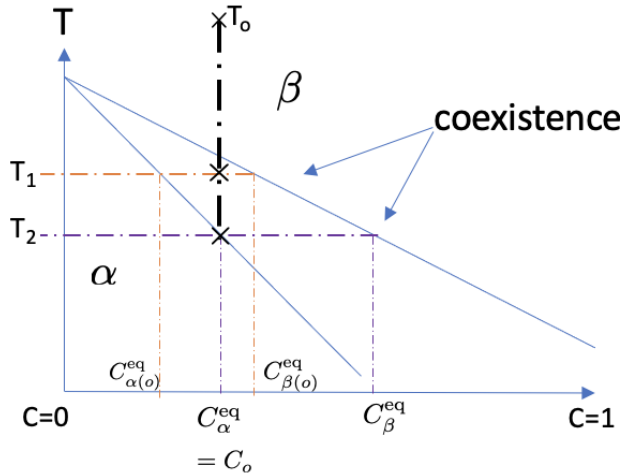


Figure 3.1: Typical phase diagram of a two-component metal alloy containing elemental species *A-B*, at dilute concentrations of the solute *B*. The regions above and below the slanted lines are single phase regions, denoted β and α , respectively. At temperatures between the slanted lines the system coexists as two phases $\alpha + \beta$. The lines defined by the concentrations where the horizontal dashed lines cut through the coexistence region (e.g., $(C_{\beta}^{\text{eq}}, C_{\alpha}^{\text{eq}})$ and $(C_{\beta(o)}^{\text{eq}}, C_{\alpha(o)}^{\text{eq}})$) are known as *tie lines*, which are used to determine the equilibrium concentrations of each phase at a given temperature, as well as the solid/liquid fraction at equilibrium.

undercooling or supersaturation (let's denote it Δ in both cases) is constant, we expect that for a typical particle

$$v = \frac{dR}{dt} \propto \Delta G_{\text{drive}} = \text{constant} \implies R \sim v t, \quad (3.3)$$

for which the density or solute diffusional interactions range is short ($\sim \text{nm}$). For slowly quenched systems constrained by a conservation law, however, grains will eventually interact via their solute diffusion fields as the system approaches equilibrium and this theory become invalid.

²Quenches from temperature T_o to T_1 , T_2 , etc, lead to nucleation and growth of α phase from β phase. Any temperature T , the driving force $\Delta G_{\text{drive}} = \omega_L(T) - \omega_{\text{eq}}(T)$ where $\omega_L(T)$ is the grand canonical potential of the metastable liquid and $\omega_{\text{eq}}(T)$ is the corresponding equilibrium value of the system. It is straightforward to show that for dilute binary alloys, $\Delta G_{\text{drive}} \propto \Delta$ where $\Delta \propto (C_o - C_{\alpha}^{\text{eq}})/(C_{\beta}^{\text{eq}} - C_{\alpha}^{\text{eq}})$ is the supersaturation, with C_o being the average system concentration and $C_{\alpha/\beta}^{\text{eq}}$ the equilibrium concentrations of the α/β phases. For more details on alloy thermodynamics the reader is referred to Chapter 6 of Ref. [24] and Section 1.7.2 of these notes.

Thus, a grain that has been growing from time t' to time t will satisfy

$$R(t, t') = v(t - t') \quad (3.4)$$

Substituting Eq. (3.4) into Eq. (3.1) and noting that I is constant yields

$$f_s(t) = \left(\frac{4\pi}{3} I \right) \int_0^t dt' v^3 (t - t')^3 dt', \quad (3.5)$$

Equation (3.5) is a little too simplistic as it assumes that there is always an infinite amount of liquid volume within which post-critical nuclei can continuously grow and/or nucleate, which is clearly nonsense in a finite size system. In fact, the liquid (or, more generally, metastable phase β using notation of Fig. (3.1)) fraction available for new grains to grow and/or nucleate into *shrinks* with time. Moreover, by changing the lower limit of the integral in Eq. (3.5) to t_o , and the upper limit to $t_o + dt$, Eq. (3.5) can be more accurately seen as representing *incremental* change in solid fraction between $t_o \rightarrow t_o + dt$. Thus, if we now denote by X_s the *true* solid fraction, the change (i.e. increase) in dX_s is equal to the incremental amount of solid df_s generated in the liquid multiplied by the available fraction of liquid denoted $X_L = 1 - X_s$, i.e., $dX_s = X_L df_s$. Integrating this last differential gives

$$\int_0^t \frac{dX_s}{1 - X_s} = \int_0^t df_s, \quad (3.6)$$

which can be solved to give

$$X_s(t) = 1 - e^{-\left(\frac{4\pi}{3} I\right) \int_0^t dt' [v(t-t')]^3 dt'} \quad (3.7)$$

It is emphasized that Eq. (3.7) is only approximate. It assumes a simple effective spherical geometry of growing particles and, as was mentioned above, non-interacting particles. In reality, particles take on different geometries (rods, dendrites, discs, polyhedra, etc). Moreover, the fact that particles do interact at late times implies that Eq. (3.7) is really only accurate over early to (at best!) intermediate times of the phase transformation. Note that Eq. (3.7) *does not* assume that particles grow at constant speed, which is a good thing, since it turns out that particle speed can go through a transient phase depending on its geometry. Nevertheless, it is not too bad an approximation to assume that in the mean-field sense, $v \sim \text{constant}$.

The importance of Equation (3.7) lies in its generic or “universal” features. Namely, it predicts that the time dependence of a first order phase transition proceeds according to a *stretched exponential* whose time exponent is of the form $d + 1$, where d is the dimension of space, and where the time scale of the exponential is inversely dependent on the homogeneous nucleation rate and the cube of the growth rate. It turns out that these universal features are also born out experimentally, where it is generally observed that

$$X_s(t) = 1 - e^{-\text{const.} \times t^{d+1}} \quad (\text{homogeneous nucleation}) \quad (3.8)$$

The qualification “homogeneous nucleation” is specified in Eq. (3.8) since we have thus far only considered homogeneous nucleation. Most practical phase transformations are, in fact, governed by heterogeneous nucleation. To model this process, the heterogeneous nucleation rate changed from a constant to

$$I_{\text{het}} = N\delta(t), \quad (3.9)$$

where N is proportional to the density impurity or *inoculant* sites on which nuclei can form. Such sites so dramatically decrease the barrier for nucleation (by many orders of magnitude!) that heterogeneous

nucleation completely overrides homogeneous nucleation as the selected mechanism by which particles appear in the liquid. Indeed, except for extremely fast cooling rates, most heterogeneous nucleation events occur on inoculant sites almost immediately, hence the appearance of the $\delta(t)$ in Eq. (3.9). It is straightforward to repeat the above steps using Eq. (3.9) and arrive at the heterogeneous analogue of Eq. (3.7), which yields a general growth law of the form

$$X_s(t) = 1 - e^{-\text{const.} \times t^d} \quad (\text{heterogeneous nucleation}) \quad (3.10)$$

To make Eq. (3.8) and Eq. (3.10) quantitative, one typically fits the capture the qualitative feature of the kinetics of a phase. The stretched exponential theories derived above are known as *KAMJ* growth laws, after their originators Kolmogorov, Avrami, Meyer and Johnson.

3.2 Grain Growth Dynamics Subject to Mass Conservation

While the KAMJ theories derived above provide a good description of the phase transformation at early to intermediate time, they become inaccurate at late times as alluded to previously. At late times particles interact by exchanging mass or density via their overlapping diffusion fields; as a result, mass conservation must be taken into account in the system. Moreover, since the system is close to equilibrium at late times, the main driving force for the phase transformation now becomes the reduction of curvature. These two effects, taken together, lead to a situation where smaller particles diffuse their mass toward larger particles, ultimately leading to a system with a few large particles. The cartoon in Fig. (3.2) illustrates these idea. This section considers both mass (or density, heat, etc)

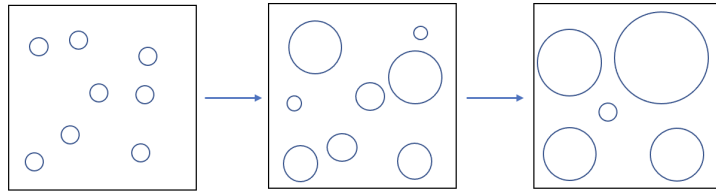


Figure 3.2: Typical sequence of particle morphologies when growth is limited by surface tension and mass conservation. At early times a particle's growth velocity is approximately constant and particles grow at a steady rate. As soon as particles start to interact via their solute diffusion fields, particles start to coalesce to reduce surface tension. In this regime growth thermodynamic driving force (i.e., supersaturation) is very small and further growth of particles is limited by mass diffusion proportional to the differences in curvature between large and small particles. In the end we are left with a few large particles.

diffusion and interface curvature in order to derive a more realistic growth law scaling of particles at late times. Before doing so, however, we first must digress and consider the physics governing particle growth in a metastable matrix more precisely than we've done previously.

3.2.1 Conditions controlling the kinetics of a phase boundary in an alloy

Considering the system in the cartoon of Fig (3.2) what must the governing equations for this system be? To answer this question we assume the system is comprised on the matrix containing some distribution of spherical grains of the stable phase. Between the slowly moving (called *coarsening*)

interfaces that separate the grains from the matrix, conserved mass transport is governed by the usual diffusion equation,

$$\frac{\partial C}{\partial t} = \nabla \cdot (D \nabla C), \quad (3.11)$$

where C is the concentration field and D is the diffusion coefficient, which in general is a function of the phase; however here we will be considering it a constant here. It is noted that mass diffusion through the bulk is typically the slowest process of grain growth and coarsening. Equation (3.11) must be supplemented by two boundary conditions applied at matrix/particle interfaces.

The first boundary condition relates the velocity of a location on the particle/matrix interface to the solute flux across the interface according to

$$(C_{\text{int}}^+ - C_{\text{int}}^-) v_n = D \{ \nabla C|_{R^-} \cdot \hat{n} - \nabla C|_{R^+} \cdot \hat{n} \}, \quad (3.12)$$

where C_{int}^+ and C_{int}^- represent the concentrations on the α/β -facing sides of the interface of any particle and \hat{n} is a unit vector that is normal to a particle and pointing into the matrix by convention, making the local normal interface speed $v_n = \hat{n} \cdot \bar{v}$, with \bar{v} being the local interface velocity. Equation (3.12) is a statement of mass conservation, representing the flux of solute accumulating in the liquid (or solid) as interface advances to the difference in fluxes toward and away from the interface.

The second boundary condition constrains the interface concentration. Specifically, when the interface is curved and moving, the local interface concentration deviates from the equilibrium value by a correction proportional to the local interface curvature and the local normal interface speed v_n . This effect, known as the *Gibbs-Thomson effect* is expressed as

$$C_{\text{int}}^\pm = C_{\alpha,\beta}^{\text{eq}} - d_o \kappa - \frac{v_n}{\mu}, \quad (3.13)$$

where $C_{\alpha,\beta}^{\text{eq}}$ are the equilibrium concentrations of the α/β phases at the quench temperature (see for example Fig (3.1)), d_o is the *capillary length* (a measure of the surface tension that is actually a function of the concentration difference across the interface but treated as a constant here) and μ is the atomic mobility. Except for very large driving forces, the last term in Eq. (3.13) can typically be neglected for most phase transformations in metals ³.

Eq. (3.11), Eq. (3.12) and Eq. (3.13) are referred to as a *sharp-interface model* and are general in describing the growth particles in a metastable phase, such as occurs in solidification, or most 1st order phase transformations. An analogous set of equations can be derived for solidification of a pure substance, the kinetics of which are controlled by the transport of heat. This is done explicitly in the next chapter, with the steps of that derivation being adaptable to obtain the equations derived above.

3.2.2 Early-time grain growth kinetics

Consider a quench to a temperature $T = T_1$ as shown on the left had side of Fig. (3.3). Initially, a post-critical size particle will start to grow while obeying the sharp interface equations Eq. (3.11), Eq. (3.12) and Eq. (3.13). The concentration levels at and away from the α/β interface is depicted on the right hand side of Fig. (3.3). Since the solid is initially small, the concentration in the α grain rapidly attains the value predicted by the Gibbs-Thomson relation throughout (not just at the interface). On the matrix side, however, the concentration follows a characteristic diffusion tail, spanning from the Gibbs-Thomson prediction at the interface to the far-field initial value of the matrix.

³The atomic mobility in metals is typically very large, allowing solute levels on either side of the a two-phase interface to rapidly attain to their equilibrium values, as predicted by the equilibrium phase diagram.

In this early-time limit of the growth process, the interface is driven largely by supersaturation and the phase transformation kinetics are thus governed, approximately anyway, by the model described in Section (3.1).

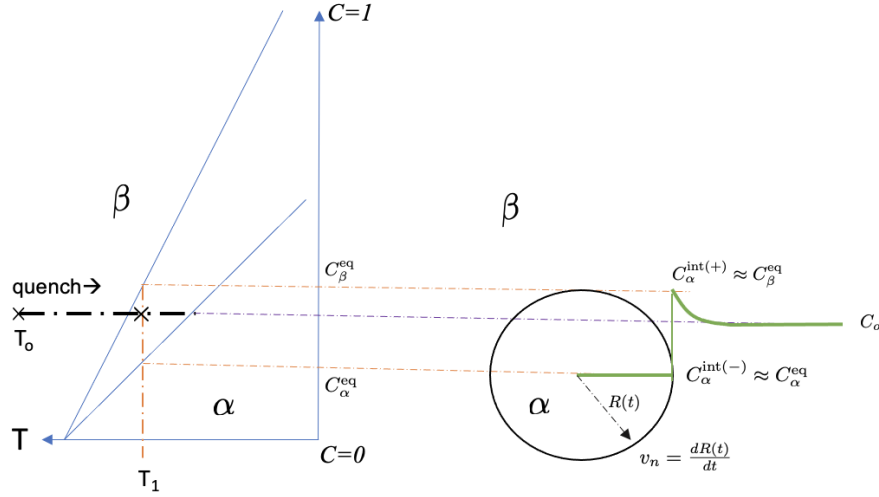


Figure 3.3: Solute concentration profiles describing the *early-time* growth of a precipitated particle of phase α growing into a matrix phase β at a quench temperature T_1 . In this time regime, particle growth is driven predominately by supersaturation of particles with respect to the matrix and curvature effects on concentration can be neglected. The interface concentration on the matrix side of the particle can be set to the equilibrium value of the β phase at T_1 , while the interface concentration on the particle side can be set to equilibrium value of the α phase at T_1 . The growth speed v_n of a particle tracks the rate of change of its radius $R(t)$.

3.2.3 Late-time grain growth kinetics

We now turn our attention to later times in the grain growth process where the phenomenon of *coarsening* starts to occur. To help visualize this process, Fig. (3.4) illustrates an example of a small particle (α) next to a very large one (α') in the late-stage of the coarsening process at a quench temperature denoted here as $T = T_2$. The area outside the particles is the matrix (β). The left side of the figure shows a phase diagram with the relevant concentration levels projected onto the corresponding locations on the particles and matrix. With reference to Fig. (3.4), we find that at late times the system is nearly in equilibrium and so the concentration within the bulk of the matrix (β) is nearly at the value on the phase diagram corresponding to the quench temperature T_2 . Also shown in the figure are the concentrations on either side of the particles' interface. For the larger particles (e.g., α'), the curvature correction of the concentration due to the Gibbs-Thomson effect of Eq. (3.13) is negligible and thus ignored. For smaller particles (e.g., α), however, we must consider the curvature effect due to the Gibbs-Thomson condition on the matrix side otherwise there would be *no* concentration gradient between the neighbouring particles to drive the coarsening growth process whereby the larger particle grows at the expense of the smaller one, i.e. by diffusing solute toward it and dissolving it ⁴.

⁴We can easily incorporate the curvature effect on the interface concentration of the larger α' grains, but they end up making the math that follows more messy, without really providing new scaling information.

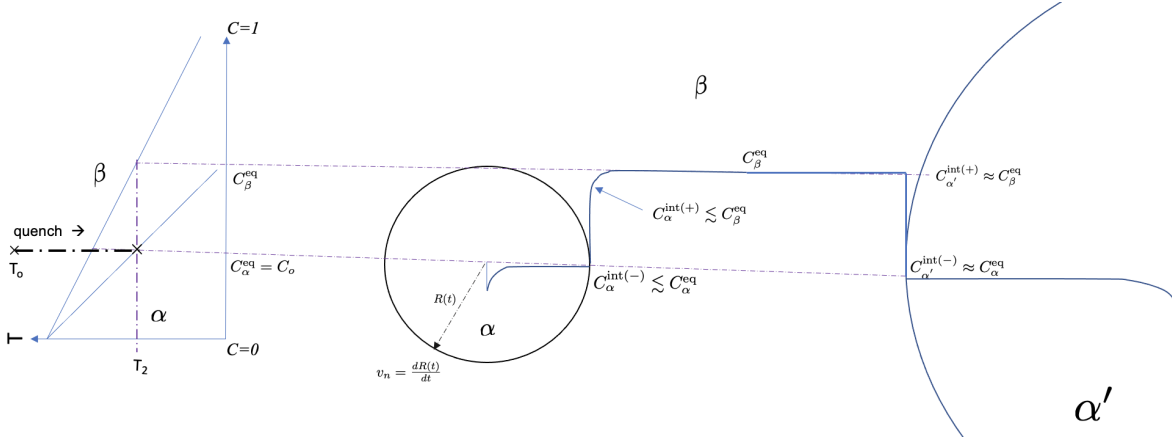


Figure 3.4: Solute concentration profiles describing the *late-time* growth of a precipitated particle of phase α growing into a matrix phase β at a quench temperature T_2 . The system is nearly in equilibrium and comprises a few large particles with very few small particles (e.g., $R_{\alpha'} \gg R_\alpha$). The matrix concentration is almost at the equilibrium value given by the phase diagram (i.e., C_β^{eq}). The concentrations on either side of the interface of *large* particles (α') can be approximated by the equilibrium values C_β^{eq} (matrix side) and $C_\alpha^{\text{eq}} = C_o$ (particle side), ignoring curvature corrections. The concentrations on either side of the interface of *smaller* particles (α), however must consider the curvature correction from equilibrium since surface tension is the *only* driver for particle growth with supersaturation being negligible. (Dips in the concentration at the centres of particles (“coring”) represent the concentration levels at the early stages of solidification.)

The above considerations allow us to simplify the sharp interface model of Section (3.2.1) and apply it to derive the time scaling for the dissolution of a small particle close to a large one, as depicted in the cartoon of Fig. (3.4). Namely, we consider a 1D line connecting the two particles, and recall that $R_{\alpha'} \gg R_\alpha$. In the region between the particles (e.g. the matrix between α and α' in Fig. (3.4)), Eq. (3.11) can be approximated by

$$\frac{d^2C}{dx^2} = 0, \quad (3.14)$$

with the Dirichlet boundary conditions

$$\begin{aligned} C_\alpha^{\text{int}(+)} &= C_\beta^{\text{eq}} - d_o/R(t) \\ C_{\alpha'}^{\text{int}(+)} &= C_\beta^{\text{eq}} \end{aligned} \quad (3.15)$$

are applied to the matrix side of the α and α' particle interfaces, respectively⁵. Finally, the Neuman boundary condition

$$\Delta C_{\text{int}} v_n = -D \left. \frac{dC}{dx} \right|_{\alpha^{\text{int}(+)}} \quad (3.16)$$

is applied on the matrix side of the α particle interface, where $\Delta C_{\text{int}} = C_\alpha^{\text{int}(+)} - C_\alpha^{\text{int}(-)}$ and where we can approximate $C_\alpha^{\text{int}(-)} \approx C_\alpha^{\text{eq}}$ to lowest order in what follows. An analogous expression to Eq. (3.16)

⁵Note that in the coarsening process, interface velocities are so small that the velocity-dependent correction in the Gibbs-Thomson effect can be ignored in most cases.

is also applied on the matrix side of the α' grain, but we do not write it here as it will not be used below.

To proceed further, we note that Eq. (3.14) implies that the concentration is approximately linear between the two particles, which allows us to approximate the concentration gradient in Eq. (3.16) as

$$\left. \frac{dC}{dx} \right|_{\alpha^{\text{int}(+)}} = \frac{C_{\alpha'}^{\text{int}(+)} - C_{\alpha}^{\text{int}(+)}}{\text{diffusion length}} \approx \frac{d_o/R(t)}{R(t)} \quad (3.17)$$

where the numerator in second equality on the RHS of Eq. (3.17) is obtained by substitution of the boundary conditions in Eq. (3.15). It is noted that the diffusion length of solute must clearly vary over the scale $R(t)$, the radius of the α grain that close to and about to be dissolved by the α' grain. Indeed, it is the radius of curvature of the α grain that causes the decreases in concentration from its equilibrium value since a fully equilibrated system comprising only straight, stationary boundaries (i.e., $R = \infty$) would lead to $v_n = 0$. Substituting Eq. (3.17) into Eq. (3.16) thus leads to

$$v_n \approx -\frac{D}{\Delta C_{\text{int}}} \frac{d_o}{R^2(t)} \quad (3.18)$$

From the first line of Eq. (3.15) it is noted that $\Delta C_{\text{int}} = C_{\beta}^{\text{eq}} - C_{\alpha}^{\text{eq}} + \mathcal{O}(1/R)$. However, when this is substituted into Eq. (3.18) and terms of order up to $1/R(t)$ are retained, we obtain

$$v_n = \frac{dR(t)}{dt} \propto \frac{1}{R^2(t)} \quad (3.19)$$

Equation (3.19) predicts that the α (or, equivalently α') interfaces evolve in time according to the time scaling

$$R(t) \sim t^{1/3}, \quad (3.20)$$

which is the classic $1/3$ -growth law governing coarsening in systems constrained by a conserved order parameter. This type of growth was designated the name *Oswald ripening* the classical work of classic work of I. M. Lifshitz and V. V. Slyozov (LS). A detailed review can be found in Ref. [29].

The scaling law of Eq. (3.20) governs the shrinking of a typical small particle that is dissolved by a much larger nearby neighbouring particle. This behaviour is prevalent in the late stages of a first order phase transition in the regime of solid fraction $X_s \approx 1$. This is deep result and is independent of the simplicity with which it was derived; a more involved treatment would give the same coarsening exponent of $1/3$. It also other interesting ramifications, one of which is to help us deduce a scaling law for the grain size distribution in the late stage of alloy precipitation.

3.2.4 Scaling of particle size distribution in the late time coarsening regime

An important application of the scaling of particles size at late time in the precipitation process is that makes it possible to work out the scaling law of the corresponding grain (also called particles here) size distribution in the system. We explore this in this subsection.

We begin by defining by $n(R, t)$ the number of particles between the size $R \rightarrow R + dR$ at time t . We tacitly assume that all particles are spherical. Formally, $n(R, t)$ is given by

$$n(R, t) = \sum_{i=1}^{N(t)} \delta(R - R_i(t)), \quad (3.21)$$

where the index $i = 1, 2, \dots, N(t)$ runs over the $N(t)$ particles present in the system at time t and $R_i(t)$ is the radius of the i^{th} particle at time t . Note that the units n are $[n] = 1/m$ (i.e., number of particles per size R). The mean particle size, denoted $\bar{R}(t)$ is given by

$$\bar{R}(t) = \frac{\int_0^L dR R n(R, t)}{\int_0^L n(R, t) dR} = \frac{\int_0^L dR R n(R, t)}{N(t)}, \quad (3.22)$$

where L denotes the size of the system. It turns our that the peak in the observed $n(R, t)$ shifts to larger R as t increases and its corresponding amplitude decreases. From Eq. (3.22), this lead to \bar{R} increasing with time, but $N(t)$ becoming smaller as t increases. This can be seen by tracking the solid fraction,

$$\phi = \frac{1}{V} \sum_{i=1}^N \frac{4\pi}{3} R_i^3(t), \quad (3.23)$$

which at late times becomes nearly a constant in coarsening systems. At late times and sufficiently deep quenches $\phi \approx 1$, which upon taking the average of Eq. (3.23) and re-arranging, gives ⁶

$$N(t) \approx \frac{V}{\frac{4\pi}{3} \bar{R}^3(t)}, \quad (3.24)$$

which shows that at a fixed time t , the number of particles $N(t)$ must clearly increases proportionately to volume V since the mean particle size \bar{R} is independent of V , or at least varies only very slowly with V at any given time t . It is also clear from the above considerations that the mean particle size defines a characteristic length for the system, which we define for later use as $l_c \sim \bar{R}(t)$.

Next, consider a quantity of the system of the form $Q(\bar{x}, R(t), t, N_p, V)$ where here \bar{x} is a position vector, N_p is the number of atoms in the system and V the volume. Since $t \sim \bar{R}(t)$ in the coarsening system under consideration, we can replace t by \bar{R} . There may be other length scales in the system that also change, like in the case of spinodal decomposition, the interface width W_ϕ , which grows with time. In that case, we can write Q as $Q(\bar{x}, R, \bar{R}(t), W_\phi(t), N_p, V)$. Let us consider the case where Q is extensive. By definition of extensive quantities, we can write $Q \rightarrow Vq(\bar{r}, R, \bar{R}, W_\phi, \rho)$, where ρ is the system density and q is a density of the original Q . Moreover, let us assume that the density of the quantity Q we are considering has units $[q] = m^p$, where p is some exponent. This makes it possible to scale out the length scale l_c from q and write $Q(\bar{r}, R, t) = V\bar{R}^p f(\bar{x}/l_c, R/l_c, W_\phi/l_c, \dots)$, where f is a dimensionless scaling function. Now, in first order phase transformations W_ϕ is a constant of order nm and does not change with time, and $W_\phi/l_c \ll 1$, so is can be dropped from f , giving

$$Q(\bar{r}, R, t) = V\bar{R}^p f\left(\frac{\bar{x}}{l_c}, \frac{R}{l_c}, \dots\right) \quad (3.25)$$

We next turn to the specific case of the number distribution $n(R, t)$ is a volume V (assumed to be very large compared to $\bar{R}^3(t)$). As discussed above, this is an extensive quantity that has units $[n] = m^{-1}$. Thus, using the format of Eq. (3.25) we can write $n(R, t)$ in the form

$$n(R, t) = V\bar{R}^p f\left(\frac{R}{\bar{R}(t)}\right) \quad (3.26)$$

⁶Since we are predominately interested in performing a dimensional analysis of the particle size distribution, can assume that $\bar{R}^3 = \text{bar}R^3$ here.

It is clear that the exponent p in Eq. (3.26) is $p = -4$, but let us derive it somewhat differently. To do so, we substitute Eq. (3.26) into $\int_0^L n(R, t) dR = N$, which using Eq. (3.24). yields,

$$\int_0^L n(R, t) dR = V \bar{R}^p f \int_0^L f\left(\frac{R}{\bar{R}(t)}\right) dR = \frac{V}{\frac{4\pi}{3} \bar{R}^3(t)} \quad (3.27)$$

Making the change of variable $\xi = R/\bar{R}(t)$ in Eq. (3.27) yields

$$\bar{R}^{p+1} \int_0^{\frac{L}{\bar{R}}} f(\xi) d\xi = \frac{3}{4\pi} \bar{R}^{-3} \quad (3.28)$$

Since we are considering late times here and $L/\bar{R} \gg 1$, it is reasonable to replace the upper limit of the integral in Eq. (3.28) by $L/\bar{R} \rightarrow \infty$ without too much loss of accuracy. This gives,

$$\underbrace{\bar{R}^{p+1} \int_0^\infty f(\xi) d\xi}_{\text{constant}} = \frac{3}{4\pi} \bar{R}^{-3}, \quad (3.29)$$

from which we immediately identify $p = -4$, consistent with our previous assumption. A more appropriate form for the particles size distribution is one that is intensive and independent of the system size. Defining by $\bar{n}(R, t)$ as the number of particles per unit volume in the range $R \rightarrow R + dR$ gives the following *a universal scaling for \bar{n}* ,

$$\bar{n}(R, t) = \bar{R}^{-4}(t) f\left(\frac{R}{\bar{R}(t)}\right) = \bar{R}^{-(d+1)}(t) f\left(\frac{R}{\bar{R}(t)}\right) \quad (3.30)$$

Precipitates grown in most alloys, such as for example Al-Cu alloys used for aerospace components, are typically nm in scale. It is common to characterize material microstructure on such scales through diffraction experiments, which essentially measure the square of the Fourier transform of density-density correlation function, which is itself proportional to the particle size distribution function (if we ignore defects and grain boundaries). The Fourier transform of $\bar{n}(R, t)$ is given by

$$\hat{\bar{n}}(k, t) = \int x^{-(d+1)} f\left(\frac{x}{\bar{R}}\right) e^{-ikx} dx \quad (3.31)$$

where k denotes wavevector and d the dimension of space. Once again, making the change of variables $\xi = x/\bar{R}$ yields

$$\hat{\bar{n}}(k, t) = \bar{R}^{-d} \underbrace{\int xi^{-(d+1)} f(\xi) e^{-i(k\bar{R})xi} d\xi}_{G(k\bar{R}(t))} \quad (3.32)$$

which shows that the integral is just some function of the argument $k\bar{R}(t)$. The *universal scaling form for the Fourier transform of \bar{n} is thus of the form*

$$\hat{\bar{n}}(k, t) = \bar{R}^{-d} G(k\bar{R}(t)) \quad (3.33)$$

Figure (3.5) shows a cartoon that show the qualitative behaviour of $\bar{n}(R, t)$ and $\hat{\bar{n}}(k, t)$ as well as the scaling functions $f(x)$ and $G(k)$.

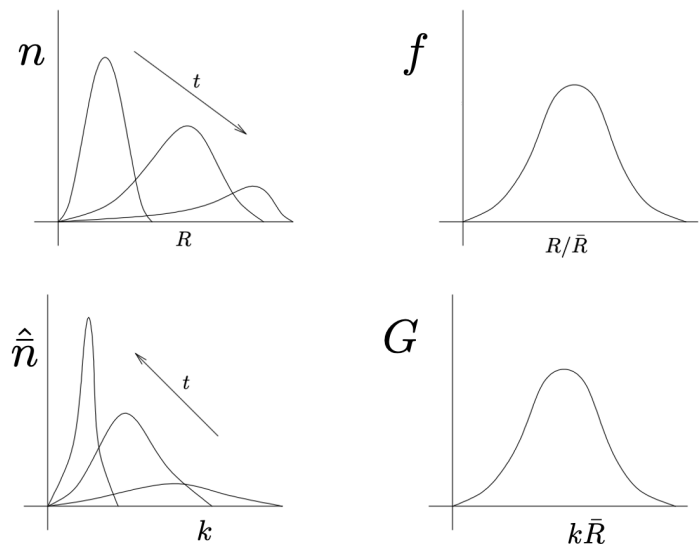


Figure 3.5: Left frames illustrate the late-time evolution of $\bar{n}(R, t)$ and $\hat{n}(k, t)$. The right hand frames show the universal scaling functions $f(x/\bar{R})$ and $G(k\bar{R})$. Reprinted from notes of Professor Martin Grant, McGill University, Department of Physics [11].

Chapter 4

Interface Instabilities and the Emergence of Solidification Microstructures

Previous chapters considered the kinetics of first order transformation in two broad phases. The first was the nucleation phase, which is governed by the rate of formation and size distribution of the first embryonic crystals to emerge in an undercooled liquid. The second described the rate at which post-critical grains grow and consume the matrix. Both stages tacitly assumed that crystals were spherical and neither considered that microscopic crystals could evolve dynamic morphologies as they grow. In fact, what emerges in an experiment are evolving grains that grow into very complex crystal structures, which include but are certainly not limited to, the well-known *snowflake* pattern. When individual crystals coalesce to form a solidified material (i.e., a solid), they leave behind a complex patterning that is typically referred to as “*microstructure*” in materials science. A detailed analysis of microstructure reveals that it contains sub-structures across scales from *nm-mm*. At the $\mu\text{m} - \text{mm}$ scales are the boundaries between merged crystals, which are referred to generically as *grain boundaries*. These are quintessential in defining the real-world mechanical properties of metals and their alloys, such as yield strength and ductility. In semiconductors, however, grain boundaries are not desirable as they wreak havoc on the pristine electronic properties of an otherwise perfect crystalline material. The second type of microstructures occurs in alloys (i.e. mixtures of two or more elemental metal components) involves the distribution of solutes throughout the bulks of crystalline grains, as well as solute segregation within the grain boundaries. Solute distribution and segregation is also critical in controlling mechanical and functional properties of materials. The third and fourth types of microstructure emerge on the scale of angstroms-nanometers and involves the formation of *vacancies* and *dislocations*. Vacancies (i.e., vacant lattice sites in the crystal lattice) are thermodynamically stable in solids at all temperatures. However, rapid rates of solidification can lead to large (i.e., non-equilibrium) vacancy densities, which change the effective properties of the solid phase. Dislocations emerge when a crystal is subjected to mechanical deformation, which leads to misfits between neighbouring atomic planes. This occurs by design when post-processing most metals and their alloys. However, dislocations can also emerge spontaneously during rapid solidification in technologies such as metal 3D printing, laser welding, splat cooling. Under extensive mechanical loading 3D dislocations can actually extend over many μm and become entangled; such tangles are perhaps the most important mechanism for dramatically mechanical strength of a metal alloy.

It is fair to say that microstructure determines by the nearly *all* the real-world properties of most materials. For a detailed and thorough review of the entire topic of solidification microstructures, from

the physics of how they emerge to their applications in engineering materials, the reader is referred to J. Dantzig and M. Rappaz book solidification [6]. In this section, we will examine the origins of complex microstructure by examining interface instabilities that occur in most 1st phase transformations. As a concrete backdrop, we will examine this topic in the context of solidification, starting first by deriving the kinetic laws governing crystallization, and following this with an investigation of how a solidifying front becomes unstable, the quintessential precursor to grain boundary formation and other complex shapes in materials.

4.1 Sharp-Interface Model of Solidification of a Pure Substance

Section 3.2.1 summarized the conditions that prevail along a moving interface separating two phases in a binary alloy. These comprise what is known as a *sharp-interface model* (or SIM for short) of a phase transformation. In this sub-section we consider the solidification of a pure substance and derive a SIM to describe this process. We derive the SIM here in more detail than we did for alloys since the thermal physics governing a pure material are simple to visualize and intuit. The steps shown here are straightforwardly adapted to the alloy case in Section 3.2.1, and are left to the reader, or can be found in the literature (e.g., Ref ([24])).

Consider a 1D front of a solid growing into a metastable liquid that is undercooled, as depicted in the cartoon in Fig. (4.1). As the interface advances, latent heat is released, which in turn diffuses into

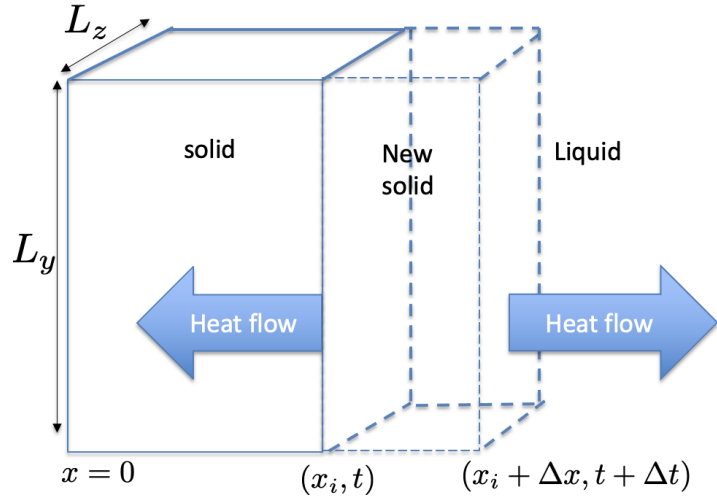


Figure 4.1: Cartoon of a 1D interface advancing toward the right into an undercooled liquid, depicting the directions of heat flow as new solid of thickness Δx is created during the advance of the solidification front. The interface position at time t is located at x_i . A cross section of area $A = L_y \times L_z$ is considered.

the bulks (solid and liquid). With reference to geometry and symbols in Fig. (4.1), the latent heat released when a slab of new solid of thickness Δx is formed over a time Δt is equal to $\rho L_f \Delta x L_y L_z$ where ρ is the density of the material (assumed for simplicity to be equal in both phases), L_f is the latent heat or enthalpy of fusion (per mass) for converting a volume of liquid to solid, $A = L_y \times L_z$ is the cross sectional area of the advancing front. We can relate the heat released to the advance speed of the front and the local temperature field as follows. The flux of heat across the liquid-facing end of the increment of the solid slab is given by Fick's law as $J_{x_i+\Delta x} = -k \partial T / \partial x|_{x_i+\Delta x}$, where T is the temperature field and k_L the thermal conductivity of the liquid. The flux of heat across the

solid-facing end of the solid slab is given by $J_{x_i} = -k_s \partial T / \partial x|_{x_i}$, where k_s is the thermal conductivity of the solid. Assuming 1D heat flow, conservation of energy requires that the difference in the heat fluxes across the two surfaces enclosing the small slab must equal the heat created, i.e.,

$$\rho L_f \Delta x L_y L_z = (J_{x_i + \Delta x} - J_{x_i}) L_y L_z \Delta t \quad (4.1)$$

Simplifying Eq. (4.1), rearranging terms and taking the limit $\Delta t \rightarrow 0$ and $\Delta x \rightarrow 0$ gives

$$\rho L_f v_n = k_s \left. \frac{\partial T}{\partial x} \right|_{x_i^+} - k_L \left. \frac{\partial T}{\partial x} \right|_{x_i^-} \quad (4.2)$$

where $v_n = \lim_{\Delta t \rightarrow 0} (\Delta x / \Delta t)$ and x_i^\pm represents the liquid(+) / solid(-) sides of the mathematically sharp (in the limit) solid-liquid interface. Similar arguments adapted to a small cross section of a complex solid-liquid interface advancing in 3D generalize Eq. (4.2) to its 3D form as

$$\rho L_f v_n = k_s \nabla T \cdot \hat{n}|_s - k_L \nabla T \cdot \hat{n}|_L \quad (4.3)$$

where \hat{n} denotes the unit normal to the interface, which by convention points into the liquid, and where v_n represents the interface velocity along the normal direction. The subscripts s and L denotes the solid/liquid sides of the interface. Equation (4.3) serves as Neumann type of boundary condition that relates derivatives in $T(x, y, z, t)$ to the local interface speed.

The temperature field $T(x, y, z, t)$ must also satisfy a Dirichlet type of boundary condition at the solid-liquid interface, which is called the *Gibb-Thomson* condition, given by

$$T_{\text{int}} = T_m - 2\Gamma\kappa - \frac{v_n}{\mu} \quad (4.4)$$

where T_{int} is the interface temperature, T_m is the melting temperature, Γ is the so-called Gibbs-Thomson coefficient, κ is the local mean curvature of the interface ¹ and μ is the atomic mobility in the liquid. The Gibbs-Thomson coefficient Γ is related to the more familiar solid-liquid interface energy γ_{sl} by

$$\Gamma = \frac{\gamma_{sl} T_m}{\rho L_f} \quad (4.5)$$

The atomic mobility μ can be in theory determined (sometimes!) from molecular dynamics simulations. It is instructive to analyze the physical meaning of Eq. (4.4). When $\kappa = 0$ (as in Fig. (4.1)) and $v_n = 0$, it reduces to the well-known condition that states that a stationary solid-liquid interface is at the melting temperature (i.e. the only temperature that can simultaneously support both phases). When $\kappa \neq 0$ and $v_n = 0$, Eq. (4.4) states that the equilibrium temperature is depressed by the local curvature of the interface. The last term in Eq. (4.4) depresses the equilibrium temperature due to non-equilibrium attachment kinetics at the interface. To see this, invert the equation for the speed of the interface in 1D, which gives $v_n = \mu (T_{\text{int}} - T_m)$, which tells us that the speed of the interface is directly proportional to the degree of undercooling at the solid-liquid interface, which makes perfect sense! It is noteworthy, however, that for very slow rates of solidification ($0 < v_n < \text{mm/s}$), the kinetic undercooling term is typically ignored in solidification modelling. This is justified for metals and their alloys because μ is quite large compared to most soft-matter systems. For higher rates of solidification,

¹The mean curvature in 3D is $\kappa = (1/R_1 + 1/R_2)/2$ where R_1 and R_2 are the local radii of curvature in the x and y directions. In 2D the mean curvature reduces to $1/2R$ (see Ref. [6] page 52) and so the factor of 2 disappears in the statement of the Gibbs-Thomson condition.

the kinetic term in the Gibbs-Thomson condition must be included and, indeed, produces quite exotic non-equilibrium effects on the morphology and composition (in alloys) of phases produced.

Away from the solid-liquid interface, the extended temperature field $T(x, y, z, t)$ must evolve in time according to the energy conservation equation, i.e.,

$$\begin{aligned}\rho c_p \frac{\partial T}{\partial t} &= -\nabla \cdot \bar{J}_q \\ &= \nabla (k \nabla T),\end{aligned}\quad (4.6)$$

where c_p is the specific heat at constant pressure and $\bar{J}_q = -k \nabla T$ is *Fick's Law*, a constitutive relation between heat flux and temperature, and where k is the thermal conductivity. Eq. (4.6) becomes

$$\frac{\partial T}{\partial t} = \nabla (\alpha \nabla T), \quad (4.7)$$

where $\alpha = k/(\rho c_p)$ is the thermal diffusivity.²

Equation (4.7) and the boundary conditions defined by Eq. (4.3) and Eq. (4.4) define a complete sharp interface model for the evolution of a solidification front, as well as the accompanying temperature field $T(x, y, z, t)$. These equations will be examined in the following pages to elucidate the physical mechanism behind the emergence of complex dendritic morphologies.

4.2 Solidification of an Undercooled Spherical Liquid Drop

This section solves the SIM model of section (4.1) in spherical geometry, a solution that will then be used in the next section to examine how linear instabilities emerge in a solidifying front. The original work on this topic was done by Mullins and Sekerka in their seminal work in Ref. [22]. For detailed solutions to numerous other solidification problems in various geometries, as well as for a comprehensive review of alloy thermodynamics, the reader is referred to the comprehensive and excellently-written work on solidification written by two pioneers in the field of solidification, Jon Dantzig and Michelle Rappaz [6].

Consider the growth of a 3D spherically symmetric crystal sphere of size $R(t)$ growing into an undercooled liquid, as depicted in the cartoon of Fig. (4.2). The sharp interface equations describing the solidification of the crystal in this geometry are described by Equation (4.7), Eq. (4.3) and Eq. (4.4), which in spherical co-ordinates (r, θ, ϕ) become

$$\begin{aligned}\frac{\partial T}{\partial t} &= \frac{\alpha_s}{r^2} \frac{\partial}{\partial r} \left(r^2 \frac{\partial T}{\partial r} \right), \quad 0 < r < R(t) \\ \frac{\partial T}{\partial t} &= \frac{\alpha_L}{r^2} \frac{\partial}{\partial r} \left(r^2 \frac{\partial T}{\partial r} \right), \quad R(t) < r < \infty \\ T_{\text{int}} &= T_m - 2\Gamma\kappa = T_m - \frac{2\Gamma}{R(t)}, \quad r = R(t)) \\ \rho_L L_f \frac{dR}{dt} &= k_s \left. \frac{\partial T}{\partial r} \right|_{r=R^-} - k_L \left. \frac{\partial T}{\partial r} \right|_{r=R^+} \\ T(r \rightarrow \infty) &= T_\infty\end{aligned}\quad (4.8)$$

²It is reasonable to approximate thermal conductivity k as constant in most phase transformations in metals. It is stressed, however, that for mass diffusion in alloys, the ratio of solute diffusivities in solid/liquid $\sim 10^{-3} - 10^{-4}$, and so the solute diffusion *cannot* be modelled as a constant as it leads to different physics from the constant-diffusion case.

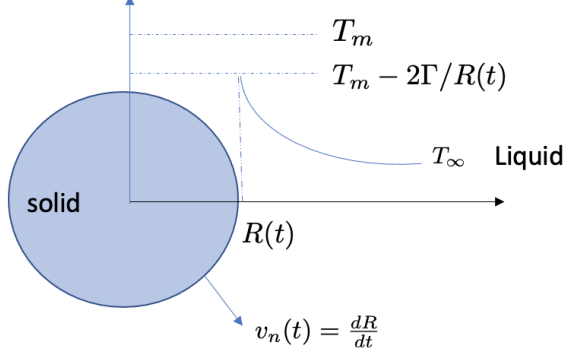


Figure 4.2: 3D crystal sphere solidifying into an undercooled liquid. At time t the interface is located at $R(t)$ and its speed is $v_n = dR/dt$. The interface temperature deviates from the equilibrium melting temperature T_m due to the curvature, where Γ is the Gibbs-Thomson coefficient. Also shown is the general shape of the temperature field away from the sphere, where T_∞ is the far-field temperature.

where α_L/α_s are the thermal diffusivities of the liquid/solid and T_∞ is the far-field temperature. Here, R^\pm refer to the liquid/solid sides of the interface at $r = R(t)$. It is also assumed that there is some initial temperature field $T(r, t = 0)$ to be determined below.

It is instructive to rescale the Equation (4.8) to make them dimensionless. We begin by making space and time dimensionless according to $\bar{r} = r/R_i$ and $\bar{t} = t/t_c$, where R_i is the initial crystal radius and $t_c = R_i^2/(\alpha_L \Delta)$ is a characteristic time, with $\Delta = c_p \Delta T / L_f$ and $\Delta T = T_m - T_\infty$. The temperature is also rescaled to $\Theta = (T - T_m)/\Delta T$. In scaled units, the radius of the crystal becomes $\bar{R}(t)$ and its curvature $\bar{\kappa} = 1/\bar{R}(t)$. We further define the ratios $k_r = k_s/k_L$ and $\alpha_r = \alpha_s/\alpha_L$ (which satisfy $k_r = \alpha_r$ if we assume the same density in both phases). We also define the dimensionless critical nucleus³ size by $\bar{R}^* = R^*/R_i$. These scalings and definitions are compactly summarized as follows:

$$\begin{aligned} \bar{r} &= r/R_i, \quad \bar{t} = (\alpha_L \Delta / R_i^2) t, \quad \Theta = (T - T_m) / \Delta T, \quad \bar{R}(t) = R(t)/R_i, \\ \Delta &= c_p \Delta T / L_f, \quad \Delta T = T_m - T_\infty, \quad k_r = k_s/k_L, \quad \alpha_r = \alpha_L/\alpha_s, \quad \bar{R}^* = R^*/R_i \end{aligned} \quad (4.9)$$

Note that in scaled units, the initial conditions are $\bar{R} = 1$, since R_i is initial crystal size. Also for future reference, Δ is referred to as the *Stefan number*.

Applying the re-scalings in Eq. (4.9) converts Eq. (4.8) to the more compact form

$$\begin{aligned} \Delta \frac{\partial \Theta}{\partial \bar{t}} &= \frac{\alpha_r}{\bar{r}^2} \frac{\partial}{\partial \bar{r}} \left(\bar{r}^2 \frac{\partial \Theta}{\partial \bar{r}} \right), \quad 0 < \bar{r} < \bar{R}(t) \\ \Delta \frac{\partial \Theta}{\partial \bar{t}} &= \frac{1}{\bar{r}^2} \frac{\partial}{\partial \bar{r}} \left(\bar{r}^2 \frac{\partial \Theta}{\partial \bar{r}} \right), \quad \bar{R}(t) < \bar{r} < \infty \\ \Theta_{\text{int}} &= -(\bar{R}^*) \bar{\kappa} = -\frac{\bar{R}^*}{\bar{R}(\bar{t})}, \quad \bar{r} = \bar{R}(t) \\ \frac{d\bar{R}}{d\bar{t}} &= k_r \left. \frac{\partial \Theta}{\partial \bar{r}} \right|_{\bar{r}=\bar{R}^-} - \left. \frac{\partial \Theta}{\partial \bar{r}} \right|_{\bar{r}=\bar{R}^+} \\ \Theta(\bar{r} \rightarrow \infty) &= -1 \end{aligned} \quad (4.10)$$

³The critical nucleus size is $R^* = 2\gamma_{sl}/\Delta G$. Using Eq. (4.5) and $\Delta G = (\rho L_f/T_m)\Delta T$ for a pure substance [6] gives $R^* = 2\Gamma/\Delta T$.

It is instructive to compute the typical magnitude Δ for Aluminum, a common metal of practical interest. For Al, $c_p = 1.19 \times 10^3$ J/kg-K and $L_f = 3.98 \times 10^5$ J/kg, and typical undercooling values during solidification are of the order $\Delta T \sim 1$ K. This gives $\Delta \approx 0.003 \ll 1$. In this limit, it is convenient to neglect the time derivatives in Eq. (4.10) in what follows.

The solution of the diffusion equations in Eq. (4.10) is of the form $\Theta(\bar{r}, \bar{t}) = a(\bar{t}) + b(\bar{t})/\bar{r}$ (with the time derivatives in Eq. (4.10) neglected). The constants a and b are found by substituting $\bar{r} = \bar{R}(\bar{t})$ into $\Theta(\bar{r}, \bar{t})$ and matching the result to the right hand side of the third line in Eq. (4.10) (the Gibbs-Thomson condition). This together with the far-field condition in Eq. (4.10) gives $a(\bar{t}) = -1$ and $b(\bar{t}) = (1 - \bar{R}^*/\bar{R}(\bar{t})) \bar{R}(\bar{t})$. The compete solution of Θ in the liquid is thus

$$\Theta(\bar{r}, \bar{t}) \equiv \Theta_o^L(\bar{r}, \bar{t}) = \left\{ 1 - \frac{\bar{R}^*}{\bar{R}(\bar{t})} \right\} \frac{\bar{R}(\bar{t})}{\bar{r}} - 1, \quad \bar{R}(\bar{t}) < \bar{r} < \infty \quad (4.11)$$

Applying the same solution form to the solid and considering that the solution must be bounded requires that $b = 0$, while the Gibbs-Thomson condition in Eq. (4.10) now gives $a = -\bar{R}^*/\bar{R}(\bar{t})$. This gives the complete solution of Θ in the solid as

$$\Theta(\bar{r}, \bar{t}) \equiv \Theta_o^s(\bar{r}, \bar{t}) = -\frac{\bar{R}^*}{\bar{R}(\bar{t})}, \quad 0 < \bar{r} < \bar{R}(\bar{t}) \quad (4.12)$$

Notice that Θ is continuous at the interface as it must from our intuition that temperature must be continuous at the interface. The notations $\Theta_o^{s,L}$ have been made for later use.

The flux conservation equation in Eq. (4.10) is next used to find an equation for $\bar{R}(\bar{t})$. The derivative of the temperature at the solid side of the interface is $\partial\Theta^s/\partial\bar{r}|_{\bar{r}=\bar{R}-} = 0$, while the derivative on the liquid side of the interface is $\partial\Theta^L/\partial\bar{r}|_{\bar{r}=\bar{R}+} = -(1 - \bar{R}^*/\bar{R}(\bar{t}))/\bar{R}(\bar{t})$. Substituting these expressions into the flux conservation equation gives

$$\frac{d\bar{R}(\bar{t})}{d\bar{t}} = \left(1 - \frac{\bar{R}^*}{\bar{R}(\bar{t})} \right) \frac{1}{\bar{R}(\bar{t})} \quad (4.13)$$

This equation, solved subject to the initial condition that $\bar{R}(\bar{t} = 0) = 1$, gives the dimensionless size of the crystal as a function of time.

It is noteworthy that there is *only* one initial condition that can be satisfied by $\Theta(\bar{r}, \bar{t})$ since we neglected the time derivatives in Equation (4.10). This given by taking the limit $\bar{R}(\bar{t} = 0) = 1$ in Eq. (4.11) and Eq. (4.12), which gives,

$$\Theta(\bar{r}, \bar{t} = 0) = \begin{cases} \Theta_o^s(\bar{r}, \bar{t} = 0) = -\bar{R}^*, & 0 < \bar{r} < 1 \\ \Theta_o^s(\bar{r}, \bar{t} = 0) = \{1 - \bar{R}^*\}/\bar{r} - 1, & 1 < \bar{r} < \infty \end{cases}$$

Moreover, when $\bar{t} = 0$, Eq. (4.13) gives

$$\frac{d\bar{R}(\bar{t})}{d\bar{t}} \Big|_{\bar{t}=0} = 1 - \frac{R^*}{R_i}, \quad (4.14)$$

where we have reverted to dimensional units on the right hand side of Eq. (4.14) for clarity. Equation (4.14) implies that only crystals whose initial size is greater than the critical nucleus size, i.e. $R_i > R^*$, can grow, which of course makes perfect sense. For the case of precisely $R_i = R^*$, the initial temperature field $\Theta(\bar{r}, \bar{t} = 0) = -1$ everywhere, which corresponds to $T(r, t = 0) = T_\infty$, and the crystal size neither grows or shrinks.

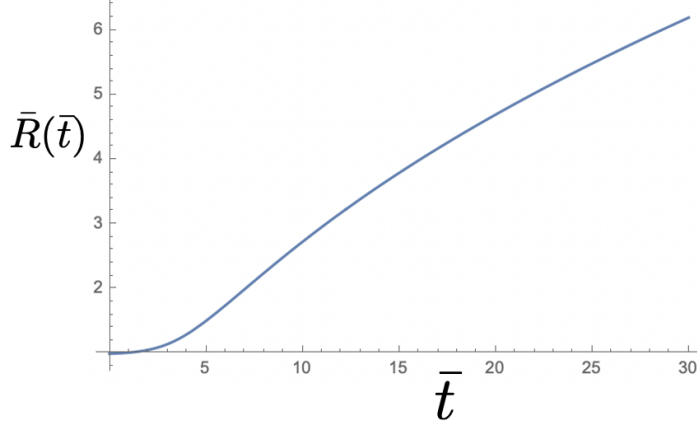


Figure 4.3: The solution of Eq. (4.13) for a crystal seed with initial radius $R_i = 1.01 R^*$, i.e. just slightly greater than the critical nucleus size. The early time growth is slow and then grows rapidly at intermediate times. At late times, the growth settles onto the usual $\bar{R}(\bar{t}) \sim \bar{t}^{1/2}$ growth law for planar, or near-planar interfaces growing into an undercooled melt.

4.3 Stability of an Undercooled Spherical Liquid Drop

In this section we examine the stability of a solidifying spherical liquid drop whose spatiotemporal evolution is described by Eqs. (4.11)-(4.13). We will show how it is impossible for a spherical crystal to remain spherical beyond some size $R(t)$, and after while its interface becomes unstable to perturbations, giving rise to wave-like undulations that are the precursors to the complex morphologies that arise in crystal microstructures, such as the tree-like patterns called *dendrites*, which give snowflakes in ice their shape, and also appear in solidified metals and their alloys.

In what follows, we assume that the base spherical crystal interface shape $\bar{R}_o(\bar{t})$ studied in Section (4.2) will become unstable as it starts to evolve very small random undulations. The radius of the crystal, from the centre to a point on the solid-liquid interface, is now represented as $\bar{R}(\theta, \phi, \bar{t}) = \bar{R}_o(\bar{t}) + \bar{R}_1(\theta, \phi, \bar{t})$, where \bar{R}_1 is a small perturbation away from the base solution. Here, θ and ϕ are the polar angles of the (r, θ, ϕ) co-ordinate system. *It is also noted that we will continue to work in the dimensionless units described in Eq. (4.9).* The undulations encoded in \bar{R}_1 can be expanded is a series of spherical harmonics $Y_l^m(\theta, \phi)$, where l and m are the integer indices of the harmonic that satisfy $l = 0, 1, 2, \dots$ and $-m < l < m$. As is typically done in perturbation analysis, we will study the growth rate of any given harmonic as it grows at early time, when its amplitude is very small. To do so, we expand the shape of the crystal as

$$\bar{R}(\theta, \phi, \bar{t}) = \bar{R}_o(\bar{t}) + \delta(\bar{t}) Y_l^m(\theta, \phi) \quad (4.15)$$

where the small amplitude of the harmonic undulation is captured by the dimensionless quantity $\delta(\bar{t}) \ll 1$. As the crystal becomes unstable, naturally so will the thermal field that accompanies its growth. We thus expect that the complete solution of the thermal field within the growing solid and outside in the liquid is given by the expansion

$$\begin{aligned} \Theta_s(\bar{r}, \theta, \phi, \bar{t}) &= \Theta_o^s(\bar{r}, \bar{t}) + \delta(\bar{t}) \Theta_1^s(\bar{r}, \theta, \phi, \bar{t}), \quad 0 < \bar{r} < \bar{R}(\theta, \phi, \bar{t}) \\ \Theta_L(\bar{r}, \theta, \phi, \bar{t}) &= \Theta_o^L(\bar{r}, \bar{t}) + \delta(\bar{t}) \Theta_1^L(\bar{r}, \theta, \phi, \bar{t}), \quad \bar{R}(\theta, \phi, \bar{t}) < \bar{r} < \infty, \end{aligned} \quad (4.16)$$

where here, $\Theta_o^{s,L}$ are the base solutions of the perfectly spherical crystal given by Eq. (4.11) and Eq. (4.12), and $\Theta_1^{s,L}$ are perturbations of the dimensionless temperature away from the base solution. These are considered of order unity and the amplitude of the temperature perturbation is carried by δ . The goal of the remainder of this section is to determine an equation satisfied by $\delta(\bar{t})$ and the associated thermal perturbation fields $\Theta_1^{s,L}$. Once that is done, we can assess what harmonic morphologies (i.e. value of l and their subharmonics in m) can become unstable and grow during solidification and which ones remain stable and do not manifest themselves in the early-time crystal morphology.

To proceed, we substitute the expansion of the thermal fields in Eq. (4.16) into the diffusion equations $\nabla_{(\theta,\phi)}^2 \Theta_L(\bar{r},\theta,\phi,\bar{t}) = 0$ and $\nabla_{(\theta,\phi)}^2 \Theta_s(\bar{r},\theta,\phi,\bar{t}) = 0$, which are just the first two lines of Eq. (4.10) with (i) the time derivatives neglected and (ii) with the laplacian written in full (\bar{r},θ,ϕ) co-ordinates. Doing so gives leads to the following equation to be satisfied by both Θ_1^s and Θ_1^L ,

$$\frac{1}{\bar{r}^2} \frac{\partial}{\partial \bar{r}} \left(\bar{r}^{-2} \frac{\partial \Theta_1^{s,L}}{\partial \bar{r}} \right) + \frac{1}{\bar{r}^2 \sin \theta} \frac{\partial}{\partial \Theta_1^{s,L}} \left(\sin \theta \frac{\partial \Theta_1^{s,L}}{\partial \theta} \right) + \frac{1}{\bar{r}^2 \sin^2 \theta} \frac{\partial^2 \Theta_1^{s,L}}{\partial \phi^2} = 0 \quad (4.17)$$

it is noted that the base solutions disappear when the forms in Eq. (4.16) are substituted into the laplacian since, *by construction*, they automatically satisfy the radial-only part of the laplacian (i.e. $\partial_{\bar{r}} (\bar{r}^2 \partial \Theta_o^{s,L} / \partial \bar{r}) = 0$), leaving only Eq. (4.17) to be satisfied by the perturbation functions in each region. Substituting a solution for $\Theta_1^{s,L} = f(\bar{r}) Y_l(\theta, \phi)$ into Eq. (4.17), and using separation of variables (or just look up in some mathematical physics text), it is straightforward to show that the general solution of Eq. (4.17) is given by

$$\Theta_1^{s,L}(\bar{r},\theta,\phi) = \left\{ A(\bar{t}) \bar{r}^l + B(\bar{t}) \bar{r}^{-l} \right\} Y_l^m(\theta, \phi) \quad (4.18)$$

The requirements of bounded solutions requires that $A = 0$ in the general solution in the liquid region, and $B = 0$ in the general solution in the solid region. The completed solution of the dimensionless temperature field is thus given by

$$\begin{aligned} \Theta^s(\bar{r},\theta,\phi,\bar{t}) &= \theta_o^s(\bar{r},\bar{t}) + \delta(\bar{t}) A_s(\bar{t}) \bar{r}^l Y_l^m(\theta, \phi), \quad 0 < \bar{r} < \bar{R}(\theta, \phi, \bar{t}) \\ \Theta^L(\bar{r},\theta,\phi,\bar{t}) &= \theta_o^L(\bar{r},\bar{t}) + \delta(\bar{t}) \frac{A_L(\bar{t})}{\bar{r}^{l+1}} Y_l^m(\theta, \phi), \quad \bar{R}(\theta, \phi, \bar{t}) < \bar{r} < \infty \end{aligned} \quad (4.19)$$

The coefficients A_s , A_L and δ will be determined from the boundary conditions in Eq. (4.10) (i.e., the last three lines), each of which will be adapted to polar co-ordinates and evaluated on the surface $\bar{R}(\theta, \phi, \bar{t})$ in Eq. (4.15).

To apply the Gibbs-Thomson boundary condition in Eq. (4.10) to the perturbed temperature solutions, it must first be upgraded from its spherically symmetric form to one suitable for an arbitrary 3D surface, i.e.

$$\Theta_{\text{int}}(\theta, \phi) = -\frac{2\Gamma}{\Delta T} \bar{\kappa}(\theta, \phi) = -\frac{R^*}{R_i} \bar{\kappa}(\theta, \phi) = -\bar{R}^* \bar{\kappa}(\theta, \phi), \quad (4.20)$$

where the dimensionless curvature $\bar{\kappa}(\theta, \phi)$ applies to a general 3D surface ⁴, such as that given by Eq. (4.15). Applying the definition of curvature for a 3D surface in polar co-ordinates to $\bar{R}(\theta, \phi, \bar{t})$

⁴Curvature is defined by $\bar{\kappa} = (1/\bar{R}_1 + 1/\bar{R}_2)/2$, where \bar{R}_1 and \bar{R}_2 are the principal radius of curvature. Readers following Ref. [22] should note that they don't have the factor of 1/2 in the definition of curvature, and so their expression for curvature must be divided by 1/2.

and expanding the answer to linear order in δ yields

$$\bar{\kappa}(\theta, \phi) = \frac{1}{\bar{R}_o(\bar{t})} \left\{ 1 - \frac{\delta(\bar{t}) Y_l^m(\theta, \phi)}{\bar{R}_o(\bar{t})} \right\} - \frac{\delta(\bar{t})}{2\bar{R}_o^2(\bar{t})} \mathcal{L}\{\partial_\theta, \partial_\phi\} Y_l^m(\theta, \phi), \quad (4.21)$$

where $\mathcal{L}\{\partial_\theta, \partial_\phi\}$ is compact notation for the operator

$$\mathcal{L}(\partial_\theta, \partial_\phi) \equiv \frac{1}{\sin \theta} \frac{\partial}{\partial \theta} \left(\sin \theta \frac{\partial}{\partial \theta} \right) + \frac{1}{\sin^2 \theta} \frac{\partial^2}{\partial \phi^2} \quad (4.22)$$

Applying the spherical harmonic identity $\mathcal{L}\{\partial_\theta, \partial_\phi\} Y_l^m(\theta, \phi) = -l(l+1) Y_l^m(\theta, \phi)$ simplifies Eq. (4.21) to the more compact form

$$\bar{\kappa}(\theta, \phi) = \frac{1}{\bar{R}_o(\bar{t})} \left\{ 1 - \frac{\delta(\bar{t}) Y_l^m(\theta, \phi)}{\bar{R}_o(\bar{t})} \right\} + \frac{\delta(\bar{t})}{2\bar{R}_o^2(\bar{t})} l(l+1) Y_l^m(\theta, \phi) \quad (4.23)$$

Finally, substituting Eq. (4.23) into Eq. (4.20) and factoring like terms yields the order- δ Gibbs-Thomson condition,

$$\Theta_{\text{int}}(\theta, \phi) = -\frac{\bar{R}^*}{\bar{R}_o(\bar{t})} - \delta(\bar{t}) \frac{\bar{R}^*}{2\bar{R}_o^2(\bar{t})} [(l+2)(l-1)] Y_l^m(\theta, \phi), \quad (4.24)$$

which is next to evaluate the complete form of the perturbed thermal solutions.

The strategy next is as follows: (1) evaluate each of the thermal solutions in Eq. (4.19) at $\bar{r} = \bar{R}_o(\bar{t}) + \delta(\bar{t}) Y_l^m(\theta, \phi)$; (2) expand the result to order δ ; (3) compare the expanded result (separately for the liquid and the solid) to Eq. (4.24) and extract the coefficients A_s and A_L . Proceeding as per the above three steps yields the following expansion for the thermal field of the liquid evaluated at $\bar{r} = \bar{R}$,

$$\Theta_{\text{int}}^L \simeq \left(-1 + \frac{C_L}{\bar{R}_o(\bar{t})} \right) + \delta(\bar{t}) \left(\frac{A_L}{\bar{R}_o^{l+1}(\bar{t})} - \frac{C_L}{\bar{R}_o^2(\bar{t})} \right) Y_l^m(\theta_1), \quad (4.25)$$

where $C_L = (\bar{R}_o(\bar{t}) - \bar{R}^*)$. Equating Eq. (4.25) to Eq. (4.24) and matching terms of order $\mathcal{O}(1)$ shows that this term is just the base solution in Eq. (4.11), evaluated at $\bar{R}_o(\bar{t})$. Matching of the $\mathcal{O}(\delta)$ terms yields

$$\begin{aligned} A_L(\bar{t}) &= \left\{ 1 - \frac{\bar{R}^*}{\bar{R}_o(\bar{t})} \right\} \bar{R}_o^l(\bar{t}) - \frac{\bar{R}^*}{2} \bar{R}_o^{l-1}(\bar{t}) [(l+2)(l-1)] \\ &= \bar{R}_o^l(\bar{t}) - \frac{\bar{R}^*}{2} \bar{R}_o^{l-1}(\bar{t}) l(l+1) \end{aligned} \quad (4.26)$$

Substituting this expression for A_L into the second line of Eq. (4.19) yields the complete *liquid* phase solution to order δ ,

$$\Theta^L(\bar{r}, \theta, \phi, \bar{t}) = \frac{\{\bar{R}_o(\bar{t}) - \bar{R}^*\}}{\bar{r}} + \delta(\bar{t}) \frac{\{\bar{R}_o^l(\bar{t}) - \frac{1}{2}\bar{R}^* l(l+1) \bar{R}_o^{l-1}(\bar{t})\}}{\bar{r}^{l+1}} Y_l^m(\theta, \phi) - 1, \quad \bar{R}(\theta, \phi, \bar{t}) < \bar{r} < \infty \quad (4.27)$$

Proceeding in exactly the same way with the solid phase solution in Eq. (4.19) and matching it to Eq. (4.24) yields the complete *solid* phase solution to order δ

$$\Theta^s(\bar{r}, \theta, \phi, \bar{t}) = -\frac{\bar{R}^*}{\bar{R}_o(\bar{t})} - \delta(\bar{t}) \left\{ \frac{\bar{R}^* [(l+2)(l-1)]}{2\bar{R}_o^{l+2}(\bar{t})} \right\} \bar{r}^l Y_l^m(\theta, \phi), \quad 0 < \bar{r} < \bar{R}(\theta, \phi, \bar{t}) \quad (4.28)$$

The final phase of the stability analysis of the base crystal solution $\bar{R}(\bar{t})$ is to find an equation for the amplification factor, or *growth rate*, coefficient $\delta(\bar{t})$. This is done via the flux conservation equation, which becomes

$$v_n = k_r \nabla \Theta^s(\bar{r}, \theta, \phi) \cdot \hat{n}|_{\bar{R}-} - \nabla \Theta^L(\bar{r}, \theta, \phi) \cdot \hat{n}|_{\bar{R}+} \quad (4.29)$$

The procedure is as follows: (1) use the perturbed thermal solutions in Eq. (4.19) to evaluate the right hand side terms of Eq. (4.29), while the surface $\bar{r} = \bar{R}_o(\bar{t}) + \delta(\bar{t}) Y_l^m(\theta, \phi)$ is used to evaluate the normal velocity. It is recalled that only terms to order $\delta(\bar{t})$ are retained in these evaluations; (2) compare terms of the same order in δ to yield differential equation satisfied by $\delta(\bar{t})$. Since $\delta(\bar{t}) \ll 1$ the normal velocity $v_n = \bar{v} \cdot \hat{n}$ can be approximated by the time derivative of $\bar{R}(\theta, \phi, \bar{t})$ and the gradients on the surface of $\bar{R}(\theta, \phi, \bar{t})$ can be approximated by radial derivatives. This simplifies Eq. (4.29) to

$$\frac{d\bar{R}_o(\bar{t})}{d\bar{t}} + Y_l^m(\theta, \phi) \frac{d\delta(\bar{t})}{d\bar{t}} \simeq k_r \left. \frac{\partial \Theta^s}{\partial \bar{r}} \right|_{\bar{R}(\bar{r}, \theta, \phi)} - \left. \frac{\partial \Theta^L}{\partial \bar{r}} \right|_{\bar{R}(\bar{r}, \theta, \phi)} \quad (4.30)$$

Proceeding with the evaluation and simplification of the first derivative term on the RHS of Eq. (4.30) gives

$$k_r \left. \frac{\partial \Theta^s}{\partial \bar{r}} \right|_{\bar{r}=\bar{R}(\bar{r}, \theta, \phi)} = -\frac{\delta(\bar{t}) k_r \bar{R}^*[(\ell+2)(\ell-1)\ell]}{2\bar{R}_o^3(\bar{t})} Y_l^m(\theta, \phi) \quad (4.31)$$

Similarly, the second term on the RHS of Eq. (4.30) can be approximated by

$$\left. \frac{\partial \Theta^L}{\partial \bar{r}} \right|_{\bar{r}=\bar{R}(\bar{r}, \theta, \phi)} = -C + \delta(\bar{t}) \left\{ \frac{2C}{\bar{R}_o(\bar{t})} - \left\{ \frac{1}{\bar{R}_o^2(\bar{t})} - \frac{\bar{R}^*}{2\bar{R}_o^3(\bar{t})} \ell(\ell+1) \right\} (\ell+1) \right\} Y_l^m(\theta, \phi), \quad (4.32)$$

where

$$C \equiv \left\{ 1 - \frac{\bar{R}^*}{\bar{R}_o(\bar{t})} \right\} \frac{1}{\bar{R}_o(\bar{t})} \quad (4.33)$$

We next substitute Eq. (4.31) and Eq. (4.32) into Eq. (4.30) and comparing orders of $\delta(\bar{t})$. To order $\mathcal{O}(1)$, we recover Eq. (4.13) as we must since this is a perturbation theory. Comparing terms of order $\mathcal{O}(\delta)$ yields, after some algebra and simplifications,

$$\frac{d\delta(\bar{t})}{d\bar{t}} = \left\{ 1 - \frac{\bar{R}^*}{2\bar{R}_o(\bar{t})} [(\ell+1)(\ell+2) + 2 + k_r \ell(\ell+2)] \right\} \frac{(\ell-1)}{\bar{R}_o^2(\bar{t})} \delta(\bar{t}) \quad (4.34)$$

where we used the identity $\ell(\ell+1) - 4 = (\ell-1)[(\ell+1)(\ell+2) + 2]$ to arrive at Eq. (4.34). It is noted that the solution of Eq. (4.34) requires the solution of Eq. (4.13) to be input on the RHS, which is also a standard outcome of most perturbation theories; higher-order perturbations to a desired solution require input from the lower order perturbation.

Analysis of Eq. (4.34) shows that an $l=0$ mode of a perturbation around the base circular seed decays in amplitude at $\bar{t} \rightarrow \infty$ regardless of the size of the $R_o(\bar{t})$. A perturbation with mode $l=1$ also never becomes unstable since $\delta(\bar{t}) = 0$ for all \bar{t} ; this is referred to as *neutral stability*). The first surface instability around $R_o(\bar{t})$ that can grow corresponds to any mode of $l=2$. Examining the expression in the curly parentheses in Eq. (4.34) reveals that the growth rate of any $l=2$ mode grows in amplitude when the base circular seed satisfies

$$\bar{R}_o(\bar{t}) > (7 + 4k_r) \bar{R}^* \quad (4.35)$$

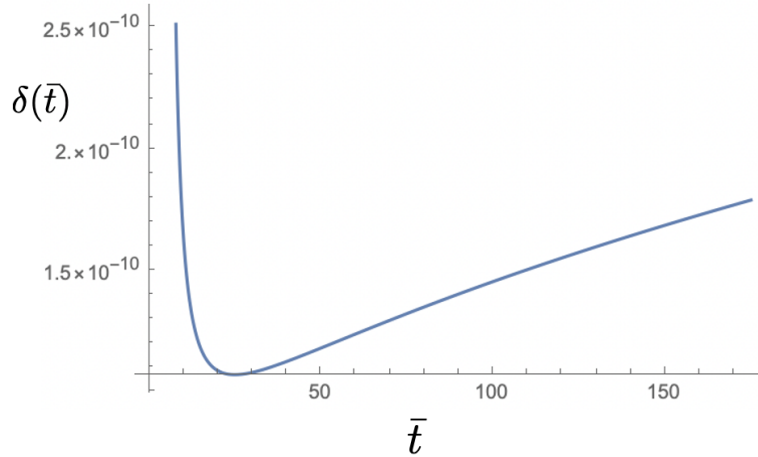


Figure 4.4: Amplification growth rate governed by Eq. (4.34) for an $l = 2$ mode around an undercooled crystal seed. This plot depicts the case of $\bar{R}^* = 0.5$ (i.e. initial seed size $R_i = 2\bar{R}^*$) and $k_r = 1$. The early time growth decays because the right hand side of Eq. (4.34) is negative when $\bar{R}(\bar{t}) \sim 1$. A changeover from decay to growth of the amplification factor occurs at about $\bar{t} \sim 25$, whereupon $\bar{R}_o(\bar{t}) > (7 + 4k_r)\bar{R}^* = 11\bar{R}^*$.

In other words when the base (i.e. first order) crystal solution becomes larger than the critical nucleus size by a factor of $(7 + 4k_r)$, the surface of an circular, undercooled, crystal seed will exhibit surface undulation that are some linear combination of the $l = 2$ family of spherical harmonics. Figure (4.4) shows this effect for the growth rate of the amplification factor $\delta(\bar{t})$ for an $l = 2$ mode. Figure (4.5) depicts the three possible modes of deformation of the surface of the base spherical crystal seeds. Specifically, the figures depicts $\bar{R}(\bar{t})$ in Eq. (4.15) with deformation modes Y_2^m , for $m = -1, 0, 1$.

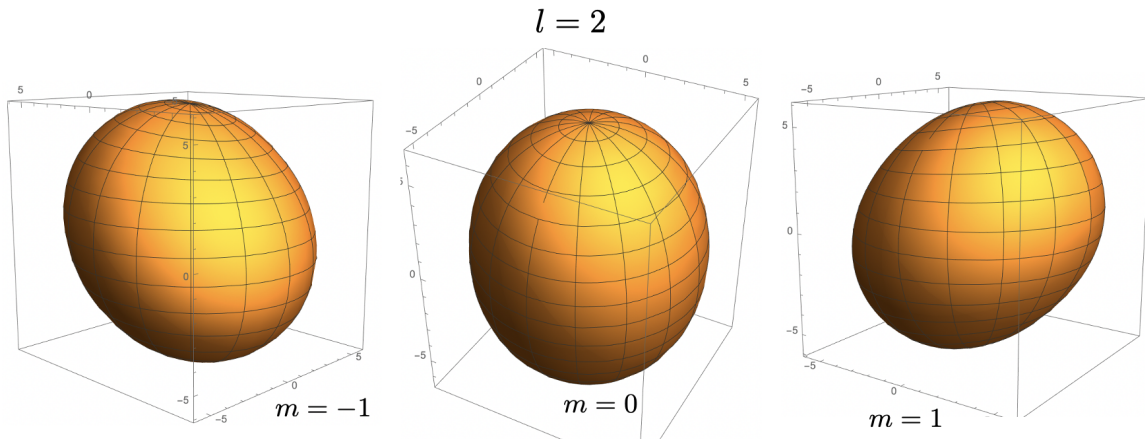


Figure 4.5: Three modes of deformation of a base circular crystal $\bar{R}_o(\bar{t})$ caused by a perturbation of its surface by the spherical harmonics $Y_2^m(\theta, \phi)$, $m = -1, 0, 1$. The amplification rate δ in Eq. (4.15) has been exaggerated in the figure to illustrate the form of the surface undulations.

The above linear stability analysis is often referred to as the *Mullins and Sekerka* stability analysis,

after the authors that first developed it in Ref. [22]. It is straightforward to extend this analysis to planar front in 2D and 3D by adapting the approach outlines in this sub-section. This is left as an exercise for the reader (the reader is referred to Ref. [6] for some of the details of these other calculations.)

4.4 Beyond Linear Stability: Dendritic Growth Forms

The Mullins and Sekerka (MS) instability outlined in the previous section is a generic instability that occurs in *any* 1st order phase transition involving the motion of a two-phase boundary driven by a thermodynamic excess energy that drives a system towards equilibrium (e.g. solid grains grow in a metastable liquid such as to transform the liquid into a solid). The pattern of the first instability to form on the interface is a competition between two factors: (1) diffusion of latent heat (or segregation of solute in the case of alloys) away from the interface and (2) interface energy. The first controls the accumulation of heat in front of the interface, which affects the local effective undercooling ahead of an advancing front. On the other hand, surface energy resists any increase of surface area, which always increases the excess free energy of a system. The diffusional element of the MS instability is depicted in Fig (4.6) for the case of a 2D solid-liquid interface. As latent heat released away from a planar interface reduces the undercooling uniformly ahead of the planar front, causing the entire interface to slow down. It turns out that the speed of an undercooled planar interface will asymptotically approach zero as $\langle v \rangle \sim t^{-1/2}$. Conversely, an interface that develops a sinusoidal perturbation exhibit

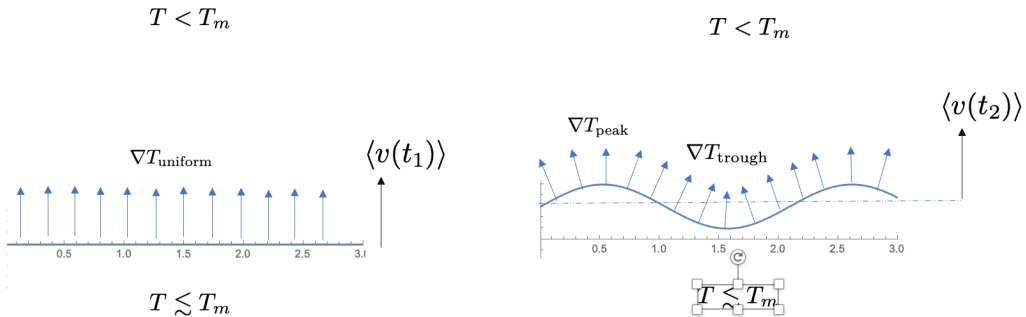


Figure 4.6: Illustration of the temperature gradients at some locations ahead of an advancing front at two times. (left) at early times, the front is planar (time= t_1), while at some later time (t_2) the interface amplifies a sinusoidal instability as it advances. The latent heat released in the planar interface reduces the undercooling uniformly ahead of the planar front, causing the entire interface to slow down. A fortuitous instability that is sinusoidal, however, can preferentially diffuse heat into the troughs of the front, allowing the regions around the peaks to maintain a larger undercooling $T < T_m$. These peaks start to grow faster than the troughs.

faster growth rates at the peaks of the front compared to the troughs. These modes grow by allowing the regions around the peaks to maintain a larger undercooling $T < T_m$. Based on Fig (4.6) alone, one might imagine that the wave modes with the highest frequency will lead to the largest growth patterns selected. However, this is not the case as larger frequency modes also lead to larger solid-liquid interface energy, which is unfavourable. Thus, there is in fact a balancing act between diffusion at the front and interface energy, which ultimately selects a characteristic length scale governing the initial

interface instability of the interface.⁵. Further pedagogical details of how to extract this characteristic length scale of unstable solid-liquid interface, in 2D and 3D, are shown round in Refs [6, 17].

The MS interface instability analysis is only accurate at very early times, specifically for $t \ll t_c = R_i/(\alpha_L \Delta)$. At times much larger than T_c , the interface evolution is governed by the highly non-linear dynamics of the sharp interface model. This requires fairly sophisticated computational techniques to solve in order to track the complex interface patterns that emerge. Figure (4.7) shows the time evolution of a solid liquid interface obtained from an experiment in which a transparent organic material is solidified. The images are in a coordinate frame that is moving with the interface, which evolves in time from right to left. The first three images show how a planar front becomes unstable and amplifies some characteristic mode, which sets a characteristic length scale. At later times, non-linear amplifications of this and other modes gives way to a more complex cellular patters, at first, followed later by thicker cellular patterns that have themselves also become unstable and given rise to transverse growth modes along their length; these are called *side branches*. This behaviour is

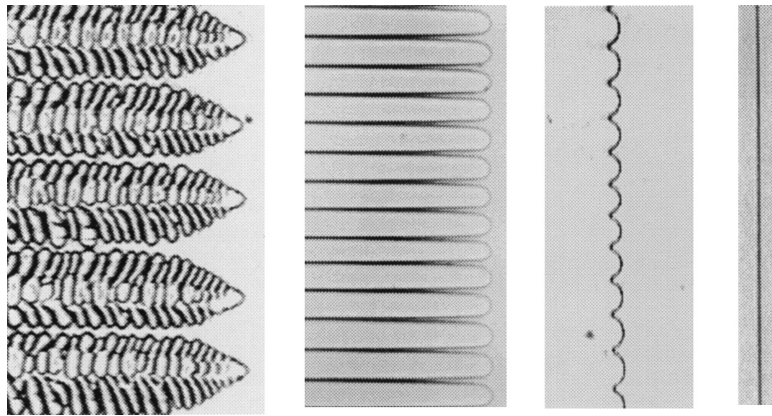


Figure 4.7: Experimental image sequence of a solid-liquid interface evolving from right to left. The sample is an organic thin-film deposited as a liquid on a microscope slide sitting on a movable stage that is slowly pulled to the right, across a thermal gradient that maintains a temperature $T < T_m$ the left side of the stage and $T > T_m$ on the right side.

typical of *all* solidification experiments in most materials. It is also manifested in solid state particle growth and pretty much any 1st order phase transformation.

4.5 Limitations of Sharp Interface Models

By this point, we have said pretty much as much as we can about pattern formation in 1st order phase transitions. As with the phase separation in 2nd order phase transitions, there is not much we can say analytically beyond what is revealed by linear analysis of the early stages of growth, which set the characteristic length and time scales. To study microscopic patterns in non-equilibrium phase transformations at late times, it appears must lower our pencil and head to the computers, armed with the full set of equations of the sharp interface model (SIM) described above. To some extent that is true, but it is noted that the simple sharp interface model itself is a simplification. It does not contain

⁵A clarification is in order here. As shown in the previous section, the harmonics comprising a noisy 3D crystal front will be amplified at different times in the growth of a spherical seed, but they will all be in multiples of the wavelength set by the $l = 2$ harmonic. The adaptation of the MS analysis to a 2D planar front shows that all modes can be amplified at the same time, but with different rates, leading again to one characteristic wavelength being selected by the system.

any information about the characteristic processes taking place within the nm scale of the interface itself. Moreover, while the SIM can describe a single topologically connected grain, it is notoriously difficult and computationally intensive to track multiple grains and nearly intractable to describe their proper coalescence. A more complete picture of the physics of solidification and other 1st order phase transformations requires that we abandon the SIM and turn to Ginzburg-Landau type theories, from which are derived another class of models known as *phase field models* (PFM). These are field-theoretic models that describe a system from a set of continuous fields, most important among which is the *order parameter of phase field*. This field is continuous in space and time and keeps attains positive values in solids or other ordered phases and zero in liquid or disordered phases, while interpolating between these extremes within a nm region that defines an interface, which comes naturally with the introduction of the order parameter in a system's thermodynamics and kinetics. The order parameter also couples to other fields such as temperature and solute distribution. Their coupled motion this gives a continuous description of a system, mapping out the properties the bulk phase and interfacial regions.

Ginzburg-Landau theories themselves arise from standard mean field theories of phase transition, in which the order parameter is assumed to be a standard thermodynamic variable that attains some values within the bulk of a phase. Examples of mean field theories that the reader may already be familiar with from undergraduate physics courses include magnetization (Ising Model), density difference between two fluids (phase separation in liquids), crystalline orientation (mean field theory of solidification), and others. For a detailed study of mean field theories, Ginzburg-Landau models and phase field modelling, the reader is referred to Ref. [25]. Some further mean field theories and phase field type models are also examined in later sections of these notes.

Chapter 5

Topics in Mean Field Theory

Mean field theory as a formalism by which to introduce an order parameter into the thermodynamic description of a system alongside the traditional thermodynamic variables like temperature, volume, particle number, pressure, chemical potential, etc. [25]. The order parameter can naturally emerge from the microscopic scale as a coarse grained descriptor of broken symmetry phases in ferromagnetism, phase separation in binary mixtures, as well as in solidifying liquids, precipitating solids, etc. The free energy describing the thermodynamics of these (and other) systems is expanded near some reference state in terms of the order parameter in such a way as to reflect the symmetries of the system as well as the type of phase transformation. If materials interfaces are to be included, the order parameter becomes a spatially extended field, and powers of its gradient must also be incorporated into the expansion of the free energy, thus leading to a Ginzburg-Landau functional.

The order fields can also be coupled to other fields that model long-wavelength phenomena accompanying phase transformations. These include temperature and concentration in solidification, vector potential in ferro-magnetic materials and strain in solid state precipitation. The free energy of such systems, written in terms of these fields and the order parameter, can be used to derive Euler-Lagrange equations for the system or dynamical equations that describe microstructure evolution in non-equilibrium phase transformations. The reader is referred to Ref. [25] for examples.

This chapter expands on the topic of mean field theory with two examples. The first derives a model of a solid that couples density and strain to a new order parameter for vacancy concentration. It is shown that this is a minimal model for describing elastic deformation in solids that incorporates the role of vacancies. The second example studies fluctuations of a Ginzburg-Landau functional around the saddle point approximation, showing how the inclusion of fluctuations renormalizes the coefficients of the mean field free energy functional from their original form in the mean-field Hamiltonian.

5.1 Landau Theory of Solids

Typically, deformation in solids is treated through a Hooke-type stress-strain response. However, deformation of real solids is intimately coupled to plastic processes, the latter of which are related to dislocations and vacancies. A proper hydrodynamic treatment of solids thus requires the inclusion of vacancy effects into the thermodynamics of deforming solids. Here, we will introduce a new vacancy order parameter which couples to density and strain to provide an accurate representation of solids.

5.1.1 Vacancy order parameter

Consider a solid with a unit cell structure with volume V and N_s lattice sites per unit cell. Denote the total number of atoms occupying the unit cell N , and the number of vacant sites in the unit cell

by N_v . In terms of these occupancy definitions, we define

$$N = N_s - N_v \quad \text{atoms per unit cell} \quad (5.1)$$

$$n = N/V \quad \text{atomic number density} \quad (5.2)$$

$$\Omega_0 = V/N_s \quad \text{volume per site of unit cell} \quad (5.3)$$

$$n_v = N_v/V \quad \text{vacancy density} \quad (5.4)$$

Substituting Eq. (5.1) into Eq. (5.2) also gives the atomic occupancy fraction,

$$n = \frac{N_s}{V} - \frac{N_v}{V} = \frac{1}{\Omega_0} - n_v \quad (5.5)$$

$$\Rightarrow \Omega_0 n = 1 - \Omega_0 n_v = 1 - \chi_v \quad (5.6)$$

where $\chi_v = \Omega_0 n_v$ is the fraction of vacancies in the unit cell. Equation (5.6) expresses the fraction of occupied sites in the unit cell as one minus the fraction of vacancies in the unit cell.

It is instructive to take the variation of the atomic density n starting from Eq. (5.5). This gives,

$$\begin{aligned} \delta n &= \delta \left(\frac{1}{\Omega_0} \right) - \delta n_v = -\frac{d\Omega_0}{\Omega_0^2} - \delta n_v \\ \Rightarrow \Omega_0 \delta n &= -\frac{\delta\Omega_0}{\Omega_0} - \Omega_0 \delta n_v \end{aligned} \quad (5.7)$$

The change of geometry of a unit cell is coupled to strain changes; in particular, relative changes to its volume are equal to the hydrostatic strain according to

$$\frac{\delta\Omega_0}{\Omega_0} = u_{ii}, \quad (5.8)$$

where the double index subscript “ ii ” implies summation. Substituting Eq. (5.8) into the last line of Eq. (5.7), gives after re-arranging,

$$\Omega_0 \delta n_v = -(u_{ii} + \Omega_0 \delta n) \quad (5.9)$$

Equation (5.9) shows that the change of vacancy fraction relative to the original number of lattice sites is due to two factors, hydrostatic strain of the unit cell and change of atomic occupancy relative to the original number of lattice sites.

The above considerations suggest introducing a new order parameter, $\psi_v = \ln(1 - \chi_v)$, that describes the relative change of vacancy fraction in a solid. This order parameter satisfies

$$\begin{aligned} \delta\psi_v &= -\frac{\delta\chi_v}{1 - \chi_v} = \frac{\delta(\Omega_0 n)}{\Omega_0 n} = \frac{\delta n}{n} + \frac{\delta\Omega_0}{\Omega_0} \\ &= \frac{\delta n}{n} + u_{ii} \end{aligned} \quad (5.10)$$

it is noteworthy that if there is a negligible change of vacancies, as happens at low temperatures in metals, then $\delta\chi_v = 0$ and we recover the usual $\delta n/n = -u_{ii}$, which means that the change of density is due only to the hydrostatic strain of the unit cell of the crystal. At temperatures near the melting point or high operating temperatures of metals $\delta\chi_v \neq 0$ and so vacancies must be included into the description of the solid state. The vacancy order parameter can be seen to vary from zero in an ideal solid without vacancies and some non-zero value when vacancies are present.

5.1.2 Vacancy-strain coupling in the free energy

When a solid deforms at a certain temperature its free energy can change due to changes in local density (i.e. atoms/volume) and local strain changes (stretching of lattice planes at constant density). Denote density here by n and strain by $u_{ij} = (\partial_i u_j + \partial_j u_i)/2$, where $\mathbf{u} = (u_x, u_y, u_z)$ is the local displacement vector. Up to quadratic order in these fields n and u_{ij} , a Landau-like free energy of a solid can be expanded relative to an undeformed state ($u_{ij}^0 = 0$) at a reference density n_0 as

$$f(n_0 + \delta n, u_{ij}) = f(n_0) + \left(\frac{\partial f}{\partial n} \right)_{n_0} \delta n + \frac{A}{2} \left(\frac{\delta n}{n_0} \right)^2 + \frac{1}{2} u_{ij} \bar{K}_{ijkl} u_{kl} + D \left(\frac{\delta n}{n_0} \right) u_{ii} \dots, \quad (5.11)$$

where n_0 is a reference density of the undeformed state. Here, the temperature T is suppressed explicitly in Eq. (5.11) but is implicitly in the dependance of the coefficients. The first term is a reference energy of the undeformed solids. The second term is the first order coupling of density to chemical potential, the third is the quadratic Hooke's law type deformation energy, with \bar{K}_{ijkl} being the tensor of elastic coefficients. The last term is the coupling of strain to density changes.

As mentioned in the last section, a proper thermodynamic treatment of solids should consider the vacancy order parameter $\delta\psi_v$ in its Landau free energy expansion. The expansion of Eq. (5.11) to quadratic order in n and u_{ij} is sufficient to do this. Namely, setting $n \rightarrow n_0$ to denote the base density implied by the variation in Eq. (5.10), and substituting it into Eq. (5.11) gives, after re-arranging,

$$\begin{aligned} f(n_0 + \delta n, u_{ij}) &= f(n_0) + \mu_0 \delta n + \frac{A}{2} \left\{ \frac{\delta n}{n_0} + u_{ii} \right\}^2 + (D - A) \left\{ \frac{\delta n}{n_0} + u_{ii} \right\} u_{ii} + \frac{1}{2} u_{ij} K_{ijkl}^v u_{kl} \\ &= f(n_0) + \mu_0 \delta n + \frac{A}{2} \delta\psi_v^2 + \frac{1}{2} u_{ij} K_{ijkl}^v u_{kl} + (D - A) \delta\psi_v u_{ii}, \end{aligned} \quad (5.12)$$

where the elastic tensor K_{ijkl}^v is defined by

$$K_{ijkl}^v = \bar{K}_{ijkl} + (A - 2D) \delta_{ij} \delta_{kl}, \quad (5.13)$$

and where the linear term coupling to δn in the third term of Eq. (5.11) has been identified with the chemical potential μ_0 at the reference density n_0 . Equation (5.12) is a Landau-type of theory of a solid that is expanded to quadratic in vacancy and strain order parameters, with a linear coupling between the two. It is noteworthy that the elastic constant tensor Eq. (5.13) takes on an important correction that emerges directly due to the coupling of vacancies to strain.

5.1.3 Vacancies in the stress tensor

The stress tensor in a solid can be decomposed as follows ¹,

$$\sigma_{ij} = -p \delta_{ij} + h_{ij}, \quad (5.14)$$

where the first term in Eq. (5.14) is the [isotropic] thermodynamic pressure, and the second component includes isotropic and non-isotropic stresses contributions arising from displacement of crystallographic planes relative to each other. The stress component h_{ij} is specific to solids where inter-atomic planes take on specific equilibrium spacings as a result of breaking translational invariance. These terms are examined further below.

¹Equation (5.14), as well as some other results used in this chapter, will be shown explicitly in Chapter 6 where the thermodynamics of a moving material volume will be examined (the reader is also referred to Ref. [5]) for a derivation of this result from dynamic or static arguments)

it will be shown in Chapter 6 that pressure for solids is given in terms of the free energy (in the notation of this chapter) as

$$-p = (f - \mu n)_{u_{ij}} = \left(f - n \frac{\partial f}{\partial n} \right)_{u_{ij}} \quad (5.15)$$

where T is temperature, f is free energy density, μ is the chemical potential per atom and n is the mass density. This is well-known thermodynamics result, but note that when applied specifically to solids, the strain is held constant when taking the derivative of the free energy. This implies that the thermodynamic pressure p takes into account only density changes due to atomic occupation and vacancies.

To obtain an expression for h_{ij} in Eq. (5.14), we combine the change of pressure derived from Eq. (5.15), i.e. $-dp = df - \mu dn - nd\mu$, with the relationship $-dp = -sdT - nd\mu + h_{ij}du_{ij}$, to be derived in Eq. (6.36) (neglecting the second order velocity contributions here). This yields,

$$df = -sdT + \mu dn + h_{ij}du_{ij} \quad (5.16)$$

Equation (5.16) immediately yields

$$h_{ij} = \frac{\partial f}{\partial u_{ij}} \Big|_{T,n} \quad (5.17)$$

Equation (5.17) relates that part of the stress tensor associated with strain in the spacing between atomic planes (or mass density waves) to the the free energy of the solid.

Using the free energy derived in Eq. (5.12) allows us to calculate explicit forms for the components of the stress tensor in Eq. (5.14). Starting with Eq. (5.17), the first line of Eq. (5.12) gives, after collecting terms,

$$h_{ij} = \bar{K}_{ijkl}u_{kl} + D \frac{\delta n}{n_0} \delta_{ij} \quad (5.18)$$

It will hereafter be assumed that $h_{ij} = 0$ in the undeformed reference state where density $n = n_0$ and $u_{ij} = u_{ij}^0 = 0$. This can be understood by assuming, for example, that the reference state is in equilibrium surrounded by some fluid at some pressure $\sigma_{ij}^0 = -p^0 \delta_{ij}$, and hence, in the reference state, $h_{ij} = h_{ij}^0 = 0$.

To calculate the change of pressure from the reference state, $\delta p = p - p^0$, we first return to the differential relation $-dp = -sdT - nd\mu + h_{ij}du_{ij}$. To linear order in the strains ², this yields,

$$dp = sdT + nd\mu \quad (5.19)$$

Making the approximation that $dp \rightarrow \delta p$ and $d\mu \rightarrow \delta\mu$ (also $dT \rightarrow \delta T$), we write

$$\delta p = s\delta T + n\delta\mu, \quad (5.20)$$

where change of chemical potential $\delta\mu$ is evaluated from Eq. (5.12) as follows,

$$\begin{aligned} \mu &= \frac{\partial f}{\partial n} \Big|_{u_{ij}} = \mu_0 + A \frac{\delta n}{n_0^2} + D \frac{u_{ii}}{n_0} \\ \implies \delta\mu &= A \frac{\delta n}{n_0^2} + D \frac{u_{ii}}{n_0} \end{aligned} \quad (5.21)$$

²Substituting Eq. (5.18) into $h_{ij}du_{ij}$ yields an expression that is second order strains, which we neglect in linear elasticity.

and where $\delta\mu = \mu - \mu(n_0)$. Substituting Eq. (5.21) into Eq. (5.20), with $n \rightarrow n_0$, and assuming isothermal conditions, gives

$$\delta p = A \frac{\delta n}{n_0} + D u_{ii} \quad (5.22)$$

Substituting both Eq. (5.22) and Eq. (5.18) into the change form of Eq. (5.14), i.e. $\delta\sigma_{ij} = -\delta p \delta_{ij} + \delta h_{ij}$, and recalling that $\delta h_{ij} = h_{ij} - h_{ij}^0$ with $h_{ij}^0 = 0$, gives

$$\delta\sigma_{ij} = - \left\{ A \frac{\delta n}{n_0} + D u_{ii} \right\} + \left\{ \bar{K}_{ijkl} u_{kl} + D \frac{\delta n}{n_0} \delta_{ij} \right\} \quad (5.23)$$

Using Eq. (5.13) to write $K_{ijkl} = K_{ijkl}^v - (A - 2D) \delta_{ij} \delta_{kl}$, and substituting for \bar{K}_{ijkl} into Eq. (5.23) gives, after some re-arranging,

$$\begin{aligned} \delta\sigma_{ij} &= (D - A) \left\{ \frac{\delta n}{n_0} + u_{ii} \right\} \delta_{ij} + K_{ijkl}^v u_{kl} \\ &= (D - A) \delta\psi_v \delta_{ij} + K_{ijkl}^v u_{kl} \end{aligned} \quad (5.24)$$

Equation (5.24) relates the changes in the stress state of a solid (relative to an equilibrium state) to both Hookian type elastic strains and to the change of vacancies in the solid. The diffusion of vacancies is a well known effect in materials science; while it is negligible at low temperatures, it becomes crucial at higher temperatures, leading to phenomena such as creep, deformation mediated precisely by the diffusive transport of vacancies. We'll study hydrodynamics of solids in Chapter 6, where we will see how $\delta\psi_v$ affects the displacement modes of a solid.

5.2 Fluctuations in Ginzburg-Landau Theory

Landau mean field theory typically begins by assuming that there exists an order parameter field (denoted by $\phi(\mathbf{x})$ here) that can describe the local ordering of a system undergoing a phase transformations. One can then, in principle, restrict the trace of the partition function over the possible states of the order parameter, each state weighted by the microscopic density of states corresponding to said order parameter configuration. By restricting ourselves to the state of this trace that minimizes the Boltzmann weight of the partition functions, we can obtain a mean field free energy. If spatial variations are neglected, the mean field free energy can help elucidate –despite its simplicity– the main features of symmetry breaking cause discontinuity in second derivatives in a 2nd order transition, or the discontinuous break in symmetry from the high temperature phase that lead to discontinuous 1st derivatives in a first order transition. When ϕ is allowed to have spatial variations, we can extract a mean field solution that incorporates an inter-phase interfaces. Here, we consider functional fluctuations around the saddle point approximation of $\phi(\mathbf{x})$ and show that this leads to the re-normalization of the coefficients of the Ginzburg-Landau free energy functional that emerges from the original form in the mean field Hamiltonian.

5.2.1 Expansion of partition function around the mean field solution

Consider the phenomenological Hamiltonian given by

$$H[\phi] = \int \left\{ \frac{K}{2} |\nabla\phi|^2 - \frac{r}{2} \phi^2 + \frac{s}{4} \phi^4 + h(x)\phi(x) \right\} d\mathbf{x} \quad (5.25)$$

where $\phi(\mathbf{x})$ is a spatially dependent order parameter describing a system. The local average of $\phi(\mathbf{x})$ describes some local quantity over many atomic lengths. It varies over some correlation length ξ that depends on whether we are talking about a 1st or second order phase transformation. Assuming we can suitably define any microscopic configuration of the system by some instance of $\phi(\mathbf{x})$, we can formally define the partition function of the system by

$$Q_V = \int \mathcal{D}(\phi) e^{-H[\phi]/k_B T} \quad (5.26)$$

where the notation $\mathcal{D}(\phi)$ means that we are to sum the Boltzmann factor $e^{-H[\phi]/k_B T}$ over all possible configurations of the field ϕ , weighting each term in this sum by the density of microscopic states compatible with each configuration of $\phi(\mathbf{x})$. It is instructive to analyze some of the properties of Q_V in the limit of small fluctuations of the order parameter.

As with most non-linear models, the partition function in Eq. (5.26) has no solution where Eq. (5.25) is concerned. To proceed we expand the Hamiltonian $H[\phi]$ around some presumed equilibrium state $\phi_0(\mathbf{x})$ (that can possibly have spatial variations in it). This leads to

$$H[\phi(\mathbf{x})] = H[\phi_0] + \int d\mathbf{x} \frac{\delta H}{\delta \phi(\mathbf{x})} \Big|_{\phi_0} \delta\phi(\mathbf{x}) + \frac{1}{2} \int d\mathbf{x} \int d\mathbf{x}' \delta\phi(\mathbf{x}) \frac{\delta^2 H}{\delta \phi(\mathbf{x}) \delta \phi(\mathbf{x}')} \Big|_{\phi_0} \delta\phi(\mathbf{x}') + \dots \quad (5.27)$$

Keeping up to second order terms in this *functional expansion* of $H[\phi]$ and substituting the truncated functional series in Eq. (5.26) leads to

$$Q_V = \int \mathcal{D}(\phi) e^{-\beta \left\{ H[\phi_0] + \int d\mathbf{x} \frac{\delta H}{\delta \phi(\mathbf{x})} \Big|_{\phi_0} \delta\phi(\mathbf{x}) + \frac{1}{2} \int d\mathbf{x} \int d\mathbf{x}' \delta\phi(\mathbf{x}) \frac{\delta^2 H}{\delta \phi(\mathbf{x}) \delta \phi(\mathbf{x}')} \Big|_{\phi_0} \delta\phi(\mathbf{x}') \right\}} \quad (5.28)$$

In the saddle point approximation, the most likely state of the system occurs at an extremum of $H[\phi]$, which gives the equilibrium properties of the system described by Eq. (5.25). This state is given by the solution of the Euler-Lagrange equation for $H[\phi]$,

$$\frac{\delta H}{\delta \phi(\mathbf{x})} \Big|_{\phi_0} = -K\nabla^2\phi_0(\mathbf{x}) - r\phi_0(\mathbf{x}) + s\phi_0^3(\mathbf{x}) - h(\mathbf{x}) = 0 \quad (5.29)$$

Eq. (5.29) implies that the second term in the exponential expansion of Eq. (5.28) is zero. Moreover, the factor $\exp(-H[\phi_0]/k_B T)$ can be brought out of the functional trace implied by Eq. (5.28) as the trace is scanning variations *around* $\phi_0(\mathbf{x})$. We can thus re-write Q_V as

$$Q_V = e^{-H[\phi_0]/k_B T} \int \mathcal{D}(\phi) e^{-\frac{\beta}{2} \left(\int d\mathbf{x} \delta\phi(\mathbf{x}) \int d\mathbf{x}' \frac{\delta^2 H}{\delta \phi(\mathbf{x}) \delta \phi(\mathbf{x}')} \Big|_{\phi_0} \delta\phi(\mathbf{x}') \right)} \quad (5.30)$$

We next calculate the second functional derivative of $H[\phi]$, which gives

$$\begin{aligned} \frac{\delta H}{\delta \phi(\mathbf{x}) \delta \phi(\mathbf{x}')} &= \frac{\delta}{\delta \phi(\mathbf{x})} \left(-K\nabla^2\phi(\mathbf{x}') - r\phi(\mathbf{x}') + s\phi^3(\mathbf{x}') - h(\mathbf{x}') \right) \\ &= -K\nabla_{\mathbf{x}'}^2 \delta(\mathbf{x}' - \mathbf{x}) - r\delta(\mathbf{x}' - \mathbf{x}) + 3s\phi^2(\mathbf{x}') \delta(\mathbf{x}' - \mathbf{x}) \\ &= \left(-K\nabla_{\mathbf{x}'}^2 - r + 3s\phi^2(\mathbf{x}') \right) \delta(\mathbf{x}' - \mathbf{x}), \end{aligned} \quad (5.31)$$

where $\nabla_{\mathbf{x}'}$ denotes differentiation with respect to \mathbf{x}' . Substituting $\phi^2(\mathbf{x}') \rightarrow \phi_0^2(\mathbf{x}')$ in Eq. (5.31) and substituting the result into Eq. (5.30) gives, after two integration by parts on the gradient term,

$$Q_V = e^{-H[\phi_0]/k_B T} \int \mathcal{D}(\phi) e^{-\frac{\beta}{2} \int (-K \delta\phi(\mathbf{x}) \nabla^2 \delta\phi(\mathbf{x}) - r \delta\phi^2(\mathbf{x}) + 3s \phi_0^2(\mathbf{x}) \delta\phi^2(\mathbf{x})) d\mathbf{x}} \quad (5.32)$$

Since the second exponential factor in Eq. (5.32) is of Gaussian form, it is possible to explore functional fluctuations of the order parameter field around its saddle point $\phi_0(\mathbf{x})$. To do so, we will re-write the Hamiltonian in the exponential of Eq. (5.32) as

$$\Delta H[\phi] = \int d\mathbf{x} \int d\mathbf{x}' \delta\phi(\mathbf{x}) \left\{ -\frac{K}{2} \nabla_{\mathbf{x}'}^2 - \frac{r}{2} + \frac{3s}{2} \phi_0^2(\mathbf{x}') \right\} \delta(\mathbf{x}' - \mathbf{x}) \delta\phi(\mathbf{x}') \quad (5.33)$$

which is often done when deriving Q_V by functional integrals of a Guassian form.

5.2.2 Guassian integration of Q_V

To analyze ΔH it will be assumed that $\delta\phi(\mathbf{x})$ can be expressed in a discrete Fourier series as follows

$$\delta\phi(\mathbf{x}) = \frac{1}{V} \sum_k c_k e^{i\mathbf{k}\cdot\mathbf{x}} \quad (5.34)$$

where V is the volume of the system, and where it is tacitly assumed that the sum has a high- k cutoff Λ_c since we are dealing with a system whose smallest microscopic length scale is on the order of a few atomic lengths. Also, since $\delta\phi(\mathbf{x})$ describes fluctuations near the saddle point solution, we will assume that it varies on much shorter length scales than $\phi_0(\mathbf{x})$. As such, the sum in Eq. (5.34) will also be assumed to have a lower k cutoff Λ_L , i.e. $\Lambda_L < k < \Lambda_c$. The discrete representation of the delta function will be approximated by

$$\delta(\mathbf{x}' - \mathbf{x}) = \frac{1}{V} \sum_k e^{i\mathbf{k}\cdot(\mathbf{x}' - \mathbf{x})}, \quad (5.35)$$

where the sum over wave modes is over the same range ³ as that in Eq. (5.34). Furthermore, the \mathbf{k} -space delta function can be represented by the standard form

$$\int d\mathbf{x} e^{i(\mathbf{k}-\mathbf{k}')\cdot\mathbf{x}} = V \delta(\mathbf{k} - \mathbf{k}') \quad (5.36)$$

To proceed, Eq. (5.34) and Eq. (5.35) are substituted for Eq. (5.33), which gives

$$\begin{aligned} \Delta H &= \frac{1}{V^3} \int d\mathbf{x} \int d\mathbf{x}' \left(\sum_{\mathbf{k}} c_{\mathbf{k}} e^{i\mathbf{k}\cdot\mathbf{x}} \right) \sum_{\mathbf{k}'} \left\{ \frac{\alpha}{2} |\mathbf{k}'|^2 - \frac{r}{2} + \frac{3s}{2} \phi_0^2(\mathbf{x}') \right\} e^{i\mathbf{k}'\cdot(\mathbf{x}' - \mathbf{x})} \left(\sum_{\mathbf{k}''} c_{\mathbf{k}''} e^{i\mathbf{k}''\cdot\mathbf{x}'} \right) \\ &= \frac{1}{V^3} \int d\mathbf{x}' \int d\mathbf{x} \sum_{\mathbf{k}} \sum_{\mathbf{k}'} \sum_{\mathbf{k}''} c_{\mathbf{k}} c_{\mathbf{k}''} \left\{ \frac{\alpha}{2} |\mathbf{k}'|^2 - \frac{r}{2} + \frac{3s}{2} \phi_0^2(\mathbf{x}') \right\} e^{i(\mathbf{k}' + \mathbf{k}'')\cdot\mathbf{x}'} e^{i(\mathbf{k} - \mathbf{k}')\cdot\mathbf{x}} \end{aligned} \quad (5.37)$$

³If the reader objects to representing the delta function on this restricted \mathbf{k} space domain, one can also proceed by completing the $\int d\mathbf{x}'$ integral in Eq. (5.33) and then simply deal with Eq. (5.34) to represent $\delta\phi(\mathbf{x})$ in the resulting expression for ΔH .

Pulling through $\int d\mathbf{x}$ and applying the integration on the rightmost exponential of Eq. (5.37) with argument $(\mathbf{k} - \mathbf{k}') \cdot \mathbf{x}$, removes, after using Eq. (5.36), the sum over the \mathbf{k}' vectors. This yields

$$\begin{aligned}\Delta H &= \frac{1}{V^2} \int d\mathbf{x}' \sum_{\mathbf{k}} \sum_{\mathbf{k}''} c_{\mathbf{k}} c_{\mathbf{k}''} \left\{ \frac{\alpha}{2} |\mathbf{k}|^2 - \frac{r}{2} \right\} e^{i(\mathbf{k} + \mathbf{k}'') \cdot \mathbf{x}'} \\ &+ \frac{3s}{2V^2} \int d\mathbf{x}' \int \sum_{\mathbf{k}} \sum_{\mathbf{k}''} c_{\mathbf{k}} c_{\mathbf{k}''} \left\{ \phi_0^2(\mathbf{x}') \right\} e^{i(\mathbf{k} + \mathbf{k}'') \cdot \mathbf{x}'}\end{aligned}\quad (5.38)$$

Pulling through $\int d\mathbf{x}'$ and applying the integration to the remaining exponential now removes the sum over the \mathbf{k}'' vectors on the first line of Eq. (5.38), yielding

$$\Delta H = \frac{1}{V} \sum_{\mathbf{k}} |c_{\mathbf{k}}|^2 \left\{ \frac{\alpha}{2} |\mathbf{k}|^2 - \frac{r}{2} \right\} + \frac{3s}{2V^2} \sum_{\mathbf{k}} \sum_{\mathbf{k}''} c_{\mathbf{k}} c_{\mathbf{k}''} \int d\mathbf{x}' \phi_0^2(\mathbf{x}') e^{i(\mathbf{k} + \mathbf{k}'') \cdot \mathbf{x}'} \quad (5.39)$$

To simplify the second term in Eq. (5.39), it is noted that $\delta\phi(\mathbf{x})$ represents small fluctuations of $\phi(\mathbf{x})$ around the saddle point solution $\phi_0(\mathbf{x})$. This is illustrated schematically in Fig. 5.1. Thus,

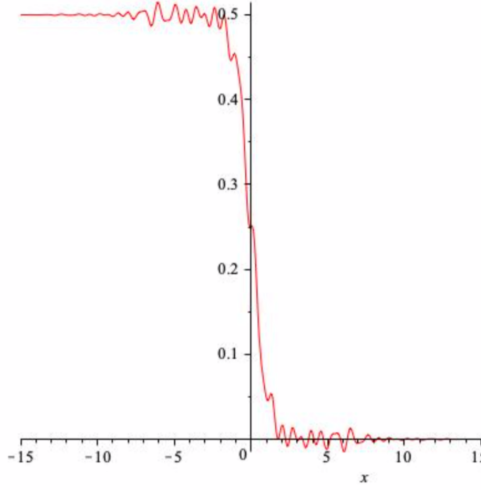


Figure 5.1: Illustration of fluctuations (wiggles) of the order parameter $\phi(\mathbf{x})$ around its saddle point solution $\phi_0(\mathbf{x})$, which varies on much longer length scales. For illustrative purposes $\phi_0(\mathbf{x})$ is shown here to have the classic hyperbolic tangent-like form characteristic of domain walls or solid-liquid interfaces.

while $\delta\phi(\mathbf{x})$ is assumed to be composed predominately of Fourier modes bound by $\Lambda_L < \mathbf{k} < \Lambda_c$, $\phi_0(\mathbf{x})$ is assumed to smooth on over these length scales, as it varies on the larger scales that define a domain walls, solid-liquid interface, etc. In other words, $W\Lambda_L \gg 1$, where W represent the correlation length that control variations in the form of $\phi_0(\mathbf{x})$. These considerations imply that the factor $\exp\{i(\mathbf{k} + \mathbf{k}'') \cdot \mathbf{x}\}$ in the integrand of Eq. (5.39) oscillates very rapidly compared to the variations $\phi_0^2(\mathbf{x})$, except in the neighbourhood of $\mathbf{k}'' = -\mathbf{k}$. As a result, the integral in Eq. (5.39) can be approximated as

$$\int d\mathbf{x}' \phi_0^2(\mathbf{x}') e^{i(\mathbf{k} + \mathbf{k}'') \cdot \mathbf{x}'} \approx \delta_{\{\mathbf{k}, -\mathbf{k}''\}} \int d\mathbf{x}' \phi_0^2(\mathbf{x}'), \quad (5.40)$$

where $\delta_{i,j}$ is the Kronecker delta function. This allows us eliminate the \mathbf{k}'' sum in second term Eq. (5.39) and re-write Eq. (5.39) as

$$\begin{aligned}\Delta H &= \frac{1}{V} \sum_{\mathbf{k}} |c_{\mathbf{k}}|^2 \left\{ \frac{\alpha}{2} |\mathbf{k}|^2 - \frac{r}{2} \right\} + \frac{3s}{2V^2} \sum_{\mathbf{k}} |c_{\mathbf{k}}|^2 \int d\mathbf{x} \phi_0^2(\mathbf{x}) \\ &= \frac{1}{V^2} \int d\mathbf{x} \sum_{\mathbf{k}} \left\{ \frac{\alpha}{2} |\mathbf{k}|^2 - \frac{r}{2} + \frac{3s}{2} \phi_0^2(\mathbf{x}) \right\} |c_{\mathbf{k}}|^2\end{aligned}\quad (5.41)$$

It is recalled that the sums in Eq. (5.39) are assumed to have the aforementioned \mathbf{k} space limits. Moreover, the sums are assumed to only go over half the \mathbf{k} space since $\delta\phi(\mathbf{x})$ is real and thus $c_{\mathbf{k}}^* = c_{-\mathbf{k}}$.

To carry out the functional integration in the second factor of Eq. (5.32), it is convenient to re-write the second line of Eq. (5.41) in discrete form as

$$\frac{\Delta H[\phi]}{k_B T} = \sum_i \sum_{\mathbf{k}} \underbrace{\frac{\Delta x^d}{2K_B T} \left\{ \alpha |\mathbf{k}|^2 - r + 3s\phi_0^2(x_i) \right\}}_{\Gamma(\mathbf{k}, \phi_i)} |\tilde{c}_{\mathbf{k}}|^2, \quad (5.42)$$

where d is the dimension of space, and where the $c_{\mathbf{k}}$ have been made dimensionless by rescaling them to $\tilde{c}_{\mathbf{k}} = c_{\mathbf{k}}/L^d$. In arriving at Eq. (5.42) use was made of the following,

$$V = L^d \quad (5.43)$$

$$\frac{1}{V} \int d\mathbf{x} = 1 \quad (5.44)$$

$$\int d\mathbf{x} \rightarrow \sum_i \Delta x_i \quad (5.45)$$

Breaking up $\tilde{c}_{\mathbf{k}}$ into its real and complex parts as $\tilde{c}_{\mathbf{k}} = \tilde{c}_{\mathbf{k}}^R + i \tilde{c}_{\mathbf{k}}^I$, the functional integral in Eq. (5.32) becomes

$$\begin{aligned}\int \mathcal{D}(\phi) e^{-\Delta H[\phi]/k_B T} &= \int \mathcal{D}(\phi) e^{-\sum_i \sum_k \Gamma(\mathbf{k}, \phi_i) |\tilde{c}_{\mathbf{k}}|^2} \\ &= \prod_i \prod_{\mathbf{k}} \int \int \tilde{c}_{\mathbf{k}}^R \tilde{c}_{\mathbf{k}}^I e^{\Gamma(\mathbf{k}, \phi_i) (\tilde{c}_{\mathbf{k}}^R)^2} e^{\Gamma(\mathbf{k}, \phi_i) (\tilde{c}_{\mathbf{k}}^I)^2} \\ &= \prod_i \prod_{\mathbf{k}} \left(\int \tilde{c}_{\mathbf{k}}^R e^{\Gamma(\mathbf{k}, \phi_i) (\tilde{c}_{\mathbf{k}}^R)^2} \right) \left(\int \tilde{c}_{\mathbf{k}}^I e^{\Gamma(\mathbf{k}, \phi_i) (\tilde{c}_{\mathbf{k}}^I)^2} \right)\end{aligned}\quad (5.46)$$

In going from the first to second lines of Eq. (5.46) the definition of a functional integral was applied, i.e., summing over all field fluctuations $\delta\phi(\mathbf{x})$ is equivalent to summing over the real and complex parts of the coefficients $\tilde{c}_{\mathbf{k}}$, which vary the possible states of $\delta\phi(\mathbf{x})$ through Eq. (5.34). The last line of Eq. (5.46) is pedantic but meant to emphasize that the solution of a product trivial Gaussian integrals. Completing the above integrals gives

$$\begin{aligned}\int \mathcal{D}(\phi) e^{-\Delta H[\phi]/k_B T} &= e^{\ln(\prod_i \prod_{\mathbf{k}} \frac{\pi}{\Gamma(\mathbf{k}, \phi_i)})} \\ &= e^{-\sum_i \sum_{\mathbf{k}} \ln\left(\frac{\Gamma(\mathbf{k}, \phi_i)}{\pi}\right)} \\ &= e^{-\frac{1}{2} \sum_i \sum_{\mathbf{k}} \ln\left(\frac{\Delta x^d}{2\pi K_B T} \left\{ \alpha |\mathbf{k}|^2 - r + 3s\phi_0^2(x_i) \right\}\right)}\end{aligned}\quad (5.47)$$

The $1/2$ in the last line of Eq. (5.47) is added in order to allow the sums in \mathbf{k} space to vary over all \mathbf{k} space. It is also noted that the argument of the exponential in Eq. (5.47) is dimensionless as the units of the coefficients r and s are J/L^d and α has units $J m^2/L^d$. The above is an application of functional integration. Readers wishing to learn more details on functional integration are referred to the text by Binney [3].

Taking the last line of Eq. (5.47) into continuum space requires that we apply Eq. (5.45) backwards and take the limit $\sum \mathbf{k} \rightarrow \int d^d\mathbf{k}/(2\pi)^d$. Doing so gives

$$Q_V = \text{const} \times e^{-H[\phi_0]/k_B T} e^{-\frac{1}{2} \int d^d\mathbf{x} \int \frac{d^d\mathbf{k}}{(2\pi)^d} \ln \{\alpha' |\mathbf{k}|^2 - r' + 3s' \phi_0^2(\mathbf{x})\}} \quad (5.48)$$

where the re-scalings $\alpha' = \alpha/k_B T$, $r' = r/k_B T$, $s' = s/k_B T$ have been made. The constant is given by $\exp(-(1/2) \sum_k \sum_i \Delta x^d / 2\pi)$ and is unimportant as it will merely add a constant to the free energy, which does not affect any of its thermodynamics. Using the definition $F = -k_B T \ln Q_V$ finally gives

$$F[\phi(\mathbf{x})] = F[\phi_0(\mathbf{x})] - \frac{k_B T}{2} \int d^d\mathbf{x} \int \frac{d^d\mathbf{k}}{(2\pi)^d} \ln \{\alpha' |\mathbf{k}|^2 - r' + 3s' \phi_0^2(\mathbf{x})\} \quad (5.49)$$

5.2.3 Renormalization of free energy coefficients

One can interpret the extra term beyond $F[\phi_0]$ in Eq. (5.49) as adding a correction to the true free energy beyond those that arise solely from the saddle point approximation. Effectively, this extra term *renormalizes* the original coefficients of $F[\phi_0]$. To see this, consider fluctuations of $\phi(\mathbf{x})$ around the bulk phase region of $\phi_0(\mathbf{x})$, which we denote $\phi_0(\pm\infty)$ since these occur far from an interface, where $\phi_0(\mathbf{x})$ is constant. Furthermore, suppose that Eq. (5.49) can be written as

$$F[\phi(\mathbf{x})] = \int \left\{ \frac{\alpha_{\text{eff}}}{2} |\nabla \phi|^2 - \frac{r_{\text{eff}}}{2} \phi^2 + \frac{s_{\text{eff}}}{4} \phi^4 \right\} d\mathbf{x} \quad (5.50)$$

Then, the second variational derivative of Eq. (5.49) gives r_{eff} according to

$$r_{\text{eff}} = - \frac{\delta^2 F[\phi(\mathbf{x})]}{\delta \phi^2} \Big|_{\phi=\phi(\pm\infty)} = r' - 3s' k_B T \int \frac{d^d\mathbf{k}}{(2\pi)^d} \left\{ \frac{1}{\alpha' |\mathbf{k}|^2 - r' + 3s' \phi_0^2(\pm\infty)} \right\}, \quad (5.51)$$

Assuming as an example, that we are considering magnetic domain wall solutions. Above T_c $\phi_0(\pm\infty) = 0$, while below T_c it would have two non-zero values. Considering the order parameter close to and above T_c (where $\phi_0 = 0$) also allows us to compute a correction for the critical transition temperature T_c by considering the renormalized r_{eff} . The fourth variational derivative of Eq. (5.49) gives s_{eff} according to

$$s_{\text{eff}} = \frac{\delta^4 F[\phi(\mathbf{x})]}{\delta \phi^4} \Big|_{\phi=\phi(\pm\infty)} = s' - \frac{54}{6} (s')^2 k_B T \int \frac{d^d\mathbf{k}}{(2\pi)^d} \left\{ \frac{1}{(\alpha' |\mathbf{k}|^2 - r')^2} \right\}, \quad (5.52)$$

Calculating the correction for α_{eff} cannot be derived from considering the first variational of $F[\phi(\mathbf{x})]$ as it becomes convolved with the other parameters. As it turns out, that at this order of Gaussian fluctuations, the parameter $\alpha_{\text{eff}} = \alpha'$.

This analysis shows that the coefficients of the free energy of Model A used in phase field modelling are actually renormalized from those that enter the Hamiltonian from which it can be derived from the partition function.

Chapter 6

Hydrodynamics of Solids

Recent years have seen the explosion of so-called *phase field models* to describe the spatiotemporal evolution microstructure in non-equilibrium phase transformations. These models couple slow quantities, like an order parameter field, to one or more other mesoscale fields such as temperature, magnetism, strain, etc. Their coupled evolution is described by a set of stochastic differential equations that describe the dissipative minimization of free energy functional of the evolving system. Fields of conserved quantities are governed by a conservation law whose flux is proportional to local chemical potential gradient, where the chemical potential is itself a variational derivative of a free energy functional. Non-conserved quantities are governed by simple gradient flow. Phase field models are examples of a more general class of *hydrodynamic* theories that describe the evolution of broken symmetry and/or conserved variables that, while spatially extended, represent a [locally] coarse grained description of a material (i.e. a many body system).

A classical example that one thinks of when hearing the word “hydrodynamic equations” is the Navier-Stokes equations. These describe the coupled evolution of density, momentum and energy, all slowly varying quantities that are conserved over the whole system. Hydrodynamic equations are mathematically closed by combining local conservation laws with constitutive relations for fluxes of mass, momentum and energy back to the various slowly varying quantities themselves [5]. While the word “hydrodynamics” typically conjures up images of flowing fluids, it is also applicable to solids and other systems as well. A hydrodynamic description of a solid must consider conservation of mass, momentum and energy, as well as strains, which reflect broken translational symmetries that emerge in crystals. In addition, solids also require another collective variable to describe their hydrodynamics, that associated with *vacancy density* [23, 5], which we studied in Chapter (5).

This Chapter will examine the hydrodynamics of solids. Beyond being important in its own right, sketching out a framework that examines the collective modes of density, momentum, strain and vacancy diffusion in solids will prove useful later on when we consider the dynamics of the PFC model, a theory based on a DFT-type of density order parameter and which can form ordered solid phases.

6.1 Microscopic Operators and Conservation Laws

Begin by considering a deforming continuum. At this point, we’ll keep it general and not specify until we are forced to whether we are talking about a fluid or solid. The continuum is assumed to be divided into small volume elements ΔV that can deform but are otherwise connected without voids. Each volume will be treated locally as a translating system that comprises of a large number of atoms. Viewed from the lab frame, a reference point (e.g. the centre) of ΔV is tracked by some position

$\mathbf{x}(t)$ and has a corresponding velocity $\mathbf{v}(t)$. Internally, ΔV is assumed to contain N particles, each of which is assumed to be positioned and moving around randomly within the volume. The volume ΔV is itself assumed to be in equilibrium with respect to the variables defining its local thermodynamic state (e.g. $T, P, \Delta V, N$, etc). Further details on these considerations are summarized in the cartoon in Figure 6.1.

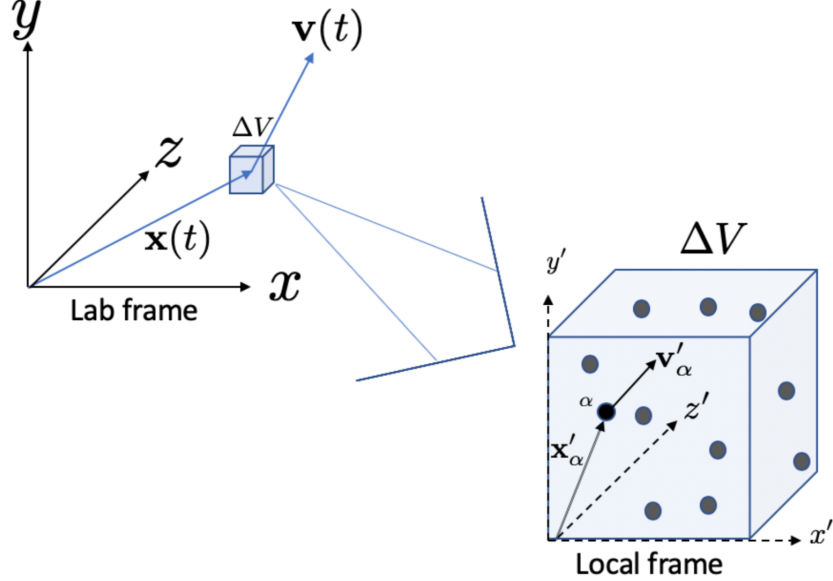


Figure 6.1: Left figure shows a volume element ΔV that is assumed to be part of a continuum. The position and velocity vectors tracking a reference point in the volume from the lab frame are $\mathbf{x}(t)$ and $\mathbf{v}(t)$, respectively. The right frame is a zoom-in of ΔV , showing that it comprises of many particles positioned and moving randomly within the volume. The position and velocity of a random particle α within ΔV relative to a coordinate system fixed in the volume element are denoted $\mathbf{x}'_\alpha(t)$ and $\mathbf{v}'_\alpha(t)$, respectively (the t label is suppressed in the zoom-in cartoon for clarity). The position of the particle α with respect to the lab frame is thus $\mathbf{x}_\alpha(t) = \mathbf{x}(t) + \mathbf{x}'_\alpha(t)$, and its lab-frame velocity is $\mathbf{v}_\alpha(t) = \mathbf{v}(t) + \mathbf{v}'_\alpha(t)$. It is assumed that $\mathbf{v}'_\alpha(t)$ and $\mathbf{v}(t)$ are uncorrelated, and that $|\mathbf{v}(t)| \ll |\mathbf{v}'_\alpha(t)|$.

We define three microscopic operators from which coarse grained averages of three key hydrodynamic variables (and associated co-called *hydrodynamic modes*) can be calculated. These are the momentum density ($\hat{\mathbf{g}}(\mathbf{x}, t)$), mass density ($\hat{\rho}(\mathbf{x}, t)$) and energy density ($\hat{\varepsilon}(\mathbf{x}, t)$) and are given, respectively, by

$$\begin{aligned}\hat{\mathbf{g}}(\mathbf{x}, t) &= \sum_{\alpha} \mathbf{p}_{\alpha} \delta(\mathbf{x} - \mathbf{x}_{\alpha}(t)) \\ \hat{\rho}(\mathbf{x}, t) &= \sum_{\alpha} m \delta(\mathbf{x} - \mathbf{x}_{\alpha}(t)) \\ \hat{\varepsilon}(\mathbf{x}, t) &= \sum_{\alpha} \frac{p_{\alpha}^2}{2m} \delta(\mathbf{x} - \mathbf{x}_{\alpha}(t)) + \sum_{\alpha} \sum_{\beta \neq \alpha} U(\mathbf{x}_{\alpha}(t) - \mathbf{x}_{\beta}(t)) \delta(\mathbf{x} - \mathbf{x}_{\alpha}(t)),\end{aligned}\quad (6.1)$$

where α and β are particle indices that count over particles in the volume ΔV , m is the mass of each particle (assumed identical here for simplicity), $\mathbf{x}_{\alpha}(t) = \mathbf{x}(t) + \mathbf{x}'_{\alpha}(t)$, $\mathbf{p}_{\alpha} = m(\mathbf{v}(t) + \mathbf{v}'_{\alpha}(t))$ is the momentum of particle α (with p_{α} denoting its magnitude) and $U(\mathbf{x}_{\alpha} - \mathbf{x}_{\beta})$ is the potential energy between two particles, where a central force field is assumed throughout.

As formal distributions, the three microscopic operators fields in Eq. (6.1) satisfy the mass, momentum and energy conservation laws, which are expressed as

$$\begin{aligned}\frac{\partial \hat{\rho}(\mathbf{x}, t)}{\partial t} &= -\nabla \cdot \hat{\mathbf{g}} \\ \frac{\partial \hat{\mathbf{g}}(\mathbf{x}, t)}{\partial t} &= -\nabla \cdot \pi_{ij} \\ \frac{\partial \hat{\varepsilon}(\mathbf{x}, t)}{\partial t} &= -\nabla \cdot \mathbf{J}_\varepsilon,\end{aligned}\tag{6.2}$$

where \mathbf{J}_ε is the microscopic energy flux and π_{ij} is the momentum flux tensor. *It is noteworthy that the conservation laws in Eq. (6.2) apply equivalently to the microscopic operators as they do to their average quantities $\rho(\mathbf{x}, t) = \langle \hat{\rho}(\mathbf{x}, t) \rangle$, $\mathbf{g}(\mathbf{x}, t) = \langle \hat{\mathbf{g}}(\mathbf{x}, t) \rangle$ and $\varepsilon(\mathbf{x}, t) = \langle \hat{\varepsilon}(\mathbf{x}, t) \rangle$ [5], where, in the latter case, averages of these hydrodynamic variables are driven by averages of the corresponding fluxes, i.e. $\pi_{ij} \rightarrow \langle \pi_{ij} \rangle$ and $\mathbf{J}_\varepsilon \rightarrow \langle \mathbf{J}_\varepsilon \rangle$.*

6.1.1 Averages of microscopic operators

In order to use mass, momentum and energy density operators, their meso-scale averages are required since hydrodynamics deals with a coarse volumes. This subsection will derive the form of local thermodynamic averages of the density, momentum and energy density using the microscopic operators in Eq. (6.1). In addition, it will be useful to know how these averages translate between lab frame co-ordinates and co-ordinates relative to the co-moving with the reference volume ΔV .

Starting with the mass density, its average is obtained by ensemble averaging the microscopic density operator,

$$\begin{aligned}\rho(\mathbf{x}, t) = \langle \hat{\rho}(\mathbf{x} - \mathbf{x}(t) - \mathbf{x}'_\alpha(t)) \rangle &= \left\langle \sum_\alpha m \left(\underbrace{\mathbf{x} - \mathbf{x}(t)}_{\mathbf{x}'} - \mathbf{x}'_\alpha(t) \right) \right\rangle \\ &= \left\langle \sum_\alpha m (\mathbf{x}' - \mathbf{x}'_\alpha(t)) \right\rangle \\ &= \rho'(\mathbf{x}', t),\end{aligned}\tag{6.3}$$

where averages are taken with respect to particle positions within the volume ΔV , and $\mathbf{x}' = \mathbf{x} - \mathbf{x}(t)$ translates the instantaneous measurement (i.e. at time t) from a point in the lab frame to a point relative to the rest frame of ΔV . The notation ρ' denotes a density measurement made entirely from within ΔV . Equation (6.3) shows, not surprisingly, that the average density in ΔV measured from within the co-moving frame (with respect to co-moving coordinates (\mathbf{x}', t)) is the same as the average density in ΔV measured relative the lab frame (with respect to lab frame coordinates (\mathbf{x}, t)).

Proceeding similarly for the momentum, its average translates between the two frames as

$$\begin{aligned}\mathbf{g}(\mathbf{x}, t) = \langle \hat{\mathbf{g}}(\mathbf{x}, t) \rangle &= \left\langle \sum_\alpha \mathbf{p}_\alpha \delta(\mathbf{x} - \mathbf{x}_\alpha(t)) \right\rangle \\ &= \left\langle \sum_\alpha m (\mathbf{v}(t) + \mathbf{v}'_\alpha(t)) \delta(\mathbf{x} - \mathbf{x}(t) - \mathbf{x}'_\alpha(t)) \right\rangle \\ &= \left\langle \sum_\alpha m \mathbf{v}(t) \delta(\mathbf{x}' - \mathbf{x}'_\alpha(t)) \right\rangle + \left\langle \sum_\alpha m \mathbf{v}'_\alpha(t) \delta(\mathbf{x}' - \mathbf{x}'_\alpha(t)) \right\rangle \\ &= \rho'(\mathbf{x}', t) \mathbf{v}(t) + \mathbf{g}'(\mathbf{x}', t) \\ &= \rho(x, t) \mathbf{v}(t),\end{aligned}\tag{6.4}$$

where it is noted that the velocity $\mathbf{v}(t)$ comes out of the average operation in going from the third to fourth lines of Eq. (6.4) since $\langle \dots \rangle$ denotes ensemble averages over particle positions and velocities relative to the co-moving frame of reference fixed in ΔV . The second term on the third line is denoted $\mathbf{g}'(\mathbf{x}', t)$ and is the average momentum in ΔV as measured relative the co-moving frame (uses rest-frame coordinates (\mathbf{x}', t)). Here, it is assumed that the microscopic motions of particles within ΔV are random and much more rapid than the hydrodynamic motion of ΔV . It will thus be assumed that $\mathbf{g}'(\mathbf{x}', t) = 0$ hereafter [5].

The translation of the average of the internal energy density in ΔV follows similarly by taking the average of the last operator in Eq. (6.1),

$$\begin{aligned}\varepsilon(\mathbf{x}, t) &= \left\langle \sum_{\alpha} \frac{p_{\alpha}^2}{2m} \delta(\mathbf{x} - \mathbf{x}_{\alpha}(t)) + \sum_{\alpha} \sum_{\beta \neq \alpha} U(\mathbf{x}_{\alpha}(t) - \mathbf{x}_{\beta}(t)) \delta(\mathbf{x} - \mathbf{x}_{\alpha}(t)) \right\rangle \\ &= \left\langle \sum_{\alpha} \frac{m}{2} (|\mathbf{v}(t)|^2 + 2\mathbf{v}(t) \cdot \mathbf{v}'_{\alpha}(t) + |\mathbf{v}'_{\alpha}(t)|^2) \delta(\mathbf{x} - \mathbf{x}(t) - \mathbf{x}'_{\alpha}(t)) \right\rangle \\ &\quad + \left\langle \sum_{\alpha} \sum_{\beta \neq \alpha} U(\mathbf{x}'_{\alpha}(t) - \mathbf{x}'_{\beta}(t)) \delta(\mathbf{x} - \mathbf{x}(t) - \mathbf{x}'_{\alpha}(t)) \right\rangle,\end{aligned}\tag{6.5}$$

where $\mathbf{x}_{\alpha}(t) - \mathbf{x}_{\beta}(t) = \mathbf{x}'_{\alpha}(t) - \mathbf{x}'_{\beta}(t)$ has been used since U depends only on position differences. Equation (6.5) gives rise to four terms,

$$\begin{aligned}\varepsilon(\mathbf{x}, t) &= \frac{|\mathbf{v}(t)|^2}{2} \underbrace{\left\langle \sum_{\alpha} m \delta(\mathbf{x}' - \mathbf{x}'_{\alpha}(t)) \right\rangle}_{\rho'(\mathbf{x}', t)} + \mathbf{v}(t) \cdot \underbrace{\left\langle \sum_{\alpha} m \mathbf{v}'_{\alpha}(t) \delta(\mathbf{x}' - \mathbf{x}'_{\alpha}(t)) \right\rangle}_{\mathbf{g}'(\mathbf{x}', t)} \\ &\quad + \underbrace{\left\langle \sum_{\alpha} \frac{m}{2} |\mathbf{v}'_{\alpha}(t)|^2 \delta(\mathbf{x}' - \mathbf{x}'_{\alpha}(t)) + \sum_{\alpha} \sum_{\beta \neq \alpha} U(\mathbf{x}'_{\alpha}(t) - \mathbf{x}'_{\beta}(t)) \delta(\mathbf{x}' - \mathbf{x}'_{\alpha}(t)) \right\rangle}_{\varepsilon'(\mathbf{x}', t)},\end{aligned}\tag{6.6}$$

where it is recalled that $\mathbf{x}' = \mathbf{x} - \mathbf{x}(t)$ translates distances relative to a reference point in the co-moving frame of ΔV ; it is also recalled that $\mathbf{v}(t)$ and $|\mathbf{v}(t)|^2$ come out of the ensemble averages. Each term in Eq. (6.6) is identified in the underbraces for clarity. By Eq. (6.3) the first becomes $\rho(x, t)$. The second is the average momentum relative to the co-moving reference frame, which vanishes. The last term $\varepsilon'(\mathbf{x}', t)$ is the internal energy density in ΔV measured relative to a rest frame fixed in ΔV (measured in co-moving co-ordinates (\mathbf{x}', t)). It can be seen as the rest-frame energy density in ΔV . Following the notation of Ref. [5], it will be denoted as $\varepsilon_0(\mathbf{x}, t)$ when measured relative to the lab frame co-ordinates. With these identifications and definitions Eq. (6.6) becomes

$$\varepsilon(\mathbf{x}, t) = \varepsilon_0(\mathbf{x}, t) + \frac{1}{2} \rho(\mathbf{x}, t) \mathbf{v}^2(t)\tag{6.7}$$

The above derivations have allowed us to compute the averages of mass, momentum and energy densities in a system represented by the volume ΔV . As $\Delta V \rightarrow dV$ and the volume becomes infinitesimal, these quantities will become constant within ΔV and come to represent thermodynamics properties between $\mathbf{x} \rightarrow \mathbf{x} + dV$ in a hydrodynamic system.

6.2 Adding Momentum into Thermodynamics

In order to derive hydrodynamic equations of a system, it is first required that its relevant hydrodynamic quantities are integrated into the statistical mechanics of a representative volume element of

said system. In the case of a deforming continuum, this translates to first working out the Hamiltonian of the system of particles moving with ΔV , and then using this to determine its partition function and free energy, which now will incorporate motional effects of the volume. Finally, this make it possible to examine the thermodynamics of the moving system, leading to an important equation for entropy production that will be the basis of the next section that works out the form of hydrodynamic fluxes.

6.2.1 Mechanics of the moving volume ΔV

Consider the Lagrangian of the system of particles in the moving volume element ΔV examined in the last subsection ¹. This is given by

$$\begin{aligned}\mathcal{L} &= \frac{1}{2} \sum_{\alpha=1}^N m |\mathbf{v}(t) + \mathbf{v}'_\alpha(t)|^2 - \sum_{\alpha} \sum_{\beta \neq \alpha} U(\mathbf{x}'_\alpha(t) - \mathbf{x}'_\beta(t)) \\ &= \frac{1}{2} \sum_{\alpha=1}^N \sum_{i=1}^3 m (v_i(t) + v'_{\alpha i}(t))^2 - U\{\mathbf{x}'_\alpha(t)\}\end{aligned}\quad (6.8)$$

where $U\{\mathbf{x}'_\alpha(t)\}$ is shorthand notation for the potential energy expression on the first line of Eq. (6.8), and the velocities are expressed in their component form in the last line of Eq. (6.8). In the notation of Hamiltonian mechanics, the canonical co-ordinates become $\mathbf{q}_\alpha(t) \rightarrow \mathbf{x}'_\alpha(t)$ and the their time derivatives $\dot{\mathbf{q}}_\alpha(t) \rightarrow \dot{\mathbf{x}}'_\alpha(t) = \mathbf{v}'_\alpha(t)$ for $\alpha = 1, \dots, N$. The canonical momentum of particle α (in component form) is given by

$$p_{\alpha i}(t) = \frac{\partial \mathcal{L}}{\partial v'_{\alpha i}} = m (v_i(t) + v'_{\alpha i}(t)), \quad (6.9)$$

or in vector form, $\mathbf{p}_\alpha(t) = m(\mathbf{v}(t) + \mathbf{v}'_\alpha(t))$. The total Hamiltonian of this system is given by

$$\begin{aligned}\mathcal{H}_T &= \sum_{\alpha=1}^N \sum_{i=1}^3 p_{\alpha i}(t) \dot{q}_{\alpha i}(t) - \mathcal{L} \\ &= \sum_{\alpha=1}^N \sum_{i=1}^3 m (v_i(t) + v'_{\alpha i}(t)) v'_{\alpha i}(t) - \mathcal{L} \\ &= \sum_{\alpha=1}^N m (\mathbf{v}(t) + \mathbf{v}'_\alpha(t)) \cdot \mathbf{v}'_\alpha(t) - \mathcal{L}\end{aligned}\quad (6.10)$$

Substituting the Lagrangian from Eq. (6.8) into Eq. (6.10), expanding and collecting terms, gives,

$$\begin{aligned}\mathcal{H}_T &= \sum_{\alpha=1}^N \frac{m}{2} |\mathbf{v}'_\alpha(t)|^2 + U\{\mathbf{x}'_\alpha(t)\} - \sum_{\alpha=1}^N \frac{m}{2} |\mathbf{v}(t)|^2 \\ &= \underbrace{\sum_{\alpha=1}^N \frac{|\mathbf{p}'_\alpha(t)|^2}{2m}}_{\mathcal{H}_R(\mathbf{x}'_\alpha, \mathbf{p}'_\alpha)} + U\{\mathbf{x}'_\alpha(t)\} - \sum_{\alpha=1}^N \frac{m}{2} |\mathbf{v}(t)|^2 \\ &= \mathcal{H}_R(\mathbf{x}'_\alpha, \mathbf{p}'_\alpha) - \frac{N m}{2} |\mathbf{v}|^2\end{aligned}\quad (6.11)$$

¹The velocity $\mathbf{v}(t)$ of the moving volume ΔV is denoted as a function of time throughout this section. However, the results derived from Newtonian mechanics translate between the lab frame the reference frame of ΔV only for Galilean translations of a uniform continuum, i.e., when $\mathbf{v}(t) = \text{constant}$. We will hereafter consider the velocity of ΔV relative to the lab frame to be small enough such as to satisfy $\mathbf{v}(t) \approx \text{constant}$ in the mechanics treatment that follows. Results obtained will be assumed to hold in hydrodynamic limit where $\mathbf{v}(t) \neq 0$, but small compared to microscopic velocities.

where the time variable was suppressed in the last line for clarity. The last line of Eq. (6.11) expresses the total Hamiltonian in terms of the rest-frame Hamiltonian (written in terms of positions and velocities relative to the co-moving reference frame) minus the total lab frame kinetic energy of the volume ΔV .

An alternate form of the Hamiltonian \mathcal{H}_T can be written by substituting $|\mathbf{v}'_\alpha|^2 = |\mathbf{v} + \mathbf{v}'_\alpha|^2 - |\mathbf{v}|^2 - 2\mathbf{v} \cdot \mathbf{v}'_\alpha$ for the first term on the first line of Eq. (6.11). Doing so, and noting that $U\{\mathbf{x}'_\alpha\} \equiv U(\mathbf{x}'_\alpha - \mathbf{x}'_\beta) = U(\mathbf{x}_\alpha - \mathbf{x}_\beta) \equiv U\{\mathbf{x}_\alpha\}$ gives,

$$\begin{aligned}\mathcal{H}_T &= \sum_\alpha \frac{|\mathbf{p}_\alpha|^2}{2m} + U\{\mathbf{x}_\alpha\} - \sum_\alpha m\mathbf{v} \cdot (\mathbf{v} + \mathbf{v}'_\alpha) \\ &= \mathcal{H}_L(\mathbf{x}_\alpha, \mathbf{p}_\alpha) - \mathbf{v} \cdot \underbrace{\left(\sum_\alpha \mathbf{p}_\alpha \right)}_{\tilde{\mathbf{P}}} \\ &= \mathcal{H}_L(\mathbf{x}_\alpha, \mathbf{p}_\alpha) - \mathbf{v} \cdot \tilde{\mathbf{P}}\end{aligned}\quad (6.12)$$

where it is recalled that the \mathbf{p}_α are given by Eq. (6.9). The quantity $\tilde{\mathbf{P}}$ in Eq. (6.12) is the total momentum. It is equivalently given as the integral over ΔV of the momentum operator in Eq. (6.1), namely,

$$\tilde{\mathbf{P}} = \sum_\alpha \mathbf{p}_\alpha = \int_{\Delta V} \sum_\alpha \mathbf{p}_\alpha \delta(\mathbf{x} - \mathbf{x}_\alpha(t)) d^3\mathbf{x} = \int_{\Delta V} \hat{\mathbf{g}}(\mathbf{x}, t) d^3\mathbf{x} \quad (6.13)$$

A quantity that will be required in what follows is the mean of the total momentum $\tilde{\mathbf{P}}$. Using information from Eq. (6.4), this becomes

$$\begin{aligned}\mathbf{P} = \langle \tilde{\mathbf{P}} \rangle &= \int_{\Delta V} \langle \hat{\mathbf{g}}(\mathbf{x}, t) \rangle d^3\mathbf{x} \\ &= \int_{\Delta V} \rho(\mathbf{x}', t) \mathbf{v}(t) d^3\mathbf{x}' + \int \underbrace{g'(\mathbf{x}', t)}_{=0} d^3\mathbf{x}' \\ &= Nm\mathbf{v}\end{aligned}\quad (6.14)$$

where the integrals on the second line of Eq. (6.14) have been translated to the co-moving reference frame.

The last lines of Eqs. (6.11) and Eqs. (6.12) offer two equivalent ways to write the total Hamiltonian of the system of particles in the volume ΔV , one with respect to positions and velocities measured in the rest frame of the volume ΔV , and other with positions and velocities measured from the stationary lab frame. Although not apparent, they are identical, implying that the lab frame Hamiltonian of the volume being equal to the rest-frame Hamiltonian plus the kinetic energy of the volume ΔV , plus a an extra term $\mathbf{v} \cdot \sum_\alpha \mathbf{p}'_\alpha$, which vanishes when averages are thus taken, making the average energy exactly as in Eq. (6.7). It is also noted that the average of the rest frame Hamiltonian gives the rest frame internal energy of the volume ΔV .

6.2.2 Statistical mechanics of the moving volume ΔV

Thus far, we have determined the local averages of key hydrodynamic quantities, and used these to find the form of the Hamiltonian of a system comprising a moving volume element in a continuum. The reason for this course of action is that we wish to investigate the volume's statistical mechanics

in order to derive a form for its free energy containing corrections due to its motion. From there, we can derive expressions for the change of entropy of the volume, and by imposing the requirement of dissipation/dissipationless entropy flow, it is possible to extract suitable forms for the mass, momentum and energy fluxes governing the corresponding conservation laws.

The starting point is to consider the partition function of the system of a moving volume ΔV . This is given by

$$Z_N(T, \Delta V, \mathbf{v}) = \int \int e^{-\beta(\mathcal{H}_L\{\mathbf{p}_\alpha, \mathbf{x}_\alpha\} - \tilde{\mathbf{P}} \cdot \mathbf{v})} d\mathbf{x}_1, \dots, d\mathbf{x}_N, d\mathbf{p}_1, \dots, d\mathbf{p}_N \quad (6.15)$$

where it is recalled that $\tilde{\mathbf{P}}$ is a function of the phase space co-ordinates, which is suppressed in Eq. (6.15) for clarity. The thermodynamics of the volume ΔV is obtained from Eq. (6.15) by the relation [14]

$$\begin{aligned} Z_N(T, \Delta V, \mathbf{v}) &= e^{-\beta F(T, \Delta V, N, \mathbf{v})} \\ &= e^{-\beta(\langle \mathcal{H}_L \rangle - T \langle S \rangle - \langle \tilde{\mathbf{P}} \rangle \cdot \mathbf{v})}, \end{aligned} \quad (6.16)$$

from which the free energy of the volume is defined as

$$F(T, \Delta V, N, \mathbf{v}) = E - TS - \mathbf{P} \cdot \mathbf{v}, \quad (6.17)$$

where the definitions $E = \langle \mathcal{H}_L \rangle$, $S = \langle S \rangle$ and $\mathbf{P} = \langle \tilde{\mathbf{P}} \rangle$ have been made. Equation (6.17) is the usual free energy of a volume of N particles, with a correction for a translation at velocity \mathbf{v} and having a momentum \mathbf{P} .

It is instructive to re-calculate the free energy of the moving volume ΔV again using the Hamiltonian form given in Eq. (6.11), written with co-ordinates in the ΔV co-moving frame of reference. The partition function in this representation becomes

$$\begin{aligned} Z_N(T, \Delta V, \mathbf{v}) &= \int \int e^{-\beta(\mathcal{H}_R\{\mathbf{p}'_\alpha, \mathbf{x}'_\alpha\} - Nm|\mathbf{v}|^2/2)} d\mathbf{x}_1, \dots, d\mathbf{x}_N, d\mathbf{p}_1, \dots, d\mathbf{p}_N \\ &= e^{\beta Nm|\mathbf{v}|^2/2} \underbrace{\int \int e^{-\beta \mathcal{H}_R\{\mathbf{p}'_\alpha, \mathbf{x}'_\alpha\}} d\mathbf{x}_1, \dots, d\mathbf{x}_N, d\mathbf{p}_1, \dots, d\mathbf{p}_N}_{Z_N(T, \Delta V, \mathbf{v}=0)}, \end{aligned} \quad (6.18)$$

where the quantity indicated in the under-brace is the partition function written entirely in terms of particle motions measured in the rest frame of ΔV . Taking logarithms of both sides of Eq. (6.18) gives

$$\begin{aligned} F(T, \Delta V, n, \mathbf{v}) &= -k_B T \ln Z_N(T, \Delta V, \mathbf{v}) \\ &= \underbrace{-k_B T \ln Z_N(T, \Delta V, \mathbf{v}=0)}_{F(T, \Delta V, N, \mathbf{v}=0)} - \frac{Nm|\mathbf{v}|^2}{2}, \end{aligned} \quad (6.19)$$

where the quantity indicated in the under-brace of Eq. (6.19) is the free energy in the co-moving reference frame of the volume ΔV . Equation (6.19) thus becomes

$$F(T, \Delta V, N, \mathbf{v}) = F_0(T, \Delta V, N) - \frac{Nm|\mathbf{v}|^2}{2}, \quad (6.20)$$

where $F_0(T, \Delta V, N)$ denotes the rest-frame free energy of the volume ΔV .

In closing this subsection, it is noted that from Eq. (6.17) the internal energy can be written as

$$E(S, \Delta V, N, \mathbf{P}) = F(T, \Delta V, N, \mathbf{v}) + TS + \mathbf{P} \cdot \mathbf{v} \quad (6.21)$$

Substituting the last line of Eq. (6.14) for \mathbf{P} in Eq. (6.21), substituting $F(T, V, N, \mathbf{v})$ from Eq. (6.20), and noting that the entropy S remains the same in both lab and rest frames of ΔV , gives,

$$E(S, \Delta V, N, \mathbf{P}) = E_0(S, \Delta V, N) + \frac{|\mathbf{P}|^2}{2mN}, \quad (6.22)$$

which is the extensive form of Eq. (6.7), i.e. integrating the former over the volume of ΔV gives Eq. (6.22). Here, $E_0(S, \Delta V, N)$ is the rest-frame internal energy. It is noted that \mathbf{v} and \mathbf{P} are conjugate variables, with the former being intensive and the latter extensive.

6.2.3 Thermodynamics of the moving volume ΔV

This subsection will use information derived thus far to derive several expressions that relate changes in thermodynamic potentials to changes in local thermodynamic and hydrodynamic variables. The section culminates with an equation for the entropy change of ΔV , which will be used in the next subsection to derive expressions for the fluxes driving the evolution of mass, momentum and energy densities. Throughout this section, it will be assumed that the continuum in the volume ΔV supports elastic deformations, without loss of generality.

The starting point is to revisit the first law of thermodynamics. Specifically, combine Eq. (6.22) and Eq. (1.6) to yield a modified version of the first law of thermodynamics,

$$dE = TdS + \sigma_{ij}du_{ij}\Delta V + \mu dN + \mathbf{v} \cdot d\mathbf{P} \quad (6.23)$$

where σ_{ij} denotes the stress tensor acting on the reference volume element ΔV and u_{ij} is the strain tensor, defined as $u_{ij} = (\partial_i u_j + \partial_j u_i)/2$, where $\mathbf{u} = (u_x, u_y, u_z)$ is the local displacement of the solid. The second term is a generalization of the usual $-Pd(\Delta V)$ term that appears for isotropic materials. Solids support shear modes, their main hydrodynamic modes of deformation. As a result, work can be done on them by volume changes working against isotropic pressure, *as well as* by other modes of mechanical deformation they support².

Next, consider the differential of the free energy in Eq. (6.17),

$$dF = dE - TdS - SdT - \mathbf{P} \cdot d\mathbf{v} - \mathbf{v} \cdot d\mathbf{P} \quad (6.24)$$

Substituting Eq. (6.23) into Eq. (6.24) gives the differential of free energy as

$$dF = -SdT + \sigma_{ij}du_{ij}\Delta V + \mu dN + \mathbf{P} \cdot d\mathbf{v} \quad (6.25)$$

Changes in the grand potential is similarly are obtained form the relation $\Omega = F - \mu N$, which implies that $d\Omega = dF - \mu dN - N d\mu$. Substituting Eq. (6.25) for dF into this expression for $d\Omega$ gives,

$$d\Omega = -SdT + \sigma_{ij}du_{ij}\Delta V - N d\mu - \mathbf{P} \cdot d\mathbf{v} \quad (6.26)$$

By consulting Eq. (6.23), Eq. (6.25) and Eq. (6.26), the driving force for momentum is derived from each potential, each under difference constraints, Namely

$$\mathbf{P} = -\left. \frac{\partial E}{\partial \mathbf{v}} \right|_{S, \Delta V, u_{ij}, N} = -\left. \frac{\partial F}{\partial \mathbf{v}} \right|_{T, \Delta V, u_{ij}, N} = -\left. \frac{\partial \Omega}{\partial \mathbf{v}} \right|_{S, \Delta V, u_{ij}, \mu} \quad (6.27)$$

²As a consistency check, when the stress is isotropic as in a fluid, $\sigma_{ij} = -p\delta_{ij}$ and $du_{ii} = d(\Delta V)/\Delta V$, which gives, $dW = -p\delta_{ij} du_{ij} \Delta V = -p(d(\Delta V)/\Delta V) \Delta V = -p d(\Delta V)$, which is the traditional expression for work in an isotropic system.

It is instructive to break up the stress tensor into the diagonal components (which gives the pressure) and the non-diagonal parts that are responsible for shear deformation and only exist for solids, which support shear. We follow the notation of Ref. [5] and write this as

$$\sigma_{ij} = -p\delta_{ij} + h_{ij}, \quad (6.28)$$

where the first term in Eq. (6.28) is isotropic and corresponds to the thermodynamic pressure, while the second component represents a tensor conjugate to elastic strains u_{ij} (i.e. gradients of the displacements, the broken symmetry variables of a solid)³. This tensor is related to the elastic coefficients of a solid and its coupling to the u_{ij} describes elastic deformations energy in solids. (*The derivation of Eq. (6.28) is in the slides for PHYS657 and will be added here as an appendix at some point*⁴). The first term accounts for density changes, which may include vacancies when vacancies are considered in solids, as was done in Section 5.1.1. It is noted that the term h_{ij} has units of $[J/m^3]$, and it vanishes for liquids. Substituting this decomposition of σ_{ij} into the above expressions for dE , dF and $d\Omega$ gives the following set of useful thermodynamic differentials for the potentials applicable to a moving system (e.g. the volume ΔV),

$$\begin{aligned} dE &= TdS - p d(\Delta V) + \mu dN + h_{ij} du_{ij} \Delta V + \mathbf{v} \cdot d\mathbf{P} \\ dF &= -SdT - p d(\Delta V) + \mu dN + h_{ij} du_{ij} \Delta V - \mathbf{P} \cdot d\mathbf{v} \\ d\Omega &= -SdT - p d(\Delta V) - Nd\mu + h_{ij} du_{ij} \Delta V - \mathbf{P} \cdot d\mathbf{v}, \end{aligned} \quad (6.29)$$

where it is recalled that the notation ΔV is just to be consistent with notation used thus far. In general these relations hold for any moving system translating at a velocity \mathbf{v} . From the differentials of the potentials in Eq. (6.29) it can be deduced that

$$h_{ij} = -\frac{1}{\Delta V} \left. \frac{\partial E}{\partial u_{ij}} \right)_{S, \Delta V, N, \mathbf{P}} = -\frac{1}{\Delta V} \left. \frac{\partial F}{\partial u_{ij}} \right)_{T, \Delta V, N, \mathbf{v}} = -\frac{1}{\Delta V} \left. \frac{\partial \Omega}{\partial u_{ij}} \right)_{T, \Delta V, \mu, \mathbf{v}} \quad (6.30)$$

The counterparts of Eq. (6.30) relating h_{ij} to changes in free energy density will be derived below. **Note: to simplify notation, in the rest of this subsection the volume of the system being considered will be denoted simply as “V” rather than “ ΔV ”.** We will re-adopt the ΔV notation again when some remaining derivations are out of the way.

Functions like E , F , Ω , \mathbf{P} and S are extensive, which means they increase linearly with system volume or number of particles. It will prove convenient in what follows to work with the corresponding densities of these functions, which assumes we can write $E = V\varepsilon$, $F = Vf$, $\Omega = V\omega$, $S = Vs$, $\mathbf{P} = Vg$, etc. Extensive variables are also known as *homogeneous functions of order 1* in the other extensive variables, which implies they can be written as follows,

$$\begin{aligned} E(S, V, N, Vu_{ij}, \mathbf{P}) &= V\varepsilon(S/V, 1, N/V, u_{ij}, \mathbf{P}/V) = V\varepsilon(s, \rho, u_{ij}, \mathbf{g}) \\ F(T, V, N, Vu_{ij}, \mathbf{v}) &= Vf(T, 1, N/V, u_{ij}, \mathbf{v}) = Vf(T, \rho, u_{ij}, \mathbf{v}) \\ \Omega(T, V, \mu, Vu_{ij}, \mathbf{v}) &= V\omega(T, V/V, \mu, u_{ij}, \mathbf{v}) = V\omega(T, \mu, u_{ij}, \mathbf{v}) \end{aligned} \quad (6.31)$$

where ε , f , ω , s , ρ and \mathbf{g} are densities of corresponding quantities (quantity/volume). Using the homogeneity properties in Eq. (6.31) allows us to re-express Eq. (6.30) in terms of the densities of the potentials according to

$$h_{ij} = -\left. \frac{\partial \varepsilon}{\partial u_{ij}} \right)_{S, N, \mathbf{P}} = -\left. \frac{\partial f}{\partial u_{ij}} \right)_{T, N, \mathbf{v}} = -\left. \frac{\partial \omega}{\partial u_{ij}} \right)_{T, \mu, \mathbf{v}}, \quad (6.32)$$

³The reader is referred to Section 5.1.3 where the properties of h_{ij} were derived by constructing a mean field theory of solids involving vacancies.

⁴This form of the stress tensor can also be derived independently from static considerations of the work done to deform a volume of solid volume [5].

where it is recalled that for simplicity of notation, the volume ΔV in Eq. (6.30) was replaced by V , as was discussed above. The homogeneity properties encapsulated in Eqs. (6.30) are useful for determining the properties of the pressure p , from which the desired equation for entropy change, needed to complete our hydrodynamics, is derived. This is examined next.

Comparing the last of Eq. (6.31) with the last line of Eq. (6.29) leads to

$$\left. \frac{\partial \Omega}{\partial V} \right|_{T, \mu_{ij}, u_{ij}, \mathbf{v}} = \omega = -p \quad (6.33)$$

Combining the definition $\Omega = F - \mu N$ with Eq. (6.17) and using the last line of Eq. (6.31) and Eq. (6.33) to write $\Omega = V\omega = -pV$ gives

$$\begin{aligned} \Omega &= -\omega V = -pV = E - TS - \mathbf{P} \cdot \mathbf{v} - \mu N \\ \implies -p &= \varepsilon - Ts - \bar{\mu}\rho - \mathbf{g} \cdot \mathbf{v}, \end{aligned} \quad (6.34)$$

where $\bar{\mu}\rho = (\mu/m)(mN/V)$ thus making $\bar{\mu}$ the chemical potential per atom and ρ the usual density (units=[mass/volume]). It is noted that this representation of pressure (p) makes it a function of $(T, \bar{\mu}, \mathbf{v}, u_{ij})$. It is instructive to compare the change in pressure dp from the second expression in Eq. (6.34), i.e.,

$$-dp = d\varepsilon - Tds - sdT - \bar{\mu}\delta\rho - \rho d\bar{\mu} - \mathbf{g} \cdot \delta\mathbf{v} - \mathbf{v} \cdot d\mathbf{g}, \quad (6.35)$$

to dp obtained from the last line of Eq. (6.29), which gives

$$\begin{aligned} d\Omega &= d(-pV) = -pdV - Vdp = -SdT - pdV - Nd\mu + h_{ij}du_{ij}V - \mathbf{P} \cdot d\mathbf{v} \\ \implies -dp &= -sdT - \rho d\bar{\mu} - \mathbf{g} \cdot d\mathbf{v} + h_{ij}du_{ij} \end{aligned} \quad (6.36)$$

Subtracting Eq. (6.36) from Eq. (6.35) finally gives

$$Tds = d\varepsilon - \bar{\mu}d\rho - h_{ij}du_{ij} - \mathbf{v} \cdot d\mathbf{g} \quad (6.37)$$

Equation (6.37) relates the change in entropy to three sources, the work done to change the density of particles, the work done to change the spacing of lattice planes in a solid, and the change of energy of the moving system. In what follows, this equation will be applied locally to the volume ΔV and combined with the locally averaged conservation laws to extract forms for the hydrodynamic fluxes, which is the main goal of this chapter.⁵

6.3 Entropy Production and Hydrodynamic Fluxes

It is typically assumed that Eq. (6.37) holds at any instant of time in moving system, which it will be recalled, going back to the start of this chapter, represents a small volume moving within a deforming

⁵It is noted that one could have taken an alternate route above by considering a slightly different free energy and grand potential, defined by $\tilde{F} = F - h_{ij}u_{ij}$ and $\tilde{\Omega} = \tilde{F} - \mu\rho$, which are Legendre transforms of the “traditional” F and Ω , respectively. Proceeding through the same steps as above would have resulted in an expression for pressure given by $-p = \varepsilon - Ts - \bar{\mu}\rho - \mathbf{g} \cdot \mathbf{v} - h_{ij}u_{ij}$, which is a Legendre transform of Eq. (6.34), which now makes pressure a function of $(T, \bar{\mu}, \mathbf{v}, h_{ij})$. This is the same expression for pressure used in Ref. [23]. It is noted that this representation of p leads to the same entropy change expression as in Eq. (6.37), and does not change any of the results that follow in the calculations below.

continuum. As a result, Eq. (6.37) can be turned into a time rate of change of entropy of the volume ΔV , i.e.,

$$T \frac{\partial s}{\partial t} = \frac{\partial \varepsilon}{\partial t} - \bar{\mu} \frac{\partial \rho}{\partial t} - h_{ij} \frac{\partial u_{ij}}{\partial t} - \mathbf{v} \cdot \frac{\partial \mathbf{g}}{\partial t} \quad (6.38)$$

$$= -\nabla \cdot \mathbf{J}_\varepsilon + \bar{\mu} \nabla \cdot \mathbf{g} - h_{ij} \nabla_i v_j + v_j \nabla_i \pi_{ji}, \quad (6.39)$$

where each time derivative on the right hand side of Eq. (6.38) has been associated with a gradient of a flux of a coarse grained microscopic quantity from Eq. (6.2). In particular, the rate of average energy density is the negative gradient of the flux of energy density, the second term similarly to momentum flux, the third term to the gradient of the local velocity and the fourth to the gradient of the momentum tensor. It is noted that $\pi_{ij} = \pi_{ji}$. For readers following [5], we use indicial notation when tensor quantities with more than two indices need to be represented, the notation $\nabla_i = \partial_{x_i}$ and repeated indices imply summation. Equation (6.37) can be turned into a vector

$$T \nabla_i s = \nabla_i \varepsilon - \bar{\mu} \nabla_i \rho - v_j \nabla_i g_j - h_{kl} \nabla_i \nabla_k u_l, \quad (6.40)$$

where each component of Eq. (6.40) gives the gradient of change of entropy in the i^{th} direction ⁶. It is noted that the form of the last term follows due to the symmetry of h_{ij} and u_{ij} . Taking the dot product of Eq. (6.40) with the velocity $\mathbf{v} = (v_1, v_2, v_3)$ of the system ΔV gives

$$T \mathbf{v} \cdot \nabla s = \mathbf{v} \cdot \nabla \varepsilon - \bar{\mu} \mathbf{v} \cdot \nabla \rho - v_i v_j \nabla_i g_j - v_i h_{kl} \nabla_i \nabla_k u_l \quad (6.41)$$

Adding Eq. (6.39) and Eq. (6.41) gives,

$$\begin{aligned} T \frac{\partial s}{\partial t} + T \mathbf{v} \cdot \nabla s &= (-\nabla \cdot \mathbf{J}_\varepsilon + \mathbf{v} \cdot \nabla \varepsilon) + \bar{\mu} (\nabla \cdot \mathbf{g} - \mathbf{v} \cdot \nabla \rho) \\ &= (v_j \nabla_i \pi_{ji} - v_i v_j \nabla_i g_j) \\ &\quad - (h_{ij} \nabla_i v_j + v_i h_{kl} \nabla_i \nabla_k u_l) \end{aligned} \quad (6.42)$$

The above important, albeit messy, equation can be simplified by implementing the following algebraic manipulations,

$$\begin{aligned} -\nabla \cdot \mathbf{J}_\varepsilon + \mathbf{v} \cdot \nabla \varepsilon &= \nabla \cdot (-\mathbf{J}_\varepsilon + \varepsilon \mathbf{v}) - \varepsilon \nabla \cdot \mathbf{v} \\ \bar{\mu} (\nabla \cdot \mathbf{g} - \mathbf{v} \cdot \nabla \rho) &= -\nabla \cdot (\bar{\mu} \{\rho \mathbf{v} - \mathbf{g}\}) + (\rho \mathbf{v} - \mathbf{g}) \cdot \nabla \bar{\mu} + \bar{\mu} \rho \nabla \cdot \mathbf{v} \\ (v_j \nabla_i \pi_{ji} - v_i v_j \nabla_i g_j) &= \nabla_i (v_j \pi_{ji} - v_j v_i g_j) - (\pi_{ji} - v_i g_j) \nabla_i v_j + v_j g_j \nabla \cdot \mathbf{v} \\ v_i h_{kl} \nabla_i \nabla_k u_l &= \nabla_i (v_i h_{kl} \nabla_k u_l) - \nabla_i (v_i h_{kl}) \nabla_k u_l, \end{aligned} \quad (6.43)$$

where ∇_i operators act only on the quantity, operation or brackets to their immediate right. Substituting the simplifications in Eq. (6.43) into Eq. (6.42), writing $\mathbf{v} \cdot \nabla s = \nabla \cdot (s \mathbf{v}) - s \nabla \cdot \mathbf{v}$, and collecting terms gives,

$$\begin{aligned} T \frac{\partial s}{\partial t} + T \nabla \cdot (s \mathbf{v}) &= (Ts - \varepsilon + \bar{\mu} \rho + \mathbf{v} \cdot \mathbf{g}) \nabla \cdot \mathbf{v} + (\rho \mathbf{v} - \mathbf{g}) \cdot \nabla \bar{\mu} \\ &\quad - \nabla_i (\mathbf{J}_\varepsilon - \varepsilon v_i + \bar{\mu} \{\rho v_i - g_i\} - v_j \pi_{ji} + v_j v_i g_j + v_i h_{kl} \nabla_k u_l) \\ &\quad - (\pi_{ji} - v_i g_j + h_{ij}) \nabla_i v_j + \nabla_i (v_i h_{kl}) \nabla_k u_l \end{aligned} \quad (6.44)$$

⁶It is noted that due to the symmetry of u_{ij} it is straightforward to show that contractions like $h_{kl} \nabla_k u_l$ or $h_{kl} \nabla_i \nabla_k u_l$ can be written as $h_{kl} u_{kl}$ or $h_{kl} \nabla_i u_{kl}$, respectively. This property will sometimes be used here for convenience.

Using Eq. (6.34) to identify pressure in the first term on the right hand side of Eq. (6.44), and defining *dissipative heat flux* \mathbf{Q}_ε by

$$\mathbf{Q}_\varepsilon = \mathbf{J}_\varepsilon - \varepsilon \mathbf{v} + \bar{\mu} (\rho \mathbf{v} - \mathbf{g}) - v_j \pi_{ji} + (\mathbf{v} \cdot \mathbf{g}) v_i + v_i h_{kl} \nabla_k u_l, \quad (6.45)$$

reduces Eq. (6.44) to the form

$$\begin{aligned} T \frac{\partial s}{\partial t} + T \nabla \cdot (s \mathbf{v}) &= -\nabla \cdot \mathbf{Q}_\varepsilon \\ &\quad - (\pi_{ji} - p \delta_{ij} + h_{ij} - v_i g_j) \nabla_i v_j \\ &\quad + (\rho \mathbf{v} - \mathbf{g}) \cdot \nabla \bar{\mu} \\ &\quad + \nabla_i (v_i h_{kl}) \nabla_k u_l, \end{aligned} \quad (6.46)$$

where we used $p \nabla \cdot \mathbf{v} = p \delta_{ij} \nabla_i v_j$ to combine the first terms on the first and last lines of Eq. (6.44), and where we reverted back to the notation $\nabla_k u_l = u_{kl}$ to represent the last term in Eq. (6.44).

To proceed further, the identity

$$\nabla \cdot \mathbf{Q}_\varepsilon = T \nabla \cdot \left(\frac{\mathbf{Q}_\varepsilon}{T} \right) + \left(\frac{\mathbf{Q}_\varepsilon}{T} \right) \cdot \nabla T \quad (6.47)$$

is substituted into Eq. (6.46). Thus chanegs the entropy production equation to

$$\begin{aligned} T \frac{\partial s}{\partial t} + T \nabla \cdot (s \mathbf{v}) + T \nabla \cdot \left(\frac{\mathbf{Q}_\varepsilon}{T} \right) &= - \left(\frac{\mathbf{Q}_\varepsilon}{T} \right) \cdot \nabla T \\ &\quad - (\pi_{ji} - p \delta_{ij} + h_{ij} - v_i g_j) \nabla_i v_j \\ &\quad + (\rho \mathbf{v} - \mathbf{g}) \cdot \nabla \bar{\mu} \\ &\quad + \nabla_i (v_i h_{kl}) \nabla_k u_l \end{aligned} \quad (6.48)$$

Equation (6.48) is next integrated on both sides over a volume that is large enough that the fluxes $s \mathbf{v}$ and \mathbf{Q}_ε can be assumed to vanish on the volume's surface. Furthermore, since we are only considering linear elasticity of solids here, only terms quadratic in the displacements, strains, velocities or their couplings is retained, which implies that the last term in Eq. (6.48) can be neglected as it is of $\mathcal{O}(u_i^3, (\delta n/n) u_i^2)$ (since by Eq. (5.18) $h_{ij} \sim K_{ijkl} u_{kl} + D (\delta n/n_o) \delta_{ij}$, where K_{ijkl} and D are constants and n_o is a reference density)⁷. These considerations give

$$\frac{dS_{\text{tot}}}{dt} = \int \frac{1}{T} \left\{ - \left(\frac{\mathbf{Q}_\varepsilon}{T} \right) \cdot \nabla T - \left\{ \pi_{ji} - p \delta_{ij} + h_{ij} - v_i g_j \right\} \nabla_i v_j + \left\{ \rho \mathbf{v} - \mathbf{g} \right\} \cdot \nabla \bar{\mu} \right\} d^3 \mathbf{x} \quad (6.49)$$

where S_{tot} is the total integrated entropy in the volume. Equation (6.49) is an entropy production equation that is driven by three terms on the right hand side, each of which is a scalar made from a tensor product of two current densities. Non-negativity of entropy production will allow us to determine constitutive relations for the hydrodynamic fluxes from the right hand side of Eq. (6.49).

The case of dissipationless deformation requires that $dS_{\text{tot}}/dt = 0$. In a general hydrodynamic state of a deforming continuum, the local gradient terms ∇T , $\nabla_i v_j$ and $\nabla \bar{\mu}$ are not zero. As a result, the

⁷It is also noted that if the alternate expression for pressure discussed in the footnote 5 was used, the last term in Eq. (6.48) would have come out to be $v_i \nabla_i (h_{kl}) \nabla_k u_l$, but this is still of $\mathcal{O}(u_i^3, (\delta n/n) u_i^2)$ and can be neglected for linear elasticity.

vanishing of the integral in Eq. (6.49) implies that: (1) the expressions multiplying the aforementioned gradient terms vanish; (2) the dissipative heat flux $\mathbf{Q}_\varepsilon = 0$. This gives,

$$\mathbf{g} = \rho\mathbf{v} \quad (6.50)$$

$$\pi_{ji} = \underbrace{p\delta_{ij} - h_{ij}}_{-\sigma_{ij}} + v_i g_j \quad (6.51)$$

$$\mathbf{J}_\varepsilon = \varepsilon\mathbf{v} + v_j \pi_{ji} - (\mathbf{v} \cdot \mathbf{g}) v_i + v_i h_{kl} \nabla_k u_l, \quad (6.52)$$

The momentum flux tensor is seen to naturally come out to be a sum of the stress tensor, as conjectured in Eq. (6.28), plus a convective term, the latter of which is only kept for fluid flow (where also $h_{ij} = 0$). It is instructive to make another simplification to Eq. (6.52), by substituting π_{ji} from Eq. (6.51). This gives $\mathbf{J}_\varepsilon = (\varepsilon + p)\mathbf{v} - v_j h_{ij} [1 - \nabla_k u_l]$, where $1 - \nabla_k u_l \approx 1$ for small strains. Writing $g_i = \rho v_i$ in the third term on the right hand side of Eq. (6.51) gives the final form of the hydrodynamic fluxes,

$$\mathbf{g} = \rho\mathbf{v} \quad (6.53)$$

$$\pi_{ij} = p\delta_{ij} - h_{ij} + \rho v_i v_j \quad (6.54)$$

$$\mathbf{J}_\varepsilon = (\varepsilon + p)\mathbf{v} - v_j h_{ij}, \quad (6.55)$$

Equation (6.53)-Eq. (6.55), along the constitutive relationship for pressure in Eq. (6.34), are the final form of the hydrodynamic fluxes driving the local conservation of mass, momentum and internal energy in deforming continuum (either solid or liquid in the general form written as above).

6.3.1 Specialization to liquids

Since liquids do not support shear, $h_{ij} = 0$, and the above equations reduce to

$$\mathbf{g} = \rho\mathbf{v} \quad (6.56)$$

$$\pi_{ij} = p\delta_{ij} + \rho v_i v_j = -\sigma_{ij} + \rho v_i v_j \quad (6.57)$$

$$\mathbf{J}_\varepsilon = (\varepsilon + p)\mathbf{v}, \quad (6.58)$$

and Eq. (6.34) for pressure, i.e. stress tensor for the liquid. Combining Eq. (6.56)-Eq. (6.58) with conservation laws discussed above leads to the Navier-Stokes equations. It is noted that if dissipation is considered in the liquid, $dS_{\text{tot}}/dt > 0$, and additional viscosity terms quadratic in the velocities must be added to the fluxes to account for this. The reader is referred to Ref. [5] for details on this.

6.3.2 Specialization to solids

In deforming solids considered in most phase transformation processes, velocities as small and so non-linear terms in velocities are also neglected. The corresponding fluxes thus become,

$$\mathbf{g} = \rho\mathbf{v} \quad (6.59)$$

$$\pi_{ij} = p\delta_{ij} - h_{ij} = -\sigma_{ij} \quad (6.60)$$

$$\mathbf{J}_\varepsilon = (\varepsilon + p)\mathbf{v} - v_j h_{ij}, \quad (6.61)$$

where the constitutive relation for pressure given by Eq. (6.34), re-written here neglecting the non-linear velocity terms,

$$\begin{aligned} -p &= f - \bar{\mu}\rho \\ &= \varepsilon - Ts - \bar{\mu}\rho \end{aligned} \quad (6.62)$$

It is recalled that Eq. (6.62) was used in Section (5.1.3) derive the pressure in a solid when considering vacancies.

6.4 Hydrodynamics of Solids: Displacement Modes

This section uses the fluxes derived above combined with the conservation relations for mass and momentum to derive equations that govern the hydrodynamics modes of $\mathbf{u} = (u_x, u_y, u_z)$, the three broken symmetry variables that characterize a solid. The equation will have the form of a wave equation doubtless seen by many in physics numerous times in their undergraduate education, with one twist however, the elastic coefficients are endowed with corrections due to vacancy effects relevant to a solid, something very rarely seen in undergraduate studies.

We start with the expression for momentum density \mathbf{g} and approximate the velocity of a volume element in a deforming solid by $\mathbf{v} \approx \partial_t \mathbf{u}$, which gives

$$\mathbf{g} = \rho(\mathbf{x}, t)\mathbf{v} = \rho(\mathbf{x}, t)\frac{\partial \mathbf{u}}{\partial t} \quad (6.63)$$

We combine Eq. (6.63) along with the momentum conservation equation,

$$\frac{\partial \mathbf{g}}{\partial t} = \nabla_j \sigma_{ij}, \quad (6.64)$$

and the mass conservation equation,

$$\frac{\partial \rho(\mathbf{x}, t)}{\partial t} = -\nabla \cdot \mathbf{g}, \quad (6.65)$$

to arrive at

$$\frac{\partial \mathbf{g}}{\partial t} = \frac{\partial}{\partial t} \left(\rho(\mathbf{x}, t) \frac{\partial \mathbf{u}}{\partial t} \right) = \nabla_j \sigma_{ij}, \quad (6.66)$$

which leads to

$$\rho(\mathbf{x}, t) \frac{\partial^2 u_i}{\partial t^2} + \underbrace{\frac{\partial u_i}{\partial t}}_{v_i} \underbrace{\frac{\partial \rho(\mathbf{x}, t)}{\partial t}}_{-\nabla \cdot \mathbf{g}} = \nabla_j \sigma_{ij} \quad (6.67)$$

Substituting $\mathbf{v} = \partial_t \mathbf{u}_i$ and $\partial_t \rho = -\nabla \cdot \mathbf{g}$ gives

$$\rho(\mathbf{x}, t) \frac{\partial^2 u_i}{\partial t^2} - (\nabla \cdot \mathbf{g}) v_i = \nabla_j \sigma_{ij} \quad (6.68)$$

We can neglect the second order velocity terms in the study of linearized hydrodynamics, hence dropping the non-linear velocity term in Eq. (6.68) is dropped. This yields

$$\rho(\mathbf{x}, t) \frac{\partial^2 u_i}{\partial t^2} = \nabla_j \sigma_{ij}, \quad (6.69)$$

which is a wave equation for dissipation-less dynamics for each of the displacement modes of a solid.

An explicit form for the right hand side of Eq. (6.69) can be obtained by using Eq. (5.24) for the relative change of stress from a reference state, which was discussed in relation to solids in Section 5.1. Since we saw that $\nabla_j \sigma_{ij} = \nabla_j \delta \sigma_{ij}$, we can write,

$$\rho(\mathbf{x}, t) \frac{\partial^2 u_i}{\partial t^2} = \frac{\partial}{\partial x_j} \left\{ (D - A) \left\{ \frac{\delta \rho}{\rho_0} + u_{ii} \right\} \delta_{ij} + K_{ijkl}^v u_{kl} \right\} \quad (6.70)$$

where we have adapted the notation of Section 5.1 to the notation of this chapter. For small deformations near the reference equilibrium state, we can approximate $\delta \rho / \rho_0 \approx -u_{ii}$, which allows us to

neglect the first term in the large brackets on the right hand side of Eq. (6.70). This finally gives the more familiar formula from continuum mechanics,

$$\rho(\mathbf{x}, t) \frac{\partial^2 u_i}{\partial t^2} = \frac{\partial}{\partial x_j} (K_{ijkl}^v u_{kl}) \quad (6.71)$$

where it is recalled that repeated indices are summed over. Equation (6.71) is the standard wave equation developed with the hydrodynamics ideas of this Chapter, and which propagates the three modes of displacement in a solid. It is stressed, however, that it contains crucial corrections to the standard Hookian elastic constants that are born out of our of considerations of vacancy thermodynamics in solids, done in Section 5.1.

Chapter 7

Classical Density Functional Theory

The above treatment of thermodynamic potentials and their application to determining equilibrium properties of a system assumes that its phases are translationally invariant, i.e. phases are uniform. Even for the case of phase coexistence, no spatial distinction between phases is made, thus neglecting any non-uniformity within and between phases (e.g. fluctuations and interfaces). To derive a theory describing spatial variation in materials, we need to introduce spatial structure into the ensemble averaging process of the grand partition function and other thermodynamic potentials. Minimization of the grand potential functional containing spatial variations will lead to an Euler-Lagrange equation, differential equation, whose solution allows for the calculation of the density profile and energy of coexisting phases at equilibrium. For more details on the processes followed in this section, the reader is referred to Ref. [13].

7.1 Statistical Mechanics Preliminaries

We begin this discussion this notion of a classical density operator given by

$$\hat{\rho}(\mathbf{x}; \mathbf{q}) = \sum_{i=0}^N \delta^{(3)}(\mathbf{x} - \mathbf{q}_i) \quad (7.1)$$

where \mathbf{x} is the spatial (vector) position where a density measurement is made, while the \mathbf{q}_i is the vector position of any of the $i = 1 \dots N$ particles in the system and \mathbf{q} represents the $3N$ dimensional vector of all particle positions. The average of the system density at a position \mathbf{x} is given by averaging $\hat{\rho}(\mathbf{x}; \mathbf{q})$ over the phase space of all N particle positions \mathbf{q}_i and all N particle momenta \mathbf{p}_i according to

$$\rho(\mathbf{x}) = \langle \hat{\rho}(\mathbf{x}; \mathbf{q}) \rangle = \sum_{N=0}^{\infty} \frac{1}{h^{3N} N!} \int \hat{\rho}(\mathbf{x}; \mathbf{q}) f(\mathbf{q}, \mathbf{p}; N) d\Gamma, \quad (7.2)$$

where h is Plank's constant and $d\Gamma \equiv d\mathbf{q}_1, \dots, d\mathbf{q}_N, d\mathbf{p}_1, \dots, d\mathbf{p}_N \equiv d\mathbf{q}^N d\mathbf{p}^N$, where \mathbf{p} denotes the $3N$ dimensional vector of momenta of all the particles. The function $f(\mathbf{q}, \mathbf{p}, N)$ denotes the N -partcile equilibrium phase space probability density, given explicitly for an open system by

$$f(\mathbf{q}, \mathbf{p}; N) = \frac{e^{-\beta(\mathcal{H}-\mu N)}}{\Xi(\mu, \beta)}, \quad (7.3)$$

where $\beta=1/k_B T$, $\mathcal{H} \equiv \mathcal{H}(\mathbf{q}, \mathbf{p})$ is the Hamiltonian, μ the chemical potential of the system and $\Xi(\mu, \beta)$ is the grand canonical partition function of the system, given by

$$\begin{aligned}\Xi &= \sum_{N=0}^{\infty} \frac{1}{h^{3N} N!} \iint \exp(-\beta(\mathcal{H} - \mu N)) d\mathbf{q}^N d\mathbf{p}^N \\ &= \sum_{N=0}^{\infty} \frac{\exp(N\beta\mu)}{h^{3N} N!} \iint \exp(-\beta\mathcal{H}) d\mathbf{q}^N d\mathbf{p}^N = \sum_{N=0}^{\infty} \frac{z^N}{N!} Z_N,\end{aligned}\quad (7.4)$$

where z denotes the *activity* (or Fugacity)

$$z = \frac{\exp(\beta\mu)}{\Lambda^3}, \quad (7.5)$$

and Λ is the *de Broglie thermal wavelength*

$$\Lambda = \left(\frac{2\pi\beta\hbar^2}{m} \right)^{1/2}, \quad (7.6)$$

while Z_N is the configurational integral

$$Z_N = \int \exp(-\beta V_N) d\mathbf{q}^N \quad (7.7)$$

It is noted that the normalization of Eq. (7.3) and Eq. (7.4) follows

$$\sum_{N=0}^{\infty} \frac{1}{h^{3N} N!} \iint f(\mathbf{q}, \mathbf{p}; N) d\mathbf{q}^N d\mathbf{p}^N = 1, \quad (7.8)$$

where the $N!$ assures we don't over-count states that involve a permutation of the indistinguishable particle labels, and h^{3N} is for consistency with quantum statistical mechanics and to make the partition function dimensionally correct. It will be seen as we progress that working in the grand canonical ensemble as we do above is practical for distilling equilibrium properties in non-uniform systems. The density $\rho(x) = \langle \hat{\rho}(x; \mathbf{q}) \rangle$ in Eq. (7.2) is also denoted as $\rho^{(1)}(\mathbf{x})$, and referred to as the *1-particle density* [13]. We will hereafter drop the superscript in what follows for convenience.

Equation (7.3) allows all thermodynamic properties of a system to be calculated, whether they have a spacial variation in them (as with $\rho(\mathbf{x})$) or not. Averages of a quantity follow the form of Eq. (7.2) where $\hat{\rho}(\mathbf{x}; \mathbf{q})$ is replaced by whatever other operator (i.e. microscopic quantity, e.g $B(\mathbf{x}, N; \mathbf{q}, \mathbf{p})$) we wish to quantify. For example, average particle number is found by replacing $B \rightarrow N$, average energy is found by replacing $B \rightarrow \mathcal{H}$, etc. Another important thermodynamic quantity is the entropy S , given by

$$S = -k_B \sum_{N=0}^{\infty} \frac{1}{h^{3N} N!} \int f(\mathbf{q}, \mathbf{p}; N) \ln[f(\mathbf{q}, \mathbf{p}; N)] d\Gamma, \quad (7.9)$$

where $S_B = -k_B \ln(f(\mathbf{q}, \mathbf{p}; N))$ is the *Boltzman entropy* corresponding to the phase space volume $d\Gamma$, averaged over all phase space and weighted by the phase space density $f(\mathbf{q}, \mathbf{p}; N)$, giving the *Gibbs entropy*.

An important result that we will need in what follows is the connection of the grand partition function with the thermodynamic grand potential Ω . That link is defined through the definition

$$\Omega = -k_B T \ln \Xi \quad (7.10)$$

Each ensemble of statistical mechanics has a link with a corresponding thermodynamic potential through the logarithm of the corresponding partition function of the ensemble.

7.2 Adding Spatial Variations in the Grand Partition Function

To incorporate spatial variations due to an external, or perturbative, influence into the system, we introduce an external field, $\Phi_N(\mathbf{q})$, in the Hamiltonian as follows,

$$\mathcal{H}(\mathbf{q}, \mathbf{p}) = K_N(\mathbf{p}) + V_N(\mathbf{q}) + \Phi_N(\mathbf{q}) \quad (7.11)$$

where

$$\Phi_N(\mathbf{q}) \equiv \sum_{i=1}^N \phi(\mathbf{q}_i) = \int \hat{\rho}(\mathbf{x}, \mathbf{q}) \phi(\mathbf{x}) d\mathbf{x} \quad (7.12)$$

The function $\phi(\mathbf{q}_i)$ is an external potential which with the i^{th} particle interacts. This external potential be interpreted as a local energy of interactions between the atoms in the system and a container wall, or the interaction of particles in the system with an external perturbation into the system. The ensemble (thermodynamic) average of the interaction energy becomes

$$\langle \Phi_N \rangle = \int \langle \hat{\rho}(\mathbf{x}, \mathbf{q}) \rangle \phi(\mathbf{x}) d\mathbf{x} = \int \rho(\mathbf{x}) \phi(\mathbf{x}) d\mathbf{x} \quad (7.13)$$

The product $\rho(\mathbf{x}) \phi(\mathbf{x})$ is the interaction energy density at the location \mathbf{x} in the system. It is noted that $\langle \Phi_N \rangle$ is a *functional* as it depends on how $\phi(\mathbf{x})$ varies at all \mathbf{x} .

We can incorporate the microscopic interaction $\Phi_N(\mathbf{q})$ into the grand canonical partition function by effectively adding another term to the hamiltonian \mathcal{H} . This leads to

$$\Xi = \sum_{N=0}^{\infty} \frac{1}{h^{3N} N!} \iint \exp \left\{ -\beta \left(\mathcal{H} - \mu N + \int \phi(\mathbf{x}) \hat{\rho}(\mathbf{x}; \mathbf{q}) d\mathbf{x} \right) \right\} d\mathbf{q}^N d\mathbf{p}^N \quad (7.14)$$

The Lagrange multipliers μ and $\phi(x)$ can be associated with constraints of average number of particles and local particle density respectively. To simplify things further, it is noted that for any given particle number N , the density operator in Eq. (7.1) must satisfy,

$$\int \hat{\rho}(\mathbf{x}; \mathbf{q}) d\mathbf{x} = N \quad (7.15)$$

Substituting Eq. (7.15) into Eq. (7.14) thus leads to

$$\Xi[\psi(\mathbf{x})] = \sum_{N=0}^{\infty} \frac{1}{h^{3N} N!} \iint \exp \left\{ -\beta \left(\mathcal{H} + \int \psi(\mathbf{x}) \hat{\rho}(\mathbf{x}; \mathbf{q}) d\mathbf{x} \right) \right\} d\mathbf{q}^N d\mathbf{p}^N, \quad (7.16)$$

where the field $\psi(x) = \mu - \phi(x)$ is defined as the *intrinsic chemical potential*; this is the part of the system's chemical potential μ not included in $\phi(\mathbf{x})$. The grand partition function is explicitly written here as $\Xi[\psi(\mathbf{x})]$ to denote that it is functional of the intrinsic chemical potential $\psi(\mathbf{x})$.

Analogously to the process above, the phase space probability distribution can now be generalized in terms of $\psi(\mathbf{x})$ as

$$f(\mathbf{q}, \mathbf{p}; N) = \frac{1}{\Xi} \exp \left\{ -\beta \left(\mathcal{H} - \int \psi(\mathbf{x}) \hat{\rho}(\mathbf{x}, \mathbf{q}) d\mathbf{x} \right) \right\}, \quad (7.17)$$

which also makes $f(\mathbf{q}, \mathbf{p}; N)$ a functional of $\psi(\mathbf{x})$, although we omit writing that dependency explicitly to keep notation tractable.

Finally, based on the definition of $\Xi[\psi(\mathbf{x})]$, the grand potential functional is now obtained,

$$\Omega[\psi(\mathbf{x})] = -k_B T \ln \Xi[\psi(\mathbf{x})] \quad (7.18)$$

It is noteworthy that, analogously to its uniform system counterpart $\partial \Xi / \partial \mu = -N$, the functional derivative $\delta \Omega[\rho(\mathbf{x})] / \delta \psi(\mathbf{x}) = -\rho(\mathbf{x})$, a result also obtained by ensemble averaging $\hat{\rho}(\mathbf{x}, \mathbf{q})$ uisng Eq. (7.17).

7.3 The Intrinsic Free Energy Functional

The significance of the external field introduced in Section 7.2 can better be appreciated by examining the way it enters the phenomenology of the first law of thermodynamics by generalizing the work done on the system by a change of volume (typically written as $dW = PdV$) by the corresponding energy caused by a change in $\delta\phi(\mathbf{x})$. Namely, the change in work on the system could be seen as mediated by a change in energy of the atoms near the container walls interacting with changing potential of the wall. This would lead to an energy change in the system of $\delta U_{\text{int}} = \int \rho(\mathbf{x})\delta\phi(\mathbf{x})d\mathbf{x}$, where the integrand decays to zero away from the walls where $\phi(\mathbf{x})$ is zero. As a result, the first law of thermodynamics can be generalized as

$$\delta U = T\delta S + \int \rho(\mathbf{x})\delta\phi(\mathbf{x})d\mathbf{x} + \mu\delta N \quad (7.19)$$

Equation (7.19) uses "δ" to signify change since U is a functional of $\phi(\mathbf{x})$, making it natural to assume that S , T and N will in general also be functionals. Consider next the Helmholtz free energy ¹ $F = U - TS$. Its variation becomes $\delta F = \delta U - T\delta S - S\delta T$. Combining this with Eq. (7.19) gives

$$\delta F = S\delta T + \int \rho(\mathbf{x})\delta\phi(\mathbf{x})d\mathbf{x} + \mu\delta N, \quad (7.20)$$

making F a functional of $\phi(\mathbf{x})$ as well. It is seen that $\phi(\mathbf{x})$ takes the role of volume V from the uniform system counterpart of the first law [13].

Equation (7.20) suggests that we define a new thermodynamic potential, the *intrinsic free energy* (\mathcal{F}), according to

$$\mathcal{F} = F - \int \rho(\mathbf{x})\phi(\mathbf{x})d\mathbf{x} \quad (7.21)$$

The functional dependence of \mathcal{F} is found by taking the variation of Eq. (7.21), and using Eq. (7.20) to yield

$$\begin{aligned} \delta\mathcal{F} &= -S\delta T - \int \delta\rho(\mathbf{x})\phi(\mathbf{x})d\mathbf{x} + \mu\delta N \\ &= -S\delta T + \int \delta\rho(\mathbf{x})\psi(\mathbf{x})d\mathbf{x} \end{aligned} \quad (7.22)$$

Equation (7.22) shows that \mathcal{F} is a functional of $\rho(\mathbf{x})$ (analogously to F , which is also a function of N).

Proceeding further, we use $\Omega = F - \mu N$ in Eq. (7.21) to express the grand potential functional in terms of \mathcal{F} ,

$$\begin{aligned} \Omega &= \mathcal{F} + \int \rho(\mathbf{x})\phi(\mathbf{x}) - \mu N \\ &= \mathcal{F} - \int \rho(\mathbf{x})\psi(\mathbf{x})d\mathbf{x} \end{aligned} \quad (7.23)$$

Combining the variation of the second line of Eq. (7.23) with the second line of Eq. (7.22) gives

$$\delta\Omega = -S\delta T - \int \rho(\mathbf{x})\delta\psi(\mathbf{x})d\mathbf{x}, \quad (7.24)$$

¹In this section we reverse the labels for the Helmholtz and Gibbs energies from Chapter 1, denoting the former with an F and the latter with a G . This is done to keep the notation consistent with numerous texts in classical density functional theory.

which shows that Ω is a functional of the intrinsic chemical potential $\psi(\mathbf{x})$, as expected from the arguments of the previous section.

It is noted in passing that the second line of Equation (7.23) can be derived more rigorously by taking the logarithm of the e probability distribution in Eq. (7.17), which gives

$$k_B T \ln [f(\mathbf{q}, \mathbf{p}, N)] = -\mathcal{H} + \int \hat{\rho}(\mathbf{x}; \mathbf{q}) \psi(\mathbf{x}) d\mathbf{x} - k_B T \ln \Xi \quad (7.25)$$

Next, take the ensemble average (as in Eq. (7.2)), and use Eq. (7.18) to obtain

$$\begin{aligned} \langle \mathcal{H} + k_B T \ln [f(\mathbf{q}, \mathbf{p}, N)] \rangle &= \int \langle \hat{\rho}(\mathbf{x}; \mathbf{q}) \rangle \psi(\mathbf{x}) d\mathbf{x} + \Omega \\ &= \int \rho(\mathbf{x}) \psi(\mathbf{x}) d\mathbf{x} + \Omega = \mathcal{F} \end{aligned} \quad (7.26)$$

Eq. (7.26) shows that Ω and \mathcal{F} are related through a functional Legendre transformation.

That \mathcal{F} as a functional of $\rho(\mathbf{x})$ can also be arrived at more formally by considering phase space density distribution $f(\mathbf{q}, \mathbf{p}; N)$. Namely, there is a proof that tells us that for a given T , μ and V_N (inter-particle potential) there is only one external potential $\phi(\mathbf{x})$ that will correspond to a specific 1-point density field $\rho(\mathbf{x})$ [13]. This makes $f(\mathbf{q}, \mathbf{p}; N)$, which we saw is a functional of $\phi(\mathbf{x})$, also a unique functional of the density $\rho(\mathbf{x})$. Taking the ensemble average on the left hand side of Eq. (7.26) then simplifies that \mathcal{F} is a unique functional of $\rho(\mathbf{x})$.

7.4 Equilibrium Density and Thermodynamic Driving Forces

We pause here to collect a couple of important results from the previous section related to the microscopic equilibrium 1-point density field in a non-uniform system. These form key results of density functional theory. They will also be very useful later to analyze the equilibrium properties of phase field crystal (PFC) models, as well as the non-equilibrium dynamics of their density fields.

Starting with the intrinsic free energy parameterized by its natural variable, $\mathcal{F}[\rho(x)]$, Equation (7.22) gives

$$\frac{\delta \mathcal{F}}{\delta \rho(\mathbf{x})} = \psi(\mathbf{x}) = \mu - \phi(\mathbf{x}), \quad (7.27)$$

at constant temperature. Thus, if $\mathcal{F}[\rho(x)]$ can be parameterized in terms of $\rho(\mathbf{x})$, Eq. (7.27) defines an equation for the [non-uniform] equilibrium particle density field of a system as a function of the external potential $\phi(\mathbf{x})$.

Approaching things from the perspective of the grand potential $\Omega[\psi(\mathbf{x})]$, Eq. (7.24) gives

$$\frac{\delta \Omega}{\delta \psi(\mathbf{x})} = -\rho(\mathbf{x}), \quad (7.28)$$

at constant temperature. Equation (7.28) is interesting as it tells us that if we can parameterize $\Omega[\psi(\mathbf{x})]$, it is possible to obtain the single particle density by functional differentiation; this also implies that the intrinsic chemical potential can be expressed in terms of $\rho(\mathbf{x})$ (more on this later). Note that Eq. (7.28) could be equivalently derived from the Legendre transformation implied in Eq. (7.23), and assuming there exists a relationship $\rho[\psi(\mathbf{x})]$ and using Eq. (7.27).

It is instructive to evaluate Ω in Eq. (7.23) with some density $\tilde{\rho}(\mathbf{x})$ that is different from the equilibrium 1-particle density $\rho(\mathbf{x})$, i.e.,

$$\Omega[\tilde{\rho}] = \mathcal{F}[\tilde{\rho}] + \int \tilde{\rho}(\mathbf{x}) \phi(\mathbf{x}) - \mu \int \tilde{\rho}(\mathbf{x}) \quad (7.29)$$

It can be shown [13] that $\Omega[\tilde{\rho}(\mathbf{x})] > \Omega[\rho(\mathbf{x})]$ for all $\tilde{\rho}(\mathbf{x})$. Equilibrium is defined by $\tilde{\rho}(\mathbf{x}) \rightarrow \rho(\mathbf{x})$, whereupon $\Omega[\tilde{\rho}(\mathbf{x})] \rightarrow \Omega[\rho(\mathbf{x})]$, and where

$$\frac{\delta\Omega}{\delta\tilde{\rho}(\mathbf{x})}\Bigg|_{\tilde{\rho}(\mathbf{x})=\rho(\mathbf{x})} = \frac{\delta\mathcal{F}}{\delta\tilde{\rho}(\mathbf{x})}\Bigg|_{\tilde{\rho}(\mathbf{x})=\rho(\mathbf{x})} + \phi(\mathbf{x}) - \mu = 0, \quad (7.30)$$

Many models in the non-equilibrium thermodynamics literature employ the expression

$$\mathcal{D} = \frac{\delta\Omega}{\delta\tilde{\rho}(\mathbf{x})} \quad (7.31)$$

to play the role of a *thermodynamic driving force* to determine the flux of density in dynamical models of non-equilibrium phase transformations. Such models typically drive the system density from some initial configuration toward its equilibrium state. There are of course limitations of how accurate this is, including that the system should be close to equilibrium initially. More on this later.

7.5 Correlation Functions

While elegant and mathematically appealing, formal expressions of the grand partition and grand potential can rarely be solved exactly for any practical system. Instead, many density functional theory (DFT) based models of non-equilibrium systems make progress by expanding the free energy, or grand potential, in a functional Taylor series about a reference state. Each term of this expansion is related to a so-called *n-point direct correlation function*. Direct correlation functions can be related to *multi-point density correlation functions* generated by the grand potential, and some of them are measurable experimentally. Given the importance of correlation functions in the development of continuum field theories, this Section will study the topic of generating correlation functions in some detail.

7.5.1 Generating the *n*-point density from the grand partition function

To explore the formalism of generating multi-point density correlation functions from the grand potential, we first must understand how to take functional derivatives of the grand partition function. We begin by re-writing Eq. (7.16) with the interaction term in the integral $\int \psi(\mathbf{x})\hat{\rho}(\mathbf{x}, \mathbf{q})d\mathbf{x}$ expressed in terms of the sum in Eq. (7.12). This allows us to express $\Xi[\psi]$ as

$$\Xi[z^*] = \sum_{N=0}^{\infty} \frac{1}{N!} \int \exp(-\beta V_N) \left(\prod_{i=1}^N z^*(\mathbf{q}_i) \right) d\mathbf{q}^N, \quad (7.32)$$

where the shorthand notation

$$z^*(\mathbf{q}_i) = \frac{\exp[\beta\psi(\mathbf{q}_i)]}{\Lambda^3} = z \exp[-\beta\phi(\mathbf{q}_i)] \quad (7.33)$$

has been defined following Ref. [13]. It is recalled that here V_N is the particle interaction potential and z is given by Eq. (7.5). Another important quantity we'll need in addition to $\Xi[z^*]$ is the *n*-particle density of a system. This gives the probability density of finding *any n* particles within a volume element $d\mathbf{q}^n$ of phase space, irrespective of all other particle positions and all particle momenta. This is obtained by integrating the distribution in Eq. (7.17) over $(N-n)$ position coordinates of the $3N$ -vector \mathbf{q} (e.g. over $\{\mathbf{q}_{n+1}, \dots, \mathbf{q}_N\}$), integrating over all particle momenta in the $3N$ -vector \mathbf{p} , and

summing over particle numbers $N \geq n$. The resulting function is the n -particle density, whose explicit form is given by

$$\rho^{(n)}(\mathbf{q}_1, \dots, \mathbf{q}_n) = \frac{1}{\Xi} \sum_{N=n}^{\infty} \frac{1}{(N-n)!} \int \exp(-\beta V_N) \left(\prod_{i=1}^N z^*(\mathbf{q}_i) \right) d\mathbf{q}^{(N-n)}, \quad (7.34)$$

where the notation $d\mathbf{q}^{(N-n)}$ implies integration over $(N-n)$ out of N particle labels. The normalization $1/(N-n)!$ arises after multiplying each term in the sum by $N!/(N-n)!$, the number of ways we can choose n out of N particle labels. It is emphasized that $\rho^{(n)}(\mathbf{q}_1, \dots, \mathbf{q}_n)$ represents the probability of finding *any* n particles at the respective positions $\mathbf{q}_1, \dots, \mathbf{q}_n$ irrespective of their labels. Equation 7.34 will next be used to link n -particle densities to functional derivatives of the grand partition function $\Xi[z^*]$ in Eq. (7.32).

Taking the first functional derivative of Ξ with respect to $z^*(\mathbf{q}_1)$ (or any index i , which is just a label on any of N identical particles in any term of the sum) gives

$$\frac{\delta \Xi}{\delta z^*(\mathbf{q}_1)} = \sum_{N=1}^{\infty} \frac{1}{(N-1)!} \int \exp(-\beta V_N) \left(\prod_{i=2}^N z^*(\mathbf{q}_i) \right) d\mathbf{q}_2 \cdots d\mathbf{q}_N \quad (7.35)$$

A few points are in order to help the reader arrive at Eq. (7.35). First, the product is absent from Eq. (7.32) when $N = 0$, and the exponential gives a constant. This makes the $N = 0$ term in Eq. (7.32) vanish upon differentiation, hence starting the sum in Eq. (7.35) from $N = 1$. Also, the factor $(N-1)!$ appearing in Eq. (7.35) comes from the fact that the variation of $\delta \Xi$ generates (for each term in its sum) N terms, each varying with respect to one $\delta z^*(\mathbf{q}_i)$ from the set $i \in \{1, \dots, N\}$. Since the integrand of Eq. (7.32) is symmetric with respect to the interchange of any two labels in $i \in \{1, \dots, N\}$, the variation $\delta \Xi$ is thus N times the variation of Ξ with respect to any one of the labels. Multiplying Eq. (7.35) by $z^*(\mathbf{q}_1)/\Xi$ and comparing with Eq. (7.34), recovers the 1-particle (the "usual") equilibrium density field), namely,

$$\begin{aligned} \frac{z^*(\mathbf{q}_1)}{\Xi} \frac{\delta \Xi}{\delta z^*(\mathbf{q}_1)} &= \frac{1}{\Xi} \sum_{N=1}^{\infty} \frac{1}{(N-1)!} \int \exp(-\beta V_N) \left(\prod_{i=1}^N z^*(\mathbf{q}_i) \right) d\mathbf{q}_2 \cdots d\mathbf{q}_N \\ &= \rho^{(1)}(\mathbf{q}_1) \end{aligned} \quad (7.36)$$

It is emphasized that $\rho^{(1)}(\mathbf{q}_1)$ represents the probability of finding *any* particle at position \mathbf{q}_1 , irrespective of its label; the 1-particle density is given equivalently by Eq. (7.2).

We continue with the second functional derivative of Ξ , i.e., the functional derivative of $\delta \Xi / \delta z^*(\mathbf{q}_1)$ with respect to the function $\delta z^*(\mathbf{q}_2)$. Applying similar considerations to those leading to Eq. (7.35) gives

$$\frac{\delta \Xi}{\delta z^*(\mathbf{q}_1) \delta z^*(\mathbf{q}_2)} = \sum_{N=2}^{\infty} \frac{1}{(N-2)!} \int \exp(-\beta V_N) \left(\prod_{i=3}^N z^*(\mathbf{q}_i) \right) d\mathbf{q}_3 \cdots d\mathbf{q}_N, \quad (7.37)$$

where again the $N = 1$ term in Eq. (7.35) vanishes and hence the sum in Eq. (7.37) starts at $N = 2$. Similarly, the product in the integrand of Eq. (7.35) has had the $z^*(\mathbf{q}_2)$ factor knocked out by the functional differentiation. Also there is now a factor $(N-2)!$ in the denominator due to the $N-1$ identical terms the functional differentiation of Eq. (7.35) generates due to the symmetry of its integrand. Multiplying Eq. (7.37) by $z^*(\mathbf{q}_1) z^*(\mathbf{q}_2)/\Xi$ and comparing with Eq. (7.34) recovers the

2-particle density, namely,

$$\begin{aligned} \frac{z^*(\mathbf{q}_1)z^*(\mathbf{q}_2)}{\Xi} \frac{\delta\Xi}{\delta z^*(\mathbf{q}_1)\delta z^*(\mathbf{q}_2)} &= \frac{1}{\Xi} \sum_{N=2}^{\infty} \frac{1}{(N-2)!} \int \exp(-\beta V_N) \left(\prod_{i=1}^N z^*(\mathbf{q}_i) \right) d\mathbf{q}_3 \cdots d\mathbf{q}_N \\ &= \rho^{(2)}(\mathbf{q}_1, \mathbf{q}_2) \end{aligned} \quad (7.38)$$

It is emphasized here that $\rho^{(2)}(\mathbf{q}_1, \mathbf{q}_2)$ represents the probability of finding *any* two particles at positions \mathbf{q}_1 , and \mathbf{q}_2 , respectively, irrespective of their labels.

It should now be straightforward to generalize the functional differentiation of Ξ by continually applying variationals successively to Eq. (7.37), first by $z^*(\mathbf{q}_3)$, then by $z^*(\mathbf{q}_4)$, and so on up to $z^*(\mathbf{q}_n)$. This gives

$$\frac{\delta\Xi}{\delta z^*(\mathbf{q}_1)\delta z^*(\mathbf{q}_2)\cdots\delta z^*(\mathbf{q}_n)} = \sum_{N=n}^{\infty} \frac{1}{(N-n)!} \int \exp(-\beta V_N) \left(\prod_{i=n+1}^N z^*(\mathbf{q}_i) \right) d\mathbf{q}_{n+1} \cdots d\mathbf{q}_N \quad (7.39)$$

Furthermore, multiplying Eq. (7.39) by $z^*(\mathbf{q}_1)z^*(\mathbf{q}_2)\cdots z^*(\mathbf{q}_n)/\Xi$ gives the n -point density in Eq. (7.34), namely,

$$\begin{aligned} \frac{z^*(\mathbf{q}_1)\cdots z^*(\mathbf{q}_n)}{\Xi} \frac{\delta\Xi}{\delta z^*(\mathbf{q}_1)\cdots\delta z^*(\mathbf{q}_n)} &= \frac{1}{\Xi} \sum_{N=n}^{\infty} \frac{1}{(N-n)!} \int \exp(-\beta V_N) \left(\prod_{i=1}^N z^*(\mathbf{q}_i) \right) d\mathbf{q}_{n+1} \cdots d\mathbf{q}_N \\ &= \rho^{(n)}(\mathbf{q}_1, \dots, \mathbf{q}_n) \end{aligned} \quad (7.40)$$

where now $\rho^{(n)}(\mathbf{q}_1, \dots, \mathbf{q}_n)$ represents the probability of finding *any* n particles at the respective positions $\mathbf{q}_1, \mathbf{q}_2, \dots, \mathbf{q}_n$, irrespective of their labels. Equation (7.40) provides the key result we'll need in order to link the grand potential functional to the density correlations, which we started out to do at the outset of this section.

7.5.2 Generating density correlation functions from the grand potential

To proceed further, we next consider variationals of the grand potential functional with respect to the intrinsic chemical potential. We start by the realtin $\Omega = -k_B T \ln \Xi$ and take the first variational,

$$\begin{aligned} \frac{\delta\Omega}{\delta\psi(\mathbf{q}_1)} &= -\beta z^*(\mathbf{q}_1) \frac{\delta\Omega}{\delta z^*(\mathbf{q}_1)} \\ &= -\frac{z^*(\mathbf{q}_1)}{\Xi} \frac{\delta\Xi}{\delta z^*(\mathbf{q}_1)} \\ &= -\rho^{(1)}(\mathbf{q}_1) \end{aligned} \quad (7.41)$$

where we have used the variational version of the chain rule to relate $\psi(\mathbf{q}_1)$ to $z^*(\mathbf{q}_1)$ in the first line of Eq. (7.41) and Eq. (7.36) to arrive at the last line.

We next take the second variation of Ω with regards to the intrinsic chemical potential at two particle positions, $\psi(\mathbf{q}_1)$ and $\psi(\mathbf{q}_2)$, or, the variational of Eq. (7.41) with respect to $\psi(\mathbf{q}_2)$. We begin by applying the functional product rule twice and collecting terms to obtain

$$\begin{aligned} \frac{\delta\Omega}{\delta\psi(\mathbf{q}_2)\delta\psi(\mathbf{q}_1)} &= \beta z^*(\mathbf{q}_2) \frac{\delta}{\delta z^*(\mathbf{q}_2)} \left(\frac{z^*(\mathbf{q}_1)}{\Xi} \frac{\delta\Omega}{\delta z^*(\mathbf{q}_1)} \right) \\ &= \beta \left\{ \left(\frac{z^*(\mathbf{q}_1)}{\Xi} \frac{\delta\Omega}{\delta z^*(\mathbf{q}_1)} \right) \left(\frac{z^*(\mathbf{q}_2)}{\Xi} \frac{\delta\Omega}{\delta z^*(\mathbf{q}_2)} \right) - \frac{z^*(\mathbf{q}_2)}{\Xi} \frac{\delta\Xi}{\delta z^*(\mathbf{q}_1)} \delta(\mathbf{q}_1 - \mathbf{q}_2) \right. \\ &\quad \left. + \frac{z^*(\mathbf{q}_1)z^*(\mathbf{q}_2)}{\Xi} \frac{\delta^2\Xi}{\delta z^*(\mathbf{q}_1)\delta z^*(\mathbf{q}_2)} \right\}, \end{aligned} \quad (7.42)$$

The middle term in the second line of Eq. (7.42) was obtained by using the relationship $\delta z^*(\mathbf{q}_1)/\delta z^*(\mathbf{q}_2) = \delta(\mathbf{q}_1 - \mathbf{q}_2)$ [5, 13]. Inspection of Eq. (7.42) shows that the first term in the large curly brackets comprises the product of two 1-point densities evaluated at two positions, respectively, while the second term can be re-written as a 1-point density multiplying a delta function. Comparing its last term with Eq. (7.40) gives a 2-point density, thus reducing Eq. (7.42) to

$$\frac{\delta\Omega}{\delta\psi(\mathbf{q}_2)\delta\psi(\mathbf{q}_1)} = \beta \left\{ \rho^{(1)}(\mathbf{q}_1)\rho^{(1)}(\mathbf{q}_2) - \rho^{(1)}(\mathbf{q}_1)\delta(\mathbf{q}_1 - \mathbf{q}_2) - \rho^{(2)}(\mathbf{q}_1, \mathbf{q}_2) \right\} \quad (7.43)$$

The right hand side of Eq. (7.43) can be made more illuminating by connecting it to the *density-density correlation function*, defined by

$$\mathcal{C}^{(2)}(\mathbf{x}, \mathbf{x}') = \langle [\hat{\rho}(\mathbf{x}) - \langle \hat{\rho}(\mathbf{x}) \rangle] [\hat{\rho}(\mathbf{x}') - \langle \hat{\rho}(\mathbf{x}') \rangle] \rangle, \quad (7.44)$$

where $\hat{\rho}(\mathbf{x})$ is the density operator in Eq. (7.1) (with the " ; \mathbf{q} " omitted for brevity). The function $\mathcal{C}^{(2)}(\mathbf{x}, \mathbf{x}')$ measures the average fluctuation of the density (relative to its average) between \mathbf{x} and \mathbf{x}' . Expanding the right hand side of Eq. (7.44) and substituting Eq. (7.1) gives

$$\begin{aligned} \langle [\hat{\rho}(\mathbf{x}) - \langle \hat{\rho}(\mathbf{x}) \rangle] [\hat{\rho}(\mathbf{x}') - \langle \hat{\rho}(\mathbf{x}') \rangle] \rangle &= \left\langle \sum_{i=0}^N \sum_{\substack{j=0 \\ j \neq i}}^N \delta^{(3)}(\mathbf{x} - \mathbf{q}_i) \delta^{(3)}(\mathbf{x}' - \mathbf{q}_j) \right\rangle \\ &+ \left\langle \sum_{i=0}^N \delta^{(3)}(\mathbf{x} - \mathbf{q}_i) \delta^{(3)}(\mathbf{x}' - \mathbf{q}_i) \right\rangle \\ &- \rho^{(1)}(\mathbf{x})\rho^{(1)}(\mathbf{x}'), \end{aligned} \quad (7.45)$$

where it is recalled that $\langle \hat{\rho}(\mathbf{x}) \rangle = \rho^{(1)}(\mathbf{x})$ and the "⟨ ⟩" denote ensemble averaging over the \mathbf{q}_i coordinates so $\rho^{(1)}(\mathbf{x})$ and $\rho^{(1)}(\mathbf{x}')$ come out of averages. The first term on the right hand side of Eq. (7.45) is just $\rho^{(2)}(\mathbf{x}, \mathbf{x}')$. This is seen by first taking the average $\langle \delta^{(3)}(\mathbf{x} - \mathbf{q}_i) \delta^{(3)}(\mathbf{x}' - \mathbf{q}_j) \rangle$ using the density in Eq. (7.17) as a weighting function² and noting that i and j are dummy indices. This implies that each term in the sum over particles is multiplied by $N(N - 1)$, which leads directly to Eq. (7.38). Similarly taking the average $\langle \delta^{(3)}(\mathbf{x} - \mathbf{q}_i) \delta^{(3)}(\mathbf{x}' - \mathbf{q}_i) \rangle$ simplifies the last term to $\delta^{(3)}(\mathbf{x} - \mathbf{x}') \rho^{(1)}(\mathbf{x})$. These simplifications of Eq. (7.45) allow us to re-express Equation (7.43) as

$$\frac{\delta\Omega}{\delta\psi(\mathbf{q}_2)\delta\psi(\mathbf{q}_1)} = -\beta \mathcal{C}^{(2)}(\mathbf{q}_1, \mathbf{q}_2) \quad (7.46)$$

It is noted that in Eq. (7.46), the variables \mathbf{x} and \mathbf{x}' were replaced by \mathbf{q}_1 and \mathbf{q}_2 , respectively to return to the previous used notation.

The above procedure can be generalized to higher order functional derivatives of the grand potential $\Omega[\psi(\mathbf{x})]$. The algebra for this is straightforward but tedious and will not be shown here. What results is the relation

$$\frac{\delta^n\Omega}{\delta\psi(\mathbf{q}_1)\cdots\delta\psi(\mathbf{q}_n)} = -\beta^n \mathcal{C}^{(n)}(\mathbf{q}_1, \dots, \mathbf{q}_n), \quad (7.47)$$

where the n -point density correlation function is given by

$$\mathcal{C}^{(n)}(\mathbf{q}_1, \dots, \mathbf{q}_n) = \langle [\hat{\rho}(\mathbf{q}_1) - \langle \hat{\rho}(\mathbf{q}_1) \rangle] \cdots [\hat{\rho}(\mathbf{q}_n) - \langle \hat{\rho}(\mathbf{q}_n) \rangle] \rangle \quad (7.48)$$

²To proceed here, express the integral $\int \psi(\mathbf{x})\hat{\rho}(\mathbf{x}, \mathbf{q})d\mathbf{x}$ in terms of the sum in Eq. (7.12) as was done in obtaining Eq. (7.32).

The function $\mathcal{C}^{(n)}(\mathbf{q}_1, \dots, \mathbf{q}_n)$ measures statistical correlations in fluctuations of the relative density between n points simultaneously.

Equations (7.40) and 7.47 are the main results of this section. The interpretation of Eq. (7.40) is that the grand partition function is a generator of *moments* of the density field $\rho(\mathbf{x})$, while that of Eq. (7.47) is that the grand potential functional is a generator of density correlation functions.

7.5.3 Generating direct correlation functions from the excess free energy

Classical field theory models of phase transformations used to study microstructure evolution do not typically use density correlation functions defined above, but rather, the so-called *direct correlation functions*, which are derived from the *excess free energy* of a system. This aim of this section is to relate the direct correlations functions to the excess free energy by considering system expanded as an ideal gas plus an excess contribution that contains all interactions. The ideal gas will thus be effectively a non-interacting reference state around which the free energy of any system can, in theory, be written as a perturbation series of direct correlations functions. This will be used in the next section to derive a density functional theory or freezing, which has motivated many of the *phase field crystal (PFC)* models encountered in the literature.

7.5.3.1 Non-Interacting ideal gas

The grand potential of an ideal gas of non-interacting particles is given by $\Omega = -k_B T \ln \Xi$, where Ξ is evaluated from Eq. (7.32) by setting the inter-atomic potential to zero, $V_N = 0$. This gives

$$\Omega_{id}[\psi] = -k_B T \ln \left\{ \sum_{N=0}^{\infty} \frac{\tilde{Z}^*[\psi(\mathbf{q})]}{N!} \right\}, \quad (7.49)$$

where

$$\tilde{Z}^*[\psi(\mathbf{q})] = \int_V \frac{e^{\beta\psi(\mathbf{q})}}{\Lambda^3} d\mathbf{q} \quad (7.50)$$

We'll see below that the density of a gas scales with \tilde{Z}^* , and thus Eq. (7.49) can be approximated to $\mathcal{O}((\tilde{Z}^*)^3)$ by keeping the first two terms in the sum. This gives,

$$\Omega_{id}[\psi] \approx -\frac{k_b T}{\Lambda^3} \int d\mathbf{q} e^{\beta\psi(\mathbf{q})} \quad (7.51)$$

Applying Eq. (7.41) to Eq. (7.51) gives the density field of the gas,

$$\rho_{id}^{(1)}(\mathbf{q}) = \frac{e^{\beta\psi(\mathbf{q})}}{\Lambda^3}, \quad (7.52)$$

which can be inverted for the intrinsic chemical potential,

$$\psi_{id}[\rho_{id}^{(1)}(\mathbf{q})] = k_B T \ln (\Lambda^3 \rho_{id}^{(1)}(\mathbf{q})) \quad (7.53)$$

It will be instructive for what follows to also calculate the intrinsic free energy \mathcal{F}_{id} of the non-interacting gas. This is straightforward to do from the grand potential, since \mathcal{F}_{id} and Ω_{id} are related by a Legendre transform (see Eq. (7.23)), and hence satisfy

$$\mathcal{F}[\rho^{(1)}(\mathbf{q})] = \Omega[\psi(\mathbf{q})] + \int \rho^{(1)}(\mathbf{q}) \psi[\rho^{(1)}(\mathbf{q})] \quad (7.54)$$

Substituting Ω_{id} and ψ_{id} into Eq. (7.54) gives

$$\mathcal{F}_{id}[\rho_{id}^{(1)}(\mathbf{q})] = k_b T \int d\mathbf{q} \left\{ \rho_{id}^{(1)}(\mathbf{q}) \ln \left(\Lambda^3 \rho_{id}^{(1)}(\mathbf{q}) \right) - \rho_{id}^{(1)}(\mathbf{q}) \right\}, \quad (7.55)$$

Note that the above results show, not too surprisingly, that the non-uniform properties of an ideal gas can be described completely by evaluating the properties of a uniform ideal gas at the local density $\rho_{id}^{(1)}(\mathbf{q})$.

7.5.3.2 Interacting systems

With the properties of the ideal non-interacting gas in hand, we can proceed to express the grand potential and intrinsic free energy of the interacting gas in terms of their reference non-interacting gas states. We express the deviation of a system from an ideal non-interacting system by factoring the ideal contribution out of the partition function, i.e.,

$$\Xi[\psi(\mathbf{q})] = \Xi_{id}[\psi(\mathbf{q})] \Xi_{ex}[\psi(\mathbf{q})], \quad (7.56)$$

Taking logs of both sides of Eq. (7.56) gives

$$\Omega[\psi(\mathbf{q})] = \Omega_{id}[\psi(\mathbf{q})] + \Omega_{ex}[\psi(\mathbf{q})] \quad (7.57)$$

Substituting Eq. (7.57) into the right hand side of Eq. (7.54) allows us to write

$$\begin{aligned} \mathcal{F}[\rho^{(1)}(\mathbf{q})] &= \Omega_{id}[\psi] + \int_V \rho^{(1)}(\mathbf{q}) \psi_{id}[\rho^{(1)}(\mathbf{q})] \\ &\quad + \Omega_{ex}[\psi] + \int_V \rho^{(1)}(\mathbf{q}) \psi_{ex}[\rho^{(1)}(\mathbf{q})] d\mathbf{q} \end{aligned} \quad (7.58)$$

where $\psi_{ex}[\rho^{(1)}(\mathbf{q})]$ is defined by

$$\psi_{ex}[\rho^{(1)}(\mathbf{q})] = \psi[\rho^{(1)}(\mathbf{q})] - \psi_{id}[\rho^{(1)}(\mathbf{q})], \quad (7.59)$$

The expression $\psi_{ex}[\rho^{(1)}(\mathbf{q})]$ represents the difference in the intrinsic chemical potential corresponding to relative to the corresponding ideal intrinsic chemical potential evaluated at $\rho^{(1)}(\mathbf{q})$. It is clear from Eq. (7.59) that we can express the change in intrinsic free energy analogously to Eq. (7.57), according to

$$\mathcal{F}[\rho^{(1)}(\mathbf{q})] = \mathcal{F}_{id}[\rho^{(1)}(\mathbf{q})] + \mathcal{F}_{ex}[\rho^{(1)}(\mathbf{q})] \quad (7.60)$$

Why did we bother to write the grand potential and intrinsic free energy in the ways shown above? The reason is that the inter-atomic potential $V(\mathbf{q})$ typically makes any direct approach to calculating the excess free energy intractable. Though perturbative method such as the so-called *cluster expansion technique* [20], it is possible to treat the interaction potential in a perturbative fashion. There are many statistical mechanics books out there that study that and other perturbative approaches. However, here, we are after more practical approaches to model interacting systems by expanding the excess free energy in Eq. (7.60) and relating it to so-called *direct correlation functions*. These are then fit phenomenologically to yield continuum models from which efficient equations of motions can be derived to study dynamical microstructure evolution over extended physical domains on diffusional time scales.

7.5.3.3 Definition of Direct correlation functions

We begin with the definition of the *single particle direct correlation function* is defined as

$$k_B T C^{(1)}(\mathbf{q}) = -\frac{\delta \mathcal{F}_{ex}[\rho^{(1)}(\mathbf{q})]}{\delta \rho^{(1)}(\mathbf{q})} \quad (7.61)$$

To see the significance of $C^{(1)}$ we can take the variational of Eq. (7.60) to yield the intrinsic chemical potential,

$$\frac{\delta \mathcal{F}[\rho^{(1)}(\mathbf{q})]}{\delta \rho^{(1)}(\mathbf{q})} = \frac{\delta \mathcal{F}_{id}[\rho^{(1)}(\mathbf{q})]}{\delta \rho^{(1)}(\mathbf{q})} - k_B T C^{(1)}(\mathbf{q}) = \psi(\mathbf{q}) \quad (7.62)$$

Recognizing the second term in Eq. (7.62) as the form of the intrinsic chemical potential of the ideal gas and replacing it with Eq. (7.53) gives

$$\psi(\mathbf{q}) = k_B T \left\{ \ln[\Lambda \rho^{(1)}(\mathbf{q})] - C^{(1)}(\mathbf{q}) \right\} \quad (7.63)$$

Considering Eq. (7.63) shows that $C^{(1)}(\mathbf{q})$ describes the role of particle interactions on the density of the system or, alternatively, the excess part of the intrinsic chemical potential.

We can generate a hierarchy of *direct correlation functions* through repeated functional differentiation of $C^{(1)}(\mathbf{q})$, or alternatively the the excess free energy. Specifically, the two-point direct correlation function is defined as

$$k_B T C^{(2)}(\mathbf{q}, \mathbf{q}') = k_B T \frac{\delta C^{(1)}(\mathbf{q})}{\delta \rho^{(1)}(\mathbf{q}')} = -\frac{\delta^2 \mathcal{F}_{ex}[\rho^{(1)}(\mathbf{q})]}{\delta \rho^{(1)}(\mathbf{q}) \delta \rho^{(1)}(\mathbf{q}')} \quad (7.64)$$

As with the density correlation functions, the n -th order correlation can be defined and related to the corresponding functional derivative of the excess intrinsic free energy according to

$$k_B T C^n(\mathbf{q}_1, \dots, \mathbf{q}_n) = -\frac{\delta^n \mathcal{F}_{ex}[\rho^{(1)}(\mathbf{q})]}{\delta \rho(\mathbf{q}_1) \dots \delta \rho(\mathbf{q}_n)} \quad (7.65)$$

7.5.3.4 Orstein-Zernike relation for $C^{(2)}(\mathbf{q}_1, \mathbf{q}_2)$

The above procedure is formal and relates the direct correlation functions to the excess free energy, which we argued above is rarely tractable. Let's do some mathematical gymnastics to obtain a more useful expression for $C^{(2)}(\mathbf{q}_1, \mathbf{q}_2)$ in terms of the density correlation functions and the multi-point density functions discussed in previous subsections.

We proceed by considering the combination of Eq. (7.46) and Eq. (7.41), which gives,

$$\mathcal{C}^{(2)}(\mathbf{q}_1, \mathbf{q}_2) = k_B T \frac{\delta \rho^{(1)}(\mathbf{q}_1)}{\delta \psi(\mathbf{q}_2)} \quad (7.66)$$

Next, from the rules of functional differentiation it follows that $\delta \rho^{(1)}(\mathbf{q}) / \delta \rho^{(1)}(\mathbf{q}') = \delta(\mathbf{q} - \mathbf{q}')$. Moreover, since $\rho^{(1)}(\mathbf{q})$ is a functional of $\psi(\mathbf{q})$ we can use the chain rule analogue for functional differentiation to write

$$\frac{\delta \rho^{(1)}(\mathbf{q}_1)}{\delta \rho^{(1)}(\mathbf{q}_2)} = \int \frac{\delta \rho^{(1)}(\mathbf{q}_1)}{\delta \psi(\mathbf{q}'')} \frac{\delta \psi(\mathbf{q}'')}{\delta \rho^{(1)}(\mathbf{q}_1)} d\mathbf{q}'' = \delta(\mathbf{q}_1 - \mathbf{q}_2), \quad (7.67)$$

Equation (7.67) implies that the functional inverse of $\mathcal{C}^{(2)}(\mathbf{q}_1, \mathbf{q}_2)$ (think of it as a matrix with continuous indices) is

$$\left[\mathcal{C}^{(2)}(\mathbf{q}_1, \mathbf{q}_2) \right]^{-1} = \frac{1}{k_B T} \frac{\delta \psi(\mathbf{q}_1)}{\delta \rho^{(1)}(\mathbf{q}_2)} \quad (7.68)$$

Substituting Eq. (7.63) into Eq. (7.68) gives

$$\left[\mathcal{C}^{(2)}(\mathbf{q}_1, \mathbf{q}_2) \right]^{-1} = \beta \frac{\delta\psi(\mathbf{q}_1)}{\delta\rho^{(1)}(\mathbf{q}_2)} = \frac{\delta(\mathbf{q}_1 - \mathbf{q}_2)}{\rho^{(1)}(\mathbf{q}_1)} - C^{(2)}(\mathbf{q}_1, \mathbf{q}_2) \quad (7.69)$$

it is noted in passing that the function $\mathcal{C}^{(2)}(\mathbf{q}_1, \mathbf{q}_2)$ in Eq. (7.69) can be identified as the so-called *Ursell function*, which is defined like the two-point density-density correlation function except that it uses the density shifted relative to its mean value (compare Eq. (7.48) to equation 2.3.5 in the text book by Chakin and Lubensky [4]).

It is more usual to relate the direct two-point correlation function to the so-called *pair correlation function*. To do so, we substitute the rightmost equality in Eq. (7.69) and Eq. (7.66) into the rightmost equality of Eq. (7.67), which gives, after some algebra, the *Orstein-Zernike relation*,

$$h^{(2)}(\mathbf{q}_1, \mathbf{q}_2) = C^{(2)}(\mathbf{q}_1, \mathbf{q}_2) + \int C^{(2)}(\mathbf{q}_1, \mathbf{q}'') \rho^{(1)}(\mathbf{q}'') h^{(2)}(\mathbf{q}'', \mathbf{q}_2) d\mathbf{q}'', \quad (7.70)$$

where $h^{(2)}(\mathbf{q}_1, \mathbf{q}_2)$ denotes the pair correlation function, which is defined by

$$h^{(2)}(\mathbf{q}_1, \mathbf{q}_2) = g^{(2)}(\mathbf{q}_1, \mathbf{q}_2) - 1, \quad (7.71)$$

and $g^{(2)}(\mathbf{q}_1, \mathbf{q}_2)$ is defined as the *pair distribution function*, given by

$$g^{(2)}(\mathbf{q}_1, \mathbf{q}_2) = \frac{\rho^{(2)}(\mathbf{q}_1, \mathbf{q}_2)}{\rho^{(1)}(\mathbf{q}_1) \rho^{(1)}(\mathbf{q}_2)}, \quad (7.72)$$

where $\rho^{(2)}(\mathbf{q}_1, \mathbf{q}_2)$ is the 2-point density (see Eq. (7.38)). In arriving at the Orstein-Zernike relation in Eq. (7.70), use is made of the relationship

$$\mathcal{C}^{(2)}(\mathbf{q}_1, \mathbf{q}_2) = \rho^{(1)}(\mathbf{q}_1) \rho^{(1)}(\mathbf{q}_2) h^{(2)}(\mathbf{q}_1, \mathbf{q}_2) + \rho^{(1)}(\mathbf{q}_1) \delta(\mathbf{q}_1 - \mathbf{q}_2), \quad (7.73)$$

which can be derived by using the definition of $h^{(2)}(\mathbf{q}_1, \mathbf{q}_2)$ to eliminate $\rho^{(2)}(\mathbf{q}_1, \mathbf{q}_2)$ from Eq. (7.43).

As an example of the use of Eq. (7.70) consider a homogenous fluid with constant density (ρ_L). In such a material, both the direct and pair correlation functions depend only of the separation between positions in the fluid, and so their arguments can be written as $r = |\mathbf{r}| = |\mathbf{q}_1 - \mathbf{q}_2|$. In this case Eq. (7.70) becomes

$$h^{(2)}(r) = C^{(2)}(r) + \rho_L \int C^{(2)}(|\mathbf{r} - \mathbf{r}''|) h^{(2)}(\mathbf{r}'') d\mathbf{r}'', \quad (7.74)$$

Taking Fourier transforms of both sides of Eq. (7.74) gives

$$\hat{C}^{(2)}(k) = \frac{\hat{h}^{(2)}(k)}{1 + \rho_L \hat{h}^{(2)}(k)}, \quad (7.75)$$

where $\hat{C}^{(2)}(k)$ and $\hat{h}^{(2)}(k)$ denote the Fourier transforms of the respective functions at the wavevector of magnitude k . The somewhat tortuous path that brought us to Eq. (7.75) shows us that, at least for a simple fluid, the direct correlation function –linkable to the second term in the expansion of the intrinsic free energy of the system– is obtainable from knowledge of the pair correlation and paid distribution functions, which in turn are both obtainable from neutron diffraction experiments [5, 13]. Figure (7.1) shows an example of $g^{(2)}(r) = g^{(2)}(|\mathbf{q}_1 - \mathbf{q}_2|)$ for aluminum as calculated by molecular dynamics. Figure (7.2) shows a second example of a pair correlation function $h(r)$ and the corresponding direct correlation function $C^{(2)}(r)$ for a hypothetical fluid whose microscopic interactions obey a Lennard-Jones inter-atomic potential. Several features are worthy of mention in $C^{(2)}$. The large negative peak near $k \rightarrow 0$; this controls the compressibility of the liquid. At higher k values (shorter wavelengths), $C^{(2)}(r)$ exhibits a small peak near characteristic length which is of order nearest neighbour distance between atoms of the liquid. We will see in the next chapter that the strength of this peak will be crucial in controlling the ordering of the liquid during solidification.

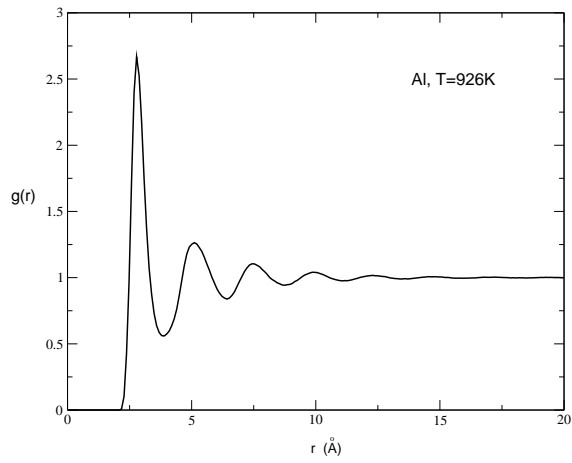


Figure 7.1: The pair distribution function $g^{(2)}(r)$ for Aluminum at $T = 926K$ calculated by molecular dynamics. Courtesy of J. J. Hoyt, Department of Materials Science and Engineering, McMaster University.

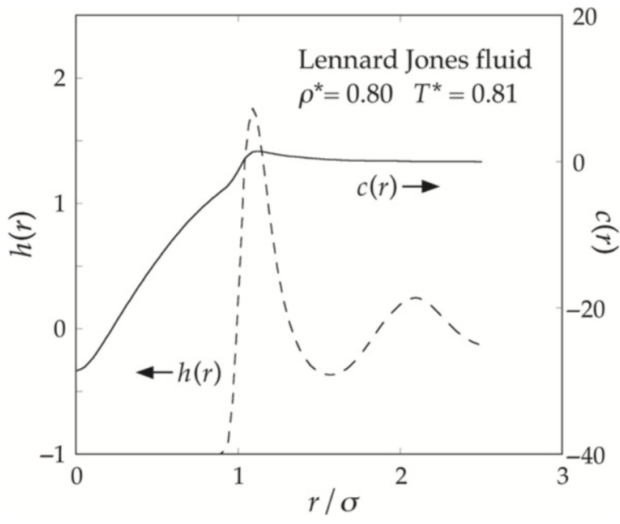


Figure 7.2: The pair correlation function $h(r)$ (left axis) and direct correlation $C(r)$ (right axis) calculated by molecular dynamics of a Lennard-Jones fluid. Reprinted from Ref. [13].

7.6 Density Functional Theory of Freezing

This theory begins by approximating the excess free energy in Eq. (7.60) by expanding around a reference homogeneous fluid with chemical potential μ_0 and corresponding density ρ_0 . To do so, we re-express the excess free energy as

$$\mathcal{F}_{ex}[\rho] = \mathcal{F}_{ex}[\rho_0] + \int \frac{\delta \mathcal{F}_{ex}}{\delta \rho(x)} \Big|_{\rho_0} \Delta\rho(\mathbf{x}) d\mathbf{x} + \frac{1}{2} \iint \Delta\rho(\mathbf{x}') \frac{\delta^2 \mathcal{F}_{ex}}{\delta \rho(\mathbf{x}) \delta \rho(\mathbf{x}')} \Big|_{\rho_0} \Delta\rho(\mathbf{x}) d\mathbf{x} d\mathbf{x}' + \dots, \quad (7.76)$$

where we defined $\Delta\rho(x) = \rho(x) - \rho_0$ and dropped the super-script from $\rho^{(1)}(\mathbf{x})$ to simplify notation. We also set the external potential to zero for now. As we saw in the last section, the excess free energy is the generating functional of *direct correlation functions*, via Eq. (7.65). The first of these is the excess contribution to the chemical potential. We may express this as the total chemical potential less the ideal contribution (see equation 7.55),

$$\frac{\delta \mathcal{F}_{ex}}{\delta \rho} \Big|_{\rho_0} = \mu^{ex}(\rho_0) = \mu(\rho_0) - \mu_{id}(\rho_0) = \mu_0 - k_b T \ln(\Lambda^3 \rho_0). \quad (7.77)$$

Truncating the expansion in equation 7.76 to second order in $\Delta\rho(x)$ and substituting the linear and quadratic terms from equation 7.77 and 7.64, we can simplify the excess free energy to,

$$\begin{aligned} \mathcal{F}_{ex}[\rho(\mathbf{x})] = & \mathcal{F}_{ex}[\rho_0] + \int \left\{ \mu_0 - k_B T \ln [\Lambda^3 \rho_0(\mathbf{x})] \right\} \Delta\rho(\mathbf{x}) d\mathbf{x} \\ & - \frac{k_B T}{2} \iint \Delta\rho(\mathbf{x}) C_0^{(2)}(\mathbf{x}, \mathbf{x}') \Delta\rho(\mathbf{x}') d\mathbf{x} d\mathbf{x}', \end{aligned} \quad (7.78)$$

where $C_0^{(2)}(\mathbf{x}, \mathbf{x}')$ denotes the two-point direct correlation function evaluated at the reference state around which we are expanding the density functional theory. Combining equation 7.55 with the simplified excess free energy in equation 7.78, we can express total change in free energy, $\Delta\mathcal{F} = \mathcal{F} - \mathcal{F}[\rho_0]$, as,

$$\begin{aligned} \Delta\mathcal{F}[\rho(\mathbf{x})] = & k_B T \int \left\{ \rho(\mathbf{x}) \ln \left(\frac{\rho(\mathbf{x})}{\rho_0} \right) - (1 - \beta\mu_0) \Delta\rho(\mathbf{x}) \right\} d\mathbf{x} \\ & - \frac{k_B T}{2} \iint \Delta\rho(\mathbf{x}) C_0^{(2)}(\mathbf{x}, \mathbf{x}') \Delta\rho(\mathbf{x}') d\mathbf{x} d\mathbf{x}'. \end{aligned} \quad (7.79)$$

We find an equivalent expression for the grand potential after a Legendre transform,

$$\begin{aligned} \Delta\Omega[\rho(\mathbf{x})] = & k_B T \int d\mathbf{x} \left\{ \rho(\mathbf{x}) \ln \left(\frac{\rho(\mathbf{x})}{\rho_0} \right) - [1 - \beta\phi(\mathbf{x})] \Delta\rho(\mathbf{x}) \right\} \\ & - \frac{k_B T}{2} \iint \Delta\rho(\mathbf{x}) C_0^{(2)}(\mathbf{x}, \mathbf{x}') \Delta\rho(\mathbf{x}') d\mathbf{x} d\mathbf{x}', \end{aligned} \quad (7.80)$$

where Eq. (7.80) has explicitly re-written the external potential $\phi(r)$ into the grand potential functional of the system. for completeness. This density functional theory like this was proposed by Ramakrishnan and Yussouff [26] to describe freezing, where ρ_0 is taken to be the density of the liquid on the first order transition line of a pure material (for a given temperature).

7.6.1 Relation of $C_0^{(2)}(\mathbf{x}, \mathbf{x}')$ to the structure factor

It was noted that $C_0^{(2)}(\mathbf{x}, \mathbf{x}')$ is formally related to the inverse of the Ursell function via in Eq. (7.69). Using the notation of Chakin and Lubensky, we denote the Ursell function as $S_{nn}(\mathbf{x}, \mathbf{x}')$, and re-write Eq. (7.69) as

$$C_0^{(2)}(\mathbf{x}, \mathbf{x}') = \frac{\delta(\mathbf{x} - \mathbf{x}')}{\rho_L} - S_{nn}^{-1}(\mathbf{x}, \mathbf{x}'), \quad (7.81)$$

where we set $\rho^{(1)}(\mathbf{x}) \rightarrow \rho_L$, which is the constant density of the liquid at the reference density around which the excess energy terms are expanded. Further, the excess term in Eq. (7.79) (or Eq.(7.80)) can be conveniently re-scaled in units of $k_B T \rho_L$ according to

$$\frac{F_{ex}}{k_B T \rho_L} = \frac{1}{2} \int \int \Delta \bar{\rho} \bar{C}_0^{(2)}(\mathbf{x}, \mathbf{x}') \Delta \bar{\rho}(\mathbf{x}') d\mathbf{x} d\mathbf{x}', \quad (7.82)$$

where $\Delta \bar{\rho} = (\rho - \rho_L)/\rho_L$ is a dimensionless density difference and where we defined the function scaled correlation function $\bar{C}_0^{(2)}(\mathbf{x}, \mathbf{x}')$ by

$$\bar{C}_0^{(2)}(\mathbf{x}, \mathbf{x}') \equiv \rho_L C_0^{(2)}(\mathbf{x}, \mathbf{x}') = \delta(\mathbf{x} - \mathbf{x}') - \rho_L S_{nn}^{-1}(\mathbf{x}, \mathbf{x}') \quad (7.83)$$

It is noted that Eq. (7.82) can be identified with the excess term of equation 4.7.4 in Chapter 4 of Chakin and Lubensky's text book [4] if $\bar{C}_0^{(2)}(\mathbf{x}, \mathbf{x}')$ is equated to $\chi_0^{-1}(\mathbf{x}, \mathbf{x}')$ in equation 4.7.5 of Ref. [4].

In closing this section, it is instructive to re-cast Eq. (7.83) in Fourier space, since in what follows the correlation kernels used in XPFC type models will be defined directly in k-space by making qualitative comparisons to $\hat{S}_{nn}(\mathbf{k})$. To do so, we will use some results about the structure factor of a liquid derived in Chapter 2, Section 2.3 of Ref. [4]. In particular, the structure factor of a liquid is given by

$$\hat{s}(\mathbf{k}) = \rho_L \left[1 + \rho_L \hat{g}^{(2)}(\mathbf{k}) \right] \quad (7.84)$$

where $\hat{g}^{(2)}(\mathbf{k})$ is the Fourier transform of the pair distribution function defined in Eq. (7.72). Using Eq. (7.71) to write $\hat{g}^{(2)}(\mathbf{k}) = \hat{h}^{(2)}(\mathbf{k}) + (2\pi)^2 \delta(\mathbf{k})$, and substituting this into Eq. (7.84) gives

$$\underbrace{\hat{s}(\mathbf{k}) - (2\pi)^2 \delta(\mathbf{k})}_{\hat{S}_{nn}(\mathbf{k})} = \rho_L \left[1 + \rho_L \hat{h}^{(2)}(\mathbf{k}) \right], \quad (7.85)$$

where the underbrace on the left hand side of Eq. (7.85) is identified with the Fourier transform of the Ursell function $\hat{S}_{nn}(\mathbf{k})$ (e.g., see equation 2.3.8 in Chapter 2 of Ref. [4]). From Eq. (7.85) we arrive at

$$\rho_L \hat{h}(\mathbf{k}) = \frac{\hat{S}_{nn}(\mathbf{k})}{\rho_L} \equiv \bar{S}_{nn}(\mathbf{k}) \quad (7.86)$$

where $\bar{S}_{nn}(\mathbf{k})$ is dimensionless as for an ideal liquid $\hat{S}_{nn}^{\text{ideal}} = \rho_L$. Since the Ursell function is identical to the structure factor for $\mathbf{k} \neq 0$, $\bar{S}_{nn}(\mathbf{k})$ is essentially the same as the dimensionless structure factor. Substituting Eq. (7.86) in Eq. (7.75) finally allows us to re-cast $\bar{C}_0^{(2)}(\mathbf{x}, \mathbf{x}')$ in Eq. (7.83) in Fourier space as

$$\hat{\bar{C}}_0^{(2)}(\mathbf{k}) \equiv \rho_L \hat{C}_0^{(2)}(\mathbf{k}) = \frac{\bar{S}_{nn}(\mathbf{k})}{1 + \bar{S}_{nn}(\mathbf{k})} \quad (7.87)$$

It is noted that $\hat{\bar{C}}_0^{(2)}(\mathbf{k})$ is a dimensionless two-point direct correlation function, and is actually what is considered (or what should be considered) when formulating the dimensionless phase field crystal models examined below, since $[\hat{C}_0^{(2)}(\mathbf{k})] = m^3 / \#$.

7.6.2 Moving on to phase field crystal models

This section has culminated with the derivation of a simple density functional theory for an inhomogeneous fluid expanded as a perturbation from a ideal reference liquid in terms of direct correlation functions defined at the reference fluid state (density and temperature). The direct correlation functions are in turn related to the density correlation functions generated by the grand potential of the system, and which can also be related to experimental measurements (at least the lower-order ones). Specifically, we have arrived at a way of relating the direct correlation functions entering the free energy functional in Eq. (7.80) to the structure factor of the reference liquid, which is measurable. While DFT type theories like that in Eq. (7.80) have been well established over the years and used to understand the properties of inhomogeneous fluids, we will at this point *get off* the "classical DFT train" and take a different turn. Namely, we used Eq. (7.79) as a starting point from which to derive various phase field phenomenologies through which to study solidification phenomena. It will be seen that two essential ingredients in developing such phase field theories will come down to the construction of the two-point direct correlation function $\hat{C}_0^{(2)}(\mathbf{k})$ at and close to the coexistence temperature and density, and the way the logarithm terms from the ideal free energy are treated. As an example, a convenient simplification that is used to map the formal density functional theory developed in this section onto the original PFC model of Ref. (??), to be examined in detail below, is to approximate the structure factor by a single peak in k-space, fit to a quartic function near $k \approx k_0$, where k_0 represents the main Bragg peak of BCC (or hexagonal in 2D) crystals to be modelled by the PFC theory.

$$\bar{S}_{nn}(\mathbf{k}) \approx \frac{\tau}{r + c(k - k_0^2)^2} \quad (7.88)$$

where $\tau = T/T_0$ with T being temperature, T_0 a reference temperature, r, c dimensionless constants and k_0 is the magnitude of the main Bragg peak of the structure factor of a liquid near coexistence.

Chapter 8

Phase Field Crystal (PFC) Theory

This section starts from Eq. (7.79), and properties of the correlation function discussed at the end of Section (7.6) to expand the derivation of the basic *phase field crystal (PFC)* model developed in Chapter 8 of Reference [24] into a class of more generalized PFC type models that are conceptually better connected to the classical DFT (cDFT) theory developed at the end of Chapter 7, but which still hold the salient features of the original PFC model introduced by Elder and Grant [8]. This new class of PFC models are coined under the name *structural PFC* models, or *XPFC* models for short. The main difference between XPFC models and the original PFC model is that the former can stabilize a wider range of crystallographically complex phases and efficiently model phase transitions between these phase in density-temperature space.

8.1 Simplifying cDFT Theory

An important step in obtaining most PFC type models is the simplification of the original second order cDFT theory described by Eq. (7.79). To do so, it is useful to work with a dimensionless relative density $n(\mathbf{x}) = (\rho(\mathbf{x}) - \rho_0)/\rho_0$, where ρ_0 is a reference density, typically taken as the density of the liquid at coexistence [24]. We will also set $\mu_0 = 0$ for simplicity as this will not alter the results of this discussion in any fundamental way. The free energy thus becomes

$$\begin{aligned} \frac{\Delta F[n(\mathbf{x})]}{k_B T_0 \rho_0} &= \int d\mathbf{x} \tau \{ (n(\mathbf{x}) + 1) \ln(n(\mathbf{x}) + 1) - n(\mathbf{x}) \} \\ &\quad - \frac{1}{2} \int \int n(\mathbf{x}) \tau \left[\rho_0 C_0^{(2)}(|\mathbf{x} - \mathbf{x}'|) \right] n(\mathbf{x}') d\mathbf{x} d\mathbf{x}', \end{aligned} \quad (8.1)$$

where we have also scaled temperature as $\tau = T/T_0$, where T_0 is a reference temperature; in what follows T_o will be chosen to correspond to the coexistence temperature at which ρ_0 is evaluated. The correlation function in Eq. (7.76) is written in translationally invariant form since it represents the direct correlation function of the liquid evaluated at (ρ_0, T_0) . The correlation function $C^{(2)}(|\mathbf{x} - \mathbf{x}'|)$ has units $[C^{(2)}] = 1/\#$ and can be expressed as a Fourier transform, shown here for later use,

$$C_0^{(2)}(|\mathbf{x} - \mathbf{x}'|) = \frac{1}{2\pi} \int \hat{C}(|\mathbf{k}|) e^{i\mathbf{k}\cdot(\mathbf{x}-\mathbf{x}')} d^3\mathbf{k} \quad (8.2)$$

where $[\hat{C}] = m^3/\#$. To proceed further, we expand the bulk (i.e. non-correlation) terms to fourth order in the n , the free energy can be re-expressed as

$$\frac{\Delta F}{k_B T_0 \rho_0} = \int d\mathbf{x} \tau \left\{ \left(\frac{n^2}{2} - \frac{n^3}{6} + \frac{n^4}{12} \right) - \frac{n(\mathbf{x})}{2} \int d\mathbf{x}' [\rho_0 C_0^{(2)}(|\mathbf{x} - \mathbf{x}'|)] n(\mathbf{x}') \right\} \quad (8.3)$$

This simplified cDFT in Eq. (8.3) is the strating point of most PFC studies in the literature.

8.2 Recovering the Traditional PFC Model

It is instructive to review here the derivation of the standard PFC model emerges from Eq. (8.3). The starting point is to specializs the direct correlation function to the simple *single-peaked* form

$$C_0^{(2)}(|\mathbf{x} - \mathbf{x}'|) = (-\hat{C}_0 - \hat{C}_2 \nabla_{x'}^2 - \hat{C}_4 \nabla_{x'}^4) \delta(\mathbf{x} - \mathbf{x}'), \quad (8.4)$$

where gradient notation $\nabla_{x'}$ implies that the operation is on the [dimensional] variable x' . The Fourier space equivalent of this correlation is

$$\hat{C}(|\mathbf{k}|) = -\hat{C}_o + \hat{C}_2 k^2 - \hat{C}_4 k^4 \quad (8.5)$$

where $k = |\mathbf{k}|$. Equation (8.5) defines a single-peaked function with a negative $k = 0$ value and a maximum at finite wavelength if $\hat{C}_o > 0$, $\hat{C}_2 > 0$ and $\hat{C}_4 > 0$. Moreover, the solution of $d\hat{C}/dk = 0$ sets the scale of the lattice spacing as (dropping the 2π)

$$a = \frac{1}{k_{\text{peak}}} = \sqrt{\frac{2\hat{C}_4}{\hat{C}_2}} \quad (8.6)$$

Papers studying the physics of the standard PFC model often work in dimensional spatial variables, where space is scaled according to $\mathbf{r} = \mathbf{x}/a$, where a is the lattice spacing of the crystal phase that emerges. They also assume isothermal conditions, thus setting the reference temperature to $T_0 \rightarrow T$, making $\tau = 1$. These scalings transform Eq. (8.3) to

$$\frac{\Delta F}{k_B T \rho_0 a^3} = \int d\mathbf{r} \left\{ \left(\frac{n^2}{2} - \frac{n^3}{6} + \frac{n^4}{12} \right) - \frac{n(\mathbf{r})}{2} \int d\mathbf{r}' [\rho_0 a^3 C_0^{(2)}(a|\mathbf{r} - \mathbf{r}'|)] n(\mathbf{r}') \right\} \quad (8.7)$$

Substituting Eq. (8.4) into Eq. (8.7) turns the correlation term in the large bracket to

$$\rho_0 a^3 C_0^{(2)}(a|\mathbf{r} - \mathbf{r}'|) \equiv C(|\mathbf{r} - \mathbf{r}'|) = \left(-\rho_0 \hat{C}_0 - \frac{\rho_0 \hat{C}_2}{a^2} \nabla_{r'}^2 - \frac{\rho_0 \hat{C}_4}{a^4} \nabla_{r'}^4 \right) [a^3 \delta(a\mathbf{r} - a\mathbf{r}')], \quad (8.8)$$

where we identify $a^3 \delta(a\mathbf{r} - a\mathbf{r}') = \delta(\mathbf{r} - \mathbf{r}')$, the dimensionless delta function ¹, and note that $[\rho_0 \hat{C}_0] = [\rho_0 \hat{C}_2/a^2] = [\rho_0 \hat{C}_4/a^4] = 1$. Furthermore, by substituting the expression of Eq. (8.6) into Eq. (8.8) we obtain

$$C(|\mathbf{r} - \mathbf{r}'|) = (1 - \Delta B - B^x (1 + \nabla_{r'}^2)^2) \delta(\mathbf{r} - \mathbf{r}'), \quad (8.9)$$

where we have define the shorthand notation

$$\begin{aligned} B^x &= \frac{\rho_0 \hat{C}_2}{2a^2} = \frac{\rho_0 \hat{C}_4}{a^4} = \frac{\rho_0 \hat{C}_2^2}{4\hat{C}_4} \\ B^l &= \rho_0 \hat{C}_o + 1 \\ \Delta B &= B^l - B^x \end{aligned} \quad (8.10)$$

¹To see this, consider re-expressing the delta function as $\lim_{\delta \rightarrow 0} \{(1/\delta^3) 1_\delta[\mathbf{x}]\}$, where $1_\delta[\mathbf{x}]$ is the indicator function, which returns unity on the measure $x \in [-\delta/2, \delta/2]$.

In terms of these definitions, Eq. (8.7) can be re-expressed as

$$\frac{\Delta F}{k_B T \rho_0 a^3} = \int d\mathbf{r} \left\{ \left(\frac{n^2}{2} - \frac{n^3}{6} + \frac{n^4}{12} \right) - \frac{n(\mathbf{r})}{2} \int d\mathbf{r}' n(\mathbf{r}') (1 - \Delta B - B^x (1 + \nabla_{\mathbf{r}'}^2)^2) \delta(\mathbf{r} - \mathbf{r}') \right\}, \quad (8.11)$$

The final form of the traditional PFC model is obtained by completing the integral in \mathbf{r}' in Eq. (8.11) and collecting terms in powers on $n(\mathbf{x})$. This gives

$$\frac{\Delta F}{k_B T \rho_0 a^3} = \int d\mathbf{r} \left\{ -\eta \frac{n^3}{6} + \chi \frac{n^4}{12} + \frac{n}{2} [\Delta B + B^x (1 + \nabla_r^2)^2] n \right\} \quad (8.12)$$

In order to make the PFC model more robust in capturing deviations away from purely ideal, the local terms in Eq. (8.11) have been scaled by free [dimensionless] parameters η and χ . In theory, these can be seen as contributions from higher order correlation terms. Finally, the [dimensionless] constants in Eq. (8.12) can be converted into corresponding free energy density units by multiplying each by $k_B T_0$. The equilibrium and dynamical properties of the standard PFC model is discussed in detail in Ref. [24] and will not be discussed further here.

The parameter ΔB is usually treated as a PFC model temperature. The dependence on temperature enters through the fact that ΔB is related to the structure factor evaluated at the peak wavevector of the triangular lattice formed (in 2D) by Eq. (8.12). Namely, it is straightforward to show that $B_l - B_x = 1 - \rho_0 \hat{C}(|\mathbf{k}_{\text{peak}}|) = 1/S(|\mathbf{k}_{\text{peak}}|)$. For a thorough analysis of the PFC model of Eq. (8.12) the reader is referred to Ref. [24]. In what follows, we expand the context of PFC to include a different class of correlation kernels.

8.3 Structural PFC Model (XPFC)

If instead of expanding $C^{(2)}(|\mathbf{x} - \mathbf{x}'|)$ in a finite series of gradients it is left as some analytic form defined over all of \mathbf{k} -space, then Eq. (8.3) becomes the *Structural PFC* model, or *XPFC* models for short. The main idea of XPFC models is to reconstruct the direct two-point correlation functions phenomenologically in \mathbf{k} -space in a way that reproduces the salient features of interest of the true direct correlation function. Of course, as a phase field theory, XPFC models must still expand the logarithmic terms in the ideal free energy to make the resulting theory tractable for dynamical simulations over experimentally relevant domain sizes ².

One convenient form used for $\rho_0 C^{(2)}(|\mathbf{x} - \mathbf{x}'|)$ used to specialize Eq. (8.3) to the XPFC model is given by

$$\rho_0 \hat{C}(\mathbf{k}) = \chi(|\mathbf{k}|) + \sum_{\alpha} e^{\frac{T}{T_0}} e^{-\frac{(|\mathbf{k}| - |\mathbf{k}_{\alpha}|)^2}{2\sigma_{\alpha}^2}} \quad (8.13)$$

where $\chi(|\mathbf{k}|)$ is non-zero and negative near $\mathbf{k} = 0$, and rapidly decays to zero for $\mathbf{k} > 0$. In the second term, the index α runs over families of point group symmetry-equivalent planes, whose reciprocal lattice vectors share a common magnitude $|\mathbf{k}_{\alpha}|$. The parameter σ_{α} is the width of the correlation peak at $\mathbf{k} = \mathbf{k}_{\alpha}$. The temperature dependence of the correlation peaks is achieved through the prefactor $\exp(T/T_0)$, which gives the correct temperature scaling of the amplitudes at temperatures much higher than the Debye temperature ³. In principle, the peaks of the XPFC correlation function

²Recently, a new class of XPFC models has emerged that retain the logarithmic structure at long wavelengths, thus allowing more quantitative control of solid-liquid-vapour properties.

³The first version of the XPFC model used a phenomenological temperature parameter to control the change of the correlation peak height according to $\hat{C}(|\mathbf{k}|) \sim \exp(-\sigma^2)$. Later, this form was changed to the one in Eq. (8.13) following Ref.[1]

can be constructed to fit the properties computed from molecular dynamics. Thus, the sum over α can run over several modes of reflection in order to stabilize exotic defect structures [2]. However, for most calculations only the α corresponding to the first 1-2 modes of reflection of the emergent crystal structures are kept. *It is also noted* that XPFC model also scales the n^3 and n^4 terms in the local free energy by η and χ , respectively.

8.4 Equilibrium Properties of the XPFC model

To understand how Eq. (8.3) in conjunction with Eq. (8.13) give rise to crystallization of metallic phases, it is instructive to explore the phase diagram supported by the model. To do so, the following ansatz will be adopted to describe the density field $n(\mathbf{x})$,

$$n(r) = n_0 + \sum_{\alpha} \phi_{\alpha} \left(\sum_{\mathbf{G} \in \{\mathbf{G}\}_{\alpha}} e^{i\mathbf{G} \cdot \mathbf{x}} \right) + c.c., \quad (8.14)$$

where *c.c.* denotes complex conjugate, while n_0 is the average density of a phase, which is zero for the liquid within coexistence (since the liquid remains at the reference density ρ_0), and takes on non-zero values for the solid, denoted $n_s = (\rho_s - \rho_0) / \rho_0$. The second term is used to describe ordering in solids. As with the XPFC correlation function, the label α in the first sum runs over families of crystal planes that share the same set of symmetry operations and are characterized by the set of reciprocal lattice vectors $\{\mathbf{G}\}_{\alpha}$. The inner sum superimposes density waves with reciprocal lattice vectors in the set $\{\mathbf{G}\}_{\alpha}$, with each such superposition weighted by an amplitude ϕ_{α} . It is noted that in equilibrium calculations, both n_0 and ϕ_{α} are taken as bulk constants of a phase.

8.4.1 Crystallography of the single mode expansion

We will first consider Eq. (8.14) for the description of BCC phase. A common set of primitive lattice vectors for the BCC lattice is given by [4, 7]

$$\bar{a}_1 = \frac{a}{2} (\hat{x} + \hat{y} + \hat{z}), \quad \bar{a}_2 = \frac{a}{2} (\hat{x} + \hat{y} + \hat{z}) \text{ and} \quad \bar{a}_3 = \frac{a}{2} (\hat{x} - \hat{y} + \hat{z}), \quad (8.15)$$

where $(\hat{x}, \hat{y}, \hat{z})$ form the axes of the conventional unit cell of BCC. From this set of real space primitive lattice vectors can be derived the corresponding set of reciprocal lattice vectors,

$$\bar{q}_1 = \frac{2\pi}{a} (\hat{x} + \hat{y}), \quad \bar{q}_2 = \frac{2\pi}{a} (\hat{x} + \hat{z}) \text{ and} \quad \bar{q}_3 = \frac{2\pi}{a} (\hat{y} + \hat{z}) \quad (8.16)$$

where each vector has a magnitude $2\pi/a$ a being the lattice constant of the BCC unit cell. Just as any lattice point in the real space lattice can be represented as a linear combination of $(\bar{a}_1, \bar{a}_2, \bar{a}_3)$, any reciprocal lattice vectors of the BCC lattice can be constructed by linear combination of $(\bar{q}_1, \bar{q}_2, \bar{q}_3)$ according to $\mathbf{G} = h\bar{q}_1 + k\bar{q}_2 + l\bar{q}_3$, where (h, k, l) are integers. Each vector \mathbf{G} defines a normal to a family of planes in real space lattice ⁴. The lattice planes causing the first (i.e dominant) mode of reflection in the BCC lattice are normal to a set of six reciprocal lattice vectors indexed by $(h k l) = (1, 0, 0), (0, 1, 0), (0, 0, 1), (1, -1, 0), (0, 1, -1), (-1, 0, 1)$. This first mode of reflection is denoted by $\alpha = 1$, and the above set of $(h k l)$ defines $\{\mathbf{G}\}_{\alpha=1}$ in Eq. (8.14). Retaining only the $\alpha = 1$

⁴The coefficients $(h k l)$ are called Miller indices and their significance is that the first plane normal to \mathbf{G} cuts through the \bar{q}_1 axis at $|\bar{q}_1|/h$, the \bar{q}_2 axis at $|\bar{q}_2|/k$ and the \bar{q}_3 axis at $|\bar{q}_3|/l$.

term in the sum of Eq. (8.14), denoting $\phi_{\alpha=1} = \phi$ and substituting the set $\{\mathbf{G}\}_{\alpha=1}$ gives, after some simple manipulations,

$$n(x, y) = n_0 + \phi[\cos(qx)\cos(qy) + \cos(qx)\cos(qz) + \cos(qy)\cos(qz)], \quad (8.17)$$

where $q = 2\pi/a$, and where we have defined $a = (\sqrt{2/3})\tilde{a}$, with \tilde{a} being a reference unit cell edge length. This somewhat strange definition of a arises as follows. We will want to later model the crystallization of both FCC and BCC phases using the same multi-peaked correlation function in the model of Eq. (8.3). The dominant mode of reflection of FCC crystals happens from $\{111\}$ planes⁵. The distance to these planes from the origin of a unit cell is the inverse of the length of any $\{111\}$ reciprocal lattice vector, which is $\sqrt{3}$ (in units of $2\pi/a$). On the other hand, the dominant mode of reflection for a BCC lattice happens off $\{110\}$ planes, whose length in reciprocal space is $\sqrt{2}$. It is thus not possible to model the first (dominant) modes of reflection for both BCC and FCC using a common first peak for $\hat{C}(\mathbf{k})$. There are two fixes. The simple one is to re-scale the lattice constant of the BCC unit cell to be $\sqrt{2}/\sqrt{3}$ time that of the FCC lattice constant, i.e. $\tilde{a} = a_{\text{FCC}}$ [12]. Perhaps a more realistic fix would be to make the peak positions in $\hat{C}(\mathbf{k})$ shift according to the local temperature, i.e. make $\hat{C}(\mathbf{k}) \rightarrow \hat{C}(\mathbf{k}; \rho_0(T))$. For simplicity, we will stick to the first method here. For convenience, we set $\tilde{a} = 1$ hereafter.

8.4.2 Mean field free energy density of BCC solid-liquid system

With Eq. (8.17) in hand, the next step is to use Eq. (8.17) to calculate the free energy density of a BCC-liquid system using the model of Eq. (8.3). This is done by substituting Eq. (8.17) into Eq. (8.3), integrating Eq. (8.3) over the volume of the conventional unit BCC unit cell cell, and normalizing by dividing by a^3 . Following this, the resulting free energy density is minimized, seeking solid solutions with $(\phi > 0, n_0 > 0)$ and liquid solutions with $(\phi = 0, n_0 > 0)$. For the moment, it is not necessary to specify a particular form for the two-point direct correlation function other than to say that it must be expandable in a Fourier series according to Eq. (8.2). *For simplicity, the scaled temperature $\tau = 1$ is assumed in what follows.*

8.4.2.1 Interaction free energy

Beginning with the non-local term in Eq. (8.3), it is instructive to go over the algebra for this important term for readers new to PFC type equilibrium calculations. To make the algebra tractable, the expansion of the form Eq. (8.14) is substituted for $n(\mathbf{x})$ and $n(\mathbf{x}')$, and Eq. (8.2) is used formally to

⁵Note that when materials science texts reference “ $\{111\}$ ”, “ $\{110\}$ ” or other families of lattice planes, they are usually using the reciprocal lattice vectors defined in the setting of the conventional unit cell of BCC or FCC.

represent $C_0^{(2)}(|\mathbf{x} - \mathbf{x}'|)$. This yields,

$$\begin{aligned}
\bar{F}_{\text{int}}[n_0, \phi] &= -\frac{1}{2V} \int n(\mathbf{x}) \left[\rho_0 C^{(2)}(|\mathbf{x} - \mathbf{x}'|) \right] n(\mathbf{x}') d\mathbf{x} d\mathbf{x}' \\
&= -\frac{\rho_0}{2V} \int \int \int \frac{d\mathbf{k}}{2\pi} d\mathbf{x} d\mathbf{x}' \left\{ n_0^2 \hat{C}(\mathbf{k}) e^{i\mathbf{k}\cdot\mathbf{x}} e^{i\mathbf{k}\cdot\mathbf{x}'} \right\} \\
&+ -\frac{\rho_0}{2V} \sum_i \int \int \int \frac{d\mathbf{k}}{2\pi} d\mathbf{x} d\mathbf{x}' \left\{ 2n_0 \phi \hat{C}(\mathbf{k}) e^{i\mathbf{G}_i \cdot \mathbf{x}} e^{i\mathbf{k}\cdot\mathbf{x}} e^{i\mathbf{k}\cdot\mathbf{x}'} \right\} \\
&+ -\frac{\rho_0}{2V} \sum_i \int \int \int \frac{d\mathbf{k}}{2\pi} d\mathbf{x} d\mathbf{x}' \left\{ 2n_0 \phi \hat{C}(\mathbf{k}) e^{i\mathbf{G}_i \cdot \mathbf{x}'} e^{i\mathbf{k}\cdot\mathbf{x}} e^{i\mathbf{k}\cdot\mathbf{x}'} \right\} \\
&+ -\frac{\rho_0}{2V} \sum_i \sum_j \int \int \int \frac{d\mathbf{k}}{2\pi} d\mathbf{x} d\mathbf{x}' \left\{ \phi^2 \hat{C}(\mathbf{k}) e^{i\mathbf{G}_i \cdot \mathbf{x}} e^{i\mathbf{G}_j \cdot \mathbf{x}'} e^{i\mathbf{k}\cdot\mathbf{x}} e^{i\mathbf{k}\cdot\mathbf{x}'} \right\} \quad (8.18)
\end{aligned}$$

Each of the integrals above can be simplified using the properties of the delta functions, analogously to the approach used in Section 5.2.1. For example, completing the $d\mathbf{x} d\mathbf{x}'$ integral on the second line gives

$$\begin{aligned}
\int \int \int \frac{d\mathbf{k}}{2\pi} d\mathbf{x} d\mathbf{x}' \left\{ n_0^2 \hat{C}(\mathbf{k}) e^{i\mathbf{k}\cdot\mathbf{x}} e^{i\mathbf{k}\cdot\mathbf{x}'} \right\} &= \frac{\rho_0 n_0^2}{V} \int \frac{d\mathbf{k}}{2\pi} \hat{C}(\mathbf{k}) \left(\int \int d\mathbf{x} d\mathbf{x}' e^{i\mathbf{k}\cdot\mathbf{x}} e^{i\mathbf{k}\cdot\mathbf{x}'} \right) \\
&= \frac{\rho_0 n_0^2}{V} \int \frac{d\mathbf{k}}{2\pi} \hat{C}(\mathbf{k}) V^2 \delta(\mathbf{k}) \\
&\rightarrow \frac{\rho_0 n_0^2}{V^2} \sum_{\mathbf{k}_i} \hat{C}_{\mathbf{k}_i} V^2 \delta_{\mathbf{0}, \mathbf{k}_i} \\
&= n_0^2 \rho_0 \hat{C}(\mathbf{0}) \quad (8.19)
\end{aligned}$$

where Eq. (5.36) was used between the first and second lines, and where the discrete limit was taken to go from the second to last line since the calculation is in a finite volume⁶. Proceeding similarly for the third and fourth lines of Eq. (8.18) reveals that they vanish since the sums do *not* include a $\mathbf{G}_i = \mathbf{0}$ term as this is explicitly represented by the n_0 term of Eq. (8.14). For the last line of Eq. (8.18), the spatial integrals are similarly done first, and the remaining $d\mathbf{k}$ integral is taken over to the discrete limit as a sum with over a Kronecker delta function. The result, combined with that in Eq. (8.19), gives

$$\bar{F}_{\text{int}}[n_0, \phi] = -\frac{1}{2} \rho_0 \hat{C}(0) n_0^2 - \frac{1}{2} \left(6 \rho_0 \hat{C}(|\mathbf{k}_{110}|) \right) \phi^2, \quad (8.20)$$

where the factor of 6 represents the total number of ways $\mathbf{G}_i + \mathbf{G}_j = \mathbf{0}$ for all (i, j) pairs in the sums implied by the first mode sum in Eq. (8.14). The notation $|\mathbf{k}_{110}|$ denotes the common magnitude of all \mathbf{G}_i in the first mode.

8.4.2.2 Local free energy terms

Moving on to the local terms of the free energy functional is more straightforward. Substituting Eq. (8.14) into Eq. (8.3) yields an integrand with a large number of simple terms each of which contains a complex exponential phase factors of the form $qx \pm qy \pm qz$. It is not practical to show

⁶The discrete limit of $\int \delta(\mathbf{k}) d\mathbf{k}/(2\pi) \rightarrow (1/V) \sum_{\mathbf{k}_i} \delta_{\mathbf{0}, \mathbf{k}_i}$, where $\delta_{\mathbf{0}, \mathbf{k}_i}$ is the Kronecker delta function. Another useful result here is the discrete limit of $\int d\mathbf{x} \exp\{i(\mathbf{k} - \mathbf{k}') \cdot \mathbf{x}\} \rightarrow V \delta_{\mathbf{k}, \mathbf{k}'}$

them here, however, the reader that has never done this type of calculation before is advised to square Eq. (8.14) to see for themselves ⁷. Carrying out the integration all complex exponential terms reveals that *only* a small fraction of them survive; namely, the ones whose phase factor vanish. All other terms contribute zero because they oscillate an integral number of times within the volume of the unit cell. The result from the non-vanishing terms gives the following local free energy density,

$$\bar{F}_{\text{loc}}[n_0, \phi] = \frac{1}{2}n_o^2 - \frac{1}{6}\eta n_o^3 + \frac{1}{12}\chi n_o^4 + 6(1 - \eta n_0 + \chi n_0^2)\phi^2 + 8(2\chi n_0 - \eta)\eta\phi^3 + 45\chi\phi^4 \quad (8.21)$$

The expression $\bar{F}_{\text{loc}}[n_0, \phi]$ corresponds to the mean field behaviour of the local terms Eq. (8.3), with the rapidly oscillating parts of the density integrated out.

8.4.2.3 Total BCC-liquid mean field free energy

The total mean field free energy approximation corresponding to Eq. (8.3) is thus the sum $\bar{F}[n_0, \phi] = \bar{F}_{\text{loc}}[n_0, \phi] + \bar{F}_{\text{int}}[n_0, \phi]$, namely,

$$\begin{aligned} \bar{F}[n_0, \phi] &= \frac{1}{2}n_o^2 - \frac{1}{6}\eta n_o^3 + \frac{1}{12}\chi n_o^4 + 6(1 - \eta n_0 + \chi n_0^2)\phi^2 + 8(2\chi n_0 - \eta)\eta\phi^3 + 45\chi\phi^4 \\ &\quad - \frac{1}{2}\rho_0\hat{C}(0)n_0^2 - 3\rho_0\hat{C}(|\mathbf{k}_{110}|)\phi^2 \end{aligned} \quad (8.22)$$

It is noted that Eq. (8.1) should also be multiplied by τ to re-introduce the correct temperature scaling inherited from Eq. (8.3). This just re-scales the coefficients η and χ , which were assumed to have a τ dependence anyway. However, the multiplication by τ adds an non-trivial temperature dependence to the correlation terms, which also contain an added temperature dependence via Eq. (8.13).

It is interesting to examine the behaviour of Eq. (8.22) as a function of $1 - \rho_0\hat{C}(|\mathbf{k}_{\text{peak}}|) = 1/S(|\mathbf{k}_{\text{peak}}|)$. Figure 8.1 shows $\bar{F}[n_0, \phi]$ for three values of $S(|\mathbf{k}_{\text{peak}}|)$, with the left figure corresponding to the lowest $S(|\mathbf{k}_{\text{peak}}|)$ (highest temperature) and the right figures corresponds to the highest $S(|\mathbf{k}_{\text{peak}}|)$ (lowest temperature). Consistent with Landau theory of first order phase transformations, there is one stable free energy well at high temperatures, which gives way two two discontinuous wells at lower temperatures, one of which is meta-stable relative to the other until some temperature that marks the first order transition point. Here, the non-conserved order parameter (ϕ) is coupled to the phase density (n_0), which is the mean of a conserved order parameter. As a result, the system below the transition temperature with n_0 running through the downward concave part of the free energy can separate into two phase volumes, each with its own density and corresponding order parameter that depends on this density. For example, a system in Figure 8.1 with $n_0 \approx 0.05$ will thus separate into a liquid with $(n_l = 0, \phi_l = 0)$ and a solid with $(n_s > 0, \phi_s(n_s) > 0)$.

8.4.3 Phase Coexistence and Construction of Diagrams

This sub-section reviews the steps to construct the phase diagram between solid and liquid analytically. First, the free energy is minimized with respect to ϕ according to $\partial\bar{F}[n_0, \phi]/\partial\phi = 0$. This yields two solutions, one is $\phi_{\min} = 0$ and the other,

$$\phi_{\min}(n_0) = \frac{1}{30\chi} \left\{ -4\chi n_0 + 2\eta + \sqrt{-44\chi^2 n_0^2 + 44\chi n_0 \eta + 4\eta^2 - 60\chi + 30\chi \rho_0 \hat{C}(|\mathbf{k}_{110}|)} \right\} \quad (8.23)$$

⁷It is not advised to do this calculation by hand, but rather to use a symbolic manipulation software such as *Mathematica* or *Maple*.

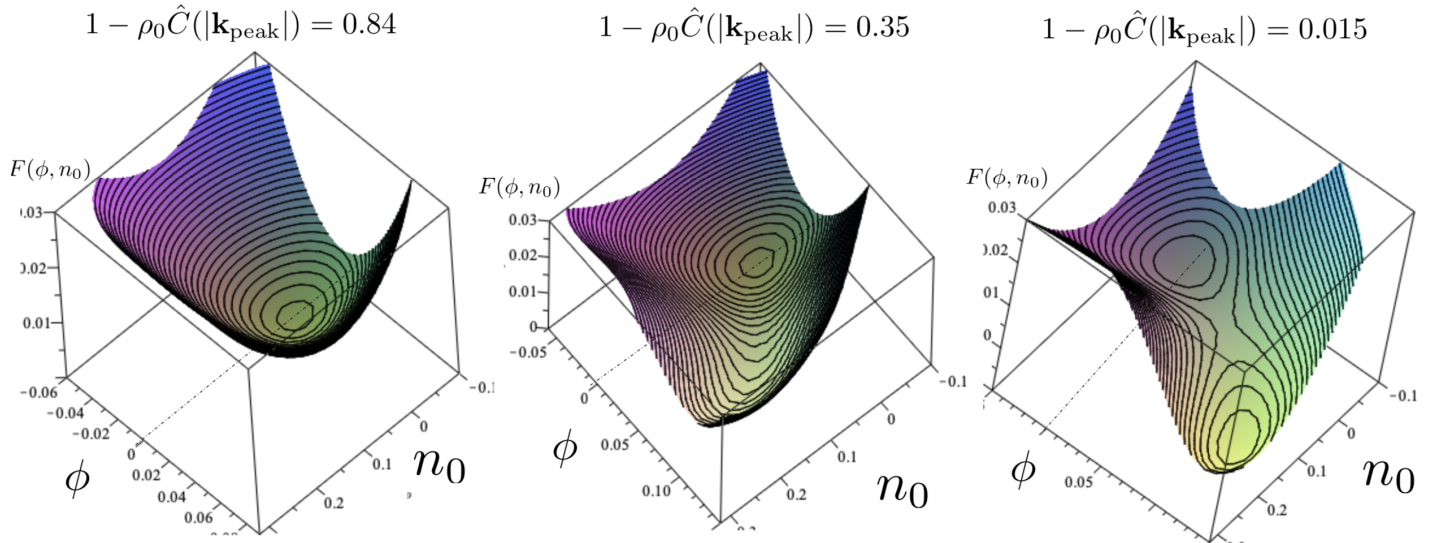


Figure 8.1: Mean field free energy of the XPFC model showing one phase (well) at $\phi = 0$ when the structure $S(|\mathbf{k}_{\text{peak}}|) = 1 - \rho_0(|\mathbf{k}_{\text{peak}}|)$ is small (left image), and the discontinuous emergence of second ordered phase with $\phi(n_0) > 0$ as $S(|\mathbf{k}_{\text{peak}}|)$ increases (middle and right images).

The $\phi_{\min} = 0$ solution corresponds to the liquid phase, while the solution of Eq. (8.23) corresponds to the BCC phase. It is Using these expressions for the order parameter, each phase's free energy can written as a function of its density, i.e.

$$\begin{aligned} f_{\text{liq}}(n_0) &= \bar{F}[n_0, 0] \\ f_{\text{BCC}}(n_0) &= \bar{F}[n_0, \phi_{\min}(n_0)] \end{aligned} \quad (8.24)$$

Figure 8.2 shows a plot of $f_{\text{liq}}(n_0)$ and $f_{\text{BCC}}(n_0)$ for typical model parameters. It is noteworthy that while the liquid mean field free energy is defined over the entire range of density shown, the solid free energy ceases to exist below a critical density. This implies that the solid phase cannot exist below this density since the radical in Eq. (8.23) becomes negative for lower values of n_0 . The line touching both curves comes from the *common tangent* or *Maxwell equal area* constructions described in Section 1.7. This construction is used to calculate the densities of coexisting phase, as well as their common chemical potential. It can be done by minimizing the total system free energy (composed of a weighted sum of the free energies of each phase) subject to mass conservation. Alternatively, one can fine the coexistence equilibrium by equating the pressures and chemical potentials of each phase. Using $f_{\text{liq}}(n_0)$ and $f_{\text{BCC}}(n_0)$ to construct the co-existence densities at different temperatures produces a phase diagrams for the BCC-liquid co-existence.

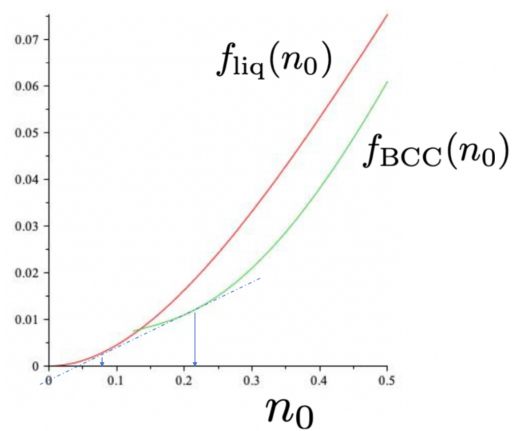


Figure 8.2: Free energy of liquid (top curve) and solid (lower curve). The solid does not exist below where $f_{\text{BCC}}(n_0)$ ceases since $\phi_{\min}(n_0)$ ceases to exist. Common tangent line is also shown.

Chapter 9

Dynamics in Classical Field Theories

From the very nature of its derivation from density functional theory, the XPFC density order parameter $n(\mathbf{x}, t)$ is a density difference. The n field in Eq. (8.3) thus expected to evolve according to conserved dynamics. Moreover, it is expected that in the diffusive limit of microstructure evolution, density dynamics must take on the form of a Langevin equation. here, the fluxes that drive density flow are determined from gradients of thermodynamic potentials [24] of an associated ensemble being considered. These fluxes serve as conjugate variables to some intensive variable. There are also rigorous treatments deriving the dynamics of classical fields from first principles, and the basic Langevin-type equations governing the PFC type models can be also be shown more formally to be spacial cases of these. They yield modifications to from Model B dynamics, but their essence remains similar, and usually requires some degree of phenomenological intervention informed by physical intuition to arrive at the final form of the dynamical equations. Three approaches for deriving XPFC dynamics for a single component density field are shown in this section.

9.1 Dynamic Density Functional Theory (DDFT)

One path to arrive at the density dynamics of the PFC density field comes is motivated from ideas of non-equilibrium statistical mechanics. This is reviewed below by examining first what is mean by a microscopic mean field density and then deriving a series of equations that approximate its dynamics.

9.1.1 Non-equilibrium statistical mechanics

The first thing to consider is how quantities that depends on the phase space coordinates and momenta of a system and are out of equilibrium are averaged. To address this question, consider a non-equilibrium probability distribution $f(\mathbf{q}, \mathbf{p}; t)$ over the phase space of a material system, as defined in Section 7.1. The dynamical evolution of $f(\mathbf{q}, \mathbf{p}; t)$ follows from classical mechanics accordng to

$$\frac{df}{dt} = \{f, \mathcal{H}\} + \frac{\partial f}{\partial t}, \quad (9.1)$$

where $\{f, \mathcal{H}\}$ is the Poisson bracket defined by

$$\{f, g\} = \sum_{i=0}^N \frac{\partial f}{\partial q_i} \frac{\partial g}{\partial p_i} - \frac{\partial g}{\partial q_i} \frac{\partial f}{\partial p_i}. \quad (9.2)$$

The distribution $f(\mathbf{q}, \mathbf{p}; t)$ must remain normalized in time as it flows through phase space, and so

$$\int d\mathbf{q}d\mathbf{p} f(\mathbf{q}, \mathbf{p}; t) = 1 \quad (9.3)$$

As a result, its total time derivative is zero $df/dt = 0$. This simplifies Eq. (9.1) to the so-called *Liouville Equation*,

$$\frac{\partial f}{\partial t} = -\{f, \mathcal{H}\} \quad (9.4)$$

Assuming ergodicity (not always guaranteed in low dimensional Hamiltonian systems!), the Liouville Equation will evolve $f(\mathbf{q}, \mathbf{p}; t)$ towards its thermodynamic equilibrium distribution $f_{eq}(\mathbf{q}, \mathbf{p})$, i.e.,

$$\lim_{t \rightarrow \infty} f(\mathbf{q}, \mathbf{p}; t) = f_{eq}(\mathbf{q}, \mathbf{p}) \quad (9.5)$$

The equilibrium distribution $f_{eq}(\mathbf{q}, \mathbf{p})$ is used to compute equilibrium averages, such as, for example the local density in equilibrium, which is done by substituting it for $f_{eq}(\mathbf{q}, \mathbf{p}, N)$ in Eq. (7.2).

In the non-equilibrium dynamics literature, the form of Eq. (7.2) is tacitly assumed to hold for calculating non-equilibrium averages of microscopic quantities by making the substitution $f_{eq}(\mathbf{q}, \mathbf{p}) \rightarrow f(\mathbf{q}, \mathbf{p}, t)$, with the proviso that the system is sufficiently close to equilibrium. For example, the non-equilibrium *coarse grained* density is thus assumed to given by

$$\rho(x, t) = \langle \hat{\rho}(x; \mathbf{q}) \rangle = \text{Tr} [\hat{\rho}(x; \mathbf{q}) f(\mathbf{q}, \mathbf{p}, t)] \quad (9.6)$$

where $\hat{\rho}(x; \mathbf{q})$ is the microscopic density operator and where the average $\langle \cdot \rangle$ denotes weighting by the non-equilibrium phase space density $f(\mathbf{q}, \mathbf{p}, t)$. Here, the $\text{Tr} [\dots]$ operation has been used to denote the sum and integrations in Eq. (7.2). Averages of other quantities operating out of equilibrium will be computed analogously to Eq. (9.6); one such other quantity examined in the next subsection is the diffusivity.

9.1.2 Density evolution as a Markov process

In the context defined by the non-equilibrium ensemble of $f(\mathbf{q}, \mathbf{p}, t)$, the spatiotemporal dynamics of a microscopic density field can also be derived as a Markov process using so-called projection operator methods¹. The mathematical details are shown in Ref. [9]. Intuitively, the main idea is to describe the evolution of the non-equilibrium density $\rho(\mathbf{x}, t)$ as a Markovian process that is driven by its [non-equilibrium] conjugate variable $\delta\mathcal{F}[\rho]/\delta\rho(\mathbf{x}, t)$ (\mathcal{F} is the system's free energy) through a so-called *Green-Kubo* type of relation. Specifically in this formalism, the dynamics of $\rho(\mathbf{x}, t)$ take on the form²

$$\frac{\partial \rho(\mathbf{x}, t)}{\partial t} = \int d\mathbf{x}' \mathcal{D}_{\mathbf{x}, \mathbf{x}'}(t) \frac{\delta\mathcal{F}[\rho]}{\delta\rho(\mathbf{x}', t)}, \quad (9.7)$$

with $\mathcal{D}_{\mathbf{x}, \mathbf{x}'}(t)$ being a non-local interaction kernel known as the *dissipation matrix*. This kernel describes the transition rate from the position \mathbf{x}' to the position \mathbf{x} (as with any Markov-type theory) and weights this transition by the local chemical potential strength at \mathbf{x}' . It then integrates all neighbouring transitions that are possible from \mathbf{x}' to \mathbf{x} . The dissipation matrix must take the form $\mathcal{D}_{\mathbf{x}, \mathbf{x}'}(t) =$

¹This is a formalism developed to approximate the time-dependent solution of the Liouville equation by an approximate solution.

²The phrase “takes on the form” should be taken with caution, since most coarse graining theories are based on microscopic formalisms that, at some point(s) in their derivation, must take several leap of faith to wash (or perhaps wish) away atomic fluctuations and leave behind equations for a mesoscale variable. Here, we follow more of an intuitive approach.

$[\nabla_{\mathbf{x}} \nabla_{\mathbf{x}'} \mathbf{D}(\mathbf{x}, \mathbf{x}', t)]$ such that Eq. (9.7) be derivable from a mass conservation law, as we we'll see below. The matrix $\mathbf{D}(\mathbf{x}, \mathbf{x}', t)$ is called the *diffusion tensor* and given by the Green-Kubo relation

$$\mathbf{D}(\mathbf{x}, \mathbf{x}', t) = \int_0^\tau dt' \text{Tr} [f(\mathbf{q}, \mathbf{p}, t) \hat{\mathbf{J}}(\mathbf{x}, 0) \hat{\mathbf{J}}(\mathbf{x}', t')], \quad (9.8)$$

where $\hat{\mathbf{J}}(\mathbf{x}, t)$ is the microscopic density flux (or particle flux) operator defined by

$$\hat{\mathbf{J}}(\mathbf{x}, t) \equiv \sum_{i=1}^N \mathbf{v}_i(t) \delta(\mathbf{x} - \mathbf{q}_i(t)) \quad (9.9)$$

with $\mathbf{v}_i(t)$, $\mathbf{q}_i(t)$ are the velocity and position of particle i , respectively, at time t . Here τ is a characteristic time scale that is longer the decay time of flux correlations but shorter than the time scale over which $f(\mathbf{q}, \mathbf{p}, t)$ changes³. The operation $\text{Tr}[f(\mathbf{q}, \mathbf{p}, t) \cdots]$ in Eq. (9.8) takes a *non-equilibrium* average of the flux correlator $\hat{\mathbf{J}}(\mathbf{x}, 0) \hat{\mathbf{J}}(\mathbf{x}', t')$ over the configuration space spanned by $\{\mathbf{q}_i(0), \mathbf{v}_i(0), \mathbf{q}_i(t'), \mathbf{v}_i(t')\}$ for $i = 1, \dots, N$ particles. It is noted that the time dependence of $\mathbf{D}(\mathbf{x}, \mathbf{x}', t)$ enters solely through the non-equilibrium phase space density $f(\mathbf{q}, \mathbf{p}, t)$.

Substituting the explicit form for $\mathcal{D}_{\mathbf{x}, \mathbf{x}'}(t)$ into Eq. (9.7), performing an integration by parts with respect to the $\nabla_{\mathbf{x}'}$ and taking the $\nabla_{\mathbf{x}}$ operator out of the integral gives a more intuitive and “Model B”-looking form for the dynamical equation for the density,

$$\frac{\partial \rho(\mathbf{x}, t)}{\partial t} = \nabla \cdot \left[\int d\mathbf{x}' \mathbf{D}(\mathbf{x}, \mathbf{x}', t) \cdot \nabla' \frac{\delta \mathcal{F}[\rho]}{\delta \rho(\mathbf{x}', t)} \right], \quad (9.10)$$

where ∇' denotes differentiation with \mathbf{x}' . Equation (9.10) describes conserved dynamics, where the expression in the large bracket plays the role of a mass flux, \mathbf{J}_{mass} , whose gradient drives changes in $\rho(\mathbf{x}, t)$. Here, \mathbf{J}_{mass} picks up non-local flux contributions at \mathbf{x} from neighbouring positions.

The diffusion matrix can be simplified. Specifically, substituting Eq. (9.9) into Eq. (9.8) gives

$$\begin{aligned} \mathbf{D}(\mathbf{x}, \mathbf{x}', t) &= \sum_{i=1}^N \sum_{j=1}^N \int_0^\tau dt' \text{Tr} [f(\mathbf{q}, \mathbf{p}, t) \mathbf{v}_i \mathbf{v}_j(t') \delta(\mathbf{x} - \mathbf{q}_i) \delta(\mathbf{x}' - \mathbf{q}_j(t'))] \\ &\approx \sum_{i=1}^N \sum_{j=1}^N \int_0^\infty dt \text{Tr} [f(\mathbf{q}, \mathbf{p}, t) \mathbf{v}_i \mathbf{v}_j(t) \delta(\mathbf{x} - \mathbf{q}_i) \delta(\mathbf{x}' - \mathbf{q}_j)] \end{aligned} \quad (9.11)$$

In the second line of Eq. (9.11) the limit $\tau \rightarrow \infty$ was taken since τ is assumed to be longer than the fluctuation-correlation decay time. Moreover, the time dependence in $\mathbf{q}_j(t')$ was ignored as the coordinates are assumed to change very slowly compared to the particles velocities and $t' \rightarrow t$ since $f(\mathbf{q}, \mathbf{p}, t)$ changes negligibly over the decay time of velocity correlations. Equation (9.11) shows that the diffusion tensor picks up large correlations between two points \mathbf{x} and \mathbf{x}' if the velocities there are strongly correlated over the characteristic time τ . Theories using equation 9.7 and or its variations are typically referred to as *Dynamic Density Functional Theories (DDFT)*.

The non-locality implied by Eq. (9.11) poses a severe limitation for simulating Eq. (9.10). It is reasonable to assume that the particle positions and coordinates can be taken as being statistically independent, which makes them decouple, giving

$$\begin{aligned} \mathbf{D}(\mathbf{x}, \mathbf{x}', t) &= \sum_{i=1}^N \sum_{j=1}^N \int_0^\infty dt \text{Tr} [f(\mathbf{q}, \mathbf{p}, t) \mathbf{v}_i \mathbf{v}_j(t)] \text{Tr} [f(\mathbf{q}, \mathbf{p}, t) \delta(\mathbf{x} - \mathbf{q}_i) \delta(\mathbf{x}' - \mathbf{q}_j)] \\ &= D_0 \mathbb{1} \rho(\mathbf{x}, t) \delta(\mathbf{x} - \mathbf{x}') \end{aligned} \quad (9.12)$$

³It is assumed through this formalism that the phase space density $f(\mathbf{q}, \mathbf{p}, t)$ changes more slowly than any relevant process in the system.

where $\mathbb{1}$ is the identity matrix (which picks up the units of the second trace) and D_0 is the standard diffusion coefficient given by

$$D_0 = \frac{1}{3} \int_0^\infty dt \text{Tr} [f(\mathbf{q}, \mathbf{p}, t) \mathbf{v}_i(0) \cdot \mathbf{v}_i(t)]. \quad (9.13)$$

Substituting Eq. (9.12) into Eq. (9.7) simplifies it to the form suggested by Ref. [19],

$$\frac{\partial \rho(\mathbf{x}, t)}{\partial t} = \nabla \cdot \left[D_0 \rho(\mathbf{x}, t) \nabla \frac{\delta \mathcal{F}[\rho]}{\delta \rho(\mathbf{x}, t)} \right]. \quad (9.14)$$

where, here, the units of $[D_0] = m^2/s$. An analogous approach can be followed to arrive at a “Model A”-type equation for a non-conserved order parameter field ϕ which has become a standard component of most phase field models.

Equation (9.14) of motion can also be extended to a Langevin equation. In this variant the equation of motion describes the evolution of the *partially* coarse-grained density operator, $\hat{\rho}(\mathbf{x}, t)$. The addition of stochastic noise is then added to Eq. (9.14) to capture fluctuations on length scales left out by the course graining procedure. This Langevin equation analogue of Eq. (9.14) for $\hat{\rho}(\mathbf{x}, t)$ then becomes

$$\begin{aligned} \frac{\partial \hat{\rho}(\mathbf{x}, t)}{\partial t} &= \nabla \cdot \left[D_0 \hat{\rho}(\mathbf{x}, t) \nabla \left(\frac{\delta \mathcal{F}[\hat{\rho}]}{\delta \hat{\rho}} \right) \right] + \xi(\mathbf{x}, t), \\ \langle \xi(\mathbf{x}, t) \rangle &= 0, \\ \langle \xi(\mathbf{x}, t) \xi(x', t') \rangle &= -\nabla \cdot [D_0 \hat{\rho}(\mathbf{x}, t) \nabla \delta(\mathbf{x} - \mathbf{x}') \delta(t - t')]. \end{aligned} \quad (9.15)$$

Equation (9.15) is essentially the governing equation used to simulate dynamics in all [nearly] all phase field (PF) or phase field crystal (PFC) models, where, in the case of PFC, $\hat{\rho} \rightarrow \rho$, with ρ representing the density operator averaged over some mesoscopic time scale (i.e., not the same ρ as in Eq. (9.14)). The noise can then be considered a spatially filtered version of the one in Eq. (9.15), representing the longer-time and longer wavelength fluctuations in the evolution of ρ . The PFC model is examined further in the next section.

9.2 Model B Limit of DDFT: PFC Dynamics

The first of Equations (9.15) can be written as a mass conservation equation of the form

$$\frac{\partial \rho}{\partial t} = -\nabla \cdot \mathbf{J}_{\text{mass}}(\mathbf{x}, t) \quad (9.16)$$

where $\mathbf{J}_{\text{mass}}(\mathbf{x}, t)$ represents the local flux of mass past a point \mathbf{x} at time t . If particle position and momenta in a given volume are taken to be uncorrelated in space and time, the flux is typically proportional to the local thermodynamic force, which drives the system toward thermal equilibrium at long times. Following Eq. (7.31), we describe the local flux according to $\mathbf{J}_{\text{mass}}(\mathbf{x}, t) = -\Gamma \nabla (\delta F / \delta \rho(\mathbf{x}, t))$, where here F is considered a free energy functional (units of J) of the field theory and Γ is a mobility factor that is proportional to the average of the inverse time scale of local density fluctuations. To reduce Eq. (9.16) to a PFC theory, we consider $\rho(\mathbf{x}, t)$ as a [locally] coarse grained field in time, and approximate $\Gamma \sim \text{constant}$. This turns Eq. (9.16) into a model B type equation of the form

$$\frac{\partial \rho}{\partial t} = \Gamma \nabla^2 \left(\frac{\delta F}{\delta \rho(\mathbf{x}, t)} \right) + \zeta \quad (9.17)$$

Here noise is added to the flux in order to account for uncorrelated microscopic motions, as described in the previous subsection. Since the noise represents fluctuations in density, it must be conserved, moreover, since Γ is taken as constant, the analogue of the noise correlations in Eq. (9.15) for a PFC theory satisfies

$$\langle \zeta(\mathbf{x}, t)\zeta(\mathbf{x}', t') \rangle = -2k_B T \bar{\rho} \Gamma \nabla^2 \delta(\mathbf{x} - \mathbf{x}') \delta(t - t') \quad (9.18)$$

Eq. (9.17) and Eq. (9.18) are a minimal reduction of the DFT type theory of the previous subsection into a Model B type phase field theory. The dimensional units of the constants appearing in this model are follows: $[\rho] = 1/m^d$, $[\delta F/\delta\rho] = J/m^d$, $[\nabla^2] = 1/m^2$ and $[\zeta] = 1/(m^d s)$ and $[\Gamma] = m^2/(J s)$.

It is desirable to work in a formalism that is expressed only in terms of the dimensionless density $n = (\rho - \bar{\rho})/\bar{\rho}$, dimensionless length $\bar{r} = \bar{x}/a$ and dimensionless free energy $\bar{F} = F/(k_B T \bar{\rho} a^3)$. Here, we express $\delta F/\delta\rho = (k_B T \bar{\rho}) \delta \bar{F}/\delta n$, where $\delta \bar{F}/\delta n$ is a dimensionless integrand of a dimensionless PFC free energy functional written in terms of n , as is done typically in the PFC literature. In these dimensionless units, Eq. (9.17) becomes

$$\frac{\partial n}{\partial t} = [k_B T \bar{\rho} M_n/a^2] \nabla_r^2 \left(\frac{\delta \bar{F}}{\delta n} \right) + \xi \quad (9.19)$$

where ∇_r acts on r , and (9.18) becomes

$$\begin{aligned} M_n &= \frac{\Gamma}{\bar{\rho}} \\ \xi &= \frac{\zeta}{\bar{\rho}}, \end{aligned} \quad (9.20)$$

where the scaled noise ξ satisfies

$$\langle \xi(\bar{r}, t)\xi(\bar{r}', t') \rangle = -2 \frac{[k_B T \bar{\rho} M_n/a^2]}{(\bar{\rho} a^3)} \nabla_r^2 \delta(\bar{r} - \bar{r}') \delta(t - t') \quad (9.21)$$

The units of $[M_n] = m^{d+2}/J \cdot s$ and $[\xi] = 1/s$, while $[\delta \bar{F}/\delta n]$ and $[n]$ are dimensionless. The a^3 term in the denominator of Eq. (9.21) comes from making the spatial delta function non-dimensional. Since a is the lattice constant of a unit cell, the product $\bar{\rho} a^3$ is the number of atoms per unit cell. In what follows, the shorthand notation, $n_u \equiv \bar{\rho} a^3$ is defined.

The above re-scalings and definitions make it possible to re-express the equations of motion in the final dimensionless form to be used hereafter,

$$\frac{\partial n}{\partial t} = \bar{M}_{PFC} \nabla_r^2 \left(\frac{\delta \bar{F}}{\delta n} \right) + \xi, \quad (9.22)$$

where the PFC noise satisfies the fluctuation-dissipation theorem,

$$\langle \xi(\bar{r}, t)\xi(\bar{r}', t') \rangle = -2 \frac{\bar{M}_{PFC}}{n_u} \nabla_r^2 \delta(\bar{r} - \bar{r}') \delta(t - t') \quad (9.23)$$

and where

$$\bar{M}_{PFC} = k_B T \bar{\rho} \frac{M_n}{a^2} \quad (9.24)$$

The units of $[\bar{M}_{PFC}] = 1/s$. Equations (9.22) and (9.23) show that XPFC dynamics are controlled by one parameter, the mobility M_n , which can effectively be seen to re-scale time. The Model B type dynamics portrayed in Eq. (9.22) and other PFC model equations in the literature [24] are the simplest dynamics that allow for consistent simulations of many salient features of microstructure and defect evolution.

9.3 “Quasi-Phononic” PFC Dynamics

As a model capable of incorporating solid-state defects and elasticity, the PFC model should be able to propagate information from elastic deformations (strains, dislocation-dislocation interactions, etc) on time scales much shorter than the diffusional time scales implied by Model B type dynamics. This requires a slightly different formulation that couples the diffusive density transport to the hydrodynamic models governing elastic modes in the solid. Doing so, however, come with severe pitfalls. Once such pitfalls is that hydrodynamic modes in a solid propagate at the speed of sound. Thus, incorporating such hydrodynamic modes into PFC solids rigorously (assuming that is even possible!) would lead to a model that is not much better than directly using molecular dynamics and which, in fact, does a much better job than PFC on these atomistic times scales. This would lead us right back to the reason we would like to have coarse grained theories that operate on long wavelengths and *diffusional* times scales. Another avenue for resolving the aforementioned problem in the dynamics of PFC (or, equivalently, XPFC) models involves using hydrodynamic considerations to adapt the PFC phenomenology to include two time scales, one diffusive and the other “inertial”, where the “inertial” merely refers to using a phenomenological time scale to emulate rapid elastic relaxation effects on the PFC n on time scales that are more rapid than any of the diffusive processes the model is emulating. This effectively allows us to separate time scales of diffusive events driven by vacancies (e.g. creep, grain boundary diffusion, dislocation climb) from those operating on much faster times scales (e.g. dislocation glide, elastic vibrations, etc). This is explored in remaining pages of this chapter.

9.3.1 Two-time dynamics in the PFC model

To incorporate diffusive and rapid relaxation dynamics into the PFC model, we re-visit the hydrodynamics concepts discussed in Section 6.4. We start by taking the time derivative of both sides of Eq. (6.65) and then substituting Eq. (6.64) on the right hand side of the result for $\partial\mathbf{g}/\partial t$. This gives

$$\begin{aligned} \frac{\partial^2 \rho}{\partial t^2} &= \nabla_i \nabla_j \pi_{i,j} \\ &= \nabla_i \nabla_j \sigma_{ij}^R + \nabla_i \nabla_j \sigma_{ij}^{\text{diss}}, \end{aligned} \quad (9.25)$$

where repeated indices imply summation. For the case of slow deformation in a solid that we will be considering here, the momentum flux tensor π_{ij} is equal to the stress tensor σ_{ij} . In the second line of Eq. (9.25) we have tacitly split σ_{ij} in two parts. The first, σ_{ij}^R , is the reactive (or thermodynamically reversible) part, while the second part, $\sigma_{ij}^{\text{diss}}$, denotes the non-reversible part of the stress tensor, which arise from dissipative sources (e.g. vacancies, friction between volume elements, etc). Following standard elasticity theory of deforming materials [16], the gradient of the reactive part of the stress tensor can be obtained form the total internal energy or fre energy functionals of the deforming body according to

$$\nabla_j \sigma_{ij}^R = \left. \frac{\delta \mathcal{E}}{\delta u_i} \right|_{s, \mathbf{g}, \psi_v} = \left. \frac{\delta \mathcal{F}}{\delta u_i} \right|_{T, \mathbf{v}, \psi_v} \quad (9.26)$$

where u_i is the i^{th} component the displacement vector $\mathbf{u} = (u_x(\mathbf{r}), u_y(\mathbf{r}), u_z(\mathbf{r}))$, which defines the displacement of a volume element at position \mathbf{r} at time t relative to its original position in the undeformed material (i.e. at some other position \mathbf{r}' in the fixed volume enclosed the system)⁴. In writing

⁴In what follows, we will only consider small (i.e. linear elastic) deformations of the solid phase around an undeformed state and thus ignore convective effects. The the instantaneous velocity of a volume element at position \mathbf{r} will thus be approximated by $\mathbf{v} = \partial_t \mathbf{u} \equiv \partial \mathbf{u} / \partial t$.

Eq. (9.26) it is tacitly assumed that there is a kinetic energy component to the energy potentials, as was done in the hydrodynamics treatment following Section 6.2.2. Another subtlety of Eq. (9.26) is that it requires a fixed *vacancy fraction* (denoted ψ_v) rather particle number to be valid [10]; this will be assumed in the following proceedings. In keeping with much of the PFC literature, we will be considering here isothermal conditions in a fixed volume and hence we will work with a free energy functional. We can thus write Eq. (9.25) as

$$\frac{\partial^2 \rho}{\partial t^2} = \nabla_i \left(\frac{\delta \mathcal{F}}{\delta u_i} \right) + \nabla_i \nabla_j \sigma_{ij}^{\text{diss}} \quad (9.27)$$

Equation (9.27) is the basis from which we derive a phenomenology for two-time-scale PFC dynamical equation.

Section 6.2.2 showed that the local free energy of a deforming volume element can be written as a sum of its frame-fixed internal energy minus its kinetic energy. We adopt this approach here and assume we can in theory write a total PFC free energy functional \mathcal{F} whose integrand is decomposable into an energy density term that is fixed with a moving volume of the materials and depends on the local PFC density $\rho(\mathbf{r}, t)$ (bulk and gradient terms, etc) minus the kinetic energy density written in terms of the local velocity \mathbf{v} (an intensive variable) and the local momentum \mathbf{g} (an extensive variable). The functional \mathcal{F} is given by

$$\mathcal{F}[s, \rho, \mathbf{v}] = \frac{1}{V} \int d\mathbf{r} \left\{ f(T, \rho(\mathbf{r}, t)) - \frac{1}{2} \mathbf{g} \cdot \mathbf{v} \right\} \quad (9.28)$$

Here, $f(T, \rho(\mathbf{r}, t))$ is the free energy density in the rest frame of volume element at position \mathbf{r} and $\mathbf{v}(\mathbf{r}, t)$ is the volume element's velocity. Integration is over the volume V of the system and \mathbf{r} describes a coordinates vector within the fixed volume V in which the entire system exists. It is recalled that a PFC-type model free energy is a type of classical density functional theory (cDFT), which implies that it is written entirely in terms of a mass density field $\rho(\mathbf{r}, t)$. What is less apparent is that PFC models *inherently* contain information about elastic strain, topological defects and vacancies. This information is encoded in the density field through the gradient and bulk expansion of $f(T, \rho(\mathbf{r}, t))$, several forms of which have been posited for different PFC models here and in the literature. As a result, it will be assumed in what follows that there exists a constitutive equation relating the PFC density to the local displacement field $\mathbf{u}(\mathbf{x})$ and the local vacancy fraction, which we denote here by $\psi_v(\mathbf{x})$.

Taking the variation of the internal energy functional in Eq. (9.28) at fixed vacancy fraction gives

$$\frac{\delta \mathcal{F}}{\delta u_i(\mathbf{y})} \Big|_{T, \mathbf{v}, \psi_v} = \int \left\{ \frac{\delta f}{\delta \rho(\mathbf{x}, t)} \Big|_T - \frac{1}{2} |\mathbf{v}|^2 \right\} \left(\frac{\delta \rho(\mathbf{x}, t)}{\delta u_i(\mathbf{y})} \Big|_{\psi_v} \right) \delta(\mathbf{x} - \mathbf{y}) d\mathbf{x}, \quad (9.29)$$

where the first expression in the curly brackets on the right hand side is the usual chemical potential $\mu(\mathbf{x}, t)$ defined in PFC models through the functional f as

$$\mu(\mathbf{x}, t) = \frac{\delta f}{\delta \rho(\mathbf{x}, t)} \Big|_T, \quad (9.30)$$

where f is the corresponding free energy density, which can in theory be substituted for any PFC model in the literature. It is emphasized that while, here, we split the total internal energy of the PFC model in terms of local and kinetic effects, in the final version of the PFC model these will subsumed back into one internal energy expression written in terms of $\rho(\mathbf{x}, t)$. The total chemical potential $\mu(\mathbf{x}, t)$ will thus be assumed to be derivable from the variational of the usual PFC free energy functional written in terms of density, i.e., $\mu(\mathbf{x}, t) = \delta F / \delta \rho(\mathbf{x}, t)$). Note: to ease up on the notation a bit in what follows, the explicit writing of the time variable will be suppressed in expressions like $\rho(\mathbf{x}, t)$, $\mu(\mathbf{x}, t)$, etc.

9.3.2 A constitutive equation for $\rho(\mathbf{x}, t)$

To proceed beyond Eq. (9.29), we require a constitutive equation that relates the local density field $\rho(\mathbf{x})$ to the local vacancy fraction $\psi_v(\mathbf{x})$ and the local deformation displacement $u_i(\mathbf{x})$, or strain $u_{ij}(\mathbf{x})$. We derived such a relationship for $\delta\rho$ in our mean-field treatment of solids, i.e., Eq. (5.10) in Section 5. Here, we motivate an extension of Eq. (5.10) to the case of the fields.

We begin by splitting the local momentum density at a point \mathbf{r} into two part as follows,

$$\mathbf{g} = \mathbf{g}^{\text{lattice}} + \mathbf{g}^{\text{vac}} = \rho(\mathbf{x}) \frac{\partial \mathbf{u}}{\partial t} + \mathbf{g}^{\text{vac}} \quad (9.31)$$

where the first term $\mathbf{g}_L = \rho(\mathbf{x}) \partial_t \mathbf{u}$ represents the momentum flux carried by the deformation of the lattice transporting atoms past some observation surface (units $\text{kg}/\text{m}^2\text{-s}$). The second term \mathbf{g}_{vac} is the momentum carried across said [hypothetical] surface by the diffusive transport (i.e., random hopping) of vacancies. These two modes of atomic transport are illustrated in Figure 9.1. Taking the divergence

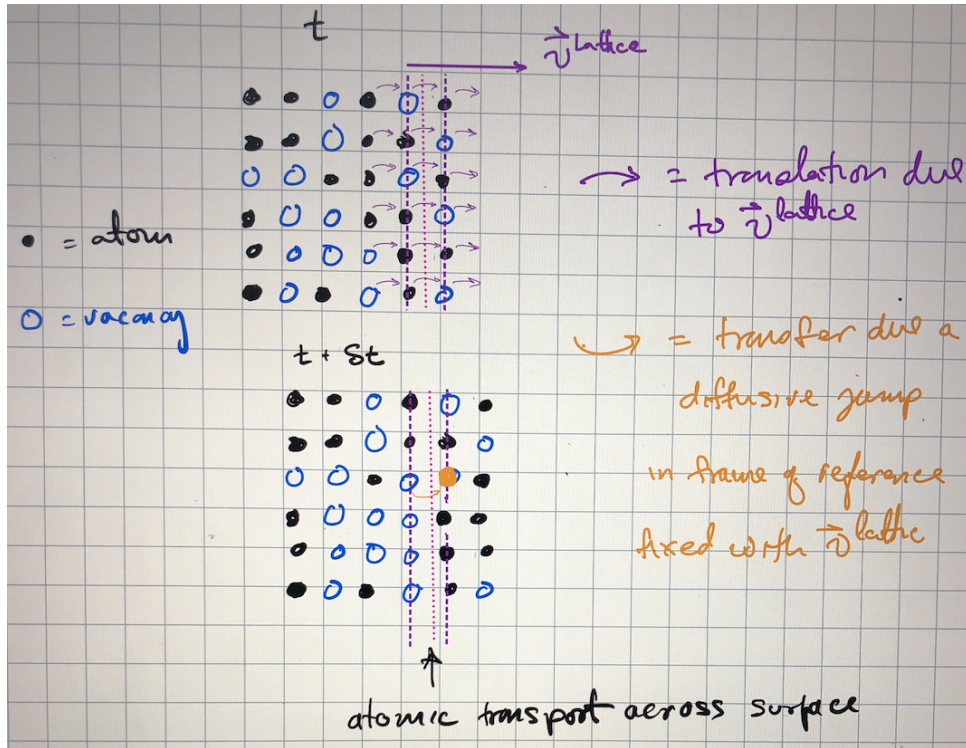


Figure 9.1: Cartoon of atoms hoping across a hypothetical surface in a crystal. Purple arrows indicated shifts in positions of atoms that are transported by displacement of the lattice, but otherwise remain in the same atomic planes. Orange arrows indicate atomic transport by a random hop from one atomic plane (or lattice site) due to the processes of diffusion, a thermally activated process.

of both sides of Eq. (9.31) and using $\partial\rho/\partial t = -\nabla \cdot \mathbf{g}$ gives

$$\frac{\partial\rho}{\partial t} = -\nabla \cdot \mathbf{g}^{\text{vac}} - \delta_{ij} \nabla_i \left(\rho \frac{\partial u_j}{\partial t} \right), \quad (9.32)$$

It is instructive to take the infinitesimal limit of Eq. (9.32), i.e. letting $\partial\rho/\partial t \rightarrow \delta\rho/\delta t$ and $\partial u_j/\partial t \rightarrow$

$\delta u_j/\delta t$, and then multiplying through by δt . This gives

$$\begin{aligned}\delta\rho &= -\delta t \nabla \cdot \mathbf{g}^{\text{vac}} - \delta_{ij} \nabla_i (\rho \dot{u}_j \delta t) \\ &= -\delta t \nabla \cdot \mathbf{g}^{\text{vac}} - \delta_{ij} \nabla_i (\rho u_j) \\ &= \delta\rho^{\text{vac}} - \delta_{ij} \nabla_i (\rho u_j),\end{aligned}\quad (9.33)$$

where we have defined $\delta\rho^{\text{vac}} \equiv -\delta t \nabla \cdot \mathbf{g}^{\text{vac}}$, which we associate with the change of mass density due to the change vacancy fraction at \mathbf{x} . Comparing Eq. (9.33) to its mean field counterpart in Eq. (5.10) $\delta\rho = \rho\delta - \delta_{ij}\rho\nabla_i u_j$ allows us to identify $\delta\rho^{\text{vac}}$ alternatively as

$$\delta\rho^{\text{vac}}(\mathbf{x}) = \rho(\mathbf{x})\psi_v(\mathbf{x}) \quad (9.34)$$

The above considerations then suggest the following generalization of Eq. (5.10) to the case of the fields,

$$\delta\rho(\mathbf{x}) = \rho(\mathbf{x})\delta\psi_v(\mathbf{x}) - \delta_{ij}\nabla_i (\rho(\mathbf{x})u_j(\mathbf{x})), \quad (9.35)$$

where δ_{ij} is the Kronecker delta. It is also noted that the displacement $u_j \equiv$ can be treated as δu_i relative to a reference undeformed state. As a result, to lowest order in the $\delta\rho$ and u_j , the term $\nabla_i (\rho(\mathbf{x})u_j) \approx \rho(\mathbf{x})\nabla_i u_j$, making the correspondence of Eq. (9.35) to its mean field counterpart complete.

Returning to Eq. (9.29) and using Eq. (9.35) yields

$$\frac{\delta\mathcal{F}}{\delta u_j(\mathbf{y})} = \int \left\{ \mu(x) + \frac{1}{2}|\mathbf{v}|^2 \right\} \left\{ -\delta_{ij} \frac{\partial [\rho\delta(\mathbf{x}-\mathbf{y})]}{\partial x_j} \right\} d\mathbf{x} \quad (9.36)$$

Integrating Eq. (9.36) by parts and dropping the $\mathcal{O}(v_i v_j)$ term (since we are considering linearized hydrodynamics) gives⁵ and substituting the result into Eq. (9.27) (after making the swap $\mathbf{y} \rightarrow \mathbf{x}$) gives,

$$\frac{\partial^2 \rho}{\partial t^2} = \nabla^2 \{ \rho(\mathbf{x})\mu(\mathbf{x}) \} + \nabla_i \nabla_j \sigma_{ij}^{\text{diss}} \quad (9.37)$$

9.4 Dissipation tensor

Continuing on to a closed form of Eq. (9.37) further requires a phenomenology for the dissipative component of the stress tensor. As with generic friction, dissipative forces in general act to dissipate the momentum of a volume element non-reversibly. To account for dissipation on two length scales, we will split of dissipative stress tensor into two sources as follows,

$$\nabla_j \sigma_{ij}^{\text{diss}} = \nabla_j \sigma_{ij}^{\text{visc}} + \nabla_j \sigma_{ij}^{\text{drag}} \quad (9.38)$$

Both components will depend on the local momentum density of a volume element, given by $\mathbf{g} = \delta\mathcal{F}/\delta\mathbf{v}$. The first term takes the standard form that relates stresses dissipated though *gradients* in the momentum density, which leads to the usual viscosity-like stress dissipation on shorter wavelengths. The second is one is more phenomenological *Aristotelian drag* force that becomes directly proportional to the momentum density, and will be operational on longer wavelengths; the latter form will also prove to be necessary to recover the Model B type limit of the modified PFC model at late times

⁵It is noted that in typical physics form, we will treat $\delta(\mathbf{x}-\mathbf{y})$ as a proper function to facilitate operations, rather than taking the more formal route of using limits of a distribution, which, while approved [somewhat more] by mathematicians, would make the algebra look alot [more] like “a dog’s breakfast”.

The first term of the dissipative stress tensor term in Eq. (9.38) is given explicitly by

$$\nabla_j \sigma_{ij}^{\text{visc}} = \mathcal{L}_{jk} \nabla_k \nabla_k \left(\frac{\delta \mathcal{F}}{\delta v_i} \right) = \nu \delta_{jk} \nabla_j \nabla_k g_i = \nu \nabla^2 \mathbf{g} \quad (9.39)$$

Taking the gradient of both sides of Eq. (9.42) and applying the mass conservation equation yields

$$\nabla_i \nabla_j \sigma_{ij}^{\text{visc}} = \nu \nabla^2 (\nabla \cdot \mathbf{g}) = -\nu \nabla^2 \left(\frac{\partial \rho}{\partial t} \right) \quad (9.40)$$

The second term of the dissipative stress tensor term in Eq. (9.38) is given explicitly by

$$\nabla_j \sigma_{ij}^{\text{drag}} = \eta \frac{\delta \mathcal{F}}{\delta v_i} = \eta \mathbf{g} \quad (9.41)$$

Taking the gradient of both sides of Eq. (9.41) and once again applying the mass conservation equation now yields

$$\nabla_i \nabla_j \sigma_{ij}^{\text{drag}} = \eta \nabla \cdot \mathbf{g} = -\eta \frac{\partial \rho}{\partial t} \quad (9.42)$$

As mentioned above, this term is necessary to recover the diffusive model B type dynamics governing diffusive transport in the PFC model ⁶.

9.4.1 Modified PFC (*MPFC*) model and its simplifications

Substituting both dissipation terms in Eq. (9.42) and Eq. (9.41) back into Eq. (9.37) gives the following PFC evolution equation for $\rho(\mathbf{x}, t)$,

$$\frac{\partial^2 \rho}{\partial t^2} + \eta (1 - \gamma \nabla^2) \frac{\partial \rho}{\partial t} = \nabla^2 \{ \rho(\mathbf{x}) \mu(\mathbf{x}) \} = \nabla^2 \left\{ \rho(\mathbf{x}) \frac{\delta \mathcal{F}}{\delta \rho(\mathbf{x}, t)} \right\} \quad (9.43)$$

where $\gamma = \nu/\eta$. Equation (9.43) is a closed equation that is a type of damped wave equation. It describes the two-time-scale evolution of the density $\rho(\mathbf{x}, t)$ in terms of total chemical potential, which can be derived from any PFC functional in the literature (here have been many!).

It is noteworthy that the dissipation sources in Eq. (9.43) act on *two* length scales differently. the ∇^2 multiplying the $\partial \rho / \partial t$ term is fundamental in its origin and acts to dissipate energy on short wavelengths. The dissipation term proportional to $\partial \rho / \partial t$ is phenomenological and acts on longer length scales. It is necessary to recover the Model B type dynamic of Eq. (9.22). Also, this type of velocity-dependent drag is critical to provide dissipating forces on microstructures like dislocations which glide as a speed set by a balance of the mechanical deformation forces and drag, which goes like $\sigma_{\text{rmdrag}} \sim \text{velocity}$.

It is inefficient to simulate Eq. (9.43) in Fourier space, which become inefficient the way the density is “sandwiched” between the two gradient operators. Two minimal models modifications exists, one better than the other. The first simplification is to remove $\rho(\mathbf{x}, t)$ on the right hand side of Eq. (9.43) out of the brackets, yielding

$$\frac{\partial^2 \rho}{\partial t^2} + \eta (1 - \gamma \nabla^2) \frac{\partial \rho}{\partial t} \approx \rho(\mathbf{x}) \nabla^2 \left\{ \frac{\delta \mathcal{F}}{\delta \rho(\mathbf{x}, t)} \right\} \quad (9.44)$$

⁶It should be noted that rigorously, only the viscosity-type first term arises due to symmetry (i.e. translational invariance) considerations in hydrodynamic treatments. However, it is straightforward to show that integrating a $\nabla \mathbf{v}$ type term over volume of an element and using the divergence theorem will yield a drag-like term on the element for the case of laminar flow. Thus, we can consider Eq. (9.38) as explicitly breaking up the dissipation into a term that obeys the local symmetries on small scales (i.e. the scale of periodic peaks in the case of a PFC model) and one that generates drag on larger scales via Eq. (9.42), which is crucial for controlling “flow” of microstructures like dislocations and grain boundaries.

This may seem crude but it is recalled that on long wavelengths (where *all* PF-type models are supposed to work well!) the density is smooth on long wavelengths and oscillates rapidly and periodically on atomic scales (see the Section of amplitude equations in chapter 8 of Ref. [24]). Expanding out the right hand side of Eq. (9.43) with the chain rule and using this smoothness property of the density gives the right hand side of Eq. (9.44) as the leading order term that is manifest at large wavelengths. The second simplification is to replace $\rho(\mathbf{x}, t)$ on the right hand side of Eq. (9.43) by the reference $\bar{\rho}$ around which the original free energy functional \mathcal{F} is expanded. This gives

$$\frac{\partial^2 \rho}{\partial t^2} + \eta (1 - \gamma \nabla^2) \frac{\partial \rho}{\partial t} \approx \bar{\rho} \nabla^2 \left\{ \frac{\delta \mathcal{F}}{\delta \rho(\mathbf{x}, t)} \right\} \quad (9.45)$$

Equation (9.45) is very crude but still provides a minimal description of two-time scale dynamics in PFC modelling. It has appeared first phenomenologically by Stefanovich et. al [28].

Bibliography

- [1] E. Alster, K. R. Elder, J. J. Hoyt, and P. W. Voorhees. Phase-field-crystal model for ordered crystals. *Phy. Rev. E*, 95:022105, 2017.
- [2] Joel Berry, Nikolas Provatas, Jorg Rottler, and Chad W. Sinclair. Defect stability in phase-field crystal models: Stacking faults and partial dislocations. *Phy. Rev. B*, 86(224112), 2012.
- [3] J. J. Binney, N. J. Dowrick, A. J. Fisher, and M. E. J. Newman. *The Theory of Critical Phenomena*. Oxford University press, 1992.
- [4] P.M. Chaikin and T.C Lubensky. *Principles of condensed matter physics*. Cambridge University Press, Cambridge, Great Britain, 1995.
- [5] P. M. Chakin and T. C. Lubensky. *Principles of Condensed Matter Physics*, page 699. Cambridge University Press, 1995.
- [6] J.A. Dantzig and M. Rappaz. *Solidification*. Engineering sciences (EPFL)., Materials. Lausanne : EPFL Press, 2009, 2009.
- [7] Martin T. Dove. *Structure and Dynamics, an atomic view of materials*. Oxford University press, 2003.
- [8] K. R. Elder and Martin Grant. Modeling elastic and plastic deformations in nonequilibrium processing using phase field crystals. *Phys. Rev. E*, 70:051605, Nov 2004.
- [9] Pep Español and Hartmut Löwen. Derivation of dynamical density functional theory using the projection operator technique. *The Journal of Chemical Physics*, 131(24):244101, 2009.
- [10] Paul D. Fleming-III and Claude Cohen. Hydrodynamics of solids. *Physical review B*, 13:500–516, 1976.
- [11] Martin Grant. Dirty tricks for statistical mechanics: time dependent things. Version 0.8, August 2005.
- [12] Michael Greenwood, Jörg Rottler, and Nikolas Provatas. Phase-field-crystal methodology for modeling of structural transformations. *Phys. Rev. E*, 83:031601, Mar 2011.
- [13] Jean-Pierre Hansen and Ian R. McDonald. *Theory of Simple Liquids with Applications to Soft Matter*. Elsevier Academic Press, fourth edition edition, 2013.
- [14] Kerson Huang. *Statistical Mechanics*. Jon Wiley and Sons, 1987.
- [15] L.D Landau and E.M. Lifsitz. *Statistical Physics*, volume 5 of *Course of Theoretical Physics*. Elsevier, Oxford, 3rd edition edition, 1980.

- [16] L.D Landau and E.M. Lifsitz. *Theory of Elasticity*. Butterworth-Heinemann, Oxford, 3rd edition edition, 1999.
- [17] J. S. Langer. Instabilities and pattern formation in crystal growth instabilities and pattern formation in crystal growth. *Rev. Mod. Phys.*, 52:1, 1980.
- [18] E.M. Lifsitz and L.P. Pitaevskii. *Physical Kinetics*, volume 10 of *Course of Theoretical Physics*. Elsevier, Oxford, 1981.
- [19] Umberto Marini Bettolo Marconi and Pedro Tarazona. Dynamic density functional theory of fluids. *Journal of Physics: Condensed Matter*, 12(8A):A413, 2000.
- [20] Joseph E. Mayer and Elliott Montroll. Molecular distribution. *The Journal of Chemical Physics*, 9(1):2–16, 1941.
- [21] James E. McDonald. Homogeneous nucleation of vapor condensation. ii. kinetic aspects. *American Journal of Physics*, 31:31–41, 1963.
- [22] W. W. Mullins and R. F. Sekerka. *J. Appl. Phys.*, 34:323, 1963.
- [23] III Paul D. Fleming and Claude Cohen. Hydrodynamics of solids. *Phy. Rev. B*, 13:500, 1976.
- [24] Nikolas Provatas and Ken Elder. *Phase Field Methods in Materials Science and Engineering*. Wiley-VCH, 2010.
- [25] Nikolas Provatas and Ken Elder. *Phase-Field Methods in Materials Science and Engineering*. Wiley-VCH Verlag GmbH & Co. KGaA, 2010.
- [26] T. V. Ramakrishnan and M. Yussouff. *Phys. Rev. B*, 19:2775, 1979.
- [27] H. Reiss. *Methods of Thermodynamics*. Dover Publishig, 1996.
- [28] P. Stefanovic, M. Haataja, and N. Provatas. *Phys. Rev. Lett.*, **96**:225504, 2006.
- [29] P.W. Voorhees. The theory of oswald ripening. *Journal of Statistical Physics*, 38:231–252, 1985.